Studies on the Effect of Nanoclay Addition on Mechanical, Thermal and Ablation Behaviour of Carbon Fiber Reinforced Polymer Composites

Submitted in partial fulfillment of the requirements for the award of the degree of

DOCTOR OF PHILOSOPHY
IN
CHEMISTRY

By

RAMARAO GOLLA
(Roll No. 716193)

Supervisors

Prof. K. Laxma Reddy

Department of Chemistry, NIT Warangal

Dr. I. Srikanth

Advanced Systems Laboratory, DRDO, Hyderabad

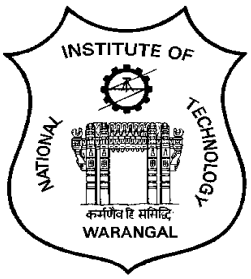

DEPARTMENT OF CHEMISTRY

NATIONAL INSTITUTE OF TECHNOLOGY WARANGAL

WARANGAL - 506004

TELANGANA, INDIA

August, 2021

CERTIFICATE

This is to certify that the thesis entitled **"STUDIES ON THE EFFECT OF NANOCLAY ADDITION ON MECHANICAL, THERMAL AND ABLATION BEHAVIOUR OF CARBON FIBER REINFORCED POLYMER COMPOSITES"** submitted to National Institute of Technolgy Warangal, by **Mr. G. Rama Rao,** bearing **Roll No 716193** for the award of **Doctor of Philosophy** in **Chemistry** is the record of the bonafide original work carried out by him under the supervisions of **Prof. K. Laxma Reddy, Professor (HAG),** Department of Chemistry, NIT Warangal and **Dr. I. Srikanth, Scientist 'F'** Advanced Systems Laboratory, DRDO, Hyderabad**.**

The results presented in this thesis have not been submitted in either part or full elsewhere for any research degree.

Signature of the External Supervisor
Dr. I. Srikanth
Scientist 'F', ASL, DRDO
Hyderabad

Signature of the Internal Supervisor
Prof. K. Laxma Reddy
Professor (HAG), Department of Chemistry
NIT Warangal

Date:

Station: NIT Warangal

DECLARATION

This is to certify that the work presented in the thesis entitled **"STUDIES ON THE EFFECT OF NANOCLAY ADDITION ON MECHANICAL, THERMAL AND ABLATION BEHAVIOUR OF CARBON FIBER REINFORCED POLYMER COMPOSITES"**.is a bonafide work done by me under the supervisions of **Prof. K. Laxma Reddy**, Professor (HAG) Department of Chemistry, NIT Warangal, and **Dr. I. Srikanth**, Scientist 'F', ASL, DRDO, Hyderabad and was not submitted elsewhere for the award of any degree or diploma.

I declare that this written submission represents my ideas in my own words and where others ideas or words have been included, I have adequately cited and referenced the sources. I also declare that I have adhered to all principles of academic honesty and integrity and have not misrepresented or fabricated or falsified any idea/data/fact/source in my submission. I understand that any violation of the above will be a cause for disciplinary action by the Institute and can also evoke penal action from the sources which have thus not been properly cited or from whom proper permission has not been taken when needed.

(RAMA RAO GOLLA)
Roll No. 716193
Date:

Dedicated to

My Parents and Teachers

Acknowledgments

I take this opportunity to express my sincere gratitude to my research supervisors **Prof. Kotha Laxma Reddy, Professor (HAG)**, Department of Chemistry, National Institute of Technology (NIT) Warangal and **Dr. Ivautri Srikanth**, **Scientist 'F'**, Advanced Systems Laboratory (ASL), DRDO, Hyderabad for their invaluable guidance, support, motivation, and suggestions from the beginning of the experiment planning phase of research work to the interpretation of the research results. I also would like to thank them for reading and correcting my research papers and thesis.

I am thankful to **Prof. N.V RamanaRao**, Director, NIT Warangal for his academic support throughout my research work. I would like to thank **Dr. Vishnu Shanker**, Head, Department of Chemistry and former heads **Prof. V. Rajeswar Rao, Prof. K. V. Gobi, and Prof. P. V. Srilakshmi**, NIT Warangal for their moral support and constant encouragement throughout my research work.

I extend my sincere thanks to the doctoral scrutiny committee (DSC), **Dr. Vishnu Shanker, Chairman and Member,** Department of Chemistry, **Prof. A. Ramachandraiah, Member,** Department of Chemistry, NIT Warangal**,** and **Prof. Shirish Sonawane, Member,** Department of Chemical Engineering, NIT Warangal for their support and valuable suggestions during DSC reviews of my research work. Their suggestions helped to improve the quality of my research work.

I would like thank **to Dr. D. Kashinath, Dr. N. Venkatathri Narayanan, Dr. Raghu Chitta, Dr. B. Srinivas, Dr. K. Hari Prasad, Dr. S. Nagarajan, Dr. M. Raghasudha, Dr. C. Jugun Prakash, Dr. Ravinder Pawar, Dr. Mukul Pradhan, Dr. G.Rajeshkhanna and Dr. V. Rajeshkumar,** Department of Chemistry, NIT Warangal for their constructive suggestions during DSC reviews of research work. I would like to thank **Dr. A. Kumar,** Head, Department of Mechanical Engineering, NIT Warangal for his encouragement throughout my research work.

I am thankful to **Dr. MRM Babu**, Director, ASL, DRDO, Hyderabad, **Mr. G. Ramaguru**, Programme Director, Agni, **Dr. Manoj Kumar Buragohain**, Technology Director, CPDC, **Mr**. **G. Venkataratnam**, Deputy Technology Director, CPDC, **Dr.Anil Kumar**, Deputy Technology Director, HTCC, **Dr. Alex Danial**, **Mr. K.Ramaswamy, Mr.N.Sudarshan**, **Mr.Y.Gangadhar Sinha, Mr**. **Ch. Ugender, Dr. M.P Raju, Dr. K. Tejasvi**, Scientists, ASL, DRDO, and **Dr.P. Ramasubba Reddy**, Scientist, DMRL, DRDO for their motivation and support throughout my research work.

I am thankful to **Mrs. Sandhya Nair**, Scientist, and **Mr. K. Kishore**, DRDL, DRDO for carrying out oxy-acetylene torch testing of various composite materials for my research work. I am thankful to **Mr. A. O Siddique** and **Dr. S. Rajesh**, Scientists, ASL for carrying out the thermal conductivity and FTIR of samples. I am thankful to **Dr. Prema Kumar**, Scientist, DMRL,DRDO for carrying out XRD of composite samples. I am thankful to **Dr. Krishnamurthy**, IIT Hyderabad, and **Dr. Suresh**, ARCI, Hyderabad for carrying out SAXS of samples. I am thankful to **Mr. K. Ganodhan Rao and Mr. P. Pranay Reddy** of CMCD/ HTCC, ASL for carryout out SEM images of various composite samples for my research work. I am thankful to **Mr. P. Chandrasekhar, Mr. S. Kannan, Mr. G. Sandeep Kumar, Mr. M. Sreenivasarao, Mr. G. Shiva Kumar, Mr.M. Madhukumar, Mr. K. Venkatesh (T), Mr. K. Venkatesh (U), and Mrs. S. Shivarani,** CPDC, ASL, for their support in conducting research work. I am thankful to **Mr. M. Saicharan, Mr. Ch. Srinivas Raju, Mr. S. Swamy, and Mr. Sankar**, CMCD/ HTCC, ASL for their support in conducting research work. I am thankful to **Mr. Sreekanth Reddy**, Scientist, DMRL, DRDO, and **Mr. A. Ramesh**, Lecturer, CMR Engineering College, Hyderabad for redrawing graphs using origin software for my research work. I am thankful to **Mr. Hemanth Kumar**, Scientist, Head TIC, ASL, for providing literature papers for my research work.

I am thankful to my seniors, **Dr. B. Mayuri** and **Dr. K. Ramaiah** for their suggestions and encouragement throughout my research work. I am thankful to **Mr. K. Venkateswara Reddy**, research scholar, Department of Metallurgy and Material Science, **Mr. T. Dhananjay Rao, Mr. G. Ambedkar, Ms. G. Shiva Paravathi, Mr. A. Ramesh, Dr. S. Rangaswamy Reddy**, research scholars, other research scholars, and administrative staff of the Department of Chemistry, NIT Warangal for their support in all administrative works at NIT Warangal and regular updates of institute academic schedules throughout my research work.

I am very much thankful to **Mr. P. Koteswara Rao,** former head of deparment of chemistry, JKC College, Guntur and **Mr. K. Prasad**, MD, Prasad Seed Pvt Ltd, Hyderabad for their encouragement throughout my research work. I am thankful to **Dr.P. Shailesh**, Methodist Engineering College, Hyderabad for his suggestions throughout my research work.

I am thankful to my wife **Mrs.Golla Sirisha,** my son **Golla Shri Ram** and my daughter **Golla Supriya Shri** for their patience and kind assistance during my research work.

Finally, I would like to thank the Almighty for His generosity and love shown to me throughout my research work.

Abstract

Carbon fiber reinforced polymer composite materials are being extensively used for thermal protection system (TPS) applications in aerospace and defence sectors. Multi-scale carbon fiber reinforced polymer composites with microscale fiber as the primary reinforcement and nanoscale filler like nanoclay as the secondary reinforcement has gained a lot of interest in a variety of applications. Present research work aims to study the effect of different weight percentages of organo modified montmorillonite nanoclay addition on mechanical, thermal, and ablation properties of carbon fiber reinforced polymer composites by choosing various prospective matrices namely phenolic resin, cyanate ester resin, and benzoxazine resin. It also aims at comparing the performance of phenolic resin, cyanate ester resin, and benzoxazine resin as a matrix for carbon fiber and nanoclay reinforced composites.

As part of experimental work, following two-phase (polymer-nanoclay) composites (type-I) were prepared by dispersion of 1, 2, 4, 6 wt% of organo modified montmorillonite (o-MMT) nanoclay in the resin system by ball milling process.

1. Phenolic Resin - Nanoclay Composite
2. Cyanate Ester Resin - Nanoclay Composite
3. Benzoxazine Resin - Nanoclay Composite

Dispersion studies of nanoclay in these resins were studied by small-angle X-ray scattering and Scanning electron microscopy. Viscosity changes, cure behaviour and thermal stability changes to these resins by the addition of nanoclay were studied. In addition to two - phase composites, following three - phase (carbon fiber-polymer-nanoclay) composites (type –II) were fabricated by adding 1, 2, 4, 6 wt% nanoclay dispersed resin to carbon fiber.

1. Carbon fiber - Phenolic Resin - Nanoclay Composite
2. Carbon fiber - Cyanate Ester Resin - Nanoclay Composite
3. Carbon fiber – Benzoxazine Resin - Nanoclay Composite

These three-phase composites were evaluated for thermal stability, mechanical properties, thermal properties, and mass ablation rate. Results from the studies of polymer - nanoclay composites (type- I) were used to understand the mechanical, thermal, and ablation behaviour of nanoclay added carbon fiber reinforced polymer composites (type–II). The process and performance mechanisms involved in each type of composite are summarised below.

Ball milling was used for dispersion of different weight percentages (0, 1, 2, 4, 6 wt%) of organo-modified montmorillonite nanoclay into the phenolic resin. Viscosity changes to resin

due to nanoclay addition were studied. On the other hand, nanoclay added phenolic matrix composites (type-I) were prepared to study the dispersion of nanoclay in the phenolic matrix by small angle X-ray scattering (SAXS), scanning electron microscopy (SEM) and thermal stability changes to the matrix by thermogravimetric analysis(TGA). This data was used to understand the mechanical, thermal, and ablation properties of nanoclay added carbon fiber- phenolic resin (C-Ph) composites (type-II) with the same weight percentages of nanoclay as that of type-I composites. Interlaminar shear strength (ILSS), flexural strength, and flexural modulus of type-II composites increased by about 29%, 12%, and 7% respectively at 2 wt% addition of nanoclay, beyond which these properties decreased. This was attributed to reduced fiber volume fraction ($\%V_f$) of type -II composites due to nanoclay addition at such high loadings. Mass ablation rate of type -II composites was evaluated using oxy- acetylene torch test at a low heat flux 125 W/cm^2 and high heat flux 500 W/cm^2. Mass ablation rates have increased at both flux levels marginally up to 2 wt% addition of nanoclay, beyond which, it has increased significantly. Increased ablation rates due to nanoclay addition were attributed to higher insulation efficiency of nanolcay, which accumulates more heat energy in the limited area behind the ablation front and also due to self-propagating ablation mechanisms triggered by thermal decomposition of organic part of nanoclay. Based on the above results, 2 wt% organo modified montmorillonite nanoclay as filler is optimum in C-Ph composites for improved thermal stability, mechanical and thermal properties without much compromising on ablative performance.

Nanoclay added cyanate ester resin (type-I) composites were prepared by dispersion of different weight percentages (0, 1, 2, 4, 6 wt%) of organo-modified montmorillonite nanoclay in resin by ball milling process and cured in oven. Cyanate ester – nanoclay composites were tested for dispersion by SAXS and SEM, thermal stability using TGA and curing behavior using DSC. This data was correlated with the thermomechanical properties of nanoclay added carbon fiber reinforced cyanate ester resin composites (type-II). ILSS and flexural strength of type-II composites increased by about 17%, 21% respectively at 2 wt% addition of nanoclay although at this loading nanoclay was found to show intercalation. Mass ablation rate of type-II composites was tested at heat fluxes 125 W/cm^2 and 500 W/cm^2.Thermal stability of type -II composites got reduced, whereas the ablation rate has increased for type -II composites with increased loading of nanoclay. However, the percentage increase in mass ablation rate was found to be lower when type-II composites were tested at 500 W/cm^2 compared to the ablation testing carried out at 125 W/cm^2. Scanning electron microscopy studies indicates significant melting of nanoclay at high

heat flux resulting in additional protection mechanisms for the composites at high flux. Based on the above results, 2 wt% organo modified montmorillonite nanoclay addition can be considered as optimum for better mechanical properties for the carbon fiber reinforced cyanate ester resin composites with minimum compromise in the thermal stability and ablation performance.

Organo modified montmorillonite nanoclay added benzoxazine resin composites (type–I) were prepared by different weight percentages (0, 1, 2, 4, 6 wt%) nanoclay in benzoxazine resin by ball milling process. Benzoxazine resin–nanoclay composites were evaluated for changes in the curing behavior using DSC and thermal stability using TGA. Dispersion of nanoclay was evaluated by SAXS and SEM. Results from these studies of type –I composites were used to understand the mechanical, thermal, and ablation behavior of nanoclay added carbon fiber reinforced benzoxazine resin composites (type–II composites). For type-II composites, ILSS, flexural strength increased by about 25%, 27% respectively at 2 wt% addition of nanoclay. Mass ablation rates have increased with the increased weight percentage of nanoclay at both heat fluxes 125 W/cm^2 and 500 W/cm^2. SEM was used to study the microstructure of the ablated composites. Increased ablation rates due to nanoclay addition are attributed to the reaction of the charred matrix with nanoclay which exposes the bare fibers to the ablation front leading to higher mechanical erosion losses. Based on the above results, 2 wt% organo modified montmorillonite nanoclay as filler is optimum for improving the performance of carbon fiber reinforced benzoxazine resin composites without much compromise in the ablation performance.

Activation energy and pre-exponential factor of phenolic resin, cyanate ester resin, and benzoxazine resin have been determined fromTGA data using Flynn-Wall-Ozawa (FWO) kinetic model as per ASMT E1641. It was observed that activation energy for 10% of decomposition for cyanate ester resin is higher than that of phenolic resin and benzoxazine resin.

Comparative performance of matrices reinforced with carbon fiber and nanoclay was studied. Cyanate ester resin composites with carbon fiber and nanoclay have higher thermal stability, ILSS, and flexural strength than phenolic resin composites and benzoxazine resin composites. The mass ablation rates are lower for cyanate ester resin composites with carbon fiber and nanoclay than phenolic resin composites and benzoxazine resin composites.

Based on thermal stability, mechanical properties, thermal properties, and mass ablation rate, it is inferred that carbon fiber reinforced cyanate ester resin composite (C-CE) and 2 wt% organo modified montmorillonite nanoclay added C-CE composite are the superior ablative composites when compared to conventional carbon fiber reinforced phenolic resin composites.

Nomenclature

Abbreviation / Symbol	Description
PMC	Polymer matrix composites
CFRC	Carbon fiber reinforced polymer composites
TPS	Thermal protection system
PAN based carbon fiber	Polyacrylonitrile based carbon fiber
Ph	Phenolic resin
CE	Cyanate ester resin
BZ	Benzoxazine resin
NC	Nanoclay
o-MMT nanoclay	Organo modified montmorillonite nanoclay / Organo montmorillonite nanoclay
C-Ph	Carbon fiber reinforced phenolic resin composite
C-CE	Carbon fiber reinforced cyanate ester resin composite
C-BZ	Carbon fiber reinforced benzoxazine resin composite
ASTM	American society for testing and materials
SAXS	Small angle x-ray scattering
cP	Centipoise
DSC	Differential scanning calorimeter
TGA	Thermogravimetric analysis
DTGA	Derivative thermogravimetric analysis
FT-IR	Fourier transform infrared spectroscopy
SEM	Scanning electron microscope

XRD	X - ray diffractometer
UTM	Universal testing machine
ILSS	Interlaminar shear strength
FS	Flexual strength
FM	Flexural modulus
MPa	Mega Pascal
GPa	Giga Pascal
nm	nanometer
g/cc	grams per cubic centimeter
mm	millimetre
OI	oxidation index
V_f	Fiber volume fraction

CONTENTS

Chapter-IV: Organo Montmorillonite Nanoclay Added Carbon Fiber - Cyanate Ester Resin Composites

List of Figures

List of Tables

Chapter - I

Introduction, Literature Review, Need and Objectives of the Present Study

Introduction, Literature Review, Need and Objectives of the Present Study

1.0 Introduction to Composite Materials

Composite materials can be defined as the combination of two or more materials (e.g. reinforcing elements, fillers, and matrix binders) differing in form or composition on a macro-scale, but acting in concert in combined form, retaining their individual identities across the interfaces between one another. The main advantages of composite materials are their high specific strength and stiffness, as well as their low density and corrosion resistance. Reinforcement and matrix are the two most important components in composite materials. The reinforcement has high strength and stiffness than the matrix phase. The reinforcement phase is the discontinuous phase, which is embedded in the continuous matrix phase. The reinforcement phase is a load-carrying member in the composite. The matrix binds with the reinforcement phase together. Matrix transfer load between reinforcements during loading, the matrix also protects the reinforcement from environmental conditions namely temperature and humidity [1-2].

The properties of composites are a function of

- The properties of the reinforcement and matrix
- Relative amounts of reinforcement and matrix
- The orientation of the reinforcement phase
- Interface bond strength between reinforcement and matrix

1.1 Classification of Composite Materials

The matrix phase and reinforcement phase of composite materials can be used to classify composite materials.

1.1.1 Classification of Composites Based on Matrix Phase

Composites are categorized into three types based on the matrix phase, thus

- Polymer matrix composites (PMC)
- Metal matrix composites (MMC)
- Ceramic matrix composites (CMC)

Among the above three types, polymer matrix composites are more common because of their low cost, simplicity of processing, chemical resistance, and low specific gravity. From the fabrication point of view, process methods of PMC's are simple and the process can be carried out at low temperatures. Thermoset polymers like phenolic resin, epoxy resin, polyester, vinyl ester, polyimide, and cyanate ester resin and thermoplastic polymers like polypropylene,

polycarbonate, polyamide, polysulphone, and polyether ether ketone (PEEK) were used in composites. In comparison to thermoplastic resins, thermoset resins are more prevalent in aerospace applications due to their ease of processing and excellent temperature stability.

1.1.2 Classification of Composites Based on Reinforcement Phase

Composites are classified into the following types based on their reinforcing phase

- Particle reinforced polymer composites
- Fiber reinforced polymer composites

1.1.2.1 Particle Reinforced Polymer Composites

A composite having particle reinforcement phase is called particle reinforced polymer composite. Particle is nonfibrous and has no long dimension, except platelets of nanoclay. The dimensions of the reinforcement determine its capability of contributing its properties to the composites. The particles in particulate composite place constraints on the plastic deformation of the matrix material between them because of their inherent hardness relative to the matrix. The particles are effective in enhancing the stiffness of the composites but do not offer the potential for much strengthening as they don't act as load-bearing members.

1.1.2.2. Fiber Reinforced Polymer Composites

A composite having fiber as reinforcement phase is called fiber reinforced polymer composite. A fiber is defined by its length is much greater than its cross-sectional dimensions. Fiber reinforced polymer composites are a combination of fibers of high strength and modulus embedded into a matrix with distinct interfaces (boundaries) between them. Different types of fibers used for the fabrication of composites include glass fiber, carbon fiber, boron fiber, kevlar fiber, and natural fibers.

Glass fibers are low-cost and high strength fiber, hence generally used as reinforcement in polymeric matrix composites for low-cost industrial applications.

Carbon fibers are the most common of all reinforcing fibers for polymeric matrix composites (PMC) especially for aerospace applications. The main features of carbon fibers are low density, high tensile strength, and high tensile modulus. Carbon fiber reinforced polymer composites (CFRC) are used in aerospace for load-bearing (structural) applications and ablative applications.

Kevlar fiber is light weight and high impact resistant fiber, hence generally used in impact resistance applications.

Fiber reinforced polymer composites are subdivided into two types as discussed below.

Discontinuous Fiber Reinforced Polymer Composites

Composites with short fibers are called discontinuous fiber reinforced polymer composites. Short fibers are generally prepared by chopping the continuous fibers. Short fibers can be aligned or randomly dispersed in the discontinuous form in the composite.

Continuous Fiber Reinforced Polymer Composites

Continuous fiber reinforced polymer composites are made with long (continuous) fibers. Continuous fibers are generally available in one direction orientation form of fiber (roving/tow) and two-directional orientation form of fiber (fabric/cloth). Roving forms of fibers are used in the fabrication of composite products by filament winding process and pultrusion process.

The following categories are used to categorize continuous fiber reinforced polymer composites.

- Unidirectional fiber reinforced polymer composites (UD composites)
- Bidirectional fiber reinforced polymer composites (2D composites)

The highest strength and modulus are produced in the fiber direction by the unidirectional orientation of continuous fibers in composites, but substantially lower strength and modulus are produced in the transverse to the fiber direction. The one-dimensional design can be used to create a multi-layered composite with unidirectional continuous fibers in each layer, but the angle of orientation from layer to layer can be altered. The disparity in strength and modulus values in different orientations can be decreased by properly orienting fibers in various layers.

With continuous fibers, the two-dimensional orientation can be made bidirectional or multidirectional. In bidirectional orientations, fiber yarns (or strands) are woven or interlaced together in two mutually perpendicular directions. These two directions are called the warp and fill directions and represent 0° and 90° orientations, respectively. The fiber yarns are crimped or undulated as they move up and down to form the interlaced structure. If the number of fiber yarns in both the warp and fill directions is the same, the characteristics in both directions are the same, and the fabric is balanced [4].

The hand layup process, autoclave molding method, compression molding method, filament winding and resin transfer molding process were employed in the manufacturing of composite products.

Carbon fiber reinforced polymer composites (CFRPC) with two-dimensional (laminated structures) are used in most thermo-structural applications where high specific strength and specific modulus are required.

Generally, CFRPC contains two -phases namely carbon fiber (reinforcement phase) and polymer (matrix phase). The advent of nanomaterials namely nanosilica, carbon nanotube, carbon nanofiber, carbon black, nanoclay, polyhedral oligomer silsesquioxane (POSS) offered scope for realizing multiscale composites. Nanofillers are added to CFRCs for enhancing their thermomechanical performance [5-12] and these composites are called nanocomposites.

1.2 Nanocomposites

Nanocomposites are the composites containing nano-sized particles, which have at least one dimension in the nanometer scale.(a nanometer is 10^{-9} m or a billionth of a meter). At low-reinforcement volume fractions, nanocomposites demonstrate superior mechanical, thermal, electrical, optical, and other capabilities. The main reasons for their superior qualities are that (a) nano-reinforcements have significantly better properties than micron-sized reinforcing fibers, and (b) their surface area to volume ratio is extremely high, resulting in a high surface area to volume ratio [13].

Nanoclay is the most adaptable nanofiller among all nanoparticles due to its inexpensive cost and ease of dispersion in resin systems. Many researchers have reported significant improvements in stiffness and strength, thermal stability and flame retardancey of pure polymeric matrices with the addition of a small amount (1 to 5 wt%) of nanoclay particles [14-21]. Thus, nanoclay has become a preferred nanofiller to improve the performance of CFRPCs for thermo structural composite products.

1.3 Literature Review

This section provide a comprehensive analysis of the current state of the art in nanoclays, polymers, carbon fiber, nanoclay added polymer composites, and nanoclay added carbon fiber reinforced polymer composites.

1.3.1 Nanoclay: Nanoclays are nanoparticles containing layered mineral silicates [22]. In the natural form, the layered smectite clay particles are 6-10 mm thick and contain >3000 planar layers. Smectite clay can be exfoliated or delaminated and dispersed as individual layers, each ~1 nm thick. In the exfoliated form, the surface area of each nanoclay particle is ~750 m^2/g and the aspect ratio are >50. The crystal structure of each layer of smectite clays contains two outer tetrahedral sheets, filled mainly with Si, and a central octahedral sheet of aluminum or magnesium. The structure of 2:1 nanoclay is shown in **Figure 1.1.**

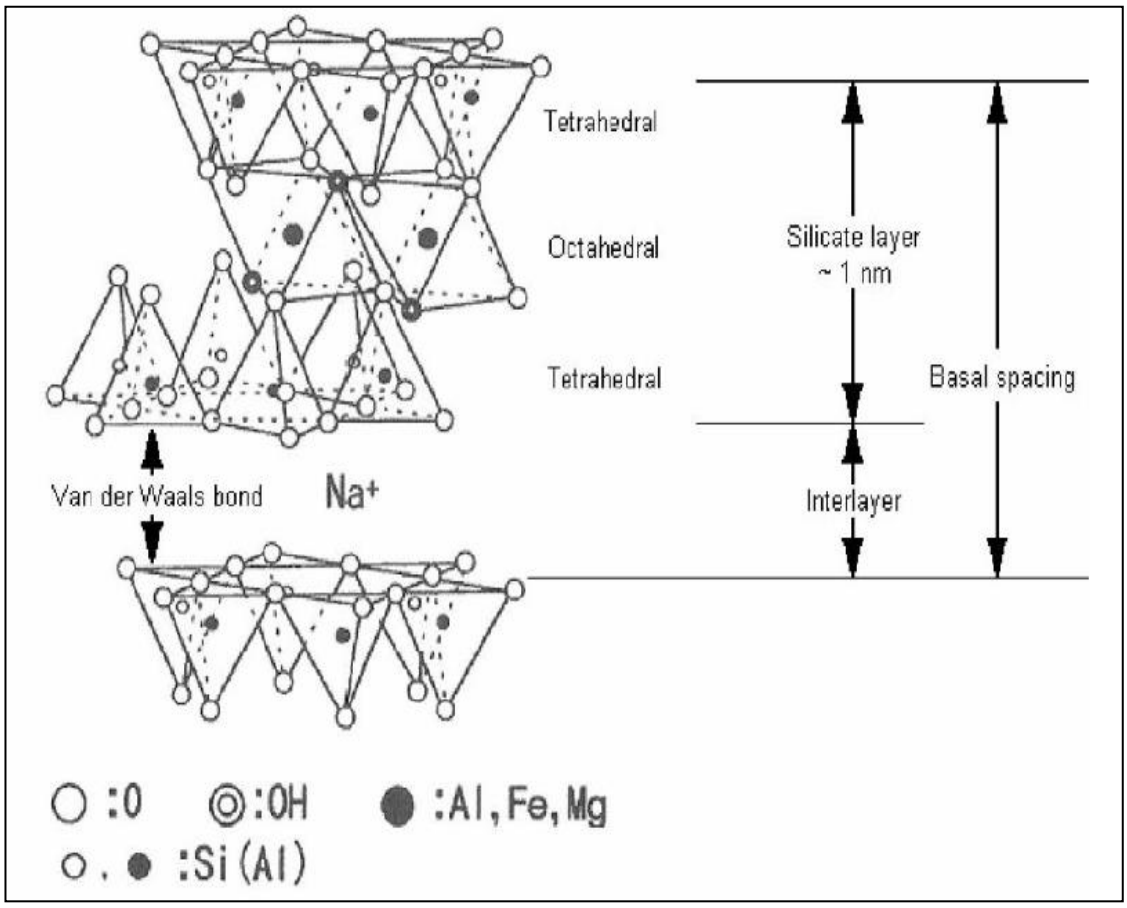

Figure 1.1 Structure of 2:1 clay mineral [22]

Each layer is reported to have a thickness of 1 nm, but their lateral dimensions might range from 200 to 2000 nm. The layers are separated by a very small gap, called the interlayer or the gallery. The negative charge, generated by isomorphic substitution of Al^{3+} with Mg^{2+} or Mg^{2+}

with Li^+ within the layers, is counterbalanced by the presence of hydrated alkaline cations, such as Na or Ca, in the interlayer. Because the forces that keep the layers together are relatively weak, tiny organic molecules can be intercalated between them.

Montmorillonite nanoclay is a popular smectite clay used in nanocomposite applications, with the chemical formula $Mx(Al_4\ xMgx)Si_8O_{20}(OH)_4$, where M indicates a monovalent cation, such as sodium, and x represents the degree of isomorphic substitution (between 0.5 and 1.3).

1.3.1.1 Structure of Surface Modified Nanoclay: Montmorillonite is hydrophilic, which makes its exfoliation in conventional polymers difficult. As the forces that hold the stacks together are relatively weak, the intercalation of small molecules between the layers is easy. To render these hydrophilic phyllosilicates into more organophilic, the hydrated cations of the interlayer can be exchanged with cationic surfactants such as alkylammonium or alkyl phosphonium (onium) (**Figure 1.2**). The modified clay (or organoclay) being organophilic, has lower surface energy and is more compatible with organic polymers. Under well-defined experimental conditions, these polymers may be able to intercalate within the galleries. The organic modification raises the d-spacing to some extent (usually over 2 nm), allowing polymer diffusion into the interlayer gap [23].

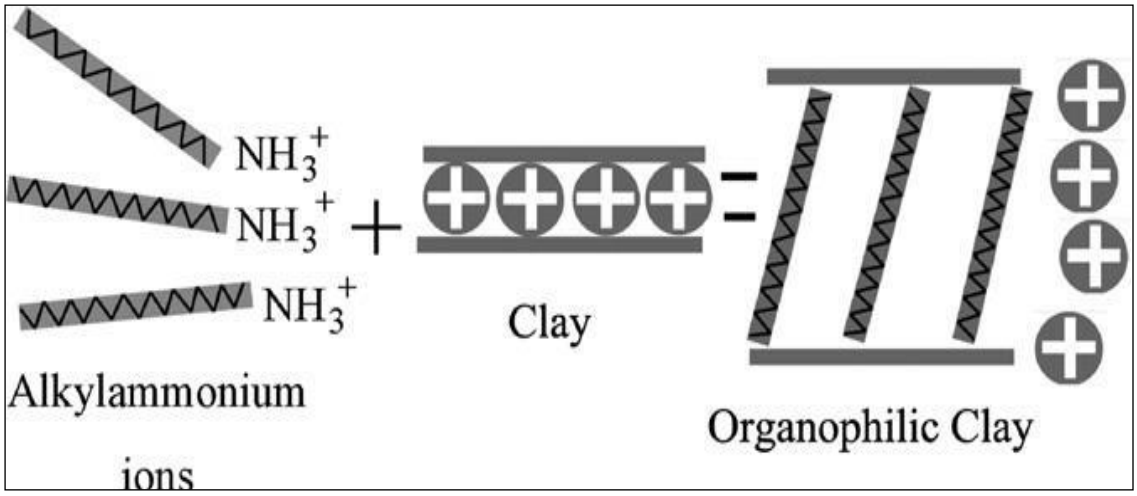

Figure 1.2: Organic modification of clay [23]

Several pristine and organo-modified clays are now commercially available. Cloisite 10A, 15A, 20A, and 30B are commercial organoclays made by Southern Clay Products (USA) [24]. Bentone 107, 108, 109 and 2010 from Elementis Specialties Company [25]. Nanomer 1.30P, 1.31PS, 1.44P, 1.44PS, 1.44PT and 1.28E from Nanocor, Inc. (U.S.A.) [26]. Nanofil 2, 5, 9, SE 3000 and SE 3010 from Sud-Chemie (Germany) [27] as well as Dellite 72T from Laviosa

Chimica Mineraria (Italy). The majority of these commercially available organoclays have been modified with ammonium cations, with only a few having been modified with silane.

1.3.1.2 Types of Polymers Used for Polymer - Nanoclay Composites

Although the chemistry of polymer intercalation, when coupled with correctly modified layered silicates, has been known for a long time [28] Polymer/clay nanocomposites are a new field that has lately gained traction. Two notable discoveries have sparked renewed interest in these materials, are the report from the Toyota research group of a nylon-6 (PA-6)/montmorillonite nanocomposite [29], which, revealed significant increases in thermal and mechanical properties, and the observation by Vaia et al. that it is possible to prepare nanocomposite by melt mixing the polymers with layered silicates [30]. Several polymer systems employed in the manufacture of nanocomposites with layered silicates can be readily classified as vinyl polymers, condensation polymers, addition polymers, polyolefins, specialty polymers, bio-degradable polymers [31].

1.3.1.3 Dispersion of Nanoclay in Polymer Systems

Uniformly dispersed silicate clay layers in a polymer matrix can improved properties, such as barrier, flame-retardance, thermal stability and mechanical properties of polymer. As a result, such polymer/clay nanocomposites have received a lot of interest in recent decades. Nanocaly has been used as a filler in both thermoplastic and thermosetting polymer composites [32].

Good dispersion of nanoclay particles in the polymer matrix is a vital component in achieving improvements in composite properties. Mechanical mixing, magnetic stirring, and sonication are the most prevalent ways of dispersing nanoclay particles in polymers. Many researchers have observed that poorly dispersed nanoparticles can decrease polymer mechanical characteristics [33-36]. Conventional nanoclay reinforced composites can be phase-separated micro composite, intercalated nanocomposites, or exfoliated nanocomposites, depending on the mixing procedure used [37]. Exfoliated nanocomposites are said to have the best interfacial contact and phase uniformity, while phase-separated micro composites offer little gain in material properties [38, 39]. As a result, the degree of exfoliation is a critical criterion for assessing the physical properties of polymer-based nanocomposites [40]. Many of these mixing approaches to disperse nanoparticles in polymers have been thoroughly investigated by numerous researchers to attain full exfoliation. The oldest method for successfully realizing nylon-montmorillonite is in-situ intercalative polymerization in

thermoplastic-based nanocomposites [41]. Melt intercalation is another method. Other approaches that use traditional shear machines like sonicators, extruders, three-roll milling, or ball milling are widely reported [37, 42, 43]. Full exfoliation of nanoclay is a challenge, due to large lateral dimensions of the layers and the high inherent viscosity of the resin that prevents effective mixing. Shear processing with an ultrasonicator or an extruder can be used to exfoliate clay particles for polymer melt intercalation. Three-roll mill was used also widely used to achieve high degree of exfoliation and dispersion of the silicate clay layers in the epoxy matrix. External shearing forces are applied to clay tactoids in this procedure [44].

Several researchers have looked into the structural changes caused by high-energy ball milling on various clay minerals. Frost et al. studied mechanically ground kaolinite up to 10 h in a planetary ball mill. Ball milling attenuated the (001) reflection until it practically vanished, showing kaolinite particle delamination, according to XRD diffraction patterns. The breakdown of hydrogen bonds between adjacent kaolinite layers was attributed to this result. [45]. Lee et al. used stirred ball milling, with water and kerosene as solvents to intercalate various alkylammonium ions. The intercalated alkyl ammonium ions proved beneficial in increasing the basal gap [46].

1.3.1.4 Methods of Preparation of Polymer - Nanoclay Composites

The most prevalent method for making polymer-nanoclay composites are listed below [13].

a) **Solution Method**: In this method, the layered silicates are exfoliated into single layers using a solvent that can be dissolve the polymer. The polymer gets absorbed into the exfoliated sheets. Exfoliated sheets with polymer molecules sandwiched between them will form a multi-layered structure while the solvent evaporates. The solution technique has been frequently used with water-soluble polymers like polyvinyl alcohol (PVA) and polyethylene oxide (PEO).

b) **In-Situ Polymerization Method**: The layered silicate is swollen within the liquid monomer in this technique, which is then polymerized by heat or radiation. As a result, the polymer molecules are produced in situ between the intercalated sheets in this process. The in-situ approach is popular with thermoset polymers like phenolic and epoxy resins.

c) **Melt Processing Method**: The liquid state of polymer is used to combine the silicate particles with the polymer. The polymer molecules can enter the interlayer space of the clay

particles and create either an intercalated or an exfoliated structure, depending on the processing condition and the compatibility between the polymer and the clay surface.

The improvement in modulus that can be achieved with only 1-5 wt% of nanoclay has been the most appealing feature of adding nanoclay to polymers. There are numerous other benefits, including reduced gas permeability, increased thermal stability, and fireretardancy [22, 47]. Exfoliation is the key for attaining better properties. Improved polymer characteristics need uniform nanoclay dispersion and interaction between nanoclay and the polymer matrix.

Ball milling can also used to exfoliate clay mineral particles. Ball milling may be particularly useful for the fabrication of polymer-nanoclay composites based on thermosets that cannot be processed using traditional melt processing methods [48].

1.3.1.4 Structure of Polymer - Nanoclay Composites

The polymer - clay nanocomposites can be divided into three categories depending upon the resulting morphology obtained [13].

Phase-Separated Microcomposites: Phase-separated microstructure results when the Polymer is unable to intercalate between the silicate sheets (**Figure 1.3 (a)**) and properties of such type of nanocomposite stay in the same range as the traditional micro composites [23].

Intercalated Nanocomposites: Intercalated structure is obtained when a single (and sometimes more than one) polymer chain is intercalated between the silicate layers resulting in a well-order multi-layer morphology built up with alternating polymeric and inorganic layers (**Figure 1.3 (b)**). The d spacing in the case of intercalated nanocomposites is in the range, 20–50 Å [23].

Exfoliated Nanocomposites: The exfoliated structure is obtained when the silicate layers are completely delaminated and uniformly dispersed in a continuous polymer matrix (**Figure 1.3 (c))** [23].

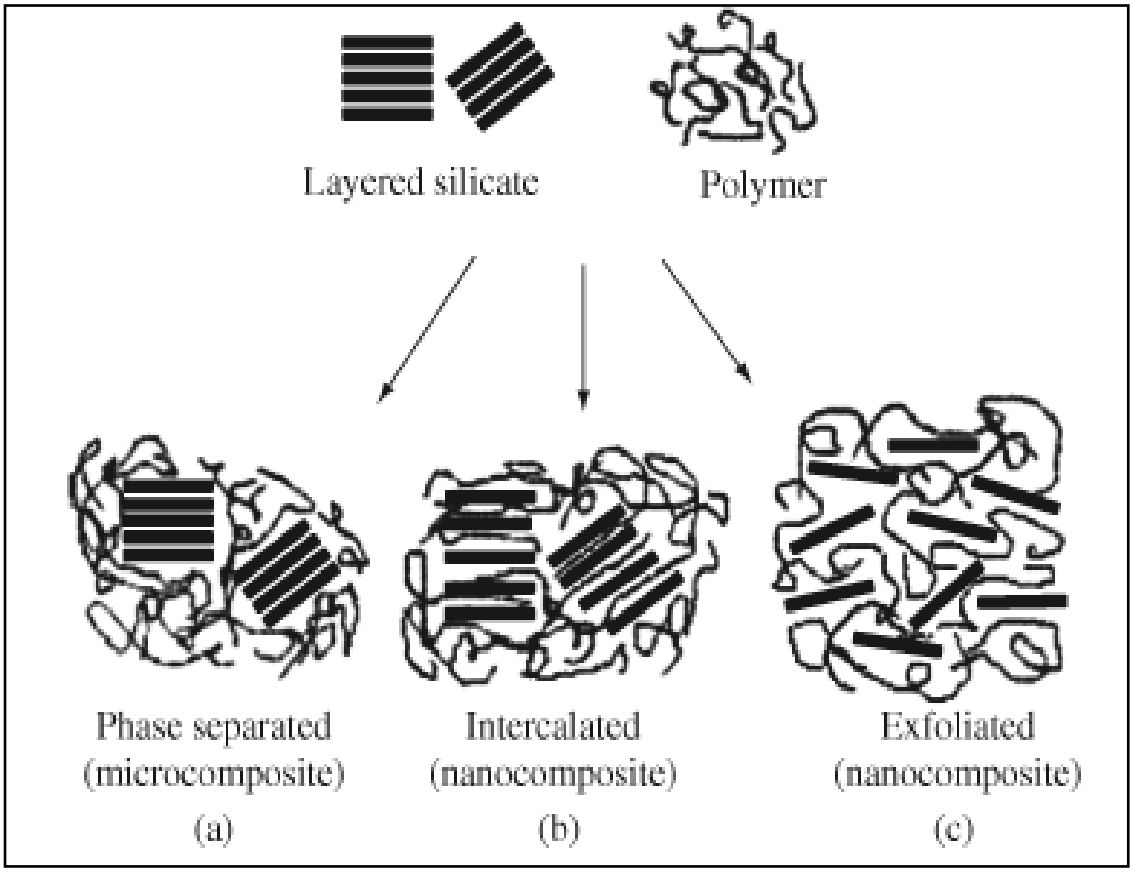

Figure 1.3: Different morphologies in Polymer-Nanoclay Composites: (a) phase-separated micro composite, (b) intercalated nanocomposite, and (c) exfoliated nanocomposite [23].

1.3.1.5 Characterisation of Polymer - Nanoclay Composite Morphology

Wide-angle x-ray diffraction (WAXD), transmission electron microscopy (TEM), and scanning electron microscopy (SEM) can be used to analyse the level and homogeneity of nanoclay platelets dispersion within the continuous polymer phase [49].

The WAXD method is widely used to characterize the structure of nanocomposites. Due to the growth of the basal spacing in an intercalated structure, the (0 0 1) characteristic peak for the organoclay tends to move to the lower angle regime. Despite the increasing layer gap, there is still an attractive force between the silicate layers that causes them to stack in an orderly form. Due to the loss of structural integrity of the layers, no peaks can be seen in the WAXD pattern for exfoliated polymer-nano clay composites [50]. The absence of Bragg diffraction peaks in the nanocomposites could imply that the clay has been exfoliated or delaminated completely [51]. However, as WAXD's data is averaged throughout the entire specimen, it does not provide information about the spatial distribution of silicate platelets in the polymer matrix.

To validate exfoliation process, transmission electron microscopic (TEM) studies are required. The shape, structure, and spatial distribution of the dispersed phase of nanocomposites can be studied by TEM in a localised area [52]. Vaia *et al.* showed that the characteristics of local microstructures obtained by TEM provide useful information that complements that acquired through WAXD [53]. Other intermediate states, such as partial intercalation and exfoliation, can exist in addition to these two well-defined structures. TEM provides a qualitative insight into the internal structure, spatial distribution of distinct phases, and defect structure for such intermediate structures through direct sight.

The small angle X-ray scattering (SAXS) technique has been widely utilised to investigate phase dispersion in matrices, polymerization, emulsification, colloidal stability, shear-induced structures, polymer crystallisation, and phase domain behaviour in polymers throughout the previous decade. One of the most significant advantages of SAXS in the case of nanostructured materials, such as clay-containing polymer nanocomposites, is that it probes materials with subnanometer resolutions (1-100 nm). SAXS, on the other hand, employs a high sample size, which covers a huge number of nanoparticles. The structure of the nanocomposites has been determined using SAXS, either from the peak shift towards a lower scattering angle side. SAXS provides information on the dispersion of partially ordered structures such as intercalated and exfoliated clays [38].

The SAXS data demonstrates clay platelet segregation, whereas the SEM shows clay distribution in the matrix on a macroscopic scale. The morphology of the experimental composites containing montmorillonite nanoclay may be observed using a scanning electron microscope (SEM). Due to the creation of three-dimensional pictures, it is a type of analysis often employed for analysing surface features in materials [54].

1.3.2 Polymer Matrices for Composites: Polymers are macromolecules made up of a huge number of smaller molecules linked together. The small molecules are called monomers. Monomers are tiny molecules that form polymer molecules by combining, and the reactions by which monomers combine are termed polymerization. A polymer molecule might include hundreds, thousands, tens of thousands, or even millions of monomer units bonded together. Examples of polymers are polyethylene, polypropylene, polyvinyl chloride, polyester resin, and phenolic resin.

Polymers are clasified into condensation and addition polymers based on polymer structure. Polymerizations are divided into step and chain polymerizations based on their polymerization mechanism. The terms condensation and step are often used synonymously, as are the addition

and chain of the term. Examples of condensation polymers are polyamides and phenolic resin and addition polymers are polyethylene and polypropylene [55].

Based on the behaviour of polymers with temperature, polymers are classified nto thermoplastic polymers and thermoset polymers. Examples of thermoplastic polymers are polyethylene, nylon, poly ether ether ketone, polysulphone. Examples of thermoset polymers are phenolic resin, polyester resin, epoxy resin, cyanate ester resin, benzoxazine resin, and silicone resins.

Low molecular weight and low viscosity monomers of thermoset polymers are available (150-20,000 centipoise). Low viscosity monomers are converted into three-dimensional crosslinked polymer structures during curing. Crosslinking is an irreversible change that occurs through a chemical reaction, such as condensation reaction, ring closure and addition reaction. As the curing process advances, the processes speed up and the accessible volume within the molecular arrangement shrinks, resulting in decreased molecule mobility and increased viscosity is not possible to remit the resin after it has gelled and formed a rubbery solid. Additional crosslinking occurs as the resin is heated further until it is entirely cured. Thermosets are known for their extended processing periods since the cure is a thermally driven procedure that necessitates chemical reactions.

Thermoplastic polymers, on the other hand, do not require extensive cure cycles since they are not chemically crosslinked with heat. They are polymers with a high molecular weight that can be melted, solidified, and cooled. Because thermoplastics do not crosslink, they can be reheated for later shaping or joining processes. However, high temperatures and pressures are usually necessary for processing due to their inherent high viscosity and melting points.

Due to processing advantages, thermoset polymers are the most commonly used resin systems in fiber reinforced polymer composites. Polymer composites are frequently employed in high-temperature thermal protection systems (TPS). Ablative materials and ablators are terms used to describe certain types of composites. Spacecraft heat shields for atmospheric re-entry and rocket nozzle liners for solid propellant rocket motors are made of ablative materials. Phenolic resin, silicone resin, and polyimide resins are among the thermoset polymers utilised as the matrix in composite materials for high-temperature applications in the aerospace and defence sectors [13].

Phenolic resins are high temperature resins that offer outstanding smoke and fire resistance with low toxicity. Phenolic resins have inherently high char yield after pyrolysis. Due to this, phenolic resins as an ablative matrix in composite materials are more popular. Ablation is a phenomenon in which a material is decomposed and eroded by high temperatures, resulting in

endothermic material loss. This process protects the underlying structure. Phenolic resin composites are extensively used in nozzles, heat shields of missiles, spacecraft vehicles, and as aircraft interior components. Phenolic resin-based ablative composites are more popular in aerospace applications due to their low thermal conductivity and low erosion rate. Resol type of phenolic resin used in ablative composites.

The preparation and curing reaction of resol type phenolic resin [56] is given below.

Resol type of phenolic resins are synthesised by alkaline reaction of phenol and formaldehyde, whereby the formaldehyde is used in excess. The two stages that follow explain a simplified version of the reaction. To make methyl phenol, phenol interacts with methylene glycol

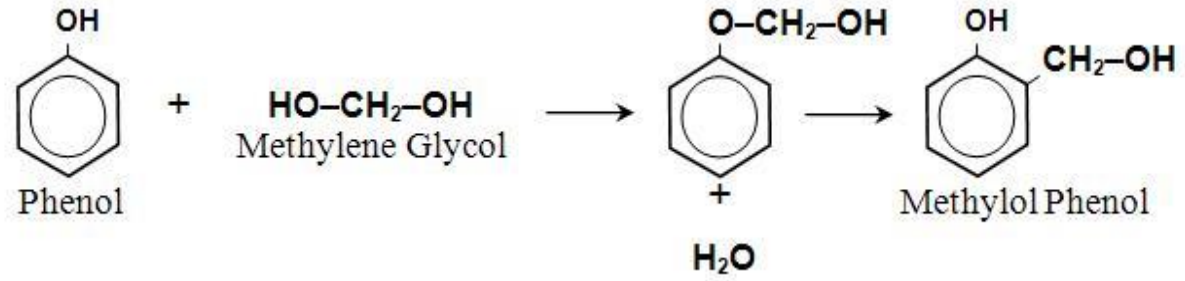

Methylol phenol can react with itself to generate a methylol phenolic with a longer chain.:

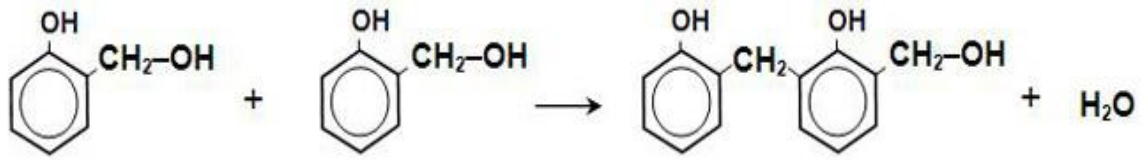

or form dibenzyl ether:

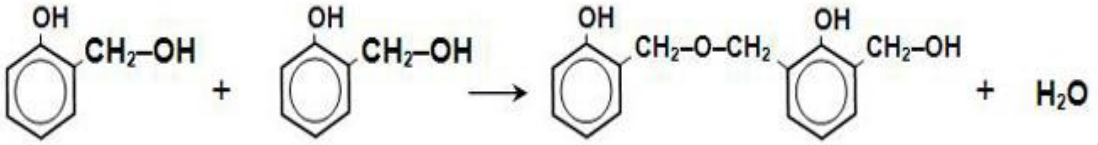

or react with phenol to form a methylene bridge.

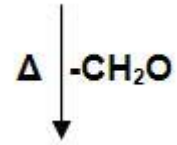

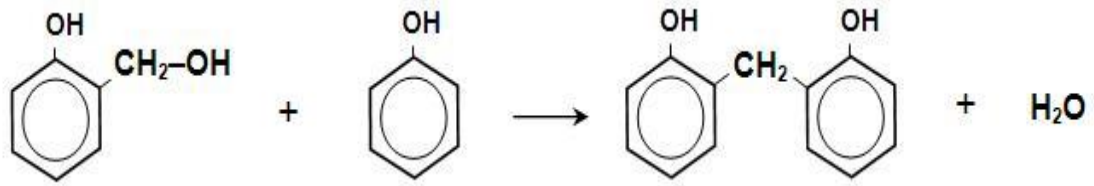

When an excess of formaldehyde is utilised, a sufficient number of methylol and dibenzyl ether groups remain reactive to complete the polymerization and cure the resin without the need for a curing agent. As a result, resol resins are frequently referred to as "single-stage" or "one-step" products in the industry. Polymerising to the necessary extent, distilling superfluous water, and quenching or tempering the polymerization reaction by quick cooling are the steps involved in the production of Resol resin. Resol resins have a limited shelf life that varies based on the resin, storage conditions, and application because they continue to polymerize at even ambient temperature.

However, phenolic resin suffers from low shelf life and out life due to the ease of crosslinking of methylol groups present in the aromatic structure leading to variation in properties of the resultant components as a function of storage life. Moreover, phenolic resin gives volatile by-products during curing leading to a large volumetric shrinkage upon cure with the formation of voids and the brittleness of the cured materials. If pressure is not applied at the gel point of resin, the end product will have porosity. Furthermore, the release of phenol and formaldehyde into the air during the curing process causes health hazards.

Cyanate ester and benzoxazine resins are two new types of resins that can compete with phenolic resin for TPS/ablative applications. These newer resins undergo additional polymerisation during curing, hence release no by-products and show low volumetric shrinkage. These resins offer other advantages in terms of lower moisture absorption, low cure shrinkage besides showing attractive thermal properties [56, 5].

The mechanism of cyanate ester resin [56] synthesis and curing reaction is shown in **Figure 1.4.**

Cyanate ester resins are a family of aromatic prepolymer which contain highly reactive cyanate (-OCN) functional groups. Cyanate ester resins are synthesized by the reaction of phenolic resin with cyanogen bromide. When three cyanate ester monomers with the –OCN functional group undergo a thermally induced cyclotrimerization (addition) reaction to generate six-member oxygen connected triazine ring, polycyanurates are generated (cyanurate). The high mass loss temperature (450 °C) of these thermosets is due to the cyanurate, which is a thermally stable cross-link. The glass transition temperature of polycyanurates generated from phenol novolac cyanate esters is around that of their thermal decomposition temperature. Polycyanurates, in addition to having great thermal stability, produce a carbonaceous char when burned, which shields the underlying material and improves fire resistance. Because

cyanate ester resins polymerize through an addition reaction, no volatiles or by-products are formed during cure. **Figure 1.4** depicts the chemical structure of cyanate ester resin.

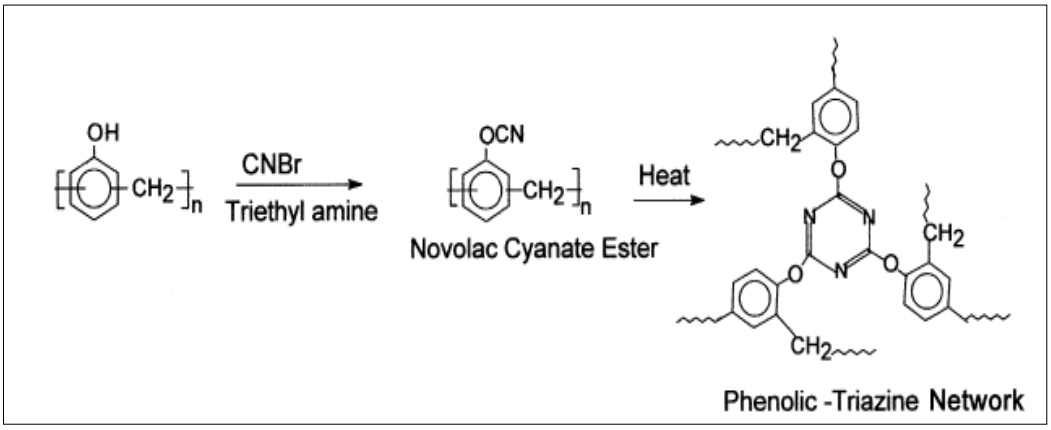

Figure 1.4. The chemical structure of cyanate ester resin

The preparation and curing reaction of benzoxazine resin is given below.

Benzoxazines are a new class of addition polymerizable phenolic resins with excellent thermal stability, high glass transition temperature (Tg), low flammability (high char yield), high modulus, low water uptake, and virtually no shrinkage upon curing, making them promising matrix materials for composites in aerospace applications.

Benzoxazine monomers as the polybenzoxazine precursors can be easily prepared from phenols, formaldehyde, and primary amines [56]. The benzoxazine monomer can be synthesized from bisphenol- A (or bisphenol- F) formaldehyde and aniline by mannich condensation reaction. Polybenzoxazine is an addition polymerized phenolic system and does not release by-products during polymerisation. Furthermore, polybenzoxazines have properties such as excellent heat resistance, electrical insulation, flame retardance, mechanical strength, and extensive molecular design flexibility for controlling the qualities of the cured material for a wide range of applications. Because there is no by-product evolution, polybenzoxazines attain required characteristics, void less state of product with long shelf life. **Figure 1.5** depicts the chemical structure of bisphenol A-based benzoxazine (BZ).

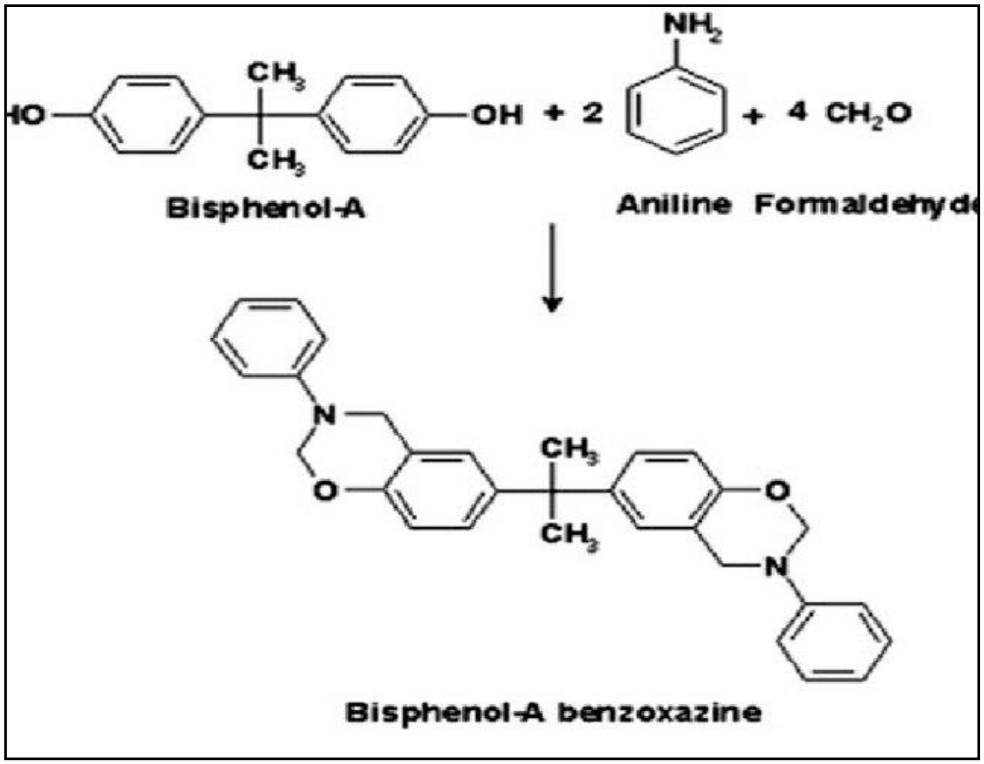

Figure 1.5. Chemical structure of benzoxazine resin (BZ)

The benzoxazine ring is known to be stable at low temperatures, but at high temperatures, the ring-opening process occurs, and novolac-type oligomers (benzoxazine resin) with both the phenolic hydroxyl group and the tertiary amine groups are generated. **(Figure. 1.6).**

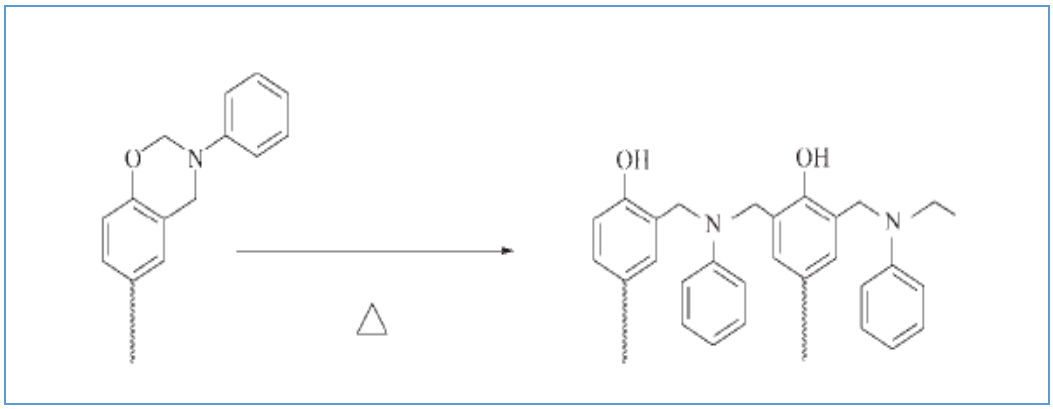

Figure 1.6. Ring-opening reaction of benzoxazine resin

1.3.3 Carbon Fibers for Composites

Carbon fibers are the most commonly used fibers for reinforcement in high-performance composite structures.They often have high modulus, higher tensile and compressive strength, and exceptional fatigue characteristics. Carbon fibers have a high carbon content (93 to 95 wt%) and are heat-treated at temperatures of 1600 °C. Carbon fibers have a low

density as well as high tensile strength and modulus and this is due to strong covalent bonding along the basal planes.

Rayon, polyacrylonitrile (PAN), and petroleum-based pitch are the precursors used for manufacturing of carbon fibers. Polymerization of the acrylonitrile monomer produces polyacrylonitrile. The manufacturing of PAN based carbon fibers can be broken down into five processes: (a) to make a fiber, spin and stretch the PAN copolymer. (b) under tension, stabilisation, and oxidation in air at 200 to 300 °C (c). carbonization in an inert atmosphere at 980 to 1595 °C (d) surface treatment and sizing [1, 2, 3, 4, 13].

Because of its high tensile strength (3500-7000 MPa) and high modulus (230-294 GPa), PAN precursor-based carbon fibers are widely used for fabricating structural composites.

1.3.4 Carbon Fiber Reinforced Polymer Composites

Carbon fiber reinforced polymer matrix composites are widely used for structural materials in the aerospace sector, sporting goods, civilian aviation, automobile, and civil infrastructure. The most frequent polymer matrix with carbon fibers is epoxy. Carbon fiber composites can also be made with phenolic resin, polyimides, cyanate ester resin polysulfone, polyimide, and polyether ether ether ketone. In most of these composites, carbon fibers are the primary load-bearing components. High performance ablative materials for spacecraft heat shields and rocket nozzle liners of solid propellant rocket motors have been made from carbon fiber reinforced phenolic resin composites [1, 2, 3, 4, 13].

The aircraft and defence sectors depend heavily on polymeric ablative composites. The primary function of polymer ablative material is to shield aerodynamic surfaces and propulsion components from harsh environmental conditions. For example, the walls of a rocket combustion chamber can reach temperatures of up to 3000 °C and pressures of up to 100 atmosphere. Ablative TPS based on a phenolic matrix are employed in these applications. Ablative materials are also employed to safeguard spacecraft during re-entry flights. Ablation, a self-regulating heat, and a mass transfer process is responsible for this protective function. Polymeric ablative composites, like any other composite, are made up of a continuous phase, the matrix, and a discontinuous phase, the reinforcements. The ablation process can involve both phases. The thermosetting resins are used in the majority of polymeric ablators. Phenolic resin is without a doubt the most widely used

matrix within this category of polymers. Phenolic-based ablative composites have good dimensional stability, thermal insulation and high thermal stability, which can be attributed to high crosslink density and the chemical structure of phenolic resin. Furthermore, phenolic matrice's high crosslinking density improves the mechanical performance of the char, resulting in improved protection of the ablator's inner layers [5].

One of the most prevalent uses of ablative materials is to protect the re-entry vehicle structure of spacecraft from the extreme heat experienced during hypersonic flight. For re-entry vehicle structures, ablative thermal protection systems (TPS) based on carbon fiber reinforced polymer composites are employed. The resin pyrolyzes when heated, releasing gaseous products (mostly hydrocarbons) that enter the solid, diffusing toward the heated external surface and proceeding into the boundary layer, where heat transfer activities take place. As a result of the resin pyrolysis, a carbonaceous residue known as 'char' is produced. The process of charring is usually endothermic. As the pyrolysis gases rise to the surface, they heat up, transferring energy from the solid to the gas. The ablation mechanism in TPS material is shown in **Figure 1.7** [5].

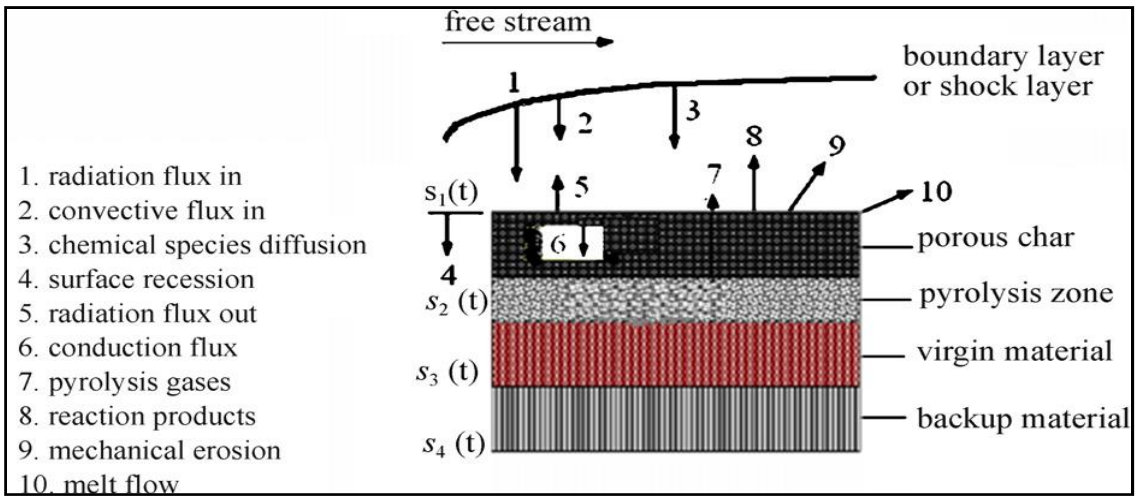

Figure 1.7. Ablation mechanism in TPS material [5]

Ablation is a heat and mass transfer process in which a significant quantity of thermal energy is dissipated through the sacrificial removal of surface material, as a result, high environmental temperatures are limited to the surface region. Numerous processes absorb, disperse, and restrict the heat input from the environment. Ablative materials are categorised in two different types. They are melting and non-melting ablative materials. In the melting type (thermoplastics based), because the liquid is evaporated soon after formation and a new surface is exposed, thermal protection is ineffective. Mechanical

ablation occurs before chemical ablation in non-melting and unreinforced materials, and a significant strength drop occurs as a result of a temperature increase. Only at extremely high temperatures (over 3000 K) does thermal ablation (sublimation) become noticeable. Non-melting ablative materials are made of char-forming thermosetting resins and are suitable for thermal protection of re-entry vehicles, probes, and ballistic missiles (high heating rates, shorter duration), and provide various degrees of protection. Thermosetting polymers, on the other hand, are frequently reinforced with continuous carbon fibers due to their poor strength and stiffness.Carbon fiber as reinforcement along with thermosetting resins are used for non-melting ablative materials [5].

Due to their char-forming capabilities and high pyrolysis heat values, polymers such as phenolic resins, polyimides, cyanate ester resins, benzoxazine resins, and polybenzimidazole are deemed ideal as a matrix (heat absorbed due to decomposition into char and gases).

1.3.5. Two -Phase Nanocomposites

When organo-modified montmorillonite nanoclay is mixed with matrices such as phenolic resin, cyanate resin, and benzoxazine resin and cured to form a composite, the result is a two-phase nanocomposite.

1.3.5.1. The Importance of Two-Phase Nanocomposites

As explained below, the preparation and testing of two-phase nanocomposites provide a thorough grasp of the numerous important aspects of nanocomposites.

i) Satae of nanoparticles dispersion in the resin system

ii) When nanoparticles interact with the resin, chemical bond formation between resin and nanoparticle, the effect of nanoparticle on curing rate and heat polymerisatio of resin.

iii)The effect of nanoparticles to resin on viscosity and thermal stability of cured reisn.

Researchers can better appreciate the role of nanoparticles as extra reinforcements in carbon fiber reinforced polymer composites, if they have a good grasp of the aforementioned factors. This is due to fact that , two-phase composites (phenolic resin - nanoclay, cyanate ester resin - nanoclay, and benzoxazine resin - nanoclay) becomes main constituents of three-phase composites (carbon fiber - phenolic resin-nanoclay, carbon fiber - cyanate ester resin - nanoclay and carbon fiber - benzoxazine resin - nanoclay).

The following sections provide an overview of recent literature trends in the field of two-phase nanocomposites of phenolic resin - nanoclay, cyanate ester resin - nanoclay, and benzoxazine resin - nanoclay.

1.3.5.2. State of the Art in Phenolic Resin - Nanoclay Composites

When compared to the virgin matrix polymer, polymer-clay nanocomposites demonstrate considerable mechanical, thermal, and physicochemical property enhancements at low clay loadings (1-5 wt%). Polymer-layered silicate nanocomposites based on montmorillonite (MMT) nanoclay have got a lot of attention since adding these nanofillers can improve mechanical, barrier, flame-retadancy and thermal properties without increasing the specific weight of the pure polymer. Previous research has demonstrated that phenolic resin-clay composites have promising high temperature ablation-resistant qualities, making them suitable for use as solid rocket propellant case liners [57-60].

Wei Jiang et al. prepared phenolic resin-montmorillonite nanoclay nanocomposites using octadecylamine (C18), benzyldimethylhexadecylammonium chloride (B2MH), benzyl triethylammonium chloride (B3E), and benzyldimethylphenylammonium chloride (B2MP) as organic modifiers. They reported that nanocomposites made of montmorillonite (MMT) modified by benzyl-containing modifiers exhibited thermal decomposition temperature higher than 783 K, with B2MP which contains both benzyl and phenyl groups. It was reported that the modifiers of montmorillonites influenced not only the curing behaviour, but also the final morphology of nanocomposites [61]. Zhihao Zhang et al. reported that the thermal stability of novolac phenolic resin decreased by the addition of nanoclay due to the catalytic activity of clay to promote decomposition. It was reported that the clay platelets restrict the molecular motion of thermoplastics in the interphase regions [62]. Min Ho Choi et al. reported modification of layered silicate and the resulting interaction between organic modifier and phenolic resin played an important role in determining the structure and final morphology of phenolic resin-layered silicate nanocomposites [63]. Gefu Ji et al. reported that intercalated nanoclay morphology reduced all properties of montmorillonite nanoclay/vinyl ester resin, whereas partially exfoliated or nearly fully exfoliated nanoclay morphology increased all properties of montmorillonite nanoclay/vinyl ester resin as compared with pure vinyl ester resin [64]. Maurizio Natali et al. reported that the introduction of well-dispersed nanoclays did not result in a consistent improvement in the thermal stability of resin [65]. A. M. Motawie et al. reported that epoxy modified novolac phenol formaldehyde (NPF) nanocomposites with 2 phr

organoclay gave optimum adhesion and scratch hardness values, thermal stability, and electrical insulation resistance as compared with epoxy/urethane, urethane modified NPF, and unfilled NPF samples [66]. P. Jahanmard et al. reported that unmodified clay (Closite Na+) has the highest influence on the mechanical properties possibly due to the good level of dispersion as well as the good interfacial interaction [67]. Sung Hun Ryu et al. reported significant improvement in the mechanical properties such as Young's modulus, tensile strength, and fracture toughness for silanized MMT nanoclay -filled epoxy nanocomposites as compared to pristine MMT nanoclay loaded system. The equilibrium water uptake was also reduced slightly for silanized MMT nanoclay filled epoxy when compared to pristine MMT nanoclay loaded epoxy system [68].

1.3.5.3 State of the Art in Cyanate Ester Resin - Nanoclay Composites

The cyanate ester (CE) resin, which is an addition-cured thermoset polymer generated by the reaction of phenolic resin with cyanogen bromide, provides a choice as an ablative matrix. Cyanate ester resin does not give any volatile by-products during curing. It has also better high temperature stability than the phenolic resin [69, 70].

It was reported that the initiation of decomposition of CE resin occurs at about 400-450 °C as compared to approximately 250-285 °C decomposition initiation temperature for phenolic resins. Char yield of the CE resins (63-65 wt%) is also higher when compared to the phenolic resin systems [71]. When compared to the processing of phenolic resin-based composites, which entails handling volatile by-products, CE resin undergoes addition curing without producing any gaseous by-products, making composite processing simple. [72, 73]. Thus, there are many technical advantages in using CE resin instead of phenolic resin. There is, however, a scarcity of information on the fabrication and properties evaluation of fiber reinforced cyanate ester resins for ablative applications.

Most of the literature on cyanate ester resin is confined to two-phase composites. Vladimir Bershtein et al. prepared amino functionalised nanoclay -cyanate resin composite with different clay loadings (0.01, 0.025, 0.05, 0.1, 0.5, 1, 2, and 5 wt%) and reported that ultra-low nanoclay content (0.025 to 0.1 wt%) improves modulus, thermal stability, and creep resistance of cyanate ester resin, whereas thermal stability of resin decreased at 5 wt% naoclay content [74]. Bibin John, et al. reported that the plasticizing action of nanoclay's organic moiety reduced the glass transition temperature of cyanate ester syntactic foams. They found that the syntactic foams thermal characteristics had not improved much [75]. Tim J. Wooster et al.

reported that the percolation of montmorillonite into the cyanate ester results in an 80 percent increase in crack resistance without sacrificing flexural strength [76]. Denis A. Kissounko, et al. reported that organic modifiers in silicate nanoclays reduced the cure temperature of the cyanate ester resin and enhanced the cure rate [77]. Jeffrey W. Gilman et al. reported that melamine treated nanoclay (10 wt% nanoclay content) reduced the flammability of cyanate ester at heat flux 35 kW/m^2 [78]. As a result, nanoclay has emerged as a popular nanofiller for improving the performance of C-CE based thermal protection system (TPS).

1.3.5.4 State of the Art in Benzoxazine Resin - Nanoclay Composites

Tarek Agag et al. prepared organo nanoclay modified polybenzoxazine nanocomposites with two different types of organoclay, allyl dimethyl stearyl ammonium-montmorillonite and propyl dimethyl stearyl ammonium- montmorillonite with different clay loadings (3,7, 10 wt%) and reported that organonanoclay catalysed the ring-opening of benzoxazine resin. They also reported that the thermal stability of resin increased with increased nanoclay content [79]. Corina Andronescu et al. prepared polybenzoxazine-nanoclay composites with different loadings (5, 10, 15 wt%) and reported that nanocomposites exhibit an intercalated structure. The addition of clays did not affect the polybenzoxazine resin's glass transition temperature or thermal stability[80]. Huei-Kuan Fu et al. prepared polybenzoxazine resin-nanoclay composites and reported that by decreasing the surface free energy of the nanocomposites, the thermal properties have improved by 10% of the organically modified montmorillonite nanoclay [81]. Hui-Wang et al. prepared nanocomposites of polybenzoxazine and exfoliated montmorillonite nanoclay using a polyhedral oligomeric silsesquioxane surfactant and reported that the incorporation of the exfoliated montmorillonite nanoclay has improved the polymer's glass transition, thermal decomposition temperatures, mechanical properties, and surface hydrophobicity [82].

1.3.6. Three -Phase Nanocomposites

Carbon fiber reinforced polymer composites (CFRCs) having additional reinforcement namely organo-modified montmorillonite nanoclay (o-MMT nanoclay) along with the conventional reinforcements like carbon fibers are referred to as three-phase composites or multi-scale composites.

1.3.6.1. The Importance of Three -Phase Nanocomposites

Carbon fiber reinforced polymer composites (CRFCs) are widely used as thermostructural systems for spacecraft vehicles. The primary function of these composites is to withstanding structural load and to tolerate high temperatures for a limited period. CFRCs, in particular, which are made with phenolic matrix reinforced with carbon fiber (carbon-phenolic), are used to shield spacecraft vehicles from high temperatures caused by high-velocity vehicle contact with the atmosphere. Such composites are called ablative composites. Carbon-phenolic is one among them. Many research groups have worked to determine the appropriateness of nanoclay reinforced carbon-phenolic (three-phase) composites for structural loads as well besides ablative applications. Apart from extensive study on phenolic resin-based systems, there were no studies on cyanate ester resin and benzoxazine resin as alternative resin systems for carbon fiber composites.

In the domain of ablative applications, the following sections present brief reported literature trends in three-phase nanocomposites of carbon fiber-phenolic resin- nanoclay, carbon fiber - cyanate ester resin- nanoclay, and carbon fiber- benzoxazine resin - nanoclay.

1.3.6.2 State of the Art in Carbon Fiber - Phenolic Resin - Nanoclay Composites

The reported literature contains a significant quantity of work that focuses on the influence of nanoclay addition on the thermal and mechanical properties of polymer systems without continuous reinforcements. With clay is added to the polymers, little research has been done on the mechanical, thermal, and ablation properties of continuous carbon fiber - polymer composite materials. Continuous carbon fiber reinforced polymer composites, on the other hand, have more immediate uses in the defence and aerospace industries. Hence the effect of nanoclay addition on carbon fiber reinforced phenolic resin composites must be investigated. A few studies that were reported are summerised below.

I. Srikanth et al. reported that using nanosilica as a filler in rayon based carbon fiber-phenolic resin composites at a 2 wt% loading increased ablation resistance, reduced thermal conductivity, and increased interlaminar shear strength [6]. A. Mirzapour et al. reported that the flexural strength of chopped rayon based arbon fiber/phenolic resin composites increases by around 13% when 3 wt% nanosilica content is added, but it reduces when 5 wt% nanosilica content is added. In comparison to pure composite, the linear and mass ablation rates for the specimen with a nanosilica concentration of 5 wt% dropped by 23.55% and 61.11%,

respectively. [9]. Ahmad Reza Bahramian reported that a cone calorimetry test at 8 x10^4 W/m^2 radiation external heat flux revealed that a 6 wt% nanoclay added asbestos cloth-phenolic resin nanocomposite loses 40% more mass than the asbestos cloth-phenolic resin composite [83].

T. M. Robert et al. developed a short silica fiber-Phenolic composite with various clay loadings (0, 1, 3, 5, and 10 wt%) and found that the nonflammability and mechanical properties of the composites were best at roughly 3 wt% nanoclay loading [84]. L Asaro et al. showed lower flexural strength in composites made with modified bentonite clay as fillers, but Suresha et al. observed enhanced flexural strength in polymeric composites made using nanoclay [85, 86]. According to Joseph Koo et al. nanoclay addition to C-Ph lowered ablation performance up to 5 wt% addition of nanoclay, but ablation performance increases at greater nanoclay content due to production of harder char [49, 87].

As a result, there are conflicting claims in the literature about the use of nanoclay as a filler in phenolic-based composites to improve mechanical and ablation properties. This could be due to differences in fiber volume fractions and the heat flux levels utilised to assess the ablation rate of the nanoclay-added composites. With systematic experimental work, the current research aims to explain the reasons for such a spread in the available data.

1.3.6.3 State of the Art in Carbon Fiber - Cyanate Ester Resin -Nanoclay Composites

Though, extensive research work was carried out in the area of cyanate ester resin-nanoclay composites, very limited research work was carried out in the area of nanoclay added carbon fiber-cyanate ester (C-CE) resin composites. K. N.Shiva Kumar et al. reported that carbon fiber-cyanate ester resin composite undergoes thermal cycling leading to reduced tensile strength and fracture strain and increased glass transition temperature [88]. Felix Abali et al. prepared carbon-carbon composite using primaset PT-30 cyanate ester resin with carbon fiber T 300 and evaluated mechanical properties [89]. S. P. Doherty et al. prepared carbon fiber-cyanate ester resin composite with high temperature organo modified nanoclay and reported that nanoclay improved thermal stability of resin, whereas addition of nanoclay marginally improved short beam shear strength and decreased open hole compression strength of carbon-cyanate ester resin composites [90].

Nanoclay is known to form a glassy phase at high heat flux as compared to low heat flux [91]. Thus, its performance as an ablation inhibitor may be higher at high heat flux. So far there are no studies reported on the effect of heat flux on the ablation performance of the nanoclay added

carbon fiber reinforced polymer matrix composites. Hence, it is aimed to address this gap in the presenst study.

1.3.6.4 State of the Art in Carbon Fiber - Benzoxazine resin -Nanoclay Composites

S. Rajesh Kumar et al. prepared glass fabric reinforced bisphenol F benzoxazine (BZ) resin with polyvinyl butyral (CA) and ethyl silicate (ES) in various weight percentages to make a glass fabric reinforced bisphenol F benzoxazine (BZ) resin. Reported that the stiffness, crosslink density, service temperature, and network branching properties of glass fabric reinforced polybenzoxazine silicate composites (GBCE) were enhanced [92]. S. Rajesh Kumar et al. made ternary mixtures of bisphenol F benzoxazine in various ratios as a hardener for bisphenol F novolac epoxy (ER) and polyethylene glycol diglycidal ether (EL) resins. Reported that, when compared to polybenzoxazine composites, these composites had better mechanical characteristics, hardness and hydrolytic stability [93].

Nonetheless, substantial study on nanoclay reinforced polybenzoxazine resin composites has been carried out. However, no studies were reported in the domain of nanoclay added carbon fiber-polybenzoxazine resin (C-BZ) composites to our knowledge. Further more, there are no studies reported on the influence of organo montmorillonite nanoclay on mechanical, thermal, and ablation behaviour of carbon fiber reinforce benzoxazine resin composites. Hence, it is aimed to addressing this gap in the present study.

1.4 Need of the Present Study

i) Extensive studies were reported on phenolic resin-based carbon fiber composites for thermal protection systems (TPS). This is due to phenolic resin has high thermal stability, char yield, and dimensional stability. However, Phenolic resin (Ph) has lower shelflife due to methylol groups and also processing disadvantages such as the evolution of volatile byproduct (water) due to condensation polymerization of the resin, which results in large volumetric shrinkage upon curing with voids and defects in the composite products. Because of this, many researchers are exploring alternate resin systems for high temperature applications like cyanate ester resins (CE) and benzoxazine resin (BZ). These resin systems undergo addition polymerization giving no process volatiles by-products and exhibit very low volumetric shrinkage upon curing. As a result, the current research work is focused on utilising cyanate ester resin and benzoxazine resin as alternate matrices to phenolic resin for carbon fiber reinforced polymer composites.

ii) To date, no studies have been published on the relationship between viscosity, curing, and thermal stability changes of polymer - nanoclay composites (two-phases) and the thermomechanical properties of nanoclay added carbon fiber reinforced polymer composites (three-phases). Present study tried to address this gap.

iii) To improve the compatibility of the nanoclay with the polymeric matrix and fiber, organic modifiers are usually added. These organic modifiers (for example o-MMT: organic modified montmorillonite clay) are generally present on clay surfaces up to 30 wt% of clay. As the thermal stability of organic modifiers is low, they may degrade during the ablation of carbon fiber reinforced polymer composites at an accelerated rate releasing various gaseous products. They may influence the ablation performance of the carbon fiber reinforced polymer composites. This aspect was not studied so far by any research group. Present study tried to address this gap.

iv) In comparison to low heat flux, nanoclay is known to generate a glassy phase at high heat flux. Thus, its performance as an ablation inhibitor may be higher at high heat flux. So far there are no studies reported on the effect of heat flux on the ablation performance of the nanoclay added polymer matrix composites. Hence, the effect of heat flux on the ablation performance of the nanoclay added carbon fiber reinforced polymer matrix composites is taken up in the present study.

v) Many researchers studied the curing behaviour and thermal stability of cyanate ester resin-nanoclay composites and polybenzoxazine -nanoclay composites. However, there are no studies reported on mechanical and the ablative performance of these matrices with carbon fiber reinforced composites. Hence carbon fiber reinforced cyanate ester resin composite and carbon fiber reinforced polybenzoxazine composites with nanoclay addition are taken up in this study to fill the gap in the literature.

1.5 Aim and Objectives of Research Work: The following aims and objectives are specified in the current research study based on the literature review.

1.5.1 The Aim of the Research Work

The research work aims at studying the effect of organo modified montmorillonite nanoclay addition on mechanical, thermal, and ablative properties of carbon fiber reinforced polymer composites by choosing various prospective matrix systems namely phenolic resin, cyanate ester resin, and benzoxazine resin.

1.5.2 The Objectives of the Research Work

i) Dispersion studies of organo modified montmorillonite (o-MMT) nanoclay in phenolic resin, cyanate ester resin, and benzoxazine resin by ball milling process using SAXS and SEM.

ii) Studying the effect of different weight percentages of o-MMT nanoclay addition on physical, mechanical, thermal, and ablation properties of following composites.

   (a) PAN based carbon fabric reinforced phenolic resin composites
   (b) PAN based carbon fabric reinforced cyanate ester resin composites
   (c) PAN based carbon fabric reinforced benzoxazine resin composites

   Understanding thermomechanical properties of above three – phase (carbon fiber – resin- nanoclay) composites under light of corresponding two - phase (resin – nanoclay) composites dispersion, viscosity, curing and thermal stability.

iii) Correlating the thermal stability and microstructure of the ablated surface with ablation properties for the above identified composites.

iv) Kinetic studies on thermal degradation of phenolic resin, cyanate ester resin, and benzoxazine resin.

v) Comparative performance of matrix systems reinforced with carbon fiber and nanoclay, which are mentioned in above ii) (a), ii) (b), and ii) (c) as TPS materials.

1.6. Structure of the Thesis

The thesis has been divided into eight chapters and its distribution is as mentioned below.

Chapter -1 deals with introduction – literature, need, aim and objectives of present study

Chapter -II deals with experimental and testing methods.

Chapter -III deals with preparation and characterisation of organo montmorillonite nanoclay added carbon fiber reinforced phenolic resin composites.

Chapter -IV deals with preparation and characterisation of organo montmorillonite nanoclay added carbon fiber reinforced cyanate ester resin composites.

Chapter -V deals with preparation and characterisation of organo montmorillonite nanoclay added carbon fiber reinforced benzoxazine resin composites.

Chapter -VI deals with kinetic studies on thermal degradation of phenolic resin, cyanate ester resin, and benzoxazine resin.

Chapter -VII deals with the comparative performance of matrices reinforced with carbon fiber and nanoclay.

In the last chapter, i.e **Chapter -VIII**, summary and conclusions of the thesis are presented

Chapters III to VI have been sub-divided into three sections namely materials, methods, results and discussion, and conclusion

Wherever the work of other researchers, authors, and scientists was used for experimental protocols, characterization, and support of interpretation of results and lead, their works were acknowledged in the list of references.

References

1. William D. Callister, Jr and David G. Rethwisch. Material science and engineering an introduction. 8th edition; John Wiley and Sons, 2009.
2. ASM Handbook Composites, Volume 21; ASM International, 2001
3. Bhagwan D. Agarwal, Lawrence J. Broutman, K. Chandrashekhara. Analysis and performance of fiber composites. 3rd edition; John Wiley and Sons, 2006
4. Krishan K. Chawla. Composite materials science and engineering. 3rd Edition; Springer, 2013.
5. G. Pulci, J. Tirillo, F. Marra, F.Fossati, C. Bartuli, T.Valente. Carbon-phenolic ablative materials for re-entry space vehicles: Manufacturing and properties. Composites: Part *A.* 2010; 41, 1483-1490.
6. I. Srikanth, Alex Daniel, Suresh Kumar, N. Padmavathi, Vajinder Singh, P. Ghosal, Anil Kumar, and G. Rohini Devi. Nano silica modified carbon–phenolic composites for enhanced resistance. Scripta Materials. 2010; 63, 200-203
7. Natali M, Monti M, Puglia D, Kenny JM, Torre L. Ablative properties of carbon black and MWNT/Phenolic composites: A comparative study. Composites Part A. 2012; 43, 174-182.
8. I. Srikanth, N. Padmavathi, Suresh Kumar, P. Ghosal, Anil Kumar, Ch. Subrahmanyam, Mechanical, Thermal and ablative properties of Zirconia, CNT modified carbon/phenolic composites. Composites Science &Technology. 2013; 80, 1-7.
9. A. Mirzapour, M.H.Asadolahy, S.Baghshahi, M.Akbari. Effect of nanosilica on the microstructure, thermal properties and bending strength of nanosilica modified carbon fiber/phenolic nanocomposite. Composites: Part A. 2014; 63, 159-167.
10. Yao Peng, Wen Wang, and Jinzhen Cao. Preparation of lignin−clay complexes and its effects on properties and weatherability of wood flour/polypropylene composites. Industrial and Engineering Chemistry Research. 2016; 55, 9657-9666.
11. Ali Asghar Jahangiri and Yasser Rostamiyan. Mechanical properties of nano-silica and nano-clay composites of phenol formaldehyde short carbon fibers. J.Composite Materials. 2020, 54; 1339-1352.
12. Zahra Eslami, Farshad Yazdani, Mir Aidin Mirzapour. Thermal and mechanical properties of phenolic-based composites reinforced by carbon fibers and multiwall carbon nanotubes. Composites: Part A. 2015; 72, 22-31.
13. P.K. Mallick. Fiber reinforced composites. 3rd Edition; CRC Press, 2008.
14. Carolina Simón-Herrero, Laura Gómez, Amaya Romero, José Luis Valverde and Luz Sanchez-Silva. Nanoclay-based PVA aerogels: synthesis and characterization. Industrial& Engineering Chemistry Research. 2018; 57, 6218-6225.
15. Yasser Rostamiyan, Abdolhosein Fereidoon, Masoud Rezaeiashtiyani, Amin Hamed Mashhadzadeh, Azam Salmankhani. Experimental and optimizing flexural strength of

epoxy-basednanocomposite: Effect of using nano silica and nano clay by using response surface design methodology. Materials and Design. 2015; 69, 96–104.

16. F. Carrasco, P. Pages. Thermal degradation and stability of epoxy nanocomposites: Influence of montmorillonite content and cure temperature. Polymer Degradation and Stability. 2008; 93, 1000-1007.
17. Zhihao Zhang, Guozhong Ye, Hossein Toghiani, Charles U. Pittman, Jr. Morphology and thermal stability of novolac phenolic resin/clay nanocomposites prepared via solution high-shear mixing, macromolecular materials and engineering. 2010; 295, 923–933.
18. Anna Czerniecka-Kubicka, Wiesław Frą cz, Marek Jasiorski, Wojciech Bła żejewski Barbara Pilch-Pitera, Marek Pyda, Iwona Zarzyka. Thermal properties of poly (3 hydroxybutyrate) modified by nanoclay**.** Journal of Thermal Calorimetry. 2017; 128, 1513- 1526.
19. Mitra Yoonessi, Hossein Toghiani, William L. Kingery, and Charles U. Pittman, Jr., Preparation, characterization, and properties of exfoliated/delaminated organically modified clay/dicyclopentadiene resin nanocomposites.Macromolecules.2004;37, 2511-2518.
20. P. Strove and Y.C. Ke. Polymer-layered silicate and silica nanocomposites. *Elsevier. Netherlands*, 2005.
21. R.V. Kurahatti, A.O. Surendranathan, S. A. Kori, Nirbhay Singh. A.V. Ramesh Kumar, and Saurabh Sri. Defence applications of polymer nanocomposites. Defence Science Journal. 2010; 60, 551-563.
22. M. Alexandre and P. Dubois. Polymer-layered silicate nanocomposites: preparation, properties, and uses of a new class of materials. Mater. Sci. Eng. 2000; 28, 1-63.
23. Asif Abdul Azeez, Kyong Yop Rhee, Soo Jin Park, David Hui, Epoxy clay nanocomposites – processing, properties, and applications: A review. Composites: Part B. 2013; 45, 308–320.
24. http://www.nanoclay.com.
25. http://www.rheox.com.
26. http://www.nanocor.com.
27. http://www.sud-chemie.com.
28. Theng, B. K. G. Formation, and properties of clay-polymer complexes, Elsevier. Scientific Publishing Co., Amsterdam, The Netherlands. 1979.
29. Okada. A., Kawasumi. M, Usuki. A Kojima. Y, Kurauchi.T, Kamigaito.O, Schaefer. D.W, Mark. J. E. Polymer based molecular composites. MRS Symposium Proceedings, Pittsburgh. 1990; 171, 45.

30. Richard A. Vaia, Hope Ishii, Emmanuel P. Giannelis. Synthesis and properties of two-dimensional nanostructures by direct intercalation of polymer melts in layered silicates. Chem. Mater. 1993; 5, 12, 1694–1696.
31. Suprakas Sinha Ray, Masami Okamoto. Polymer/layered silicate nanocomposites: a review from preparation to processing. Progress Polymer Science. 2003; 28, 1539–1641.
32. Hai-jun Lu, Guo-Zheng Liang, Xiao-yan Ma,Bao-yan Zhang, and Xiang-bao Chen. Epoxy/clay nanocomposites: further exfoliation of newly modified clay induced by shearing force of ball milling. Polym International, 2004; 53, 1545–1553.
33. Jo B, Park.S, Kim.D. Mechanical properties of nano - MMT reinforced polymer composite and polymer concrete. Constr. Build. Mater. 2008; 22, 14–20.
34. Zainuddina.S, Hosura. M.V, Zhou.Y, Narteh .A.T, Kumar. A, Jeelani. S. Experimental and numerical investigations on flexural and thermal properties of nanoclay-epoxy nanocomposites. Mater. Sci. Eng. 2010; 527, 7920–7926.
35. Peng-Cheng.M, Siddiqui. A.N, Marom .G, Kim.J.K, Dispersion and functionalization of carbon nanotubes for polymer-based nanocomposites. Composites Part A. 2010; 41, 1345–1367.
36. Mirzadeh. A, Lafleur.P.G, Kamal.M.R, Dubois.C. The effects of nanoclay dispersion levels and processing parameters on the dynamic vulcanization of TPV nanocomposites based onPP/EPDM prepared by reactive extrusion. Polym. Eng. Sci. 2012; 52, 1099–1110.
37. Wu .C.L, Zhang. Q.M, Rong. Z.M, Klaus. F. Tensile performance improvement of low nanoparticles filled polypropylene composites. Compos. Sci. Technol. 2002; 62, 1327–1340.
38. Bandyopadhyay .J, Suprakas. S.R. The quantitative analysis of nano - clay dispersion in polymer nanocompositesby small angle X-ray scattering combined with electron microscopy. Polymer. 2010; 51, 1437–1449.
39. Manitiu .M, Horsch.S, Gulari .E. Kannan. M.R. Role of polymer-clay interactions and nano-clay dispersion on the viscoelasticresponse of supercritical CO_2 dispersed polyvinyl methyl ether (PVME) -clay nanocomposites. Polymer. 2009; 50, 3786–3796.
40. Crosby .J.A, Lee.J.Y. Polymer nanocomposites: The nano effect on mechanical properties. Polym. Rev. 2007; 47, 217–229.
41. Tsai.J.L, Huang.J.C. Strain rate effect on mechanical behaviors of nylon 6–clay nanocomposites. Compos. Mater. 2006; 40, 925–938.
42. Yasmin. A Abot. J.L, Daniel. I.M. Processing of clay/epoxy nanocomposites by shear mixing. Scr. Mater. 2003; 49, 81–86.
43. Vaia .R.A, Jant. K.D, Kramer. E.J, Giannelis. E.P. Microstructural evolution of melt intercalated polymer-organically modified layered silicates nanocomposites. Chem. Mater. 1996; 8, 2628–2635.

44. Ngo.T.D, Ton-That.M.T, Hoa, S.V. Cole, K.C. Effect of temperature, duration and speed of pre-mixing on the dispersion of clay/epoxy nanocomposites. Compos. Sci. Technol. 2009; 69, 1831–1840.

45. Ray L. Frost, Éva Makó, János Kristóf, Erzsébet Horváth, J.Theo Kloprogge. Mechanochemical treatment of kaolinite. Journal of Colloid and Interface Science. 2001; 239,458–466.

46. Yu-Chen Lee, Chia-Lung Kuo, Shaw-Bing Wen, Chih-Peng Lin. Changes of organo-montmorillonite by ball-milling in water and kerosene. Applied Clay Science. 2007; 36, 265–270.

47. S.J. Ahmadi, Y.D. Huang, and W. Li. Synthetic routes, properties and future applications of polymer-layered silicate nanocomposites. J. Mater. Sci. 2004;39,1919-1925.

48. Adham R. Ramadan, Amal M.K. Esawi Ahmed Abdel Gawad. Effect of ball milling on the structure of Na+-montmorillonite and organo-montmorillonite (Cloisite 30B). Applied Clay Science. 2010, 47, 196–202.

49. Vaia RA, Price G, Ruth PN, Nguyen HT, Lichtenhan J. Polymer/layered silicate nanocomposites as high performanceablative materials. Appl Clay Sci 1999; 15:67–92.

50. Joseph H. Koo. Polymer Nanostructured materials for propulsion systems,*41st* AIAA/ASME/SAE/ASEE Joint Propulsion Conference & Exhibit. 10 - 13 July, 2005, Tucson.

51. Richard A. Vaia, Hope Ishii, Emmanuel P. Giannelis. Synthesis and properties of two-dimensional nanostructures by direct intercalation of polymer melts in layered silicates. Chem. Mater. 1993; 5, 1694–1696.

52. Richard A. Vaia, Emmanuel P. Giannelis. Polymer melt intercalation in organically-modified layered silicates: Model predictions and experiment. Macromolecules. 1997; 30, 8000–8009.

53. Deborah F. Eckel, Michael P. Balogh, Paula D. Fasulo, William R. Rodgers. Assessing organo-clay dispersion in polymer nanocomposites. J. Appl. Polym. Sci. 2004; 93, 1110-1117.

54. Vaia, RA.; Jandt, K. D.; Kramer, E. J., Giannelis, E. P. Microstructural evolution of melt intercalated polymer−organically modified layered silicates nanocomposites. Chem. Mater. 1996; 8, 2628-2635.

55. Luiza MP Campos, Letı´cia C Boaro, Tamiris MR Santos, Pamela A Marques, Sonia RY Almeida, Roberto R Bragaand Duclerc F Parra. Evaluation of flexural modulus, flexural strength and degree of conversion in BISGMA/TEGDMA resin filled with montmorillonite nanoparticles. Journal of composite materials. 2016; 51, 927-937.

56. George Odian. Principles of polymerization. Fourth Edition. John Wiley & Sons, Inc; 2004.

57. Louis Pilato. Phenolic Resins: A Century of Progress, *Springer*; 2010.

58. R. H. Alonso, L. Estevez, H. Lian, A. Kelarakis, E. P. Giannelis. Nafion–clay nanocomposite membranes: Morphology and properties. Polymer. 2009; 50, 2402-2410

59. Yaru Shi, Takashi Kashiwagi, Richard N. Walters, Jeffrey W. Gilman, Richard E. Lyon, Dotsevi Y. Sogah. Ethylene-vinyl acetate/layered silicate nanocomposites prepared by a surfactant-free method: Enhanced flame-retardant and mechanical properties. Polymer. 2009; 50, 3478-3487.

60. R. J. Blanski, J. H. Koo, P. Ruth, H. Nguyen, C. U. Pittman, Jr., S. H. Phillips. Proceedings of the 52nd JANNAF Propulsion Meeting. May 10–14, 2004; Las Vegas, pp. 1–18.

61. C. U. Pittman, Jr., R. J. Blanski, S. H. Phillips, J. H. Koo, P. N. Ruth. US Patent application air force invention No. AFB 00685, initiated Sept. 2, 2005.

62. Wei Jiang, Shinn-Horng Chen, Yun Chen. Nanocomposites from phenolic resin and various organo-modified montmorillonites: preparation and thermal stability. Journal of Applied Polymer Science. 2006; 102, 5336–5343.

63. Zhihao Zhang, Guozhong Ye, Hossein Toghiani, Charles U. Pittman, Jr. Morphology and thermal stability of novolac phenolic resin/clay nanocomposites prepared via solution high-shear mixing. Macromolecular Materials and Engineering. 2010; 295, 923–933.

64. Min Ho Choi, In Jae Chung, and Jong Doo Lee. Morphology and curing behaviors of phenolic resin-layered silicate nanocomposites prepared by melt intercalation. Chem. Mater. 2000; 12, 2977-2983.

65. Gefu Ji , Guoqiang Li. Effects of nanoclay morphology on the mechanical, thermal, and fire-retardant properties of vinyl ester-based nanocomposite, Materials Science and Engineering A. 2008; 498, 327–334.

66. Maurizio Natali, Josè Kenny, Luigi Torre. Phenolic matrix nanocomposites based on commercial grade resols: Synthesis and characterization. Composites Science and Technology. 2010; 70, 571–577.

67. A. M. Motawie, M. Z. Mohamed, S. M. Ahmed, D. El-Komy, N. A. Badawy, A. Y. Abd El All, and E. M. Sadak. Synthesis and characterization of modified novolac phenolic resin nanocomposites as metal coatings. Russian Journal of Applied Chemistry. 2015; 88, 970-976.

68. P. Jahanmard, A. Shojaei1, M. Faghihi1. Experimental and theoretical study on the mechanical properties of novolac phenolic resin nanocomposites: effects of nanoclay and multiwalled carbon nanotube. ECCM15 – 15th European conference on composite materials. Venice, Italy, 24-28 June, 2012.

69. Sung Hun Ryu, M Jeevan Kumar Reddy, and AM Shanmugharaj. Role of silane concentration on the structural characteristics and properties of epoxy-silane-modified montmorillonite clay nanocomposites. Journal of Elastomers and Plastics. 2016; 49, 1-19.

70. Ian Hamerton, John N. Hay. Recent developments in the chemistry of cyanate esters. Polymer International. 1998; 47, 465 – 473.

71. Schellhase, K. J., Koo, J. H., Buffy, J., & Brushaber, R. (2017). Development of new thermal protection systems based on silica/polysiloxane composites. 58th AIAA/ASCE/AHS/ASC Structures, Structural Dynamics, and Materials Conference. doi:10.2514/6.2017-1367

72. Michael L. Ramirez, Richard Walters, Richard E. Lyon, Edward P. Savitski. Thermal decomposition of cyanate ester resins, Polymer Degradation and Stability. 2002; 78:73–82.

73. C.P.Reghunadhan Nair, Dona Mathew, K.N.Ninan. Cyanate ester resins, recent developments. Advances in Polymer Science. 2000; 155, 1–80.

74. P.D. Mangalgiri. Polymer-matrix composites for high-temperature applications Defence Science Journal. 2005; 55, 175-193.

75. Vladimir Bershtein, Alexander Fainleib, Larisa Egorova, Kristina Gusakova, Olga Grigoryeva, Demid Kirilenko, Semen Konnikov, Valery Ryzhov, Pavel Yakushev, and Natalia Lavrenyuk. The impact of ultra-low amounts of amino-modified MMT on dynamics and properties of densely cross-linked cyanate ester resins. Nanoscale Research Letters. 2015; 10, 165-179.

76. Bibin John, C.P. Reghunadhan Nair, K.N. Ninan. Effect of nanoclay on the mechanical, dynamic mechanical and thermal properties of cyanate ester syntactic foams. Materials Science and Engineering A. 2010; 527, 5435–5443.

77. Tim J. Wooster, Simmi Abrol, Douglas R. MacFarlane. Rheological and mechanical properties of percolated cyanate ester nanocomposites. Polymer. 2005; 46, 8011–8017.

78. Denis A. Kissounko, Joseph M. Deitzel, Shawn P. Doherty, Apoorva Shah, John W.Gillespie. Understanding the role of clay silicate nanoparticles with organic modifiers in thermal curing of cyanate ester resin. European Polymer Journal. 2008; 44, 2807–2819.

79. Jeffrey W. Gilman, Richard H. Harris Jr., Douglas Hunter. Cyanate ester clay nanocomposites: Synthesis and flammability studies.International SAMPE Symposium / Exhibition, 44th Proceedings. 1999; May 23-27.

80. Tarek Agag, Tsutomu Takeichi. Preparation and cure behavior of organoclay-modified allyl- functional benzoxazine resin and the properties of their nanocomposites. Polymer Composites. 2008; 29, 750-757.

81. Corina Andronescu, Sorina Alexandra Gârea, Georgeta Voicu, Eugeniu Vasile, Horia Iovu. Nanocomposites based on a new polybenzoxazine resin and MMT. U.P.B. Sci. Bull., Series B. 2012; 74, 69-76.

82. .Huei-Kuan Fu, Chih-Feng Huang, Shiao-Wei Kuo,Han-Ching Lin,Ding-Ru Yei, FengChihChang. Effect of an organically modified nanoclay on low-surface-energy

materials of polybenzoxazine. Macromolecular Rapid Communications. 2008; 29, 1216-1220.

83. Hui-Wang, Cui, Shiao-Wei Kuo. Nanocomposites of polybenzoxazine and exfoliated montmorillonite using a polyhedral oligomeric silsesquioxane surfactant and click chemistry. Journal Polymer Research. 2013; 20, 114.

84. Ahmad Reza Bahramian.Mehrdad Kokabi. Ablation mechanism of polymer layered silicate nanocomposites heat shield. Journal of Hazardous Materials.2009; 166,445-454.

85. Temina Mary Robert, M. Satheesh Chandran, S. Jishnub, K. Sunitha, R. S. Rajeev, Dona Mathew, N. Sreenivas, L. Aravindakshan Pillaic, and C. P. Reghunadhan Nair. Nanoclay modified silica phenolic composites: mechanical properties and thermal response under simulated atmospheric re-entry conditions. Polym. Adv. Technol. 2015; 26, 104-109.

86. Asaro .L, Rivero G, Manfredi. L, Alvarez. V, Rodrigue. E. Development of carbon fiber/phenolic resin prepregs modified with nanoclays. Journal of Composite Materials. 2015; 50, 1287-1300.

87. B Suresha and Manpinder S Saini. Influence of organo-modified montmorillonite nanolayers on static mechanical and dynamic mechanical behaviour of carbon/epoxy composites. Journal of Composite Materials. 2016; 50, 3589-3601.

88. Kunigal Shivakumar and Huanchun Chen. Effect of thermal fatigue on tensile and flexural properties of carbon/cyanate ester pultruded composite. Journal of Reinforced Plastics and Composites. 2009; 28, 675-689.

89. Felix Abali, Kunigal Shivakumar, Nasrollah Hamidi, Robert Sadler. An RTM densification method of manufacturing carbon-carbon composites using Primaset PT-30 resin. Carbon. 2003; 41, 893–901.

90. S.P. Doherty, M. Takimori, J.M. Deitzel, D. Heider, J.W. Gillespie Jr., A. Shah, A. Giaya. Thermal degradation of carbon fiber/cyanate ester resin composites filled with clay silicate nanoparticles. Presented at a meeting of the Thermoset Resin Formulators Association at the HyattRegency Montreal in Montreal, Quebec, Canada, September 11 through 12, 2006.

91. D. Njoyaa, F.S. Tadjuidjea, E.J.A. Ndzanaa, A. Pountouonchia, N. Tessier-Doyenb,G. Lecomte-Nana. Effect of flux content and heating rate on the microstructure and technological properties of Mayouom (Western-Cameroon) kaolinite clay based ceramics, Journal Asian Ceramic Societies. 2017; 5, 422-426.

92. S. Rajesh Kumar, S. Krishna Mohanb, J. Dhanasekaran. Novel glass fabric reinforced Polybenzoxazine-silicate composites along with polyvinyl butyral for high service temperature applications. New Journal Chemistry. 2018; 19, 15499 – 16386.

93 S. Rajesh Kumar, S. Krishna Mohanb, J. Dhanasekaran. Epoxy benzoxazine based ternary systems of improved thermo-mechanical behavior for structural composite applications. RSC Advances. 2015; 5, 3709-3719.

Chapter - II

Experimental and Characterisation Methods

Experimental and Characterisation Methods

2.0 Experimental Methods

The experimental work involves preparation and characterisation of two-phase composites (type –I) namely phenolic resin - nanoclay, cyanate ester resin - nanoclay, benzoxazine resin – nanoclay and corresponding three-phase composites (type -II) namley carbon fiber - phenolic resin - nanoclay, carbon fiber - cyanate ester resin - nanoclay and carbon fiber - benzoxazine resin - nanoclay.

Initially, different weight percentages (1, 2, 4, 6 wt%) of organo modified montmorillite (o-MMT) nanoclay were dispersed in thermosetting resin (phenolic resin, cyanate ester resin and benzoxazine resin) by ball milling process.The following two-phase(polymer - nanoclay) composites (type - I) were cured in hot air circulating oven as per cure cylce of resin.

1. Phenolic Resin - Nanoclay Composite
2. Cyanate Ester Resin - Nanoclay Composite
3. Benzoxazine Resin - Nanoclay Composite

Dispersion studies of nanoclay in the above polymer – nanoclay composited were studied by small-angle X-ray scattering and scanning electron microscopy. Viscosity changes, cure behaviour and thermal stability changes to these resins by the addition of nanoclay were studied.

In addition to two - phase composites, following three-phase (carbon fiber – polymer - nanoclay) composites (type –II) were fabricated by adding 1, 2, 4, 6 wt% nanoclay dispersed resin to carbon fiber and cured in autoclave under pressure and vaccum as per cure cycle of resin.

1. Carbon fiber - Phenolic Resin - Nanoclay Composite
2. Carbon fiber - Cyanate Ester Resin - Nanoclay Composite
3. Carbon fiber - Benzoxazine Resin - Nanoclay Composite

Three-phase composites were characterised for physical, mechanical, thermal, and ablation properties to explore the effects of nanoclay on the performance of carbon fiber reinforced polymer composites.

The fabrication and characterisation methods for above two-phase composites and three-phase composites are covered in detail in the chapters III, IV, and V.

The typical experimental work for preparation and characterisation of two-phase and three-phase composites are depicted in **Figure 2.1**

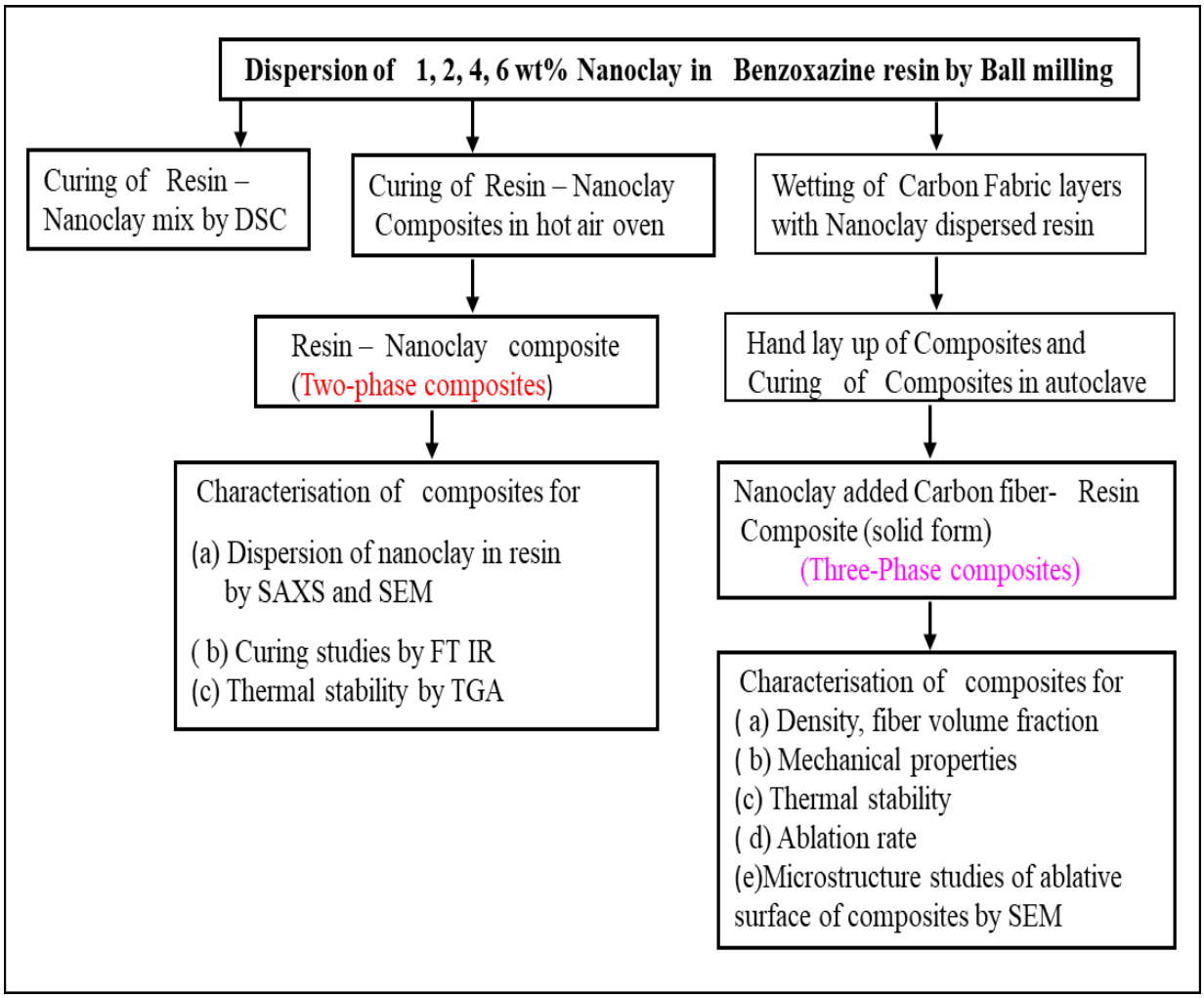

Figure 2. 1: A schematic flow diagram for experimental work and characterisation

2.1 Testing Methods: Various testing methods used in this study are briefly explained below.

2.1.1 Brookfield Viscometer

The viscosity of a fluid is a measurement of its resistance to flow. The viscosity of the resins and nanoclay dispersed resin were measured using Brookfield viscometer at room temperature. Brookfield viscometer (Model; DV-II + Pro) with spindle number 62 and 60 rpm were used for viscosity measurement as per ASTM D2196 standard [1].

2.1.2 Small Angle X - ray Scattering (SAXS)

Small angle X - ray scattering (SAXS) is a small angle scattering (SAS) technique where the elastic scattering of X-rays (wavelength 0.1 ... 0.2 nm) by a sample that has inhomogeneities in the nm-range, is recorded at very low angle (typically 0.1 - 10°). This

angular range comprises information regarding macromolecule shape and size, partially ordered material characteristic distances, pore diameters, and other data. SAXS can offer structural information on macromolecules between 5 and 25 nm, as well as repeat distances in partially ordered systems up to 150 nm in partially ordered systems [2]. Scanning the samples from 1 to 10° using a sample-detector at distance of 1.119 m and a 20 x 20 cm^2 two-dimensional position-sensitive area detector with each virtual cell (element) of around 3 mm apart. Instrumental background, dark current owing to cosmic radiation, electrical disturbances in the detector circuitry, detector nonuniformity, and efficiency were all corrected on a cell-by-cell basis (using a Fe 55 radioactive isotope standard, which emits X-rays isotropically by electron capture). Data obtained was radially (azimuthally) averaged in the q range, $0.01 < Q < 0.4A^{-1}$, scattering vector $q = (4\pi/\lambda)\sin\Theta$, and $q=2\pi/d$ where, q is scattering vector, λ is the X-ray wavelength, Θ is the scattering angle and d is the interlayer distance between crystal planes. Then, using recalibrated secondary standards, these results were transformed to an absolute differential scattering cross-section. The absolute scattering intensity is in cm^{-1} [2].Two-phase composites were evaluated for the dispersion of the nanoclay in resin-nanoclay composites using small angle X-ray scattering (SAXS: Antonpaar, Model: SAXS Point 2.0). In the present study dispersion of nanoclay in two - phase composites were characterised by SAXS.

2.2. Testing of Composites: Several testings were carried out on the fabricated composites, which are listed below.

2.2.1. Density: Three-phase composites were tested for density as per ASTM D 792 using Archimedes method [4]. The procedure consists of the following steps:

1. Weighing specimen in the air to the nearest 0.1 mg
2. Attaching specimen to analytical balance with a thin wire and weigh while the specimen and portion of the wire are immersed in distilled water.
3. Weighing wire alone, which is partially immersed up to the same point as in the previous step.

At 25°C, the density of the substance is calculated as follows:

$$\rho = (a/a+w-b)*0.9975$$

Where, ρ = Density, (g/cc)

a = Weight of specimen in air, (g)

b = Apparent weight of fully immersed specimen and partiallyimmersed wire, (g)

w = Apparent weight of partially immersed wire, (g)

Density of distilled water at 25 °C is 0.9975 g/cc

Three test specimens were tested for each type of the three-phase composite, and average values were recorded.

2.2.2 Fiber Volume Fraction

The volume proportion of fibers in composites determines their mechanical properties. Three-phase composites were tested for fiber volume fractions as per ASTM D 3171 [5]. Acid digestion method is employed with composites that have a matrix that is soluble in inorganic acid, as stated in ASTM specification D3171. This technique works well with carbon fiber reinforced polymer composites. It invovles taking 0.5 - 1.0 grams sample of the composite material and drying and weighing it. The matrix is then dissolved by immersing it in strong nitric acid. The acid used dissolves the matrix without causing damage to the fibers. Because concentrated nitric acid does not damage the fibers, they remain undigested. The residue (carbon fibers) is filtered, washed, dried, and weighed after the matrix portion of the composites is dissolved. The fiber volume fraction is calculated as per the following formula,

$$V_f = (W_f / p_f) / (W_c / p_c)$$

Where V_f = Fiber Volume fraction
W_f = Weight of fiber (g)
W_c = Weight of composite (g)
p_c = Density of composite (g/cc)
p_f = Density of fiber (g/cc)

Three test specimens were tested for each type of three-phase composite, and average values were recorded.

2.2.3 Barcol-Hardness

Hardness is defined as the resistance of a substance against the penetration by a sharp steel point indentor. The instrument, called the Barcol impressor, gives a direct reading on a 0 to 100 scale. The hardness value of composite material is frequently used to determine its degree of cure. The hardness of the three-phase composites was measured with a Bar-col measurement device, according to ASTM D2583 [6].

2.2.4 Interlaminar Shear Strength (ILSS)

ILSS is a shearing force that tends to cause a relative displacement between two laminae in a laminate along their interface plane. The shear strength test determines the fiber's bonding strength to the matrix as well as the inter-filament bond strength. ILSS determines interface strength between fiber and resin. It is a property that is dominated by resin system. However,

the observed ultimate strength value is a mixture of matrix strength and matrix-to-reinforcement bonding, rather than a straight measure of matrix strength [7, 8].

This test method is utilised as a quality control measure as well as a comparison of different composite materials. ILSS test is carried out as per ASTM D 2344[9]. ILLS of composite is determined by a universal testing machine (UTM) using a three-point bending fixture with a short span length. ILSS test is also called a short beam shear test. The span length to thickness ratio should be four to ensure shear failure rather than bending for ILSS testing of composites. Interlaminar shear strength (ILSS) is calculated using the following formula:

$$ILSS = 3P/4bd$$

Where, P = Maximum load, (Newtons)

b = Width of specimen, (mm)

d = Thickness of specimen, (mm)

ILSS value is expressed in MPa, or N/mm^2

In the present work, samples from three-phase composites with dimensions of 40 mm x 10 mm x 4 mm were collected for ILSS testing. ILSS test was carried out using a three-point bending fixture of UTM (M/s ADMET Model 2505) with load cell capacity 10KN. Support span to thickness ratio of 4:1 and crosshead speed of 1.0 mm/min was used for ILSS testing. Six test specimens were tested for each composite, and average values and standard deviation were reported.

2.2.5 Flexural Strength and Flexural Modulus

Flexural strength is the maximum stress that can be sustained by the sample in a beam in bending. The ratio of applied stress on a test specimen in flexure to the equivalent strain in the specimen's outermost fibers, within the elastic limit, is known as flexural modulus [7, 8].

A three-point test fixture with large support span length is used to determine the flexural strength and modulus, according to ASTM D790 [10]. The specimen's length dimension must be aligned with the material direction under investigation. The specimen may fail in one of three modes: tension, compression, or shear, or a combination of these mechanisms. The specimen geometry must be set so that shear stresses are kept low in comparison to bending. This is accomplished by maintaining a high ratio between the specimen's support span (L) and thickness (d). The L/d ratio for a three-point bending test is 16:1.

The flexural strength (FS) is calculated using the following formula,

$$FS = 3PL /2bd^2$$

Where P= Maximum load, (Newtons)

L = Support span length, (mm)

b = Width of specimen, (mm)

d = Thickness of specimen, (mm)

Flexural strength value is expressed in MPa or N/mm^2

Based on the linear portion of the load versus displacement curve, the flexural modulus (FM) was calculated using the equation.

$$FM = L^3 m / 4bd^3$$

Where, P = Maximum load, (Newtons)

L = Support span length, (mm)

m = Slope of Load vs displacement curve, (Newton/mm)

b = Width of specimen, (mm)

d = Thickness of specimen, (mm)

Flexural Modulus value is expressed in GPa

In this study, samples of three-phase composites with dimensions of 100 mm x 10 mm x 4 mm were collected for flexural testing. A flexural test was carried out using a three-point bending fixture of UTM (M/s ADMET Model 2505) with load cell capacity 10KN. Support span to thickness ratio of 16:1 and crosshead speed of 1.0 mm/ min was used for flexural testing. Six test specimens were tested for each composite. Average values and standard deviations reported.

2.2.6 Differential Scanning Calorimetry (DSC)

DSC is a technique in which the heat flow rate difference into a substance and a reference is measured as a function of temperature, while the sample is subjected to a controlled temperature program [11]. Indium was used to calibrate the DSC for cell constant and temperature. The curing behaviour of neat resin, two-phase composites was studied by DSC (DSC: M/s TA instruments, Q200). DSC runs were carried out from 30 to 400 °C with a sample mass of 10 ± 2 mg at a heating rate of 10 °C /min under nitrogen flow of 50 mL/min. Specific heat of three-phase composites was determined by DSC as per ASTM E 1269 [12] by three runs method with sapphire as standard material.

2.2.7 Thermogravimetric Analysis (TGA)

Thermogravimetric analysis (TGA) is a technique for measuring the mass of a substance as a function of temperature or time when the sample is subjected to a controlled temperature program in a controlled environment [11]. Before the thermal stability studies, thermogravimetric analysis (TGA: Make TA Instruments, Model Q-500) was calibrated for

temperature, weight accuracy using standard reference samples (calcium oxalate), standard weights, and standard nickel (for curie temperature). Thermal stability of as received nanoclay, two-phase and three-phase composites were evaluated using TGA from room temperature to 900 °C with a sample mass of 10 ± 2 mg at a heating rate of 10 °C /min in nitrogen atmosphere. Weight of the carbonaceous char (CR) and temperature at which 5% weight loss ($T_{5\ \%}$ /°C) observed for the samples were recorded. In the present study, two samples from each composition of type –I and type –II composite were tested for thermal decomposition temperatures and char yield. The average value is reported.

2.2.8 Thermal Conductivity

Thermal conductivity of three - phase composites was measured by hot disc thermal constants analyser (M/s Hot disc AB, Sweden; Model: TPS 2500S) at room temperature as per ISO 22007-2 [13]. Two samples having an approximate size of 80 mm x 80 mm x 4 mm were collected from each of the fabricated composites. These samples were used to sandwich a sensor that acts as both a heat source for increasing the temperature of the sample and as a resistance thermometer. The sensor was electrically heated, and the increase in temperature of the sensor surface is monitored as a function of time. The thermal conductivity and diffusivity of the material that is used to sandwich the sensor strongly influence the temperature rise of the sensor. From this, the thermal conductivity of the test samples is calculated. In the present study, two samples from each composition of type –II composites were tested for thermal conductivity and the average value is reported.

2.2.9 Oxy - Acetylene Torch Test

To assess the material's ablation resistance, it is required to recreate the harsh circumstances of the hyper-thermal environment to which thermal protection system is exposed (high heat fluxes and extremely high temperatures) in real-world service circumstances. The oxy-acetylene torch test as per ASTM E 285 is the most widely used and cost-effective method for determining the ablative (erosion rate) resistance of materials in the laboratory [14].

Test specimens having size 100 mm × 100 mm x 4 mm were used for carrying out oxy-acetylene torch test. The heat flux of oxy-acetylene torch was calibrated with a heat flux gauge by adjusting the distance between the sample and the source of flame. One set of three - phase composite specimens were subjected to a constant heat flux of 500 W/cm^2 for 60 seconds, while the other set of three-phase composite specimens were subjected to a constant heat flux of 125 W/cm^2 for 60 seconds. Mass ablation rate for three-phase composite specimens was

calculated as mass loss per second. In the present study, two samples from each composition of type –II composites were tested under each category at each flux and the average ablation rate is reported.

2.3. Morphology and Composition Characterisation

Morphology and compositional changes in three-phase composites after exposure to the oxy-acetylene torch test were studied using scanning electron microscopy (SEM) and X-ray diffractometer (XRD) respectively.

2.3.1 X-ray Diffractometer (XRD)

The intensity of the diffracted X-ray as a function of the incident, scattered angle, and wavelength is studied using this technique, which involves hitting the sample with X-rays [15]. In the present study, compositional changes in three - phase composites after exposure to the oxy-acetylene torch test were studied using an X-ray diffractometer (Philips PWD, Model: 1830 The Netherland).

2.3.2 Scanning Electron Microscope (SEM)

It involves utilising electromagnetic lenses to concentrate an electron beam flowing through an evacuated column onto the specimen. The SEM analysis of the material can yield two types of images, they are secondary electron image and backscattered electron image. The first mode of imaging provides topographic information about the material, whereas the second mode provides information on the compositional distribution of various elements inside the material. Previously, electrons generated from thermionic sources such as heated tungsten filament were utilised in scanning electron microscopes (SEMs). Field emission scanning electron microscopes (FESEMs) are advanced versions of electron microscopes that create electrons via the field emission effect [15]. They can magnify up to 10 lakhs and have a resolution of 2 nanometers. Morphology changes in three-phase composites after exposure to the oxyacetylene flame were studied using scanning electron microscopy (Table Top SEM, Make: SEC, Korea, and Model: SN4500 Plus).

In the present study, dispersion of nanoclay in polymer – nanoclay composites was characterised by using a scanning electron microscope (SEM). Before SEM studies, the surface of the samples was coated with a thin gold film with a sputtering unit (Make: M/s Hind HiVacuum India, Model: Scancoat Six). Also microstructure of ablated surface of three - phase composite specimnes after oxy- acetylene torch test was characterised by SEM.

References

1. ASTM D2196 – 18: Standard test methods for rheological properties of non-newtonian materials by rotational viscometer. American society for testing and materials. 100 Barr Harbor Drive, West Conshohocken, PA 19428, USA.
2. Bandyopadhyay. J, Suprakas, S.R. The quantitative analysis of nano-clay dispersion in polymer nanocomposites by small angle X-ray scattering combined with electron microscopy. Polymer. 2010; 51, 1437–1449.
3. Mitra Yoonessi, Hossein Toghiani, William L. Kingery, and Charles U. Pittman, Jr. Preparation, characterization, and properties of exfoliated/delaminated organically modified clay/dicyclopentadiene resin nanocomposites.Macromolecules.2004;37, 2511-2518.
4. ASTM D792 - 20: Standard test methods for density and specific gravity (relative density) of plastics by displacement. American society for testing and materials. 100 Barr Harbor Drive, West Conshohocken, PA 19428, USA.
5. ASTM D3171 - 15: Standard test methods for constituent content of composite materials. American society for testing and materials. 100 Barr Harbor Drive, West Conshohocken, PA 19428, USA.
6. ASTM D2583 – 13: Standard test method for indentation hardness of rigid plastics through a Barcol impressor. American society for testing and materials. 100 Barr Harbor Drive, West Conshohocken, PA 19428, USA.
7. J M Hodgkinson, Mechanical testing of advanced fiber composites, CRC Press, 2000.
8. Leif A. Carlsson, Donald F. Adams, R. Byron Pipes. Experimental characterization of advanced composite materials. Fourth edition, CRC Press, 2014.
9. ASTM D2344 / D2344M – 16: Standard test method for short-beam strength of polymer matrix composite materials and their laminates. American society for testing and materials. 100 Barr Harbor Drive, West Conshohocken, PA 19428, USA,
10. ASTM D790: Standard test methods for flexural properties of unreinforced and reinforced plastics and electrical insulating materials. American society for testing and materials. 100 Barr Harbor Drive, West Conshohocken, PA 19428, USA.
11. Joseph D. Menczel, R. Bruce Prime. Thermal analysis of polymers fundamentals and applications, John Wiley & Sons, Inc., Hoboken, New Jersey, 2009.
12. ASTM E1269 –11: Standard test method for determining specific heat capacity by differential scanning calorimetry. American society for testing and materials. 100 Barr Harbor Drive, West Conshohocken, PA 19428, USA.
13. ISO 22007-2- 2015: Plastics-Determination of thermal conductivity and thermal diffusivity - Part 2: Transient plane heat source (hot disc) method.
14. ASTM E285 – 08: Standard test method for oxyacetylene ablation testing of thermal insulation materials. American society for testing and materials. 100 Barr Harbor Drive, West Conshohocken, PA 19428, USA.
15. William D. Callister, Jr and David G. Rethwisch, Material science and engineering an introduction. 8th Edition. USA: John Wiley & Sons, 2009.

Chapter - III

Organo Montmorillonite Nanoclay Added Carbon Fiber –Phenolic Resin Composites

Preparation and Characterisation of Organo Montmorillonite Nanoclay Added Carbon Fiber – Phenolic Resin Composites

3.0 Introduction: Due to the high tensile strength and modulus of the PAN based carbon fiber and the high char yield and high thermal stability properties of the phenolic matrix, PAN based carbon fiber reinforced phenolic (C-Ph) composites have been used to realise high performance ablative materials for thermal protection systems (TPS) in aerospace applications [1-3]. General requirements of TPS are, it should withstand harsh aerodynamic shear loads, while simultaneously acting as a heat insulator to protect the subsystems that are behind them. Though C-Ph composites have established themselves as the best TPS materials, there is always an urge to further improve their properties to realize relatively thinner TPS, which can reduce the overall weight of aerospace systems.

Researchers have explored the addition of various nanomaterials like nanosilica, carbon nanotube, carbon black, nanoclay, polyhedral oligomer silsesquioxane (POSS) to C–Ph composites for enhancing their thermomechanical performance [4-10]. Among all these, nanoclay is the most versatile nanofiller due to its low cost and ease of dispersion in the resin systems. Many researchers have reported significant improvements in stiffness and strength of pure polymeric matrices with the addition of a small amount of nanoclay particles [11-18]. This is due to the high aspect ratio (200-1000) and modulus (170 GPa) of nanoclay and its ability to offer a higher surface area (750 m^2/g) as a filler which restricts the mobility of polymer chains under stress. However, exfoliation of the nanoclay platelets in the polymer matrix is the primary condition to get improved thermomechanical properties for the composites [19]. On the other hand, nanoclay addition to the polymeric systems results in improved thermal stability and reduced thermal conductivity which are intended for ablative applications [20]. Thus nanoclay has become a preferred nanofiller to improve the performance of C-Ph based TPS. However, there are varying reports in the literature on the utility of nanoclay as a filler in fiber reinforced phenolic based composites in improving mechanical and ablation properties. Present work latently addresses the reasons for such a scatter in the reported property variation due to nanoclay as a filler for carbon fiber reinforced phenolic resin composites. Preparation and characterisation of organo montmorillonite nanoclay added carbon fiber-phenolic resin composites is taken up in the present study with an aim to understand mechanical, thermal and abliation behaviour of composites.

3.1 Materials: Major raw materials used in this work are phenolic resin, PAN based carbon fabric, and surface modified montmorillonite (o-MMT) nanoclay. Below is a detailed specifications for each of the raw materials.

3.1.1 Phenolic Resin: Resol type phenolic resin was selected as matrix material. It has a solid content of about 62 wt% and volatile content (ethanol) of about 38 wt%. Resin has high thermal stability and char yield of about 54 wt% at 900 °C in an inert atmosphere. The technical specifications of phenolic resin are given below.

Sl.No	Test Parameter	Specification
1	Chemical name	Resol type phenolic resin
2	Viscosity at 30 °C	230 cP
3	Point of trouble (at a specific gravity of diluted resin 0.859)	7.2 ml
4	Specific gravity at 30 °C	1.14
5	Solid resin content	60-65 wt%
6	Volatile content	32-38 wt%
7	Free Phenol content	6% (Maximum)
8	Free formaldehyde content	3% (Maximum)
9	Gel time at 160 °C	15 minutes
10	Commercial name	IVA REZ Resin

The resin was procured from M/s IVP, Tarapur, India and it was used without any modification in the present study. **Figure 3.1** depicts the chemical structure of resol type phenolic resin.

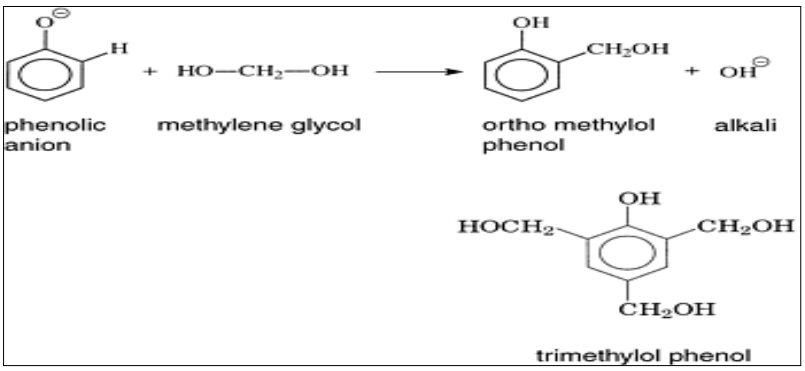

Figure 3.1. The chemical structure of resol type phenolic resin

3.1.2 PAN Based Carbon Fabric: A polyacrylonitrile (PAN) based high strength carbon fabric (bidirectional) woven with 3K fiber of T-300 grade was chosen for the fabricating of three- phase (carbon fiber - phenolic resin - nanoclay) composites. The technical specifications of the fabric are given below.

Sl.No	Test Parameter	Specification
1	Tow type	3k (3000 filaments in tow)
2	Grade of carbon fiber	T- 300 Fiber (M/s Torayca carbon)
3	Thickness of fabric	0.38 ± 0.05 mm
4	Areal density	380 ± 20 g/m^2
5	Fabric weave style	8 Harness satin
6	Fabric count (warp direction)	24 ± 1 Ends /inch
7	Fabric count (weft direction)	24 ± 1 Ends /inch
8	Fabric breaking strength	250-300 kg/inch (in both warp &weft)
9	Carbon content	93 wt%
10	Density	1.8 g/cc

PAN based woven carbon fabric was procured from M/s Urja Products Pvt Ltd, Ahmedabad, India and it was used without any modification in the present study. The image of the fabric is shown in **Figure 3.2.**

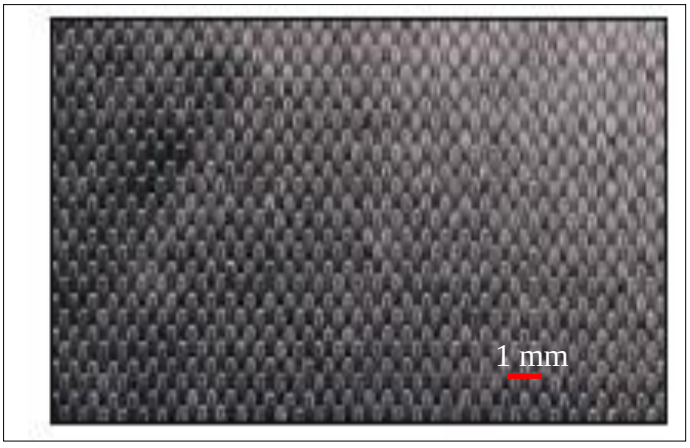

Figure 3.2 PAN based woven carbon fabric

3.1.3 Organo Montmorillonite (o-MMT) Nanoclay: o-MMT nanoclay used in this study is nanomer 1.31PS. Nanomer 1.31PS nanoclay was surface-modified montmorillonite (o-MMT) with 0.5-5 wt% aminopropyltriethoxysilane, 15-35 wt% Octadecyl amine. The nanoclay (Nanomer 1.31 PS) was supplied by Sigma-Aldrich Chemical Pvt Limited, Hyderabad, India. Brief specifications of the nanomer 1.31PS nanoclay are given below.

\

Sl.No	Test Parameter	Specification
1	Appearance	Off white free-flowing powder
2	Surface modifier	Octadecyl ammonium /silane
3	Bulk density	250- 300 kg/m^3
4	Specific gravity	1.9
5	Particle size(mean)	14-18 micron

Figure 3.3 shows the structure and composition of organo modified montmorillonite (o-MMT) nanoclay.

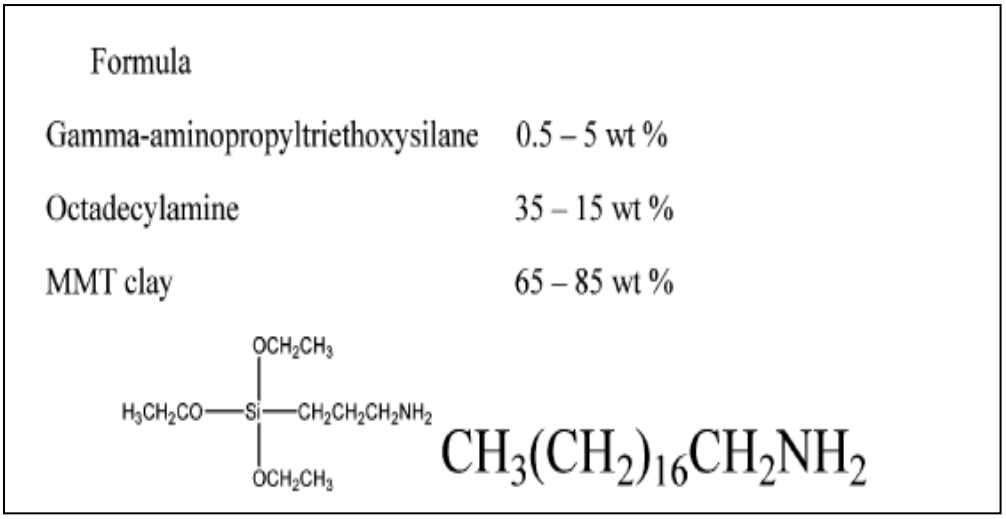

Figure. 3.3. Structure and composition of organo modified montmorillonite nanoclay

3.2. Experimental Work: The flow chart below provides a quick overview of the experimental work carried out.

Flow chart: Schematic flow of experimental work

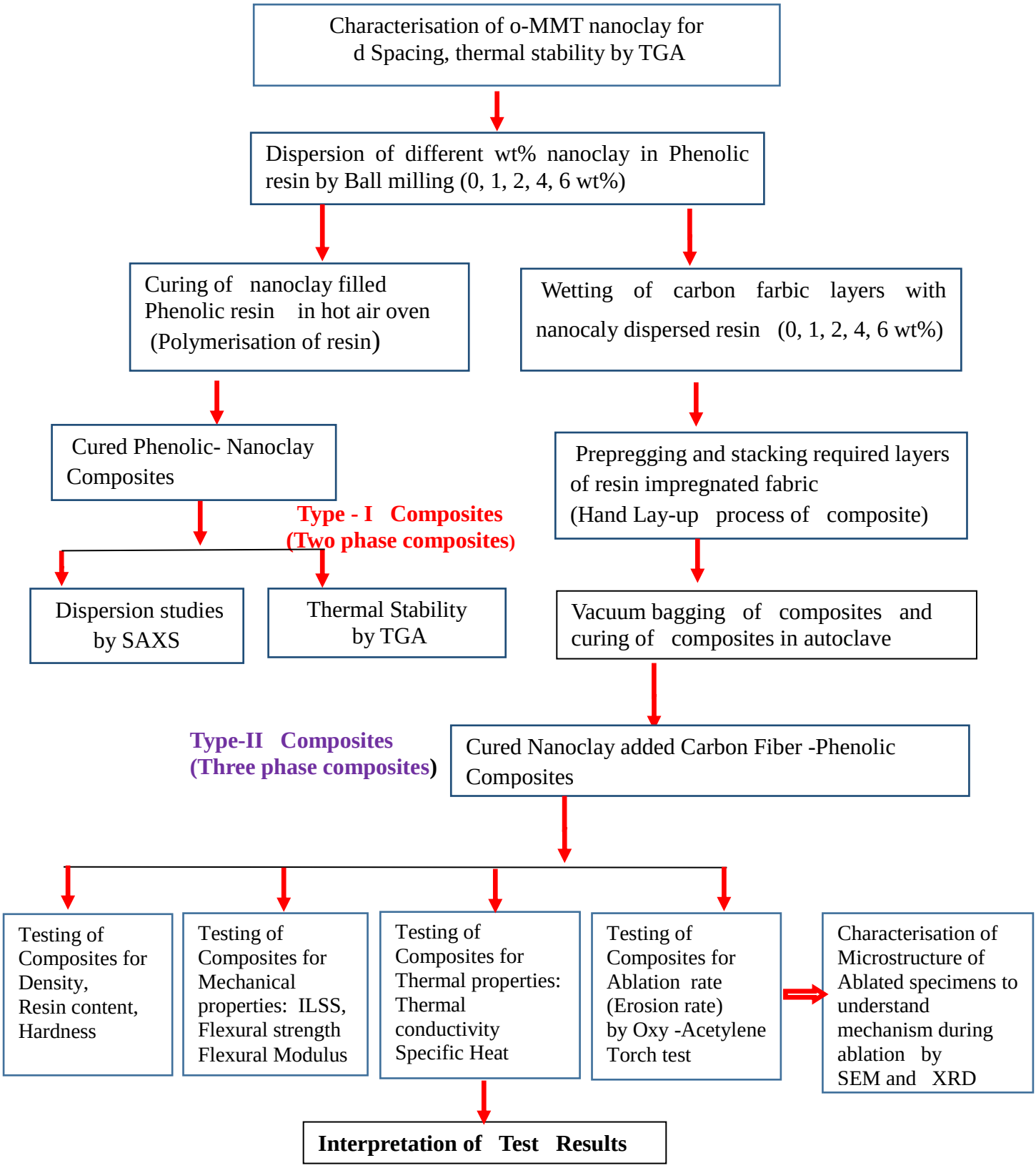

3.2.1 Dispersion of Nanoclay in Phenolic Resin

Ball milling process was employed for dispersion of o-MMT nanoclay in phenolic resin **[**21, 22]**.** The o-MMT nanoclay particles were dried in an oven at 70 °C for 2 h**.** Dispersion of nanoclay in resin was carried out by ball milling**.** The o-MMT nanoclay was dispersed in .phenolic resin using a planetary ball mill (M/s Insmart Systems) by taking approximately 198 grams of resin and 2 grams of o-MMT nanoclay in a 500 ml stainless steel (SS) jar for preparation of 1 wt% nanoclay filled phenolic resin. This mixture was ball milled for 2 hours at 250 rpm using SS balls. Ball to charge ratio was maintained at 0.5:1. Thus, four different phenolic resin - nanoclay compositions were prepared by dispersion of 1, 2, 4, and 6 wt% of nanoclay to phenolic resin. The composition of two-phase (phenolic resin - nanoclay) composites are given below in **Table 3.1.**

Table 3.1.The composition of phenolic resin - nanoclay composites (Type - I) fabricated.

Composite designation	**Nanoclay (NC) (wt%) loading in resin**	**Composition**
Phenolic resin (Ph)	0	
1 NC - Ph	1	99 g of resin + 1 g of nanoclay
2 NC - Ph	2	98 g of resin + 2 g of nanoclay
4 NC - Ph	4	96 g of resin + 4 g of nanoclay
6 NC - Ph	6	94 g of resin + 6 g of nanoclay

Images of ball milling of nanoclay into the phenolic resin at different stages are shown in **Figure 3.4.** (SS bowl shown in image has a volume of 500 ml).

Empty SS Jar with balls

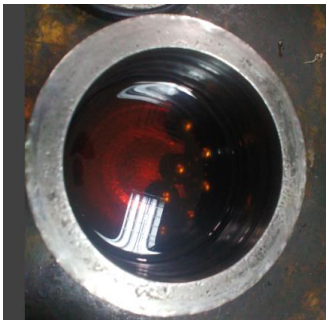

Phenolic resin added to Jar

Nanoclay added to resin

Closed Steel Jar

Ball Milling of Clay and Phenolic resin

Nanoclay dispersed in Resin

Figure 3.4. Ball milling process for dispersion of nanoclay in resin

Viscosity changes to the phenolic resin due to the addition of nanoclay was measured using Brookfield viscometer at 30 °C and shown in **Figure 3. 5.**

Figure 3.5. Measurement of viscosity of resin by Brookfield viscometer

3.2.2. Preparation of Phenolic Resin - Nanoclay Composites (Type –I)

Nanoclay dispersed phenolic resin was poured into a petri dish and the volatiles were allowed to evaporate by heating the mixture to 50 °C for one hour in a hot air circulating oven. Subsequently, the mixture was cured in a hot air oven at 90 °C for 1h, 120 °C for 1.5 h, 150 °C for 1 h, and 170 °C for 2 h. Thus, five different variants of type- I composites were prepared along with a blank phenolic matrix sample. The details of the prepared type - I composites are given in **Table 3.1**. Blank cured phenolic resin and phenolic resin – nanoclay composite are shown in **Figure 3.6.**

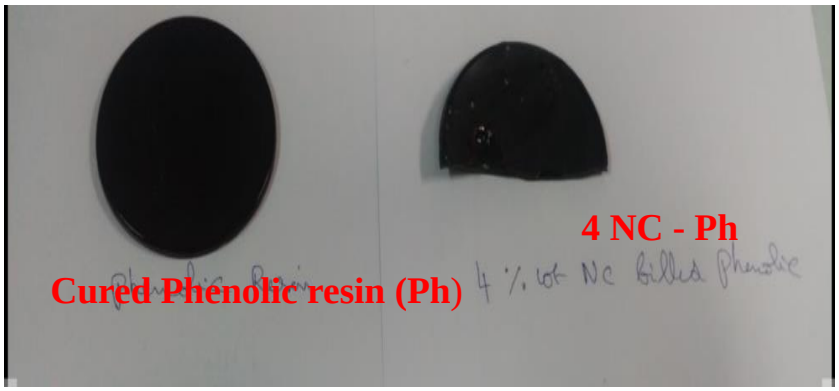

Figure 3.6. Blank cured phenolic resin and phenolic resin- nanoclay composite

These type - I composites were used for dispersion studies of nanoclay in resin by SAXS, SEM and thermal stability by the thermogravimetric analysis (TGA).

3.2.3. Preparation of NanoclayAdded Carbon Fiber -Phenolic Resin Composites (Type-II)

Preparation of composite involves six steps: (i) mould preparation, (ii) impregnation of fabric layers with resin (iii) Hand lay-up of impregnated layers stack, (iv) vacuum bagging of composite stack (vi) curing of stack in autoclave (vi) demolding.

Twelve carbon fabric layers of 300 mm x 300 mm X 0.38 mm size were cut and impregnated with nanoclay dispersed phenolic resin. The resin impregnated layers were stacked on a flat metal plate by hand lay-up process. Stacked layers were subjected to vacuum bagging, followed by curing in the autoclave. The curing was carried at 90 °C for 1h followed by 120 °C for 1.5 h, 150 °C for 1 h, and 170 °C for 2 h under a pressure of five bar and vacuum of one bar and then cool to room temperature. Processing steps for the preparation of type-II composites are shown in **Figure 3.7.** The cure cycle followed for curing type- II composites are given in **Figure 3.8.**

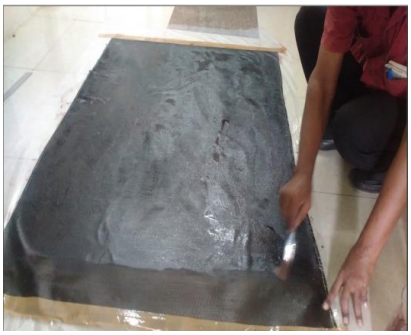

Hand impregnation of carbon cloth (fabric) with clay filled phenolic resin

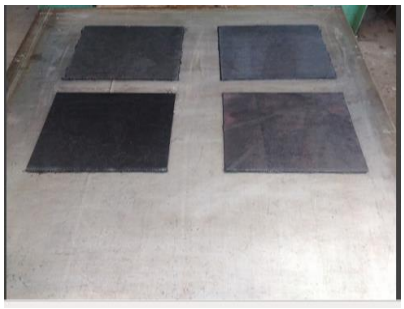

Hand Lay - up of composites (12 Layers, Size: 300 x 300 mm)

Vacuum bagging of composites and vacuum application

Curing of composite by Autoclave process

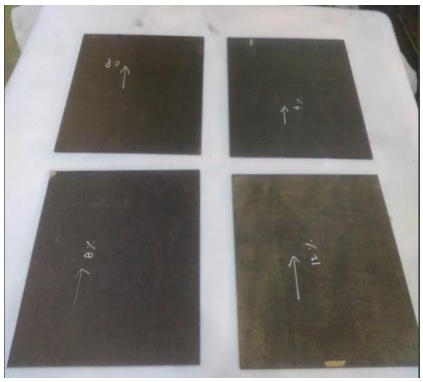

Cured C- Ph composites with 1, 2, 4, 6 wt% nanoclay

Figure 3.7. Images showing different stages of processing of nanoclay added C-Ph composites

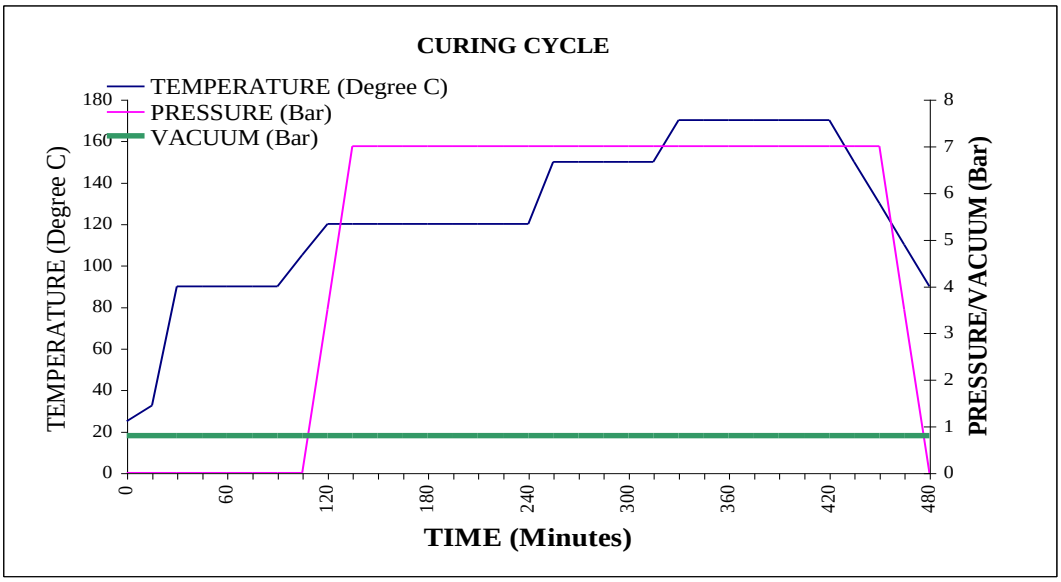

Figure 3 8. Cure cycle followed for curing of nanoclay added C-Ph composites

Five different variants of the type - II composites were fabricated along with the blank carbon-phenolic composite. Details of the prepared nanoclay added C-Ph composites (type- II) are given in **Table 3. 2.**

Table.3.2. Details of the prepared nanoclay added carbon fiber – phenolic resin composites (Type-II).

Composite designation	**Nanoclay (wt%) in resin**	**Composition**
C - Ph (blank)	0	Carbon Fabric (C) + Resin
1 NC/ C - Ph	1	Carbon Fabric + Resin + 1 wt% nanoclay
2 NC/ C - Ph	2	Carbon Fabric + Resin + 2 wt% nanoclay
4 NC/ C - Ph	4	Carbon Fabric + Resin + 4 wt% nanoclay
6 NC/ C - Ph	6	Carbon Fabric + Resin + 6 wt% nanoclay

3.3. Characterisation and Testing

3.3.1 Dispersion Studies of Nanoclay in Phenolic Resin - Nanoclay Composites

Phenolic resin – nanoclay composites (type- I) were evaluated for the dispersion of the nanoclay in phenolic resin using small angle X-ray sattering (SAXs: Antonpaar, Model: SAXS Point 2.0) by scanning the samples from 1° to 10°. Dispersion of nanoclay in resin is also evaluated using a scanning electron microscope (SEM) (Table Top SEM, Make: SEC, Korea, and Model: SN4500 Plus). Before SEM studies, the surface of the samples was coated with a thin gold film with a sputtering unit (Make: M/s Hind HiVacuum India, Model: Scancoat Six).to increase surface conductivity,

3.3.2 Density and Fiber Volume Fraction of Type – II Composites

Nanoclay added carbon fiber reinforced phenolic resin composites (type –II) were tested for density as per ASTM D792 using the Archimedes method. The fiber content of composites was measured by the acid digestion technique as per ASTM D3171. The test involves taking the known weight of the fabricated composite and digesting the matrix part of it by refluxing in concentrated nitric acid. Subsequently, the left over fabric was washed, dried, and weighed. The fiber volume fraction was calculated from the weight of

the fiber, density of fiber, and density of the composite. Images of resin content test by acid digestion method are shown in **Figure 3.9.**

Figure. 3.9. Resin content test by acid digestion

3.3.3 Barcol - Hardness

Barcol- Hardness of the type-II composites was measured with a Barcol impressor as per ASTM D2583 and shown in **Figure 3.10.**

Figure 3.10. Measurement of hardness on carbon fiber – phenolic resin composite

3.3.4 Thermal Stability of Type –I and Type –II Composites

Thermal stability of type - I and type - II composites in nitrogen atmosphere was evaluated by a thermogravimetric analysis (TGA). TGA, make TA Instruments, and model Q 500 was used and is shown in **Figure 3.11.**

Figure 3.11. Thermogravimetric analysis (TGA)

In a typical thermal stability test, a sample mass of 10±2mg was collected from the fabricated composites. TGA runs were carried out for these samples, from room temperature to 900 °C at a heating rate of 10 °C /min under a continuous flow of nitrogen (flow rate 60ml/min). Weight of the carbonaceous char (CR) and temperature at which 5% weight loss ($T_{5\ \%}$ /°C) observed for the samples were recorded. Thus two samples from the type -I and type-II composites were subjected to thermal stability tests.

From CR, the oxidation index (OI) of the type -I and type -II composites were calculated using empirical **equation (1)** [25-27].

$$OI \times 100 = 17.4 \times 0.4CR \text{ ---------- } (1)$$

3.3.5 Thermal Conductivity

Thermal conductivity of type-II composites were measured by hot disc thermal constants analyser (M/s Hot disc AB, Sweden; Model: TPS 2500S) at room temperature as per ISO 22007-2.

3.3.6 Specific Heat

The specific heat of the type-II composites was measured as per ASTM E 1269 by differential scanning calorimetry (DSC, Q200 TA Instrument make). The specific heat was measured by three-run methods. Run 1 is a blank run (equal weight of two empty aluminium crucibles). Run 2 is a standard Sapphire sample run (one crucible is empty and the second crucible with sapphire). Run 3 is a test sample run (one crucible is empty and the second crucible with test sample). A sample mass of 10 ± 2mg was collected from the fabricated type -II composites. DSC runs were carried out for these samples, from room temperature to 400 °C

at a heating rate of 10 °C /min under a continuous flow of nitrogen (flow rate 60 ml/min) was used for the measurement of specific heat of composite samples.

3.3.7 Interlaminar Shear Strength (ILSS)

ILSS test was carried out for type -II composites as per ASTM D 2344 using a three - point bending fixture with short span length by UTM (M/s ADMET Model 2505). Support span to thickness ratio of 4:1 and crosshead speed of 1.0 mm/min was used for ILSS testing. ILSS testing by UTM is shown in **Figure 3.12**. Six samples were tested for the ILSS test. The average value and standard deviation were calculated for each of the compositions. Standard deviation is shown as an error bar in the results.

Figure 3.12. ILSS of nanoclay added C-Ph composites by UTM

3.3.8 Flexural test

Flexural strength was carried out for type –II composites as per ASTM D790 by using a three-point bending fixture with a large span length by UTM (M/s ADMET Model 2505). Support span to thickness ratio of 16:1 and crosshead speed of 1.0 mm/min was used for flexural testing. Flexural testing by UTM is shown in **Figure 3.13**. Six samples were tested for the flexural test. The average value and standard deviation were calculated for each of the compositions. Standard deviation is shown as an error bar in the results.

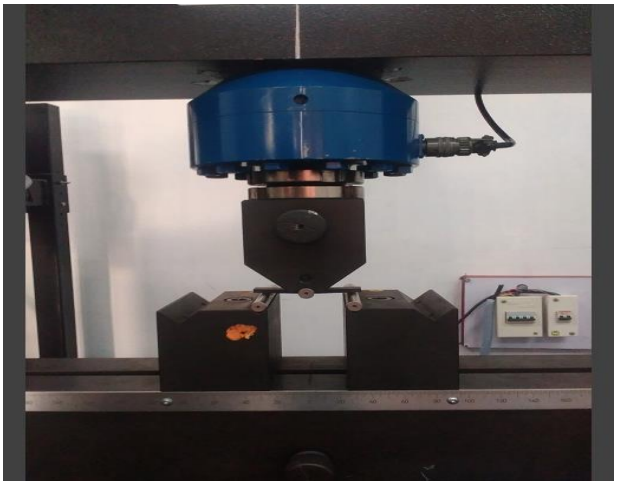

Figure 3.13. Flexural test of nanoclay added C-Ph composites by UTM

3.3.9 Oxy-acetylene Torch Test of Nanoclay Added Carbon Fiber Reinforced Phenolic Resin Composites

Type -II composites were subjected to an oxy-acetylene torch test as per ASTM E285. Test specimens having a size of 100 mm × 100 mm x 4.2 mm were used. Heat flux of oxy-acetylene torch was calibrated with heat flux gauge by adjusting the distance between the sample and the source of torch. One set of type- II composite specimens were subjected to a constant heat flux of 500 W/cm^2 for 60 seconds, while the other set of type - II composites were subjected to a constant heat flux of 125 W/cm^2 for 60 seconds. Mass ablation rate for type-II composites was calculated as mass loss per second. The test set up oxy-acetylene flame test is shown in **Figure 3.14**. Two samples were tested under each category at each flux and the average ablation rate is reported. Images of ablated samples tested at a heat flux 500 W/cm^2 are shown in **Figure 3.15.**

Figure 3.14. Oxy-acetylene torch test of nanoclay added C-Ph composites

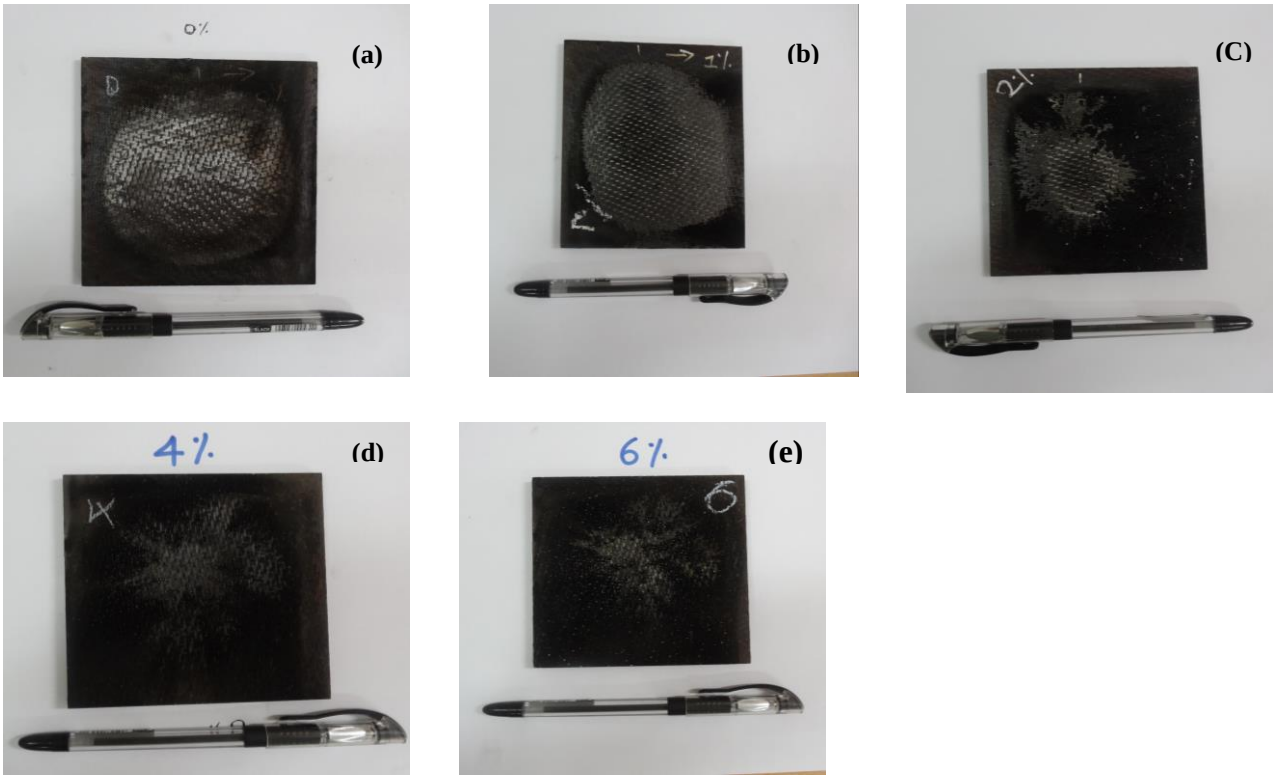

Figure 3.15. Ablated samples tested at heat flux 500 W/cm^2 (a) blank C-Ph (b) 1 wt% nano clay added C-Ph composite (c) 2 wt% nanoclay added C-Ph composite (d) 4 wt% nanoclay added C-Ph composite (e) 6 wt% nanoclay added C-Ph composite. (**Size of each specimen: 100 mm x 100 mm x 4.2 mm)**

3.4 Microstructure and Composition Characterisation

Microstructure and compositional changes in type - II composites after exposure to the oxy-acetylene torch were studied using scanning electron microscopy (ESEM: FEI Quanta 400) and X-ray diffractometer (Philips PWD, Model: 1830 The Netherland) respectively.

3.5 Results and Discussion

3.5.1 Effect of Nanoclay Content on Viscosity of Phenolic Resin

The viscosity changes to the phenolic resin due to different loadings of nanoclay is shown in **Figure 3.16.**

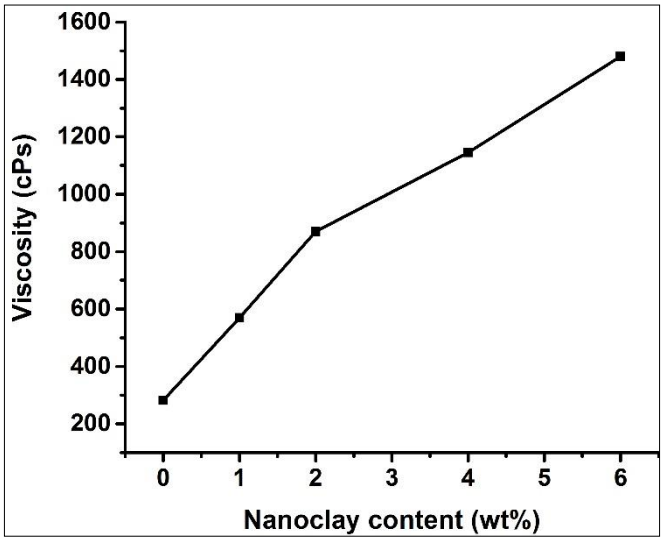

Figure 3.16 Effect of nanoclay content (wt%) on the viscosity of the phenolic resin

The viscosity of pure phenolic was 280 cP. Viscosity increased up to five times as compared to the pure phenolic at 6 wt% of nanoclay addition. It is reported that, when the nanoclay interacts with the phenolic resin, significant swelling of the clay galleries takes place due to monomer entrapment into the clay platelets [24, 25]. These swollen platelets lead to the formation of weak gels with increased viscosity. Resin viscosity is an important parameter in the processing of the composite material. The higher viscosity of the nanoclay modified phenolic resin can reduce the resin extraction during the processing, resulting in a higher resin content in the fabricated composites [26].

3.5.2 Dispersion of Nanoclay in Phenolic Resin - Nanoclay Composites

SAXS patterns of as received nanoclay and type - I composite are shown in **Figure 3.17**. The d- spacing values of type - I composites are calculated using Bragg's law and results are given in **Table 3.3**. The d-spacing of the pure nanoclay before dispersion in the phenolic resin was

found to be 3.2 nm. It can be seen from **Figure 3.17**, that, characteristic peak observed for the pure nanoclay (o-MMT nanoclay) got subsided up to 6 wt% of nanoclay addition in type-I composites, indicating that clay platelets are singular and got exfoliated in the phenolic resin. This result indicates that the shearing force exerted during ball milling of clay- phenolic mixture is sufficient enough to exfoliate the clay platelets. This is essential to improve the mechanical and thermal properties of the host matrix [21].

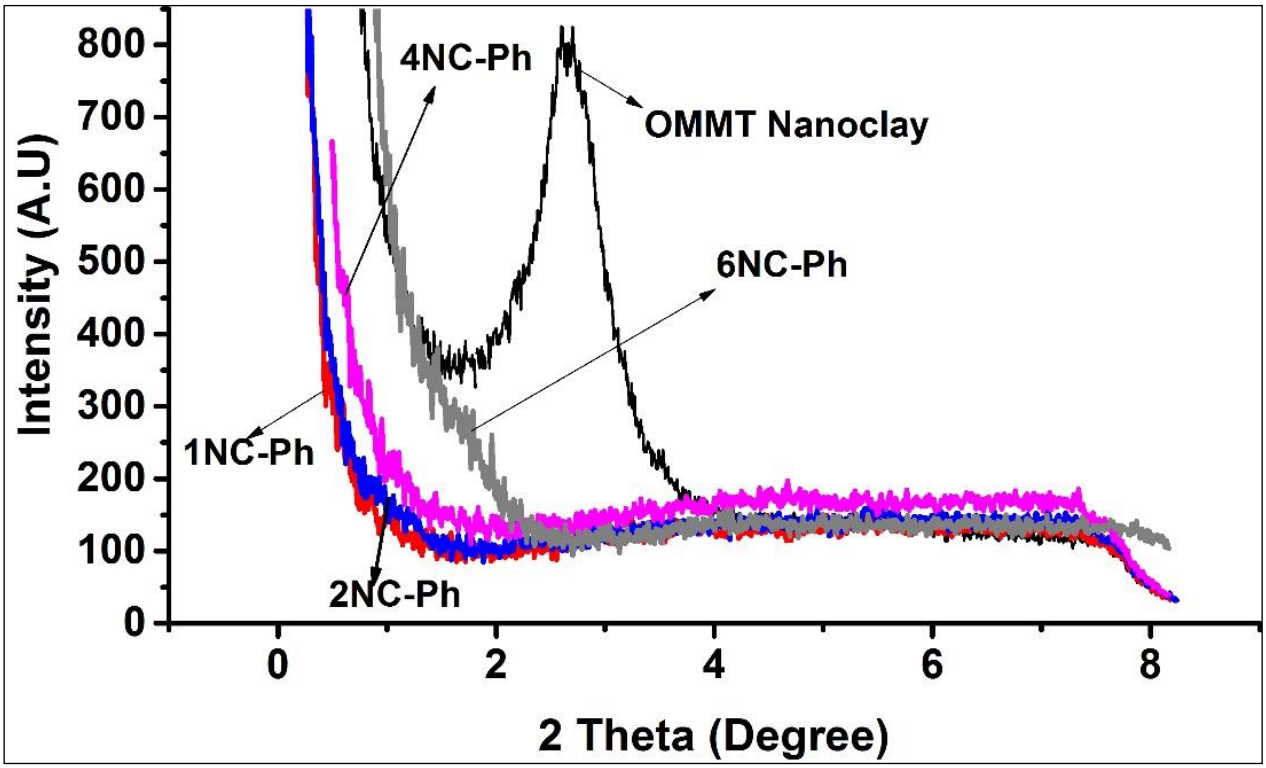

Figure 3.17: SAXS scans of nanoclay and phenolic resin- nanoclay composites

Table 3.3 *d* spacing values of nanoclay and phenolic – nanoclay composites

Sl.No	**Nanocomposites description**	**Nanoclay loading in resin (wt%)**	**2θ**	***d* 001 (nm)**
1	o-MMT nanoclay	Nanomer 1.31 PS	2.7	3.2
2	1 NC-Ph	1 wt%	No crystalline peak	
3	2 NC-Ph	2 wt%	No crystalline peak	
4	4 NC-Ph	4 wt%	No crystalline peak	
5	6 NC-Ph	6 wt%	No crystalline peak	

SAXS data indicates clay platelet segregation, whereas the SEM shows the macroscopic distribution of clay in the matrix. **Figure 3.18** shows SEM images of nanoclay dispersed in type -I composites. The white spots visible in the images shown in **Figure 3.18**, are associated with silicon molecule, one of the main o-MMT nanoparticle constituents. Thus, the larger amount of white spots with uniform spread over the exposed area suggests the presence of o-MMT nanoclay in the matrix uniformly [24].

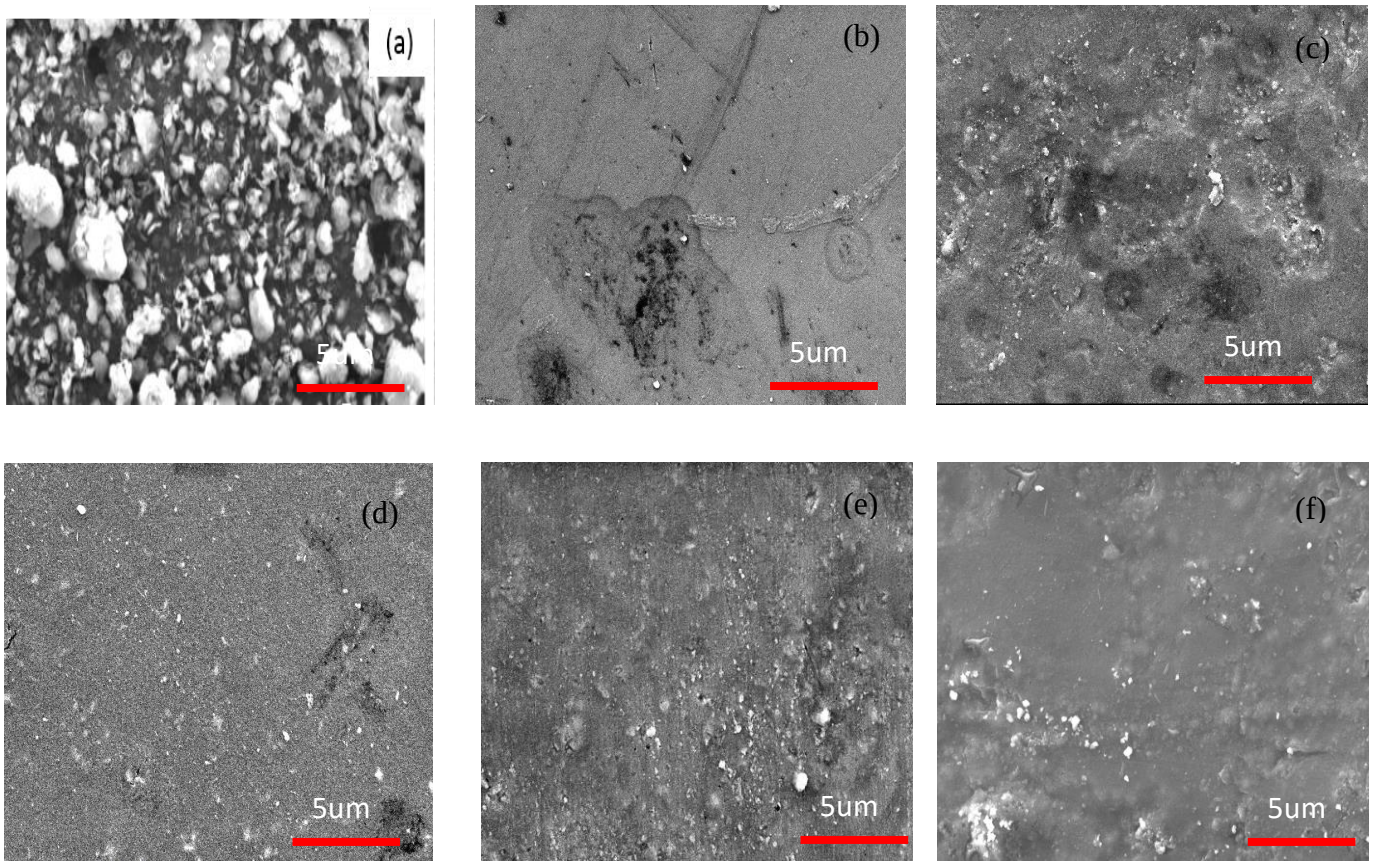

Figure 3.18. SEM images (a) as received o-MMT nanoclay (b) neat phenolic resin (c) 1 wt% o-MMT nanoclay added phenolic composite (d) 2 wt% o-MMT nanoclay added phenolic composite (e) 4 wt% o-MMT nanoclay added phenolic composite (f) 6 wt% o-MMT nanoclay added phenolic composite

3.5.3. Density and Fiber Volume Fraction of Nanoclay Added C-Ph Composites

Density and fiber volume fraction (%V_f) of fabricated composites are shown in **Table 3. 4.**

Table 3.4 Density and the fiber volume fraction of nanoclay added C-Ph composites

Sl. No	Composite description	Nanoclay in resin (wt%)	Density (g/cc)	Fibre volume fraction (%V_f)
1	C-Ph	0	1.55	63
2	1 NC/ C-Ph	1	1.52	61
3	2 NC/ C-Ph	2	1.52	61
4	4 NC/ C-Ph	4	1.49	53
5	6 NC/ C-Ph	6	1.48	52

It can be seen that, as the loading of nanoclay in resin increased, %V_f of the composite is coming down. This effect is maximum for composites processed with 4 wt% and 6 wt% nanoclay added resin systems. This could be attributed to the fact that, at these nanoclay loadings, the viscosity of the resin increased significantly, which restricted its squeeze out during the processing of composites [26]. This has reduced the fiber volume fraction of composites processed with 4 wt% and 6 wt% nanoclay added carbon fiber – phenolic resin composites. The above changes in the fiber volume fraction of the composites should have a significant effect on the mechanical, thermal properties of these composites which are discussed in detail in subsequent sections.

3.5.4. Barcol Hardness of Nanoclay Added C-Ph Composites: Barcol hardness of fabricated composites is shown in **Table 3.5**. Barcol Hardness values are found to be the same for blank C-Ph composite and nanoclay added C-Ph composites.

Table. 3.5 Barcol Hardness of nanoclay added C-Ph composites

Sl. No	Composite description	Nanoclay in resin (wt%)	Barcol Hardness
1	C-Ph (blank)	0	55-60
2	1 NC/ C-Ph	1	55-60
3	2 NC/ C-Ph	2	55-60
4	4 NC/ C-Ph	4	50-52
5	6 NC/ C-Ph	6	50-58

Barcol hardness value indicates the extent of curing of composite. Nanoclay added C- Ph composites and blank C-Ph composites were completely cured.

3.5.5 Thermal Stability of the Type -I and Type - II Composites: The TGA and DTGA scans for o-MMT nanoclay, neat phenolic resin, and phenolic –nanoclay composites (type-I) are shown in **Figures 3.19 (a), 3.19 (b**) respectively.

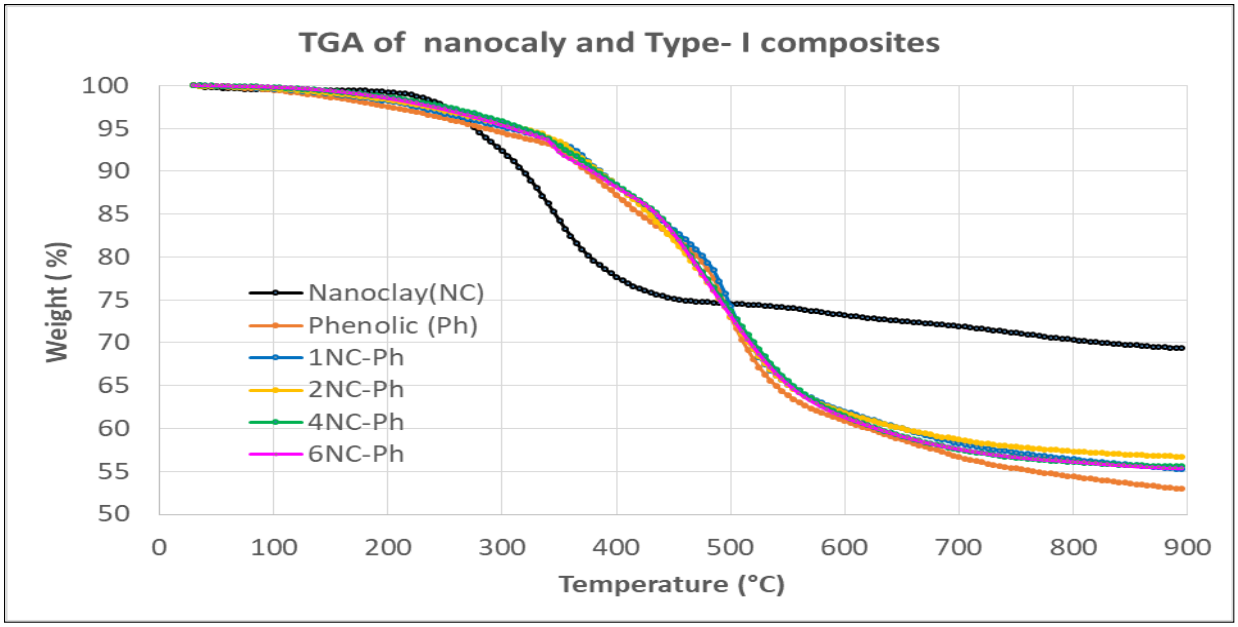

Figure 3.19 (a) TGA scans of nanoclay and phenolic- nanoclay composites

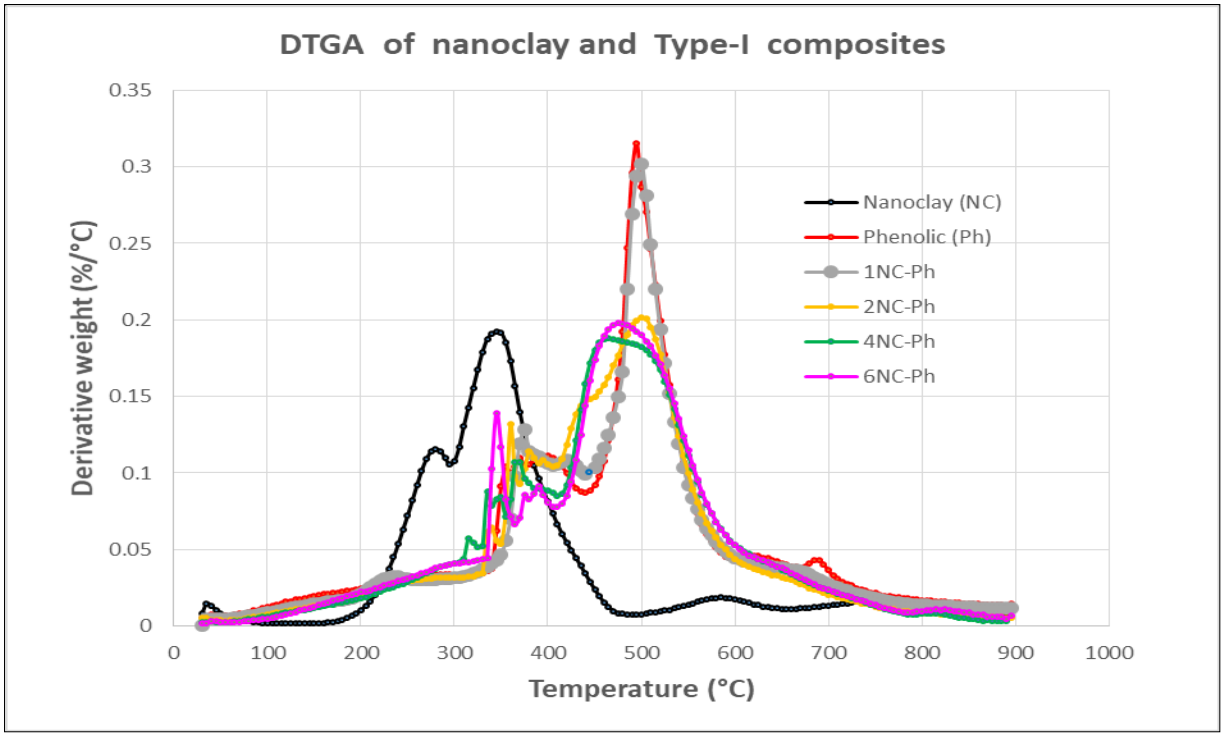

Figure 3.19 (b) DTGA scans of nanoclay and phenolic resin- nanoclay composites

The TGA and DTGA plots for blank C-Ph and nanoclay added C-Ph composites (type-II) are shown in **Figures 3.20 (a), 3.20 (b**) respectively.

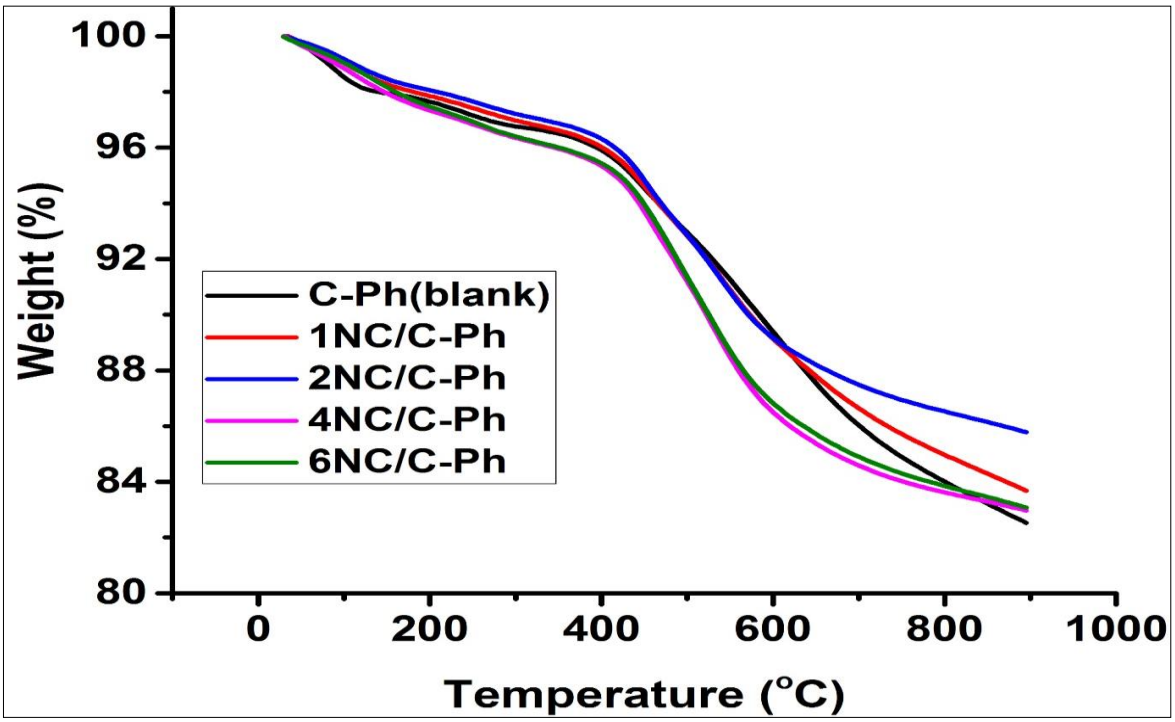

Figure 3.20 (a) TGA scans of nanoclay added carbon fiber – phenolic resin composites

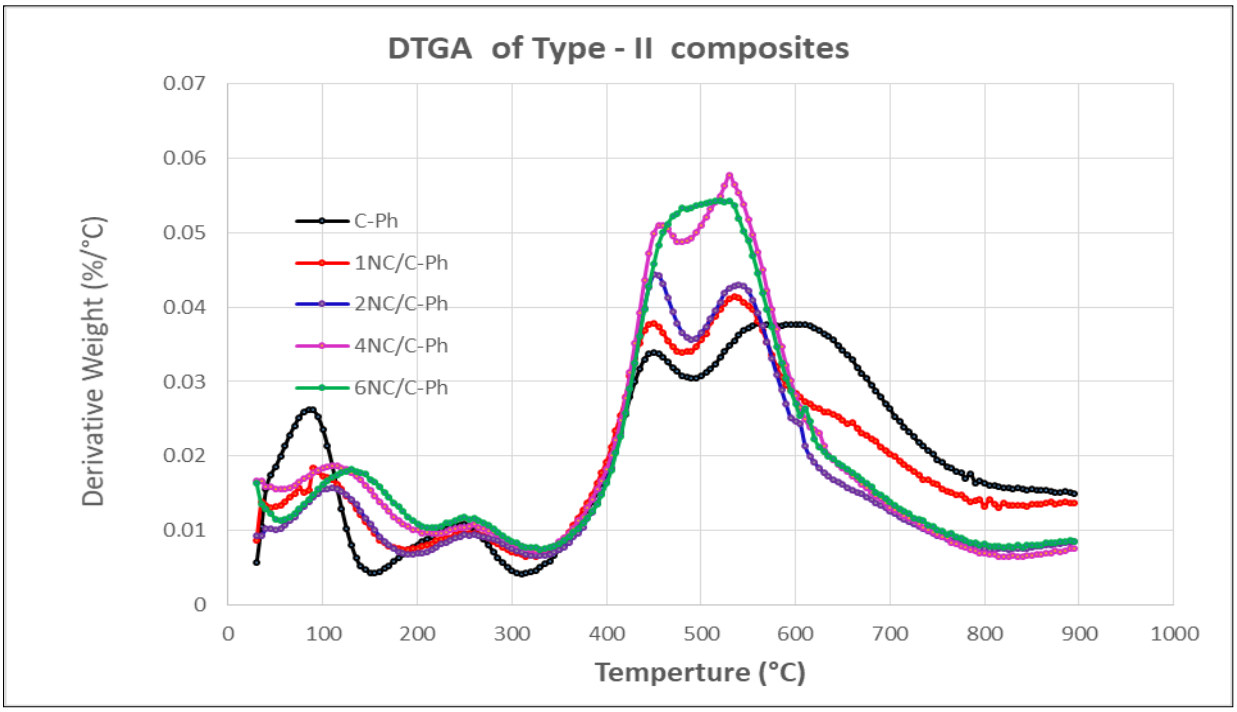

Figure 3.20 (b) DTGA scans of nanoclay added carbon fiber- phenolic resin composites

The characteristic temperature at which 5% weight loss ($T_{5\ \%\ /°C}$), char residue at 900 °C obtained from thermogravimetric analysis of composites and oxidation index are shown in **Table.3.6.**

Table 3.6. Characteristic temperature and oxidation index of type - I and type -II composites.

Nanoclay (wt%)in composite	*$T_{5\ \%\ /\ °C}$		% Residue at 900 °C		Oxidation Index	
	Type- I	Type-II	Type-I	Type-II	Type -I	Type -II
0	285	430	53	82.50	3.68	5.74
1	305	440	55	83.64	3.83	5.82
2	315	445	57	85.77	3.97	5.97
4	320	420	56	83.00	3.89	5.78
6	305	420	55	83.00	3.83	5.78

***Temperature at 5% weight loss of the sample**

The observed trends were found to be matching with the previously reported data of other researchers [20, 27]. The higher value of oxidation index indicates, higher thermal stability for the material under the study [28]. Increased thermal stability can be attributed to the strong interaction of the nanoclay layers with the matrix thereby hindering the interaction of oxygen. Temperature at 5 wt% loss of the sample, percentage residue at 900 °C, indicates that thermal stability has increased for both type -I up to 6 wt% and for type -II composites up to 2 wt% percentage addition of nanoclay, beyond that, thermal stability is showing a downward trend. Increased thermal stability up to 2 wt% of nanoclay addition is due to hindrance offered by nanoclay in oxygen and matrix interactions [30, 31]. Decreasing thermal stability beyond 2 wt% nanoclay addition can be attributed to the reasons discussed below.

From TGA scan **(Figure 3),** it was observed that the thermal degradation of organo modified montmorillonite (o-MMT) nanoclay occurs between 250 °C and 450 °C. This low temperature degradation of nanoclay is primarily due to the degradation of organic modifier part of clay. The residual mass of clay at 900 °C is about 70%. This indicates around 30% of the initial weight of the o-MMT nanoclay is organic.

During the high temperature degradation of the nanoclay added composites under an inert atmosphere, two possible reactions can occur. The first possible reaction is pyrolytic degradation of the phenolic matrix as shown in equation 2 [32].

Phenolic resin $\longrightarrow$ C (Char) + CO_2 + H_2O+ CO + CH_4 – Heat ----- (2)

At a higher heating rate or with more input heat flux, the rate of reaction (2) increases significantly [33].

Another possible reaction is that, beyond 250 °C, organic part of the nanoclay degrades as shown in equation 3 and the resultant oxygen species can react with the pristine matrix as shown in equation 4.

NH_2-$(CH_2)_3$ –Si $(O\text{-}C_2H_5)_3$ + NH_2 $(CH_2)_{17}CH_3$ $\longrightarrow$ NH_3 + NH_4-OH+ SiO_2+ O_2 +CO_2+CO ---- (3)

Phenolic matrix + O_2 $\longrightarrow$ CO_2 + H_2O+ CO – Heat ---------- (4)

In the absence of nanoclay, the limited amount of oxygen species that have evolved from reaction (2) can interact with the phenolic matrix (as shown in reaction 4) and oxidise it leading to marginal weight loss. However, when nanoclay is present, additional oxygen that was released reacts with the pristine matrix thereby increasing the rate of matrix degradation.

Thus two competing mechanisms are operating in nanoclay added composites during high temperature exposure. Up to a certain critical weight percentage (2 wt% in presence case) the hindrance offered by the nanoclay in blocking the interaction of the matrix with the oxygen dominates which results in increased thermal stability, whereas beyond the critical amount, additional degradation mechanisms triggered by the reactions (3) and (4) dominates leading to a reduction in the thermal stability of the composite. As the SAXS data is showing the nanoclay got exfoliated indicating good dispersion of nanoclay throughout the matrix, and that itself was acting as a source for generating oxidising species, the matrix degradation rate increased for type -II composites at higher loadings of the nanoclay.

3.5.6 Thermal Conductivity of Nanoclay Added Carbon Fiber–Phenolic Resin Composites

Thermal conductivity of the type -II composites is shown in **Table 3 .7**. It can be seen that the thermal conductivity of the composite is decreasing as the nanoclay content in the composite was increasing. This can be attributed to the fact that, nanoclay acts as scattering centers for the heat energy-carrying phonons [4]. This results in energy loss at these inclusions, thereby reducing the overall thermal conductivity of the composite.

Table. 3.7. Thermal conductivity data of nanoclay added C-Ph composites (type- II)

Sl. No	Composite description	Nanoclay (wt%)	Thermal conductivity (W/ m °C) at 30 °C
1	C-Ph (blank)	0	1.30
2	1 NC/ C-Ph	1	1.23
4	2 NC/C-Ph	2	1.12
3	4 NC/ C-Ph	4	1.03
5	6 NC/C-Ph	6	0.85

3.5.7 Specific Heat of Nanoclay Added Carbon Fiber –Phenolic Resin Composites

Specific heat of each composition of type - II composites was measured by differential scanning calorimetry DSC at different temperatures from 50 °C and 350 °C. **Table 3.8** shows the results of the specific heat of type - II composites samples.

Table 3.8. Results of Specific heat of nanoclay added C-Phcomposites

Composite description	Specific heat (J/Kg °C) at different temperatures						
	50 °C	100 °C	150 °C	200 °C	250 °C	300 °C	350 °C
C-Ph	915	968	1022	1104	1182	1276	1351
1 NC/ C-Ph	920	978	1055	1157	1258	1344	1419
2 NC/ C-Ph	928	986	1068	1167	1274	1356	1432
4 NC/ C-Ph	940	992	1092	1191	1292	1382	1451
6 NC/ C-Ph	980	1023	1117	1213	1311	1400	1484

Comparison of specific heat of blank C-Ph composite with different weight percentages of nanoclay added C-Ph composites were plotted and shown in **Figure 3.21.**

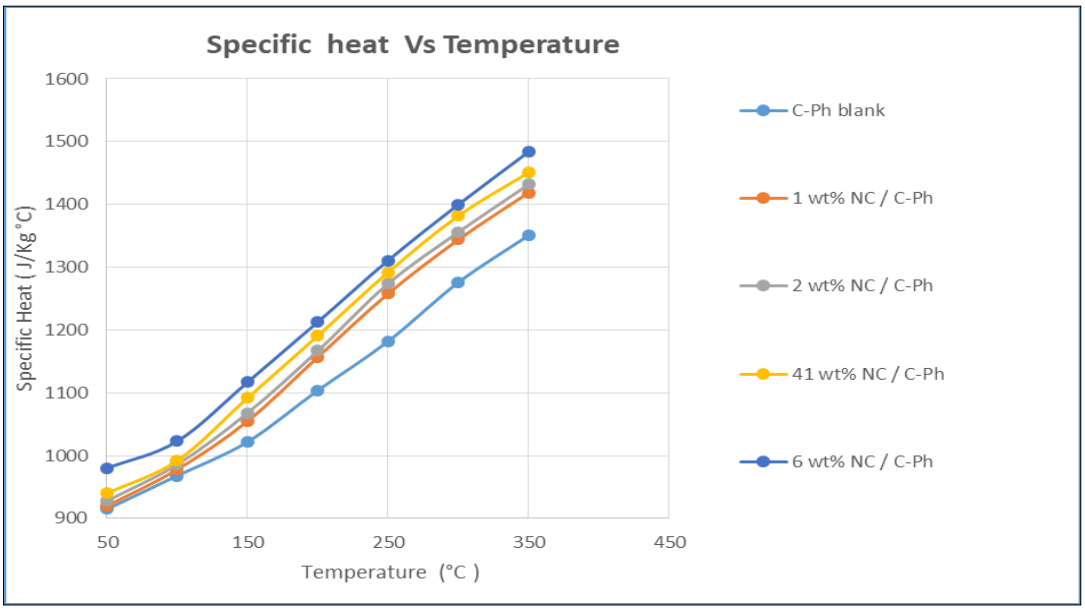

Figure 3.21. Specific heat versus temperature of nanoclay added C-Phcomposites

Specific heat has increased for 1, 2, 4, 6 wt% nanoclay added C-Ph composite by about 5.0%, 6.0%, 7.40%, and 10% respectively at 350 °C when compared to blank C-Ph composite. Thermally stable, inorganic residue of silicate layers is responsible for the enhanced value of specific heat for nanoclay added C-Ph composites. This indicates that, in comparison to standard unfilled C-Ph composites, nanoclay added C-Ph composites can have better insulating qualities.

3.5.8 ILSS of Nanoclay Added Carbon Fiber –Phenolic Resin Composites

ILSS values of individual specimens for each composition of nanoclay added C-Ph composites (type –II) are shown in **Table 3.9**. The effect of the weight percentage of nanoclay on the ILSS of type - II composite is shown in **Figure 3.22**. ILSS value increased by 29% at 2 wt% addition of nanoclay as compared to the blank sample (C-Ph composites). Beyond, 2 wt% addition of nanoclay, ILSS values have started to come down even though there is a good dispersion of nanoclay (inferred from SAXS studies). This can be understood as below.

ILSS of the layered composites is due to two factors namely

(i) The chemical binding force of matrix in keeping adjacent fabric interfaces together,

(ii) Mechanical locking between the two fabric interfaces due to overlap of the trough and peaks of the fabric weaves of two adjacent layers.

In the case of nanoclay addition up to 2 wt%, matrix content increased marginally **(Table 3.9)** while the interface area between the two adjacent layers increased significantly. This is because of the higher surface area of nanoclay. Besides, this, the chemical functional groups present in o-MMT are known to enhance the chemical bonding between the matrix to the nanoclay [33-35]. This strengthens the matrix further. Increased interfacial area between the adjacent layers, coupled with the increased matrix strength, leads to higher interfacial strength. As the matrix content has not decreased up to 2 wt% nanoclay addition, the mechanical locking between the adjacent layers is intact. This resulted in higher ILSS with the nanoclay addition.

However, beyond 2 wt% loadings of nanoclay, the interlayer mechanical locking has come down as the fiber volume fraction of the composites got reduced. This resulted in reduced ILSS. On the other hand, higher nanoclay may degrade the matrix strength itself as the higher amount of additives can hinder the crosslinking of the resin system, thereby leading to poor strength for the matrix [36].

Table 3.9 ILSS test values of o- MMT nanoclay added C-Ph composites

Specimen No	**ILSS (MPa)**				
	C-Ph	**1 NC/ C-Ph**	**2 NC/ C-Ph**	**4 NC/ C-Ph**	**6 NC/ C-Ph**
1	21	23	26	23	21
2	22	25	25	21	22
3	22	25	28	23	21
4	20	26	27	21	20
5	22	25	27	21	20
6	21	27	27	21	21
Average	**21**	**25**	**27**	**22**	**21**
Standard deveiation	**0.82**	**1.33**	**1.03**	**0.95**	**0.75**

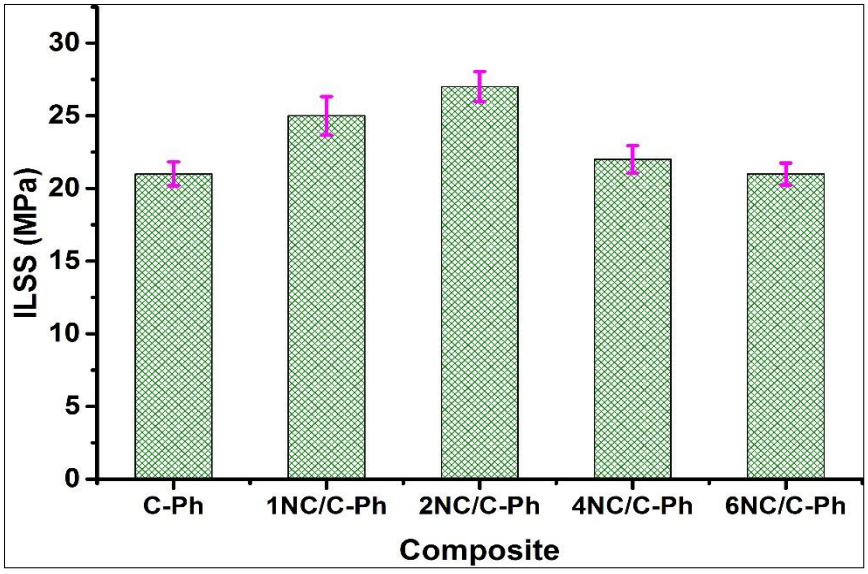

Figure 3.22. ILSS of o-MMT nanoclay added C-Ph composites

3.5.9 Flexural Strength and Modulus of Nanoclay Added C-Ph Composites

Flexural strength and flexural modulus values of individual specimens for each composition of nanoclay added C-Ph composites (type –II) are shown in **Table 3.10**. The effect of nanoclay loading on flexural strength and modulus of type -II composites are shown in **Figure 3.23**. Flexural strength increased up to 2 wt% nanoclay addition by about 12%. Flexural failure is a combination of shear, compression, tensile failure. In general, tensile strength is not known to increase significantly with nanoclay addition for the fiber reinforced composites [37]. Hence the improved flexural strength up to 2 wt% clay addition can be ascribed to the increased shear strength of the layers. As the shear strength is coming down beyond 2 wt%, flexural strength is also coming down for the composites. Besides this, reduction in the fiber volume fraction at higher loading of the nanoclay also contributed to the reduced flexural properties of the composites.

Flexural modulus also increased up to 2 wt% addition of nanoclay to C-Ph composites even though there is a slight reduction in the fiber volume fraction as compared to the blank C-Ph composite. As the carbon fiber is the main contributor to the strength/modulus, an increase in these properties even when the carbon fiber volume fraction is reducing is indicating that, clay galleries present in the composite are acting as a source for higher and efficient stress transfer between fibers to the matrix. This enabled in harnessing the maximum ability of reinforcement against the applied bending forces which resulted in higher flexural modulus for the composites added with the limited amount of nanoclay (up to 2 wt%). As there is a huge reduction in the fiber volume fraction of the composites beyond 2 wt% addition of nanoclay, the positive

contribution of the nanoclay towards the modulus improvement got nullified and thus there is a net reduction of modulus was observed.

Table 3.10 Flexural strength (FS) and Flexural modulus (FM) of o- MMT nanoclay added C-Ph composites

Specimen No	C-Ph		1 NC/ C-Ph		2 NC/ C-Ph		4 NC/ C-Ph		6 NC/ C-Ph	
	FS (MPa)	FM (GPa)	FS (MPa)	FM (GPa)	FS (MPa)	FM (GPa)	FS (MPa)	FM (GPa)	FS (MPa)	FM (GPa)
2	410	61	408	61	485	66	387	46	393	43
2	405	62	446	62	454	63	406	47	383	45
3	438	62	415	62	462	65	384	48	385	42
4	404	61	438	60	482	65	394	47	385	42
5	430	58	408	60	447	65	381	48	390	43
Average	**417**	**61**	**423**	**61**	**466**	**65**	**390**	**47**	**387**	**43**
Standard deviation	**15.58**	**1.64**	**17.80**	**1.0**	**16.86**	**1.09**	**9.96**	**0.84**	**4.15**	**1.09**

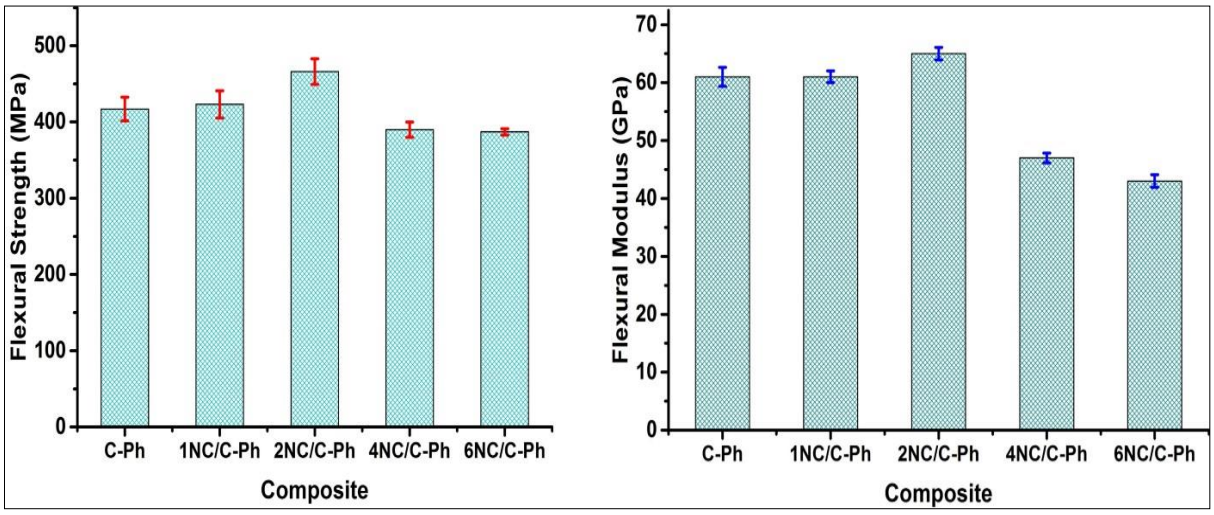

Figure 3.23. Flexural strength and Flexural modulus of nanoclay added C-Ph composites (type-II composites)

3.5.10 Effect of Nanoclay Content on Mass Ablation Rate of Type-II Composites

The results of the mass ablation rate of blank carbon fiber - phenolic resin composite and nanoclay added carbon fiber - phenolic composites tested for mass ablation rate at a low heat flux 125 W/cm^2 and high heat flux 500 W/cm^2 are presented in **Table.3.11.**

Table 3.11 Mass ablation rate of o- MMT nanoclay added C-Ph composites

Sl. No	Composite description	Nanoclay (wt%)	Mass ablation rate (mg/sec) at heat flux :125 W/cm^2	Mass ablation rate (mg/sec) at heat flux :500 W/cm^2
1	C-Ph (blank)	0	100	138
2	1 NC/ C-Ph	1	110 (10)*	168 (27)*
3	2 NC/ C-Ph	2	110 (10)*	176 (22)*
4	4 NC/ C-Ph	4	130 (30)*	233 (69)*
5	6 NC/ C-Ph	6	135 (35)*	213 (54)*

****Values shown in parenthesis indicate a percentage of increase in mass ablation rate as compared to blank.***

The mass ablation rates have increased with an increasing weight percentage of nanoclay content in type - II composites when compared to blank type -II composites at both heat fluxes 125 W/cm^2 and 500 W/cm^2. During the oxy-acetylene torch ablation, several degradation processes operate simultaneously. The first one is the chemical degradation of composite which involves endothermic pyrolysis of phenolic resin matrix into char and other gaseous products as shown in equation (2). Another one is mechanical erosion and removal of the char and fibers. The microstructure of the ablated surface gives inference on the mechanisms operated during the ablation. Ablation mechanisms are discussed in light of the microstructure of the ablated surface in the subsequent sections.

3.5.11. Microstructural Behaviour of Ablated Surface of Nanoclay Added C-Ph Composites

The microstructure of the ablated surface gives inference on the mechanisms operated during the ablation. **Figure 3.24** depicts the microstructures of ablated surfaces.

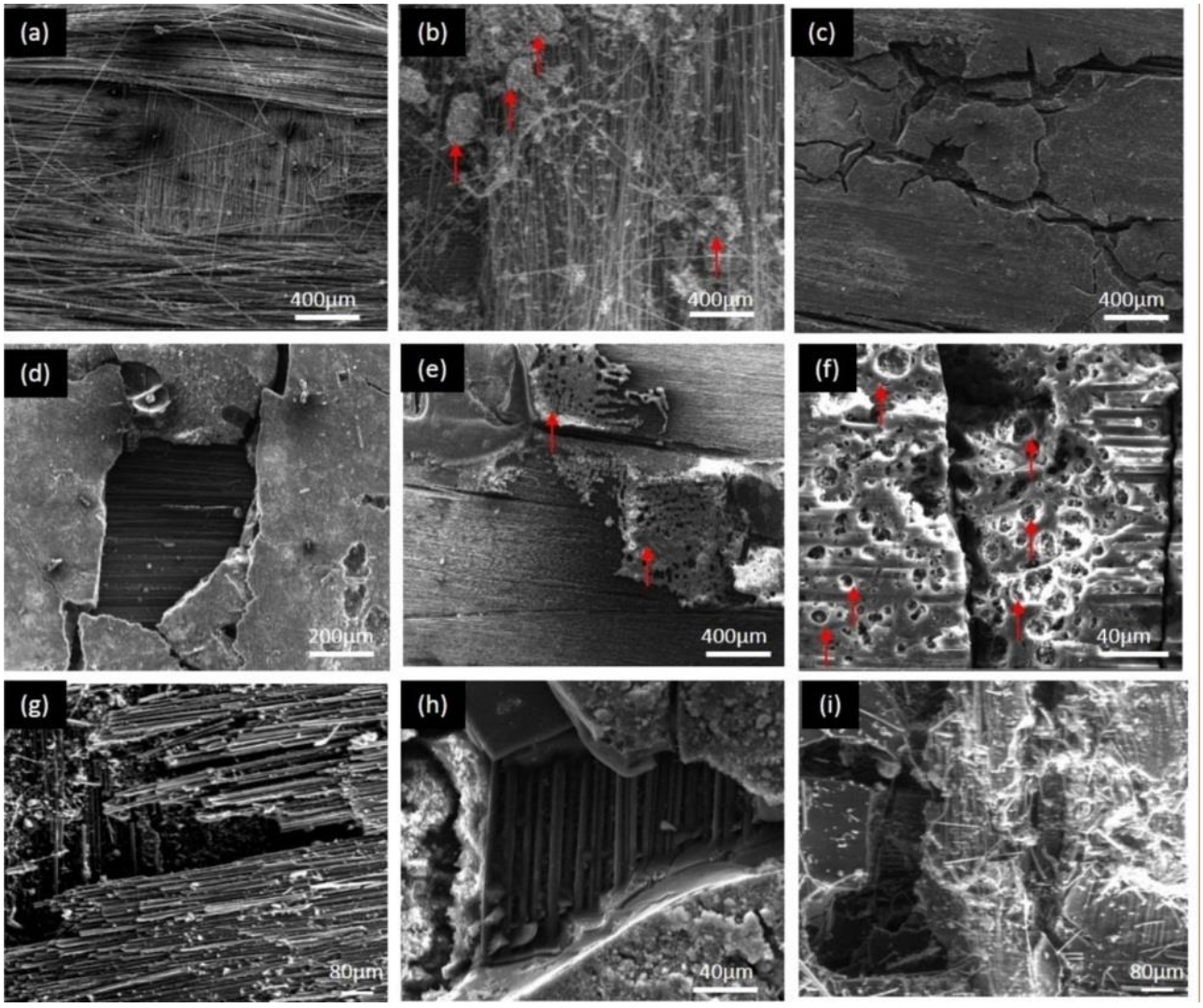

Figure 3.24. Showing SEM images of the ablated samples (a) blank C-Ph after ablation test at 125 W/cm^2 (b) blank C-Ph after ablation test at 500 W/cm^2 (c) 2 wt% nanoclay added C-Ph showing loosely held char after ablation test at 125 W/cm^2 (d) 4 wt% nanoclay C-Ph showing patches of char free zones after ablation test at 125 W/cm^2 (e) and (f) 2 wt%, 4 wt% nanoclay C-Ph showing porous char after ablation testing at 125 W/cm^2 respectively (g) 2 wt% nanoclay C-Ph showing severe damage to fibers after ablation testing at 500 W/cm^2 (h) and (i) 4 wt% and 6 wt% nanoclay added C-Ph composites showing deep pits formed after ablation testing at 500 W/cm^2 due to self-propagating ablation zones

In the case of blank C-Ph, at low heat flux, fibers are intact after ablation, whereas at high heat flux fiber breakage can be seen (as indicated with arrows in **Figue 3.24**). This resulted in a slightly increased ablation rate **(Figure 3.24.a and b)** for blank C-Ph composite. Mass ablation rates have increased marginally up to 2 wt% nanoclay addition as compared to the blank C-Ph at low heat flux. Microstructure of the ablated surfaces indicates that there is no appreciable damage to the composite surface for 1 wt% of nanoclay added C-Ph as compared to the C-Ph composites loaded with high wt% of nanoclay. However, there is a marginal increase in ablation rates even at 2 wt% nanoclay loading (**Figure 3.24.c to 3.24.i).** This could be attributed to the fact that char formed in presence of nanoclay is found to be brittle with many cracks, which flies off leading to increased mass ablation rate. Beyond 2 wt% nanoclay loading, mass ablation rates increased drastically even when the heat flux for ablation testing was low.

On the other hand, at higher heat flux, mass ablation rates have increased drastically at all levels of nanoclay loading. One possible explanation given by previous researchers for increased ablation rate for the nano silica added C-Ph composites is the reaction of the char with silica forming silicon carbide as shown in reaction 5 [4,7]. Since nanoclay contains a significant amount of silica, similar reactions are possible. However, XRD data of the ablated samples show the formation of SiC only at 6 wt% addition of nanoclay to C-Ph composites that too at a very low concentration (as inferred from the intensities of the XRD peaks of **Figure 3.25).**

$$SiO_2 + 3C \longrightarrow SiC\ (Solid\ State) + 2\ CO \quad \text{--------} \ (5)$$

Hence, the observed trends in the increased ablation rates with the nanoclay addition are to be understood based on the mechanisms as given below.

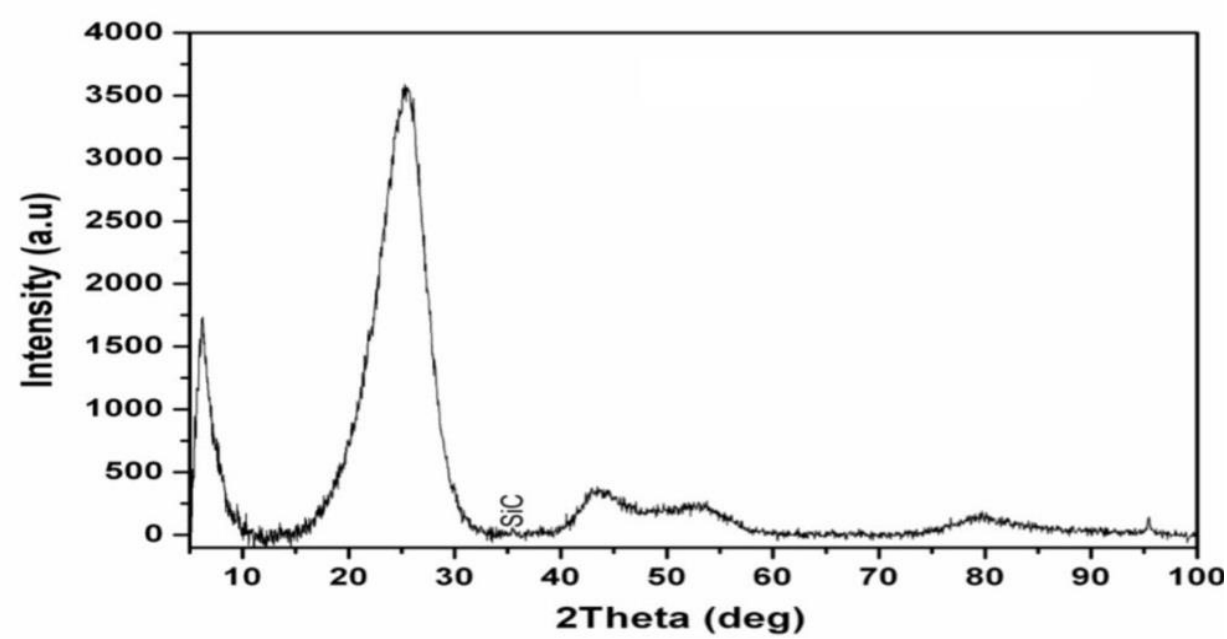

Figure 3.25 XRD of the ablated surface of 6 wt% nanoclay added carbon- phenolic composite

The mechanism I: As the nanoclay amount is increasing in the type-II composites, thermal conductivity is coming down **(Table 3.7).** This results in poor propagation of heat energy through the thickness of the composite. As the heat energy is localised, effective conversion of the matrix into char is higher in the nanoclay added composites. Thus by the time the ablation front advances, the conversion of the matrix into char is complete with no traces of pristine matrix present. As the matrix that is binding the composite is absent in the ablation front, large chunks of the ablated surface were flying off leading to a higher ablation rate **(Figure 3.24, Table 3.11).** At higher flux and higher nanoclay content, this effect was more pronounced. This is because, at higher nanoclay content, the lower thermal conductivity of the composite confines more heat energy in the vicinity of the advancing ablation front thereby creating a fully charred matrix.

Mechanism II: During the ablation, from the surface of the ablating material towards the core char front and heat front will form with the later moving ahead of the former. In the heat front zones, with the rise in the temperature, organic part of the nanoclay starts degrading as per the reaction.3. The oxygen that was available due to nanoclay decomposition, oxidises the matrix in the charred front as shown in reaction 4. Due to the removal of the matrix, large craters/perforations forms in the charred front **(Figure 3.24**). This perforation allows non-uniform exposure of the buried layers (char front) present under the ablation front to the flame, leading to selective acceleration of reactions 3 and 4 at these zones. This allows more heat to reach these zones directly from the ablation front. This results in one more cycle of decomposition of the organic part of the nanoclay, reaction of resultant oxygen with char, and

its transformation to a gaseous product leading to an increase in the depth of the crater. This repeated cycle of self-propagating mechanism leads to removal of large chunks of matrix and fibers which forms pits thus leading to increased ablation rate. This mechanism becomes more severe at high clay content and higher flux. This can be evidenced by the fact that the ablated surface of 2 wt% nanoclay got severely damaged with large pits in case of high heat flux as compared to the minimum damage without surface pits in case of low heat flux ablation **(Figure 3.24).**

Thus, as the amount of the nanoclay was increasing, the degradation rate of the matrix was increasing. On the other hand, when the heat flux increased, the energy required for reactions 2 and 3 were supplied at a faster rate thereby increasing the overall ablation rate. Thus both higher nanoclay content, as well as higher flux, were imparting higher ablation rate to the type -II composites.

3.6. Conclusions: This study has been carried out using organo montmorillonite nanoclay as filler in carbon fiber reinforced phenolic (type -II) composites. The influence of parameters such as the amount of loading of nanoclay in type -II composites was studied on mechanical, thermal, and ablation properties. Type-I composites were prepared by adding different amounts of nanoclay to the pure phenolic matrix. Changes in the viscosity of the phenolic resin due to nanoclay addition were correlated with the mechanical properties of the type -II composites. The thermal stability of o-MMT nanoclay, as well as type -I composites, was correlated with the thermal and ablative properties of type -II composites. The results obtained in this research work are summarised as below.

- 2 wt% nanoclay as filler is optimum in carbon fiber– phenolic resin composites for increased mechanical properties, thermal stability without much compromising on ablative properties.
- Thermal insulation of carbon fiber – phenolic resin composites increases due to nanoclay addition which is the intended attribute for thermal protection systems. However, oxidative degradation of organic part of nanoclay accelerates the ablative degradation of host composite.
- Ablative performance of nanoclay added carbon fiber–phenolic resin composites varies significantly as a function of heat flux used for ablation testing. Higher heat flux (500 Watts/cm^2 in the present study) and higher loading of nanoclay (beyond 2 wt% in the present study) results in increased ablation rate for nanoclay added carbon-phenolic composite.

References

1. G.Pulci, J.Tirillo, F.Marra, F.Fossati, C. Bartuli, and T.Valente. Carbon-phenolic ablative materials for re-entry space vehicles: Manufacturing and Properties. Composites: Part A. 2010; 41, 1483-1490.

2.Asaro L, Rivero G, Manfredi LB, ES Rodrı´guez**.** Study of the ablative properties of phenoliccarbon composites modified with mesoporous silica particles**.** Journal of Composite Materials. 2018; 52, 4139-4150.

3**.** Eslami Z, Yazdani F and Mirzapour MA. Thermal and mechanical properties of phenolic-based composites reinforced by carbon fibers and multiwall carbon nanotubes. Composites Part A, 2015, 72, 22–31.

4. I. Srikanth, Alex Daniel, Suresh Kumar, N. Padmavathi, Vajinder Singh, P. Ghosal, Anil Kumar, and G. Rohini Devi. Nano Silica modified carbon–phenolic composites for enhanced ablation resistance. Scripta Materials. 2010; 63, 200-203.

5. Natali M, Monti M, Puglia D, Kenny JM, Torre L. Ablative properties of carbon black and MWNT/Phenolic composites: A comparative study. Composites Part A. 2012; 43, 174-182.

6. I. Srikanth, N. Padmavathi, Suresh Kumar, P. Ghosal, Anil Kumar, Ch. Subrahmanyam. Mechanical, thermal and ablative properties of zirconia, CNT modified carbon/phenolic composites. Composites Science and Technology. 2013; 80, 1-7.

7. A.Mirzapour, M.H.Asadolahy, S.Baghshahi, M.Akbari. Effect of nanosilica on the microstructure, thermal properties and bending strength of nanosilica modified carbon fiber /phenolic nanocomposite. Composites: Part A. 2014**;** 63, 159-167.

8. Yao Peng, Wen Wang, and Jinzhen Cao. Preparation of lignin−clay complexes and its effects on properties and weatherability of wood flour/polypropylene composites. Industrial and Engineering Chemistry Research. 2016; 55, 9657-9666.

9. Ali Asghar Jahangiri and Yasser Rostamiyan. Mechanical properties of nano-silica and nano-clay composites of phenol formaldehyde short carbon fibers. Journal of Composite Materials. 2020, 54; 1339-1352.

10. Zahra Eslami, Farshad Yazdani, Mir Aidin Mirzapour. Thermal and mechanical properties of phenolic-based composites reinforced by carbon fibers and multiwall carbon nanotubes. Composites: Part A. 2015**;** 72, 22-31.

11. Carolina Simón-Herrero, Laura Gómez, Amaya Romero, José Luis Valverde and Luz Sanchez-Silva. Nanoclay-based PVA aerogels: synthesis and characterization. Industrial

and Engineering Chemistry Research. 2018; 57, 6218-6225.

12. Yasser Rostamiyan, Abdolhosein Fereidoon, Masoud Rezaeiashtiyani, Amin Hamed Mashhadzadeh, Azam Salmankhani. Experimental and optimizing flexural strength of epoxy-based nanocomposite: Effect of using nano silica and nano clay by using response surface design methodology. Materials and Design. 2015; 69, 96–104.

13 F.Carrasco, P. Pages. Thermal degradation and stability of epoxy nanocomposites: Influence of montmorillonite content and cure temperature. Polymer Degradation and Stability. 2008; 93, 1000-1007.

14. Zhihao Zhang, Guozhong Ye, Hossein Toghiani, Charles U. Pittman, Jr. Morphology and thermal stability of novolac phenolic resin/clay nanocomposites prepared via solution high-shear mixing. Macromolecular Materials and Engineering. 2010; 295, 923–933.

15. Anna Czerniecka-Kubicka, Wiesław Frącz, Marek Jasiorski, Wojciech Bła żejewski Barbara Pilch-Pitera, Marek Pyda, Iwona Zarzyka. Thermal properties of poly (3 hydroxybutyrate) modified by nanoclay. J. Thermal Calorimetry. 2017; 128, 1513- 1526.

16. Mitra Yoonessi, Hossein Toghiani, William L. Kingery, and Charles U. Pittman, Jr. Preparation, characterization, and properties of exfoliated/delaminated organically modified clay/dicyclopentadiene resin nanocomposites. Macromolecules. 2004; 37, 2511-2518.

17. P. Strove and Y.C. Ke. Polymer-Layered silicate and silica nanocomposites. Elsevier, Netherlands, 2005.

18. RV. Kurahatti, A.O. Surendranathan, S. A. Kori, Nirbhay Singh. A.V. Ramesh Kumar and Saurabh Sri. Defence applications of polymer nanocomposites, Defence Science Journal. 2010; 60, 551-563.

19. LI- Yu Lin, Joong – Hee Lee, Chang-Eui Hong, Gye-HyoungYoo, Suresh G. Advani. Preparation and characterization of layered silicate/glass fiber/epoxy hybrid nanocomposites via vacuum-assisted resin transfer moulding (VARTM). Composite Science and Technology. 2006; 66, 2116-2125.

20. Ahmad Reza Bahramian. Mehrdad Kokabi. Ablation mechanism of polymer layered silicate nanocomposites heat shield. Journal of Hazardous Materials. 2009; 166,445-454.

21. Hai-jun Lu, Guo-Zheng Liang, Xiao-yan Ma, Bao-yan Zhang, and Xiang-bao Chen. Epoxy/clay nanocomposites: further exfoliation of newly modified clay induced by shearing force of ball milling. Polymer International. 2004; 53, 1545–1553.

22.Yu-Chen Lee, Chia-Lung Kuo, Shaw-Bing Wen, Chih-Peng Lin. Changes of organo-montmorillonite by ball-milling in water and kerosene. Applied Clay Science. 2007; 36, 265–270.

24. Luiza MP Campos, Letı´cia C Boaro, Tamiris MR Santos, Pamela A Marques, Sonia RY Almeida, Roberto R Bragaand Duclerc F Parra. Evaluation of flexural modulus, flexural strength and degree of conversion in BISGMA/TEGDMA resin filled with montmorillonite nanoparticles. Journal of composite materials. 2016; 51, 927-937.

24. L. Le Pluart, J. Duchet, H. Sautereau, P.Halley, and J.-F. Gerard. Rheological properties of organoclay suspensions in epoxy network precursors. Applied Clay Science. 2004; 25, 207– 219

25. S. T. Knauert, J. F. Douglas, and F. W. Starr. The effect of nanoparticle shape on polymer - nanocomposite rheology and tensile strength. Journal of Polymer Science, Part B: Polymer Physics. 2007; 45, 1882–1897.

26. L Asaro, G Rivero, LB Manfredi, VA Alvarez, and ES Rodriguez. Development of carbon fiber /phenolic resin prepregs modified with nanoclays. Journal of Composite Materials. 2016; 50, 1287-1300.

27.Temina Mary Robert, M.Satheesh Chandran, S.Jishnu, K.Sunitha, R.S.Rajeev, Dona Mathew, N. Sreenivas, L. Aravindakshan Pillai and C. P. Reghunadhan Nair. Nanoclay modified silica phenolic composites: mechanical properties and thermal Response under simulated atmospheric re-entry conditions. Polymers Advanced Technologies. 2014; 26, 104-109.

28.Shahryar Pashaei, Siddaramaiah, and Akheel Ahmed Syed. Investigation on thermal, mechanical and morphological behaviours of organo nanocly incorporated epoxy nanocomposites. ARPN Journal of Engineering and Applied sciences. 2010; 5, 76-86.

29. Ahmed Akelah, Ahmed Rehab, Mohamed Abdelwahab & Mohamed A.Betiha. Synthesis and thermal properties of nanocomposites based on exfoliated organoclay polystyrene and poly (methylmethacrylate). Nanocomposites. 2017; 3, 20-28.

30. M.S. Senthil Kumar, N. Mohana Sundara Raju, P.S. Sampath, M.Chithirai Pon Selvan. Influence of nanoclay on mechanical and thermal properties of glass fiber reinforced polymer nanocomposites. Polymer Composites. 2016; 39, 1861-1868.

31. Brody K. Bessire, Sridhar A. Lahankar, and Timothy K. Minton. Pyrolysis of phenolic imprenated carbon ablator (PICA). Applied Materials and Interfaces. 2014;7, 1383-1395.

32. Brody K Bessire, and Timothy K. Minton. Decomposition of phenolic impregnated carbon ablator (PICA) as a function of temperature and heating rate. Applied Materials and Interfaces. 2017; 9, 21422-21437.

33. Yongsheng Zhao, Kejian Wang, Fuhua Zhu, Ping Xue, Mingyin Jia. Properties of Poly (Vinyl chloride)/ wood flour/montmorillonite: effect of coupling agents and layered silicate. Polymer Degradation and Stability. 2006; 91, 2874-2883.

34. Q. Wu, Y. Lei; F. Yao; Y. Xu; K. Lian. Properties of HDPE/clay/wood nanocomposites, J. Plastic Technology. 2007; 27, 108-124.

35. Yong Lei, Qinglin Wu, Craig M. Clemons, Fei Yao, Yanjun Xu. Influence of nanoclay on properties of HDPE/wood composites. Journal of Applied Polymer Science. 2007; 106, 3958-3966.

36.Tsutomu Takuchi, Rachibzeidan, Tarek Agag. Polybenzoxazine/clay hybrid nanocomposites: Influence of preparation method on curing behaviour and properties of polybenzoxazines. Polymer. 2002; 43, 45-53.

37. Jeena Jose Karippal, H.N. Narasima Murthy, K.S Rai, M.Sreejith and M. Krishna. Study of mechanical property of epoxy/glass/nanoclay hybrid composites. Journal of Composite Materials. 2011; 45, 1893-1899.

Chapter - IV

Organo Montmorillonite Nanoclay Added Carbon Fiber – Cyanate Ester Resin Composites

Preparation and Characterisation of Organo Montmorillonite Nanoclay Added Carbon Fiber – Cyanate Ester Resin Composites

4.0 Introduction: One of the alternate choices for the phenolic ablative matrix is cyanate ester resin, which is an addition cured thermoset polymer synthesized by the reaction of phenolic resin with cyanogen bromide [1, 2]. Though, extensive research work was carried out in the area of cyanate ester resin –nanoclay composites, very limited research work was reported in the area of nanoclay added carbon fiber-cyanate ester (C-CE) resin composites. Since nanoclay is widely known to improve the thermomechanical properties of the composites used for thermal protection systems (TPS), the objective of the research is to investigate the effects of nanoclay on the thermomechanical characteristics of C-CE. For nanoclay to act as an efficient ablation inhibitor in TPS, its melting and formation of glassy phases are critical. Nanoclay is known to form a glassy phase at high heat flux when compared to low heat flux [3]. Thus, its performance as an ablation inhibitor may be higher at high heat flux. So far there are no studies reported on the effect of heat flux on the ablation performance of the nanoclay added polymer matrix composites. This chapter is aimed at addressing this gap. Hence, preparation and characterisation of organo montmorillonite nanoclay added carbon fiber-cyanate ester composites is taken up in the present study.

4.1 Materials: Major raw materials used in this work are cyanate ester resin, PAN based carbon fabric, and surface modified montmorillonite (o-MMT) nanoclay. Detailed specifications for each of the raw materials are give below.

4.1.1 Cyanate Ester Resin: Novolac phenolic based cyanate ester resin (PT 30 S) was selected as a matrix of composites. Cyanate ester resin has solid resin content of about 75 wt% and methyl ethyl ketone solvent content of about 25%. Cyanate ester resin has high thermal stability and char yield of about 64 wt% at a temperature of 1000 °C in an inert atmosphere. The technical specifications of cyanate ester resin are as given below.

Sl.No	Test Parameter	Specification
1	Chemical name	Cyanate ester resin
2	Viscosity at 30 °C	30 cP
3	Specific gravity at 30 °C	1.2
4	Solid resin content	75 (% by weight)
5	Volatile content	25 (% by weight)
6	Gel time at 200 °C	30 minutes
7	Commercial name	PT 30S

The resin was procured from M/s Lonza Pvt Ltd, Switzerland and it was used without any modification in the present study. The chemical structure of cyanate ester resin is shown in **Figure 4.1.**

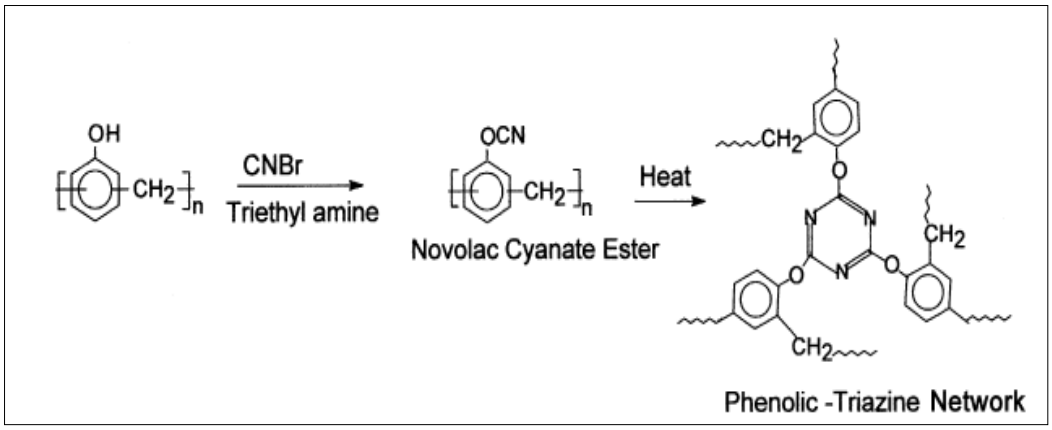

Figure 4.1. The chemical structure of Novolac cyanate ester resin

4.1.2 PAN Based Carbon Fabric: A polyacrylonitrile (PAN) based high strength carbon fabric (bidirectional) woven with 3K fiber of T-300 grade was chosen for the manufacturing of three-phase (carbon fiber – cyanate ester resin-nanoclay) composites. The technical specifications of the fabric are given below.

S. No	Test Parameter	Specification
1	Tow type	3k (3000 filaments in tow)
2	Grade of carbon fiber	T- 300 Fiber (M/s Torayca carbon)
3	Thickness of fabric	0.38 ± 0.05 mm
4	Areal density	380 ± 20 g/m^2
5	Fabric weave style	8 Harness satin
6	Fabric count (warp direction)	24 ± 1 Ends /inch
7	Fabric count (weft direction)	24 ± 1 Ends /inch
8	Fabric breaking strength	250-300 kg/inch (in both warp &weft)
9	Carbon content	93 wt%
10	Density	1.8 g/cc

PAN based woven carbon fabric was procured from M/s Urja Products Pvt Ltd, Ahmedabad, India and it was used without any modification in the present study. The image of fabric is shown in **Figure 4.2.**

Figure 4.2 PAN based woven carbon fabric

4.1.3 Organo Modified Montmorillonite (o- MMT) Nanoclay: o-MMT nanoclay used in this study is nanomer 1.31 PS. Nanomer 1.31PS nanoclay was surface-modified montmorillonite (o-MMT) with 0.5-5 wt% aminopropyltriethoxysilane, 15-35 wt% octadecyl amine. The nanoclay (Nanomer 1.31 PS) was supplied by Sigma-Aldrich Chemical Pvt Limited, Hyderabad, India. Brief specifications of the Nanomer 1.31PS nanoclay are given below.

S. No	Test Parameter	Specification
1	Appearance	Off white free-flowing powder
2	Surface modifier	Octadecyl ammonium /silane
3	Bulk density	250-300 kg/m^3
4	Specific gravity	1.9
5	Particle size (mean)	14-18 micron

Figure 4.3 depicts the structure and composition of organo modified montmorillonite (o-MMT) nanoclay.

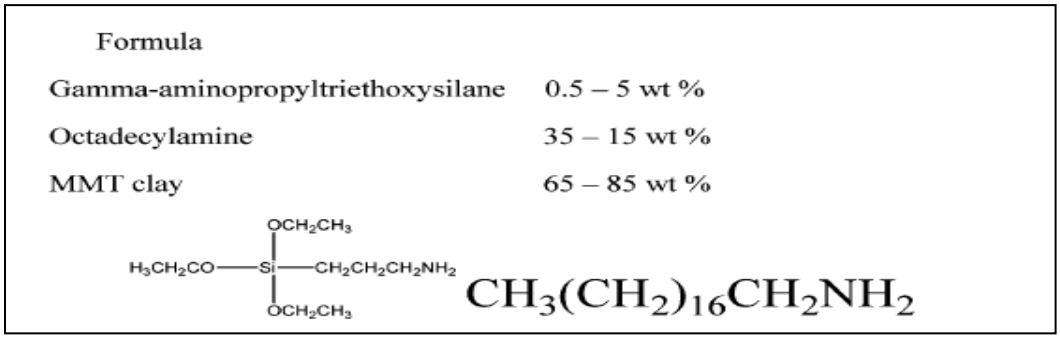

Figure 4.3. Structure and composition of organo modified montmorillonite nanoclay

4.2 Experimental Work: The flow chart below provides a quick overview of the experimental work carried out.

Flow chart: Schematic flow of experimental work

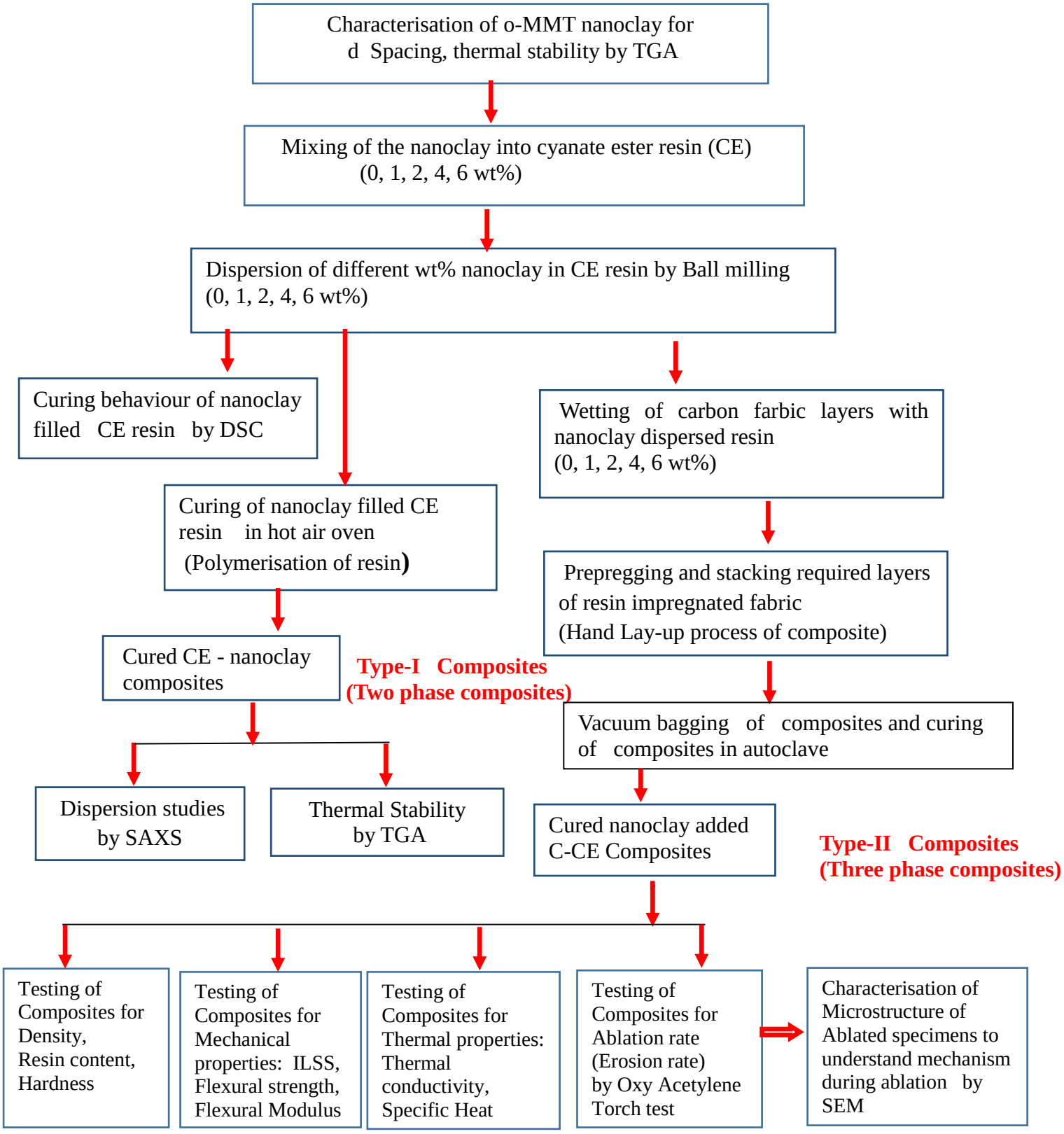

4.2.1. Dispersion of Nanoclay in Cyanate Ester Resin: Approximately 198 grams of cyanate ester resin and 2 grams of o-MMT nanoclay were taken into a 500 ml stainless steel (SS) bowl for preparation of 1 wt% nanoclay filled cyanate ester resin. This mixture was initially stirred with a glass rod for approximately 5 mins. Then this mixture along with the bowl was placed into a planetary ball mill (M/s Insmart Systems) and ball milled for 2 h at 250 rpm using SS balls. Ball to charge ratio was maintained at 0.5:1. Thus, four different o-MMT nanoclay CE resin compositions were prepared by adding 1, 2, 4, and 6 wt% of nanoclay to CE resin. The composition of two-phase (cyanate ester resin - nanoclay) composites are given in **Table 4.1.**

Table 4. 1. The composition of cyanate resin-nanoclay composites (Type - I).

Composite designation	**Nanoclay (NC) (wt%) loading in resin**	**Composition**
Cyanate ester resin (CE)	0	
1 NC - CE	1	99 g of resin + 1 g of nanoclay
2 NC - CE	2	98 g of resin + 2 g of nanoclay
4 NC - CE	4	96 g of resin + 4 g of nanoclay
6 NC - CE	6	94 g of resin + 6 g of nanoclay

Viscosity changes to the cyanate ester resin due to the nanoclay addition were measured using Brookfield viscometer at 30 °C.Typical measurement of viscosity of 4 wt% nanoclay filled CE resin by Brookfield viscometer is shown in **Figure 4.4.**

Figure 4.4 Measurement of viscosity of 4 wt% nanoclay filled CE resin by Brookfield viscometer.

4.2.2. Preparation of Cyanate Ester Resin - Nanoclay Composites (Type -1)

Nanoclay dispersed cyanate resin was poured into a petri dish and the volatiles were allowed to evaporate by heating the mixture to 60 °C for one hour. Subsequently, nanoclay resin was cured in a hot air oven by heating the resin to 120 °C for 1 hour, 150 °C for 1 h, and 177 °C for 3 h and then cooled to room temperature. To ensure complete polymerisation of the resin, samples further post cured at 100 °C for 30 minutes, 150 °C for 30 minutes, 200 °C for 30 minutes, and 250 °C for 3 h. Thus, four different variants of type-I composites were prepared along with a blank cyanate ester resin matrix sample. Details of the prepared type -I composites are given in **Table 4.1**. Cured cyanate ester resin and cyanate ester resin - nanoclay composites are shown in **Figure 4.5**.

Figure 4.5 Cured cyanate ester resin and cyanate ester resin - nanoclay composites

These type -I composites were used for characterisation of dispersion studies of nanoclay in resin by SAXS, SEM and thermal stability by the thermogravimetric analysis (TGA).

4.2.3. Preparation of Nanoclay Added Carbon Fiber - Cyanate Ester Resin Composites (Type-II).

Carbon fabric (thickness 0.38 mm) layers having a size of 300 x 300 mm were cut and impregnated with nanoclay dispersed cyanate ester resin. Twelve such layers were stacked on a flat metal plate by hand lay-up process. These stacked layers were subjected to vacuum bagging, followed by curing in the autoclave. Curing was carried at 120 °C for 1h, 150 °C for 1 h, 177 °C for 3 h under a pressure of five bar and vacuum of one bar and then cooled to room temperature. Cured composites were again post cured to get complete polymerization as per the post cure cycle mentioned for type -I composites. Thus, five different variants of the type -II composites were prepared along with the blank carbon fiber - cyanate ester resin composite. Details of the prepared type -II composites are given in **Table 4.2.**

Table 4.2 Details of the prepared nanoclay added carbon fiber - cyanate ester resin composites (Type-II)

Composite designation	**Nanoclay(NC) (wt%) in resin**	**Composition**
C-CE (blank)	0	Carbon Fabric + Resin
1 NC/ C-CE	1	Carbon Fabric + Resin+ 1 wt% nanoclay
2 NC/ C-CE	2	Carbon Fabric + Resin+ 2 wt% nanoclay
4 NC/ C-CE	4	Carbon Fabric + Resin + 4 wt% nanoclay
6 NC/ C-CE	6	Carbon Fabric + Resin + 6 wt% nanoclay

Blank carbon fiber - cyanate ester resin composite and different weight percentages of nanoclay added carbon fiber - cyanate ester resin composite (type -II) are shown in **Figure 4.6.**

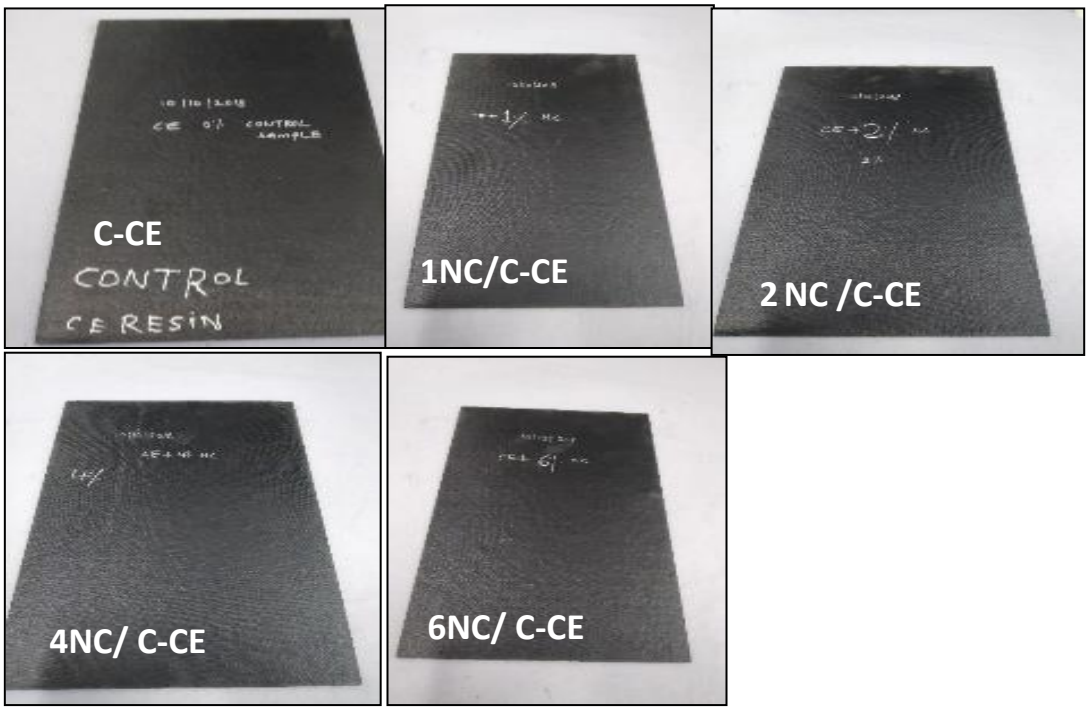

(Size of each composite: 300 mm x 300 mm x 4 mm)

Figure 4.6. Nanoclay added carbon fiber - cyanate ester resin composites (Type -II)

4.3 Characterisation and Testing

4.3.1 Curing Behaviour of Cyanate Ester Resin-Nanoclay Composites

Differential scanning calorimetry (DSC: M/s TA instruments, Q200) was used to monitor the curing reaction of the neat resin and cyanate ester resin - nanoclay composites (type-I). DSC runs were carried out from 30 to 400 °C with a sample mass of 10 ± 2 mg at a heating rate of 10 °C /min under nitrogen flow of 50 mL/min.

4.3.2 Dispersion Studies of Nanoclay in Cyanate Ester Resin- Nanoclay Composites

Type-I composites were evaluated for the dispersion of the nanoclay in resin using small angle X-ray scattering (SAXS: Antonpaar, Model: SAXS Point 2.0) by scanning the samples from 1° to 10°. Dispersion of clay in cyanate ester resin was studied with a scanning electron microscope (SEM) (Table Top SEM, Make: SEC, Korea, Model: SN4500 Plus) to identify clay particles in type -I composites. Before SEM studies, the surface of the samples was coated with a thin gold film with a sputtering unit (Make: M/s Hind HiVacuum India, Model: Scancoat Six) to increase surface conductivity.

4.3.3 Density and Fiber Volume Fraction of Type-II Composites

Density and fiber volume fraction of type -II composites were determined as per ASTM D792 and ASTM D 3171 respectively.

4.3.4 Thermal Stability Test of Type -I and Type -II Composites

Thermal stability of type -I and type -II composites in nitrogen atmosphere were evaluated. A sample mass of approximately 10 mg was collected from the composites. Thermogravimetric analysis (TGA) runs were carried out for these samples, from room temperature to 900 °C at a heating rate of 10 °C /min under a continuous flow of nitrogen (flow rate 60 ml/min). Weight of the carbonaceous char (CR) and temperature at which 5% weight loss ($T_{5\,\%}$ /°C) observed for the samples were recorded. The thermal stability of the o-MMT nanoclay as received was also carried out by TGA.

4.3.5 Interlaminar Shear Strength and Flexural Strength of Type -II Composites

ASTM D 2344 was followed for interlaminar shear strength (ILSS) test, whereas for the flexural strength test, ASTM D 790 was followed for testing of type-II composites. Tests were carried out with UTM (M/s ADMET Model 2505). From each of the fabricated type -II

composite, six samples were tested. The average value and standard deviation were calculated for each of the compositions.

Figures 4.7 and 4.8 show images of ILSS test specimens and flexural test specimens of type - II composite, respectively.

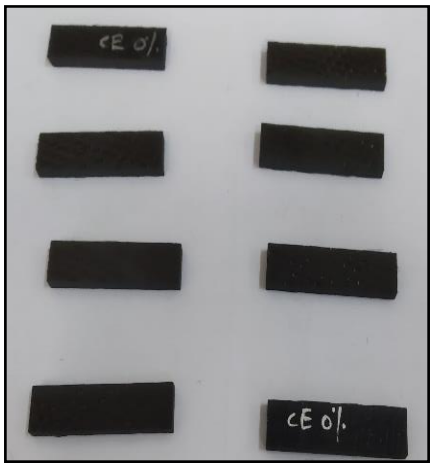

C-CE

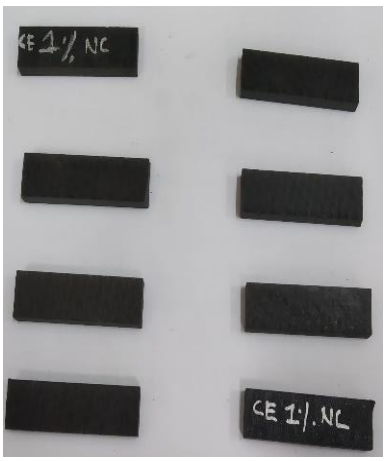

1 wt% NC/ C-CE

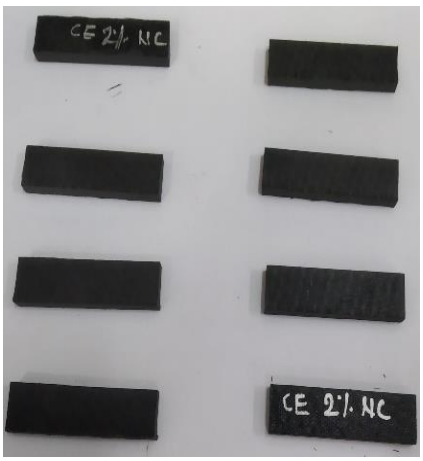

2 wt% NC/ C-CE

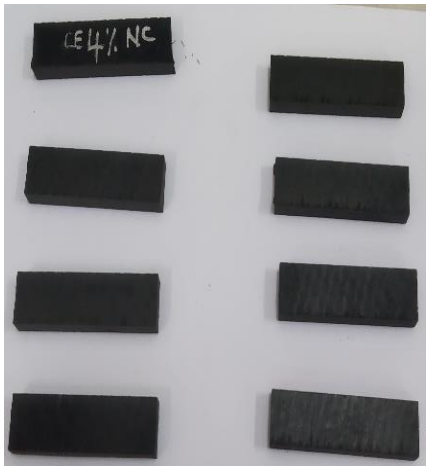

4 wt% NC/ C-CE

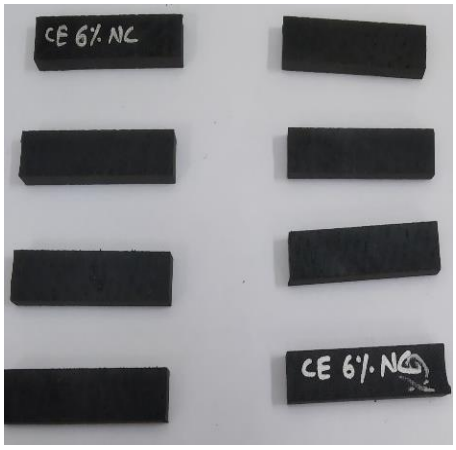

6 wt% NC/ C-CE

(**Size of each specimen: 40 mm x 10 mm x 4 mm)**

Figure 4.7 ILSS test specimens of nanoclay added carbon fiber-cyanate ester resin composites

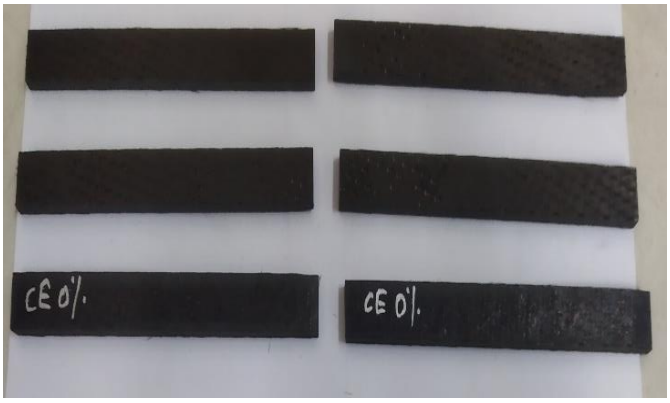

C-CE

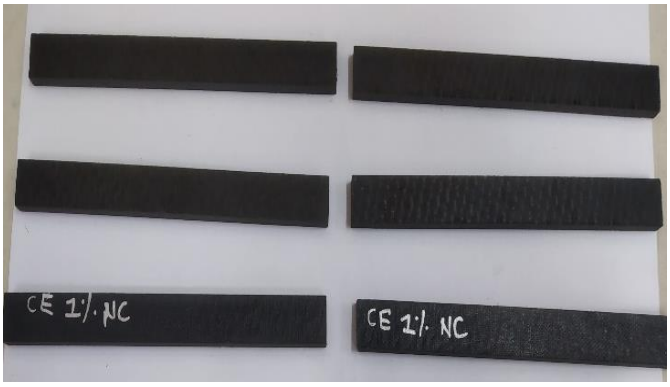

1NC/ C- CE

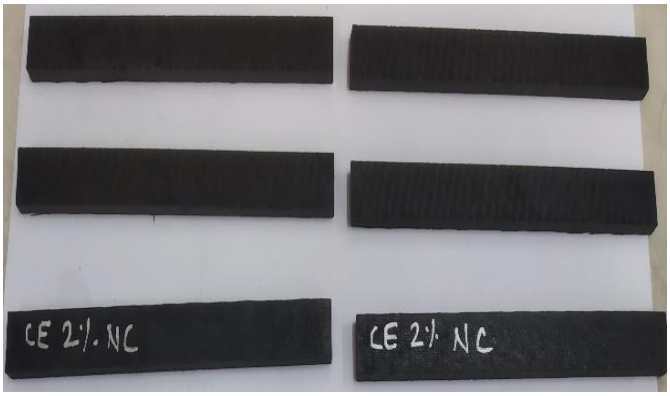

2 NC/ C-CE

4 NC/ C-CE

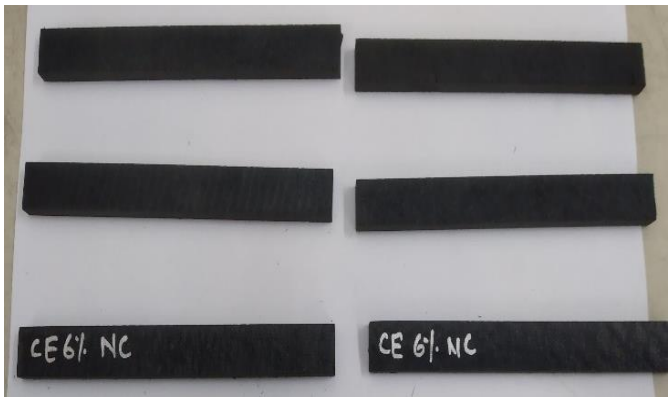

6 NC/ C-CE

(Size of each specimen: 100 mm x 10 mm x 4 mm)

Figure 4.8. Flexural test specimens of nanoclay added carbon fiber - cyanate ester resin composites

4.3.6 Oxy-Acetylene Torch Test of Nanoclay Added Carbon Fiber - Cyanate Ester Resin Composites

The oxy-acetylene torch test was carried out as per ASTM E 285 for type -II composites by collecting samples having a size of 100 mm × 100 mm x 4.0 mm. By adjusting the flame source to sample distance, heat flux was adjusted to the required level. Thus, one set of samples of type-II samples were subjected to a constant heat flux of 500 W/cm^2 for 60 seconds, while the other set of type-II composites were subjected to a constant heat flux of 125 W/cm^2 for 60 seconds. The mass ablation rate for these samples was calculated as mass loss per second. Two samples were tested at each flux and the average ablation rate was reported.

4.4. Microstructure Characterisation

Samples exposed to oxy-acetylene torch test were tested for the changes in the microstructure using a scanning electron microscope (Table Top SEM, Make: SEC, Korea, and Model: SN4500 Plus).

4.5 Results and Discussion

4.5.1 Effect of Nanoclay Content on Viscosity of Cyanate Ester Resin: The changes in viscosity of the cyanate ester resin due to different loadings of nanoclay is shown in **Figure 4.9.**

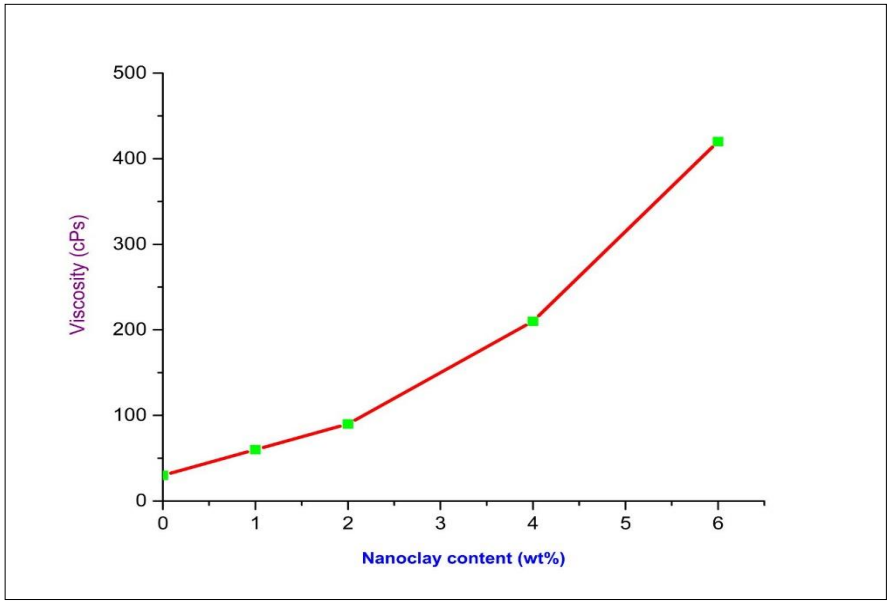

Figure 4.9 Effect of nanoclay content (wt%) on the viscosity of cyanate ester resin

The viscosity of pure cyanate ester resin is 30 cP which increased by around 50% at 1 wt% loading of o-MMT clay, which further increased to 420 cP at 6 wt% addition. As o-MMT nanoclay is showing good interactions with the cyanate ester resin, significant swelling of the clay galleries by the monomer was obtained. These swollen particles lead to the formation of

weak gels which after shearing give fluid with high relative viscosity [10-11]. Resin viscosity is an important parameter in the processing of the composite material. The higher viscosity of the nanoclay modified resins can reduce the resin extraction of the bleeder during the processing, resulting in a higher resin content for the fabricated composites [12].

4.5.2. Effect of Nanoclay Content on Curing Behaviour of Cyanate Ester Resin

Figure 4.10 shows the curing behaviour of the neat CE resin and type-I composites.

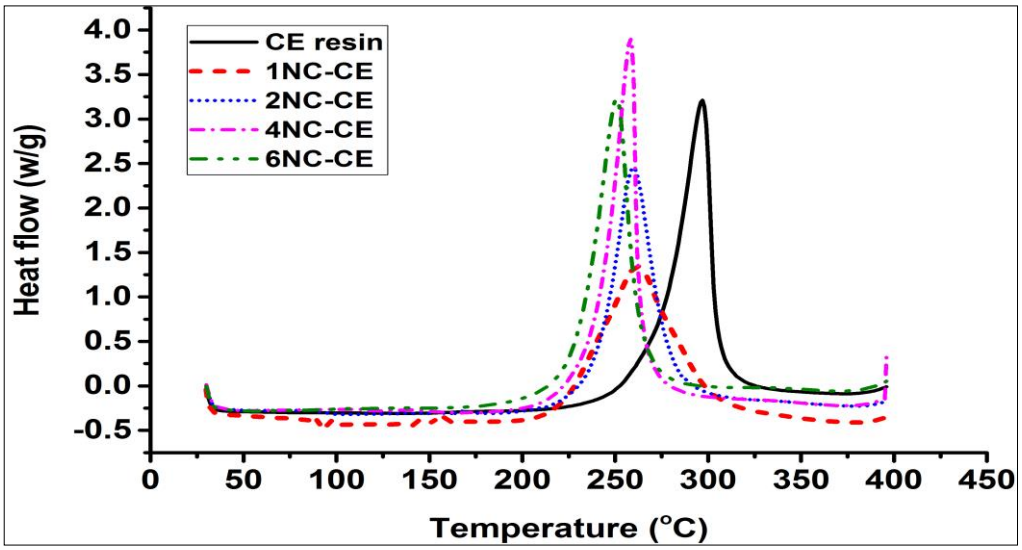

Figure 4.10. DSC scans of neat cyanate ester resin and cyanate ester - nanoclay composites

It can be seen that the broadness of the peak is increasing with the nanoclay addition to CE resin. **Table 4.3** shows the cure initiation temperature (T_i), cure onset temperature (T_e) and peak cure temperature (T_p), end set of cures exotherm (T_f), heat generated during curing (ΔH).

Table 4.3 Effect of nanoclay content on cure characteristics of cyanate ester resin-nanoclay composites

Composite description	Nanoclay content (wt%)	T_i (°C)	Te (°C)	Tp (°C)	T_f (°C)	ΔH (J/g)
CE	0	192	273	297	374	526
1 NC-CE	1	182	212	258	374	550
2 NC-CE	2	184	239	260	377	518
4 NC-CE	4	182	239	258	369	540
6 NC-CE	6	172	229	251	361	547

The heat curing of cyanate ester resin (CE) monomers creates cross-linked polycyanurate by polycyclotrimerization of the -OCN (cyanate) group. The cure reaction of cyanate ester resin can be catalysed by transition metal complexes, Lewis acids, and active hydrogen groups [4]. In the o-MMT nanoclay, active hydrogen groups (amine) are on the surface of the o-MMT part of nanoclay, therefore, the o-MMT nanoclay may exhibit a similar catalytic effect on the curing of the CE. This effect can be evidenced from the data shown in **Table 4.3,** where Ti, Te, Tp values shifted to lower temperatures with an increase in heat of polymerisation (ΔH) for type-I composites as compared to that of neat CE resin due to the catalytic effect of active hydrogen. With the increase in ΔH, it can also be inferred that cross-link density increased due to addition of nanoclay to cyanate ester resin matrix. This can be attributed to amino functional groups present on the nanoclay that can react with cyanate ester resin. The observed trends were found to be matching with the previously reported data of other researchers [5]. Thus, the present study indicates that o-MMT nanoclay acts as a catalyst for the curing of cyanate ester resin. However, the change in ΔH is not uniform with the increased amount of addition of nanoclay. It can be seen that ΔH value increased significantly for 1 wt% addition of nanoclay as it got exfoliated and thus interacted with more volume of the matrix. At 2 wt% addition of nanoclay, as the intercalation started restricting the availability of nanoclay across the space of the matrix, ΔH value decreased marginally as compared to the reference sample. Though nanoclay is intercalated at 4 wt% and 6 wt% added composites, the increased amount of nanoclay causes more interaction of amine groups of nanoclay with resin, resulting in a higher value of ΔH.

4.5.3. Dispersion of Nanoclay in Cyanate Ester Resin - Nanoclay Composites: SAXS is chosen for dispersion studies considering its ability to probe the large area of material with subnanometer resolution [6]. It is reported to give useful insight on the dispersion of partly ordered structures like intercalated, exfoliated clays [7]. **Figure 4.11** shows the SAXS patterns of the as-received nanoclay and cured cyanate ester resin- nanoclay composites**.**

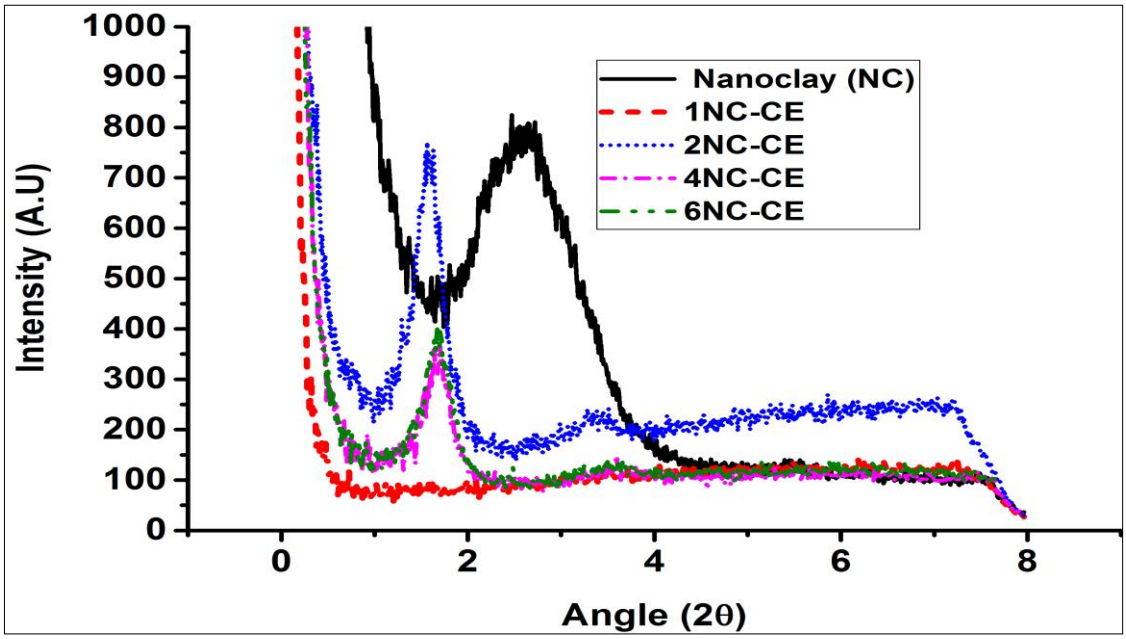

Figure 4.11 SAXS scans of nanoclay and cyanate ester resin - nanoclay composites

Bragg's law is used to study the *d* spacing values of nanoclay and cyanate ester resin-nanoclay composites (type -I). The results of d spacing values are shown in **Table 4.4.**

Table 4.4. *d* spacing values of nanoclay and cyanate ester resin-nanoclay composites

Composite description	**Nanoclay loading in resin (wt%)**	**2Θ**	**d 001 (Å)**
Nanoclay	Nanomer 1.31 PS	2.720	32.0
1 NC- CE	1 wt%	No crystalline peak	
2 NC- CE	2 wt%	1.565	56.0
4 NC- CE	4 wt%	1.702	52.0
6 NC - CE	6 wt%	1.702	52.0

It can be seen from **Figure 4.11**, that, the characteristic peak observed for the pure nanoclay (o-MMT nanoclay) got subsided for 1 wt% of nanoclay addition in type -I composites, indicating that, clay platelets got exfoliated in the cyanate ester resin. However, beyond 1wt% addition of clay, the characteristic peaks of clay can be seen in type -I composites. The d spacing value of the as-received o-MMT nanoclay, which has shown 32 A°. 2, 4, and 6 wt% of nanoclay filled cyanate ester resin composites have shown crystalline peaks with a d spacing of about 57 A°,

52 A°, and 52 A°, respectively. These results indicated that CE molecules are intercalating with the nanoclay layers there by expanding the gap between the layers. Poor exfoliation of o-MMT nanolayers when they are loaded at higher wt% into the CE can be attributed to the ability of organic part of o-MMTnanoclay which catalyse the curing of CE resin, leading to rapid gelation. This is known to retard the diffusion of the resin molecules into the galleries of nanoclay thereby inhibiting extensive layer separation in 2, 4, and 6 wt% of nanoclay filled cyanate ester resin composites [8].

SAXS data indicates clay platelets segregation, whereas the SEM shows the macroscopic distribution of clay in the matrix. **Figure 4.12** shows SEM images of nanoclay dispersed in type-I composites. The white spots highlighted in **Figure 4.12** images are associated with silicon molecule, one of the main MMT nanoparticle constituents. Thus, the larger number of white spots with uniform spread over the exposed area suggests the presence of o-MMT nanoclay in the matrix uniformly [9].

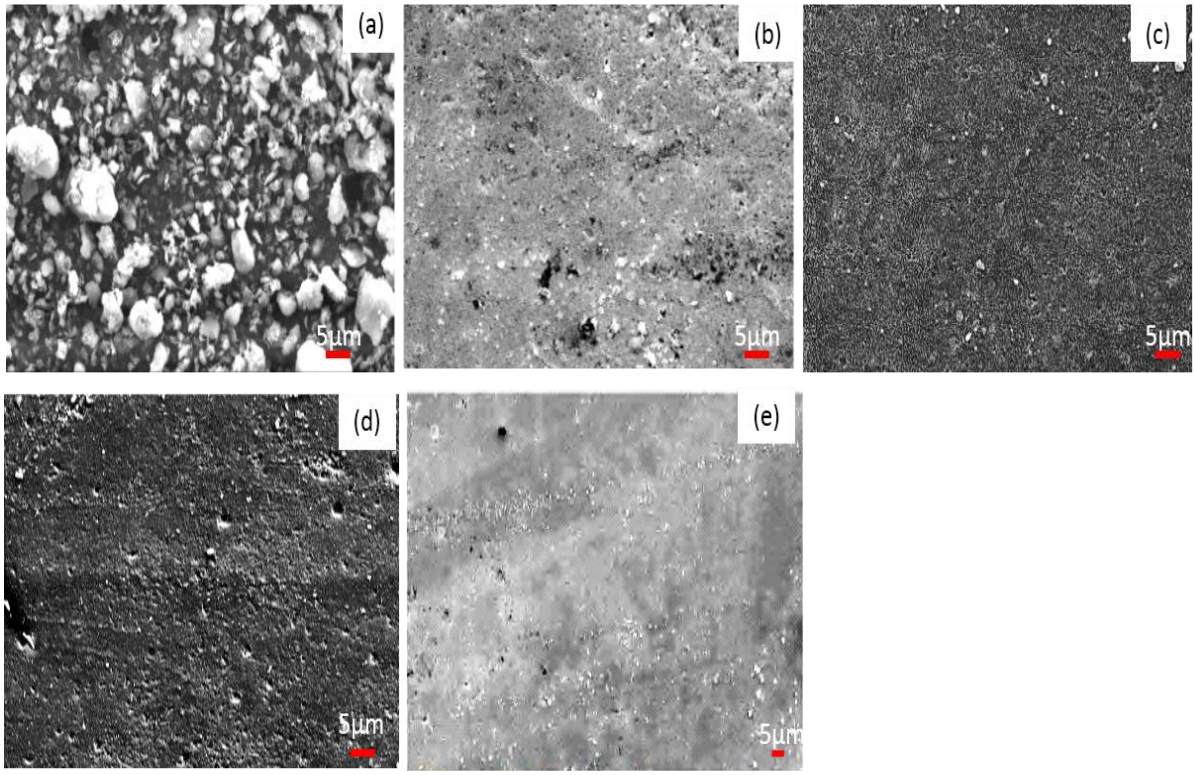

Figure 4.12. SEM images of nanoclay and cyanate ester resin-nanoclay composites (a) As received o-MMT nanoclay (b) 1 wt% o-MMT nanoclay added cyanate ester composite (c) 2 wt% o-MMT nanoclay added cyanate ester composite (d) 4 wt% o-MMT nanoclay added cyanate ester composite (e) 6 wt% o-MMT nanoclay added cyanate ester composite.

4.5.4. Density and Fiber Volume Fraction of Nanoclay Added Carbon Fiber-Cyanate Ester Resin Composites

It can be seen from **Table 4.5** that, the density, fiber volume fraction ($\%V_f$) of the composites decreases as the nanoclay content in cyanate ester resin increased.

Table 4.5 Density and fiber volume fraction of nanoclay added C-CE composites

Composite description	Nanoclay in resin (wt%)	Density (g/cc)	Fiber Volume Fraction ($\%V_f$)
C-CE (blank)	0	1.60	68
1 NC / C-CE	1	1.59	65
2 NC / C-CE	2	1.59	63
4 NC / C-CE	4	1.58	61
6 NC / C-CE	6	1.54	59

This is because of the poor resin squeeze out of the high viscous compositions when compared to the blank cyanate ester resin [12, 13]. This has resulted in reduced fiber volume fraction for the nanoclay added cyanate ester resin composites. As the fiber volume fraction is coming down and the density of the composites is also coming down.

4.5.5 Barcol Hardness of Nanoclay Added C-CE Composites: Barcol hardness of fabricated composites is shown in **Table 4.6.** Barcol Hardness values are found to be the same for blank C-CE composite and nanoclay added C-CE composites.

Table. 4.6 Barcol hardness of nanoclay added C-CE composites

Sl. No	Composite description	Nanoclay in resin (wt%)	Barcol Hardness
1	C-CE (blank)	0	72-74
2	1 NC/ C-CE	1	65-74
3	2 NC/ C-CE	2	65-72
4	4 NC/ C-CE	4	65-72
5	6 NC/ C-CE	6	65-72

Barcol hardness value indicates the extent of curing of composite. All nanoclay added carbon fiber – cyanate ester resin composites and blank C-CE composite were completely cured.

4.5.6. Thermal Stability of the Type - I and Type - II Composites: The TGA and DTGA scans of o-MMT nanoclay, neat cyanate ester resin, and cyanate ester resin - nanoclay composites (type-I) are shown in the **Figure 4.13 (a), 4. 13 (b)** respectively.

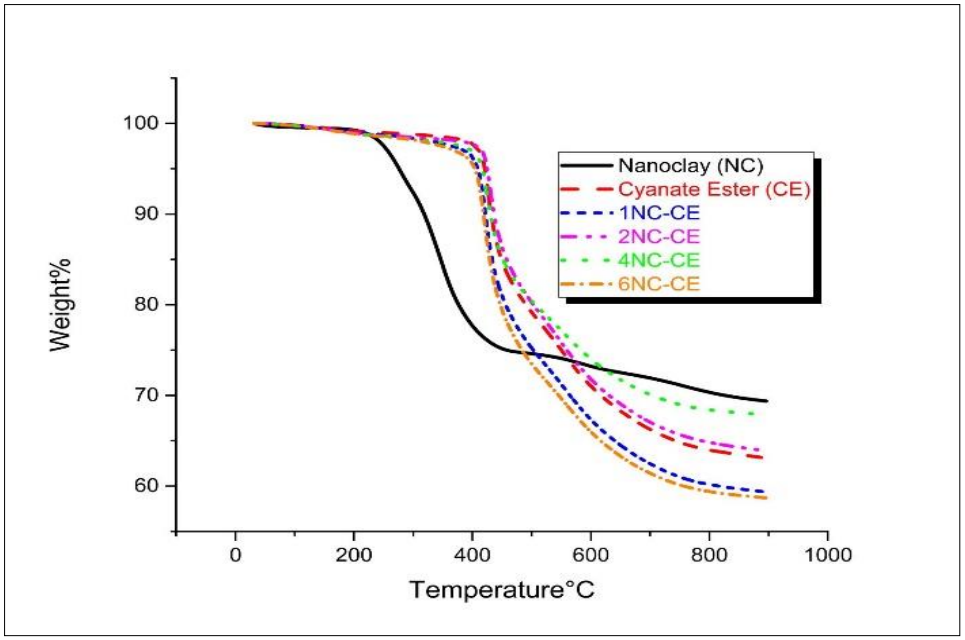

Figure 4.13 (a) TGA scans of nanoclay and cyanate ester-nanoclay composites (type-I)

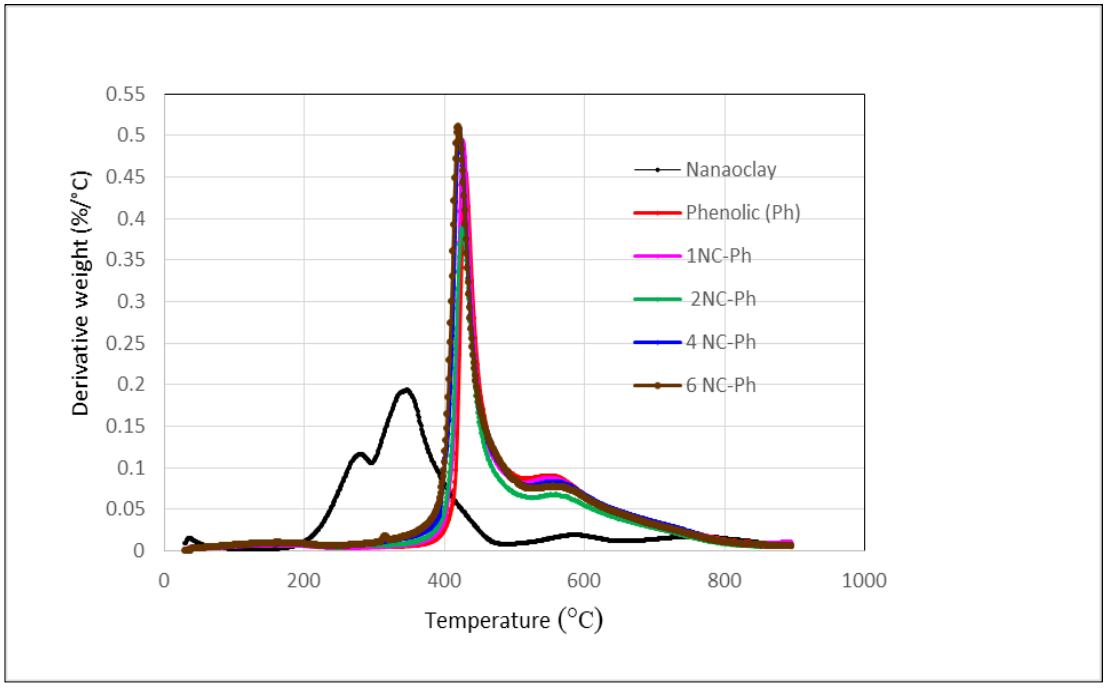

Figure 4.13 (b) DTGA scans of nanoclay and cyanate ester-nanoclay composites (type-I)

TGA and DTGA scans of carbon fiber - cyanate ester resin composite and nanoclay added carbon fiber-cyanate ester resin composites (type-II) are shown in **Figure** 4.14 **(a), 4.14 (b)** respectively.

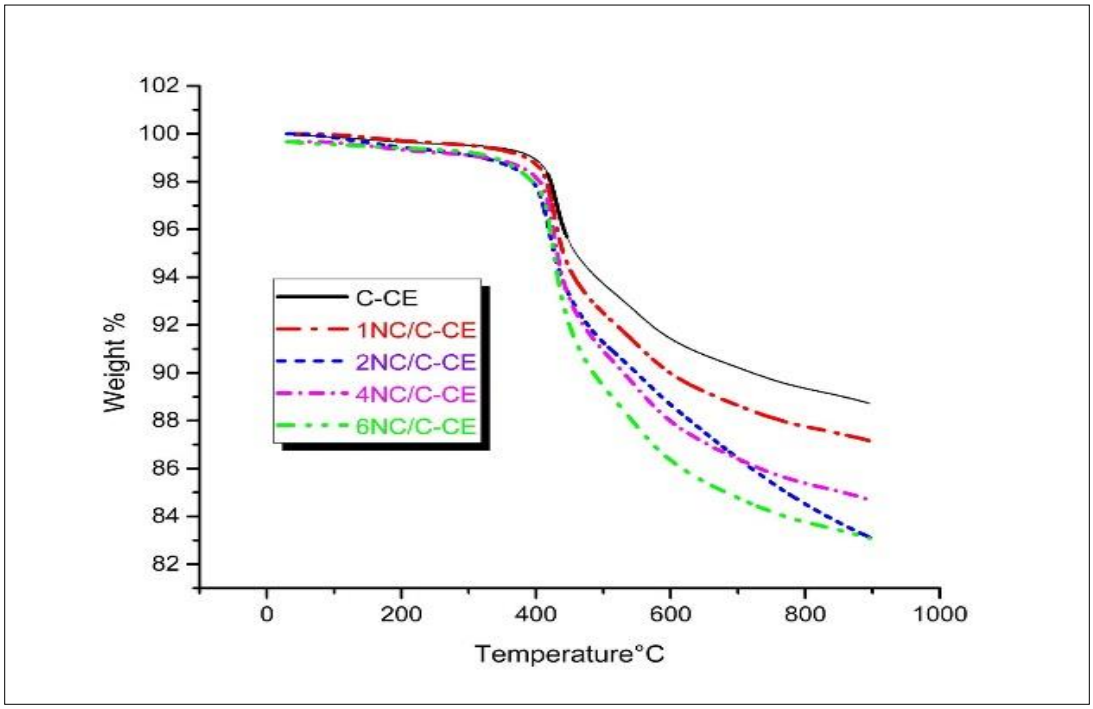

Figure 4.14 (a) TGA thermograms of nanoclay added C - CE composites (type-II)

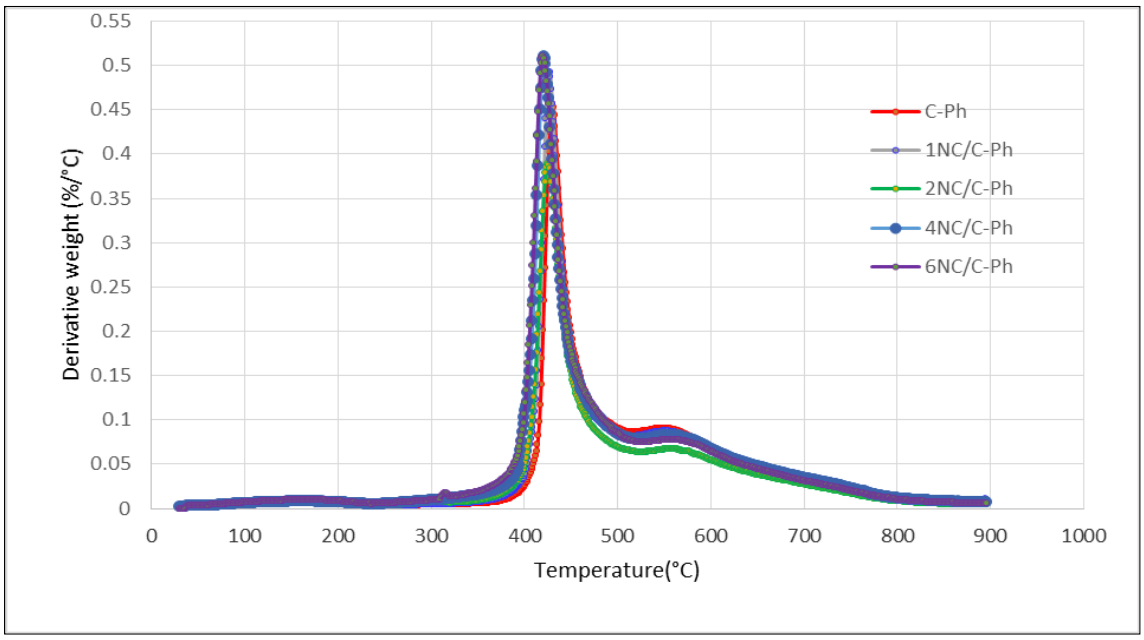

Figure 4.14 (b) TGA thermograms of nanoclay added C-CE composites (type-II)

Char residue at 900 °C and temperature at 5% weight loss ($T_{5\ \%}$ /°C) are shown in **Table. 4.7** for type - I and type - II composites.

Table 4.7 Thermal stability of Type - I and Type - II composites

Nanoclay (wt%) in composite	T 5% / °C		% Residue at 900 °C	
	Type-I	Type-II	Type-I	Type-II
0	425	459	63.89	88.73
1	420	444	63.06	86.27
2	416	440	67.84	87.16
4	410	433	60.34	85.78
6	405	427	59.00	83.11

It can be seen that the thermal decomposition and resultant weight loss of the o-MMT nanoclay started at around 250 °C and completed at around 450 °C. From the residual weight at 900 °C, it can be inferred that around 70% of the weight of clay is inorganic in nature and the rest is organic in nature. It is observed that from **Figure 4.13(a),** that the degradation of cyanate ester resin is a single-step process, wherein degradation starts at 425 °C with a resultant end char of 64 wt% at 900 °C. It can be seen that both the temperature at 5% weight loss (**$T_{5\ \%}$ /°C**) and final char yield got decreased with an increasing weight percentage of nanoclay content in both type-I and type-II composites when compared to their corresponding blank composites. This is due to the increasing agglomerates which act as defects in the CE matrix [14]. Reasons for the same are discussed below.

The thermal degradation of the cyante ester resin in an inert atmosphere can undergo as per reaction shown in equation -1 [15].

Cyanate ester resin $\longrightarrow$ C (Char) + CO + CO_2 + HOCN + NH_3 - Heat ----- (1)

On the other hand, simultaneously along with the reaction (1), degradation of organic part of the nanoclay takes place as per equation -2 [13].

NH_2-$(CH_2)_3$ –Si (O-$C_2H_5)_3$+NH_2 $(CH_2)_{17}CH_3$ $\longrightarrow$ NH_3 + NH_4-OH+ SiO_2+ O_2 +CO_2+CO ---(2)

However, the oxygen species formed in the reaction (2) can trigger the degradation of the matrix and char further as per equations 3 and 4.

Cyanate ester resin + O_2 $\longrightarrow$ CO_2 + H_2O+ CO – Heat ---------- (3)

$$Char + O_2 \longrightarrow CO_2 - Heat \text{ ---------- (4)}$$

As a result, oxygen released from o-MMT nanoclay degrades matrix and char, reducing the thermal stability of the host matrix and char.

4.5.7 ILSS of Nanoclay Added C - CE Composites

ILSS values of individual specimens for each composition of nanoclay added C - CE composites (type-II) are shown in **Table 4.8.**

Table 4.8 ILSS test results of o- MMT nanoclay added C-CE composites

Specimen No	ILSS (MPa)				
	C-CE	1 NC/ C-CE	2 NC/ C-CE	4 NC/ C- CE	6 NC/ C-CE
1	31	32	33	30	22
2	31	35	34	31	21
3	29	32	36	30	21
4	31	30	34	32	22
5	29	33	37	31	22
Average	**30**	**32**	**35**	**31**	**22**
Standard deviation	**1.1**	**1.8**	**1.6**	**0.8**	**0.5**

Figure 4.15 shows the effect of weight percentage of nanoclay on ILSS, which increased by 17% at 2 wt% addition of nanoclay when compared to the blank C-CE composites.

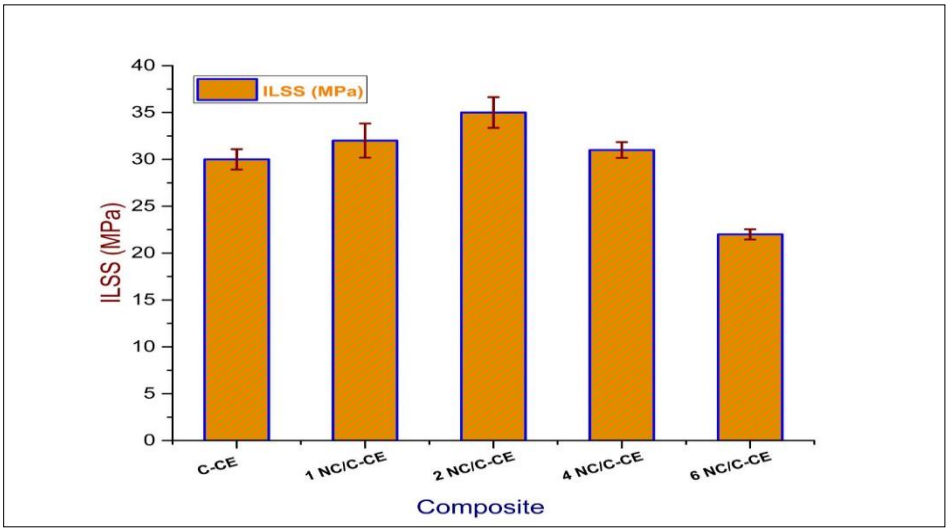

Figure 4.15. The effect of nanoclay content on ILSS of type –II composite

It can be observed from the SAXS data that up to 1 wt% addition of nanoclay got dispersed in CE resin, from 2 wt% onwards, intercalation of nanoclay was observed. But the ILSS got improved significantly up to 2 wt%. Even at 4 wt% nanoclay addition to CE resin, ILSS is better than the blank C-CE composite indicating that intercalated nanoclay platelets can impart increased ILSS up to a critical concentration due to higher interface area and strong chemical bonds that they form at the interface [16-18]. In the present study at 6 wt% of o-MMT, ILSS has come down due to a significant reduction in the fiber volume of the resultant composites.

4.5.8 Flexural Strength and Flexural Modulus of Nanoclay Added C - CE Composites

Table 4.9 shows the individual specimen flexural strength and flexural modulus values for each type-II composite.

Table 4.9. Flexural strength (FS) and Flexural modulus (FM) of o- MMT nanoclay added C - CE composites

Specimen No	C - CE		1 NC/ C - CE		2 NC/ C - CE		4 NC/ C - CE		6 NC/ C- CE	
	FS (MPa)	FM (GPa)	FS (MPa)	FM (GPa)	FS (MPa)	FM (GPa)	FS (MPa)	FM (GPa)	FS (MPa)	FM (GPa)
1	529	75	638	67	664	--	553	58	462	55
2	544	--	678	68	663	68	524	57	462	56
3	542	72	639	---	657	68	554	60	433	58
4	542	78	650	68	631	65	523	60	413	55
5	518	77	640	69	633	65	567	---	428	--
Average	**535**	**75**	**649**	**68**	**650**	**67**	**544**	**59**	**440**	**56**
Standard deviation	**11.22**	**2.65**	**16.91**	**0.82**	**16.30**	**1.73**	**19.69**	**1.50**	**21.73**	**1.41**

Figure 4.16(a) depicts the influence of nanoclay loading on the flexural strength of type -II composites.

.

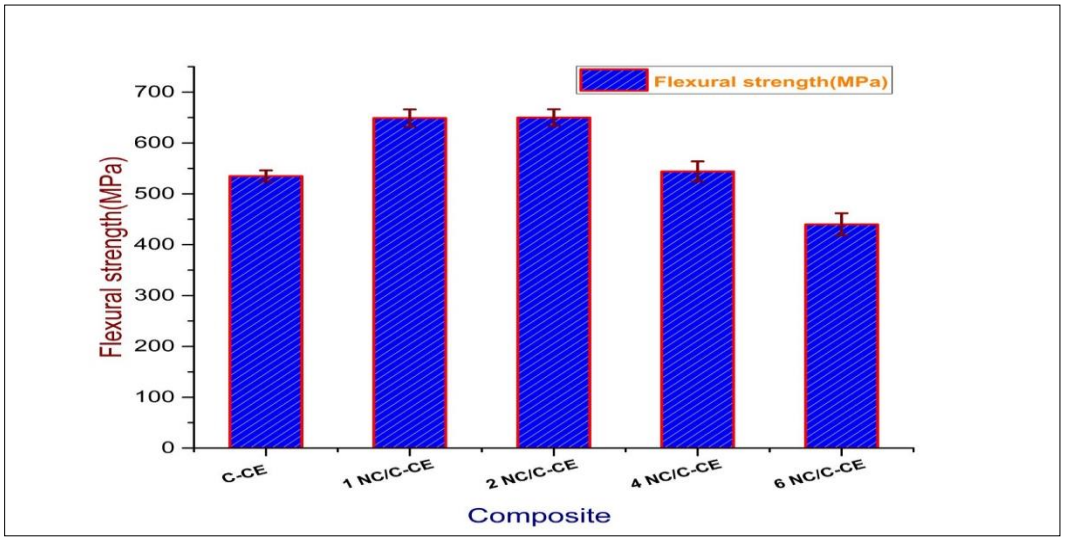

Figure.4.16 (a) The effect of weight percentage of nanoclay on flexural strength of type –II composite

Flexural strength increased up to 2 wt% nanoclay addition by about 21%. It can be seen that, in the case of 1 wt% nanoclay and 2 wt% nanoclay addition, flexural strength increased by the same degree even when at 2 wt% nanoclay got only intercalated against the good dispersion of nanoclay at 1 wt% addition. Moreover, at 2 wt%, the $\%V_f$ of the composites is around 2% lower than the 1 wt% composite. Even under such conditions, 2 wt% nanoclay added composite has shown similar flexural strength as that of the 1 wt% nanoclay added composite. At 4 wt% nanoclay addition, V_f of the composite is significantly lower when compared to the blank C-CE composite, yet it has displayed a similar degree of flexural strength. This indicates nanoclay platelets under intercalated conditions could impart a significant positive influence on the overall flexural properties of the composites. This is because, flexural failures are the combination of shear, compression, and tensile failure. Intercalated nanoclay galleries offer significant resistance to tensile strength/ compression of the matrix around them due to strong chemical bonds of the organic part of the nanoclay with the CE resin system which resists the change in the bond length. Thus, additional chemical bonds add to the overall strength of the composites [19-21]. However, beyond a critical reduction in V_f of the composite (6 wt%) in the present case, overall flexural strength has come down due to poor contribution from the fibers to the overall strength

of the composite. **Figure 4.16 (b)** shows the effect of nanoclay content on the flexural modulus of type-II composites.

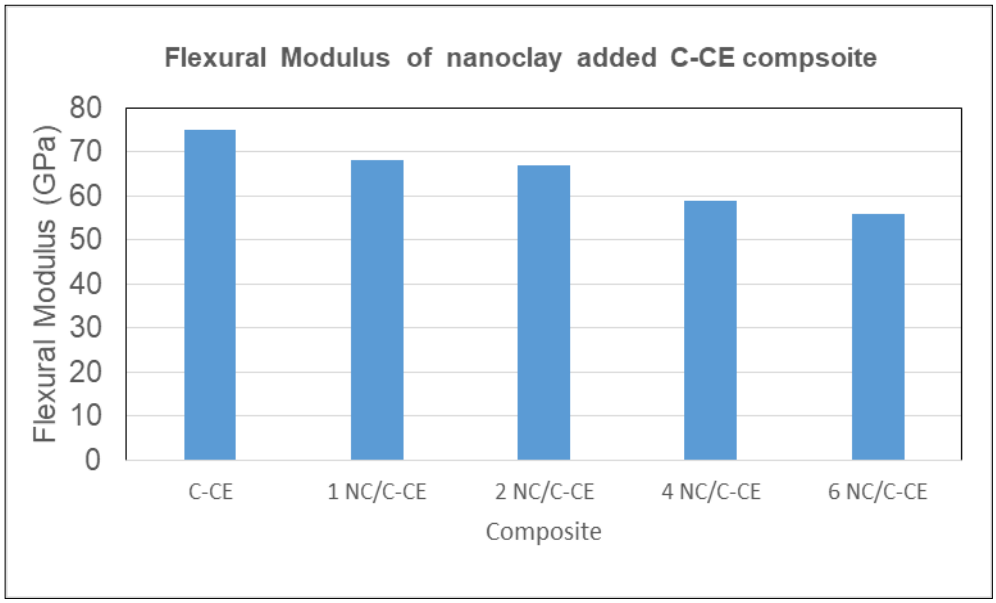

Figure 4.16 (b) The effect of nanoclay content on flexural modulus of type -II composites.

Flexural modulus decreased for 1, 2, 4 and 6 wt% nanoclay added C-CE composite by about 9%, 11%, 21%, and 25% respectively when compared to blank C-CE composite. This is because of the reduction in the fiber volume fraction of the composites as nanoclay loading content increases in the resin.

4.5.9 Thermal Conductivity of Nanoclay Added C-CE Composites

Thermal conductivity values of the type-II composites are shown in **Table 4.10**. It can be seen that the thermal conductivity of the composite is decreasing as the nanoclay content in the composite is increasing. This can be attributed to the fact that, nanoclay acts as scattering centres for the heat energy-carrying phonons [22]. This results in energy loss at these inclusions, thereby reducing the overall thermal conductivity of the composite.

Table. 4.10 Thermal conductivity data of nanoclay added C-CE composites

Sl. No	Composite description	Nanoclay (wt%)	Thermal Conductivity (W/ m °C) at 30 °C
1	C-CE (blank)	0	1.35
2	1 NC/ C-CE	1	1.28
4	2 NC/C- CE	2	1.16
3	4 NC/ C-CE	4	1.08
5	6 NC/C- CE	6	0.94

4.5.10 Specific Heat of Nanoclay Added C-CE Composites

Specific heat of each composition of type -II composites was measured by differenial scanning calorimetry (DSC) at different temperatures from 50 °C and 350 °C. The following **Table 4.11** shows the results of the specific heat tests on type -II composite samples.

Table 4.11 Results of Specific heat of nanoclay added C-CE composites

Composite description	Specific heat (J/Kg °C) at different temperatures						
	50 °C	100 °C	150 °C	200 °C	250 °C	300 °C	350 °C
C-CE (blank)	957	1109	1245	1369	1477	1585	1643
1 NC/ C-CE	991	1190	1356	1479	1589	1678	1713
2 NC/ C-CE	1031	1204	1343	1460	1563	1674	1729
4 NC/ C-CE	1122	1292	1441	1555	1651	1756	1840
6 NC/ C-CE	878	1038	1174	1271	1351	1428	1481

Comparison of specific heat of blank carbon fiber - cyanate ester resin composite with different weight percentages of nanoclay added carbon fiber- cyanate ester resin composites were plotted and shown in **Figure 4.17.**

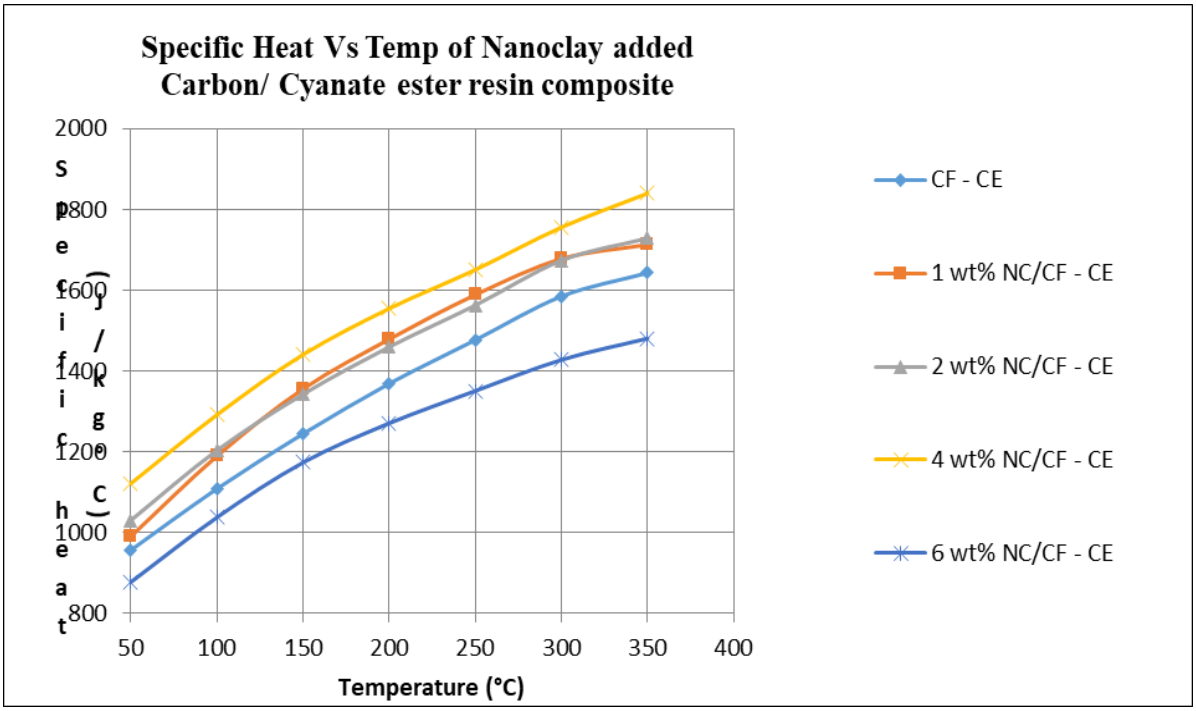

Figure 4.17 Specific heat versus temperature of nanoclay added C - CE composites

Specific heat has increased for 1, 2, 4 wt% nanoclay modified C-CE composites by about 4.26%, 5.23%, 12.40% respectively at 350 °C when compared to blank C-CE composite. However, Specific heat values decreased for 6 wt% nanoclay modified C-CE composite by about 9.86% at 350 °C when compared to blank C-CE. This is because of the reduction in the fiber volume fraction of the composites as nanoclay loading content increases in the resin. Thermally stable, inorganic residue of silicate layers is responsible for the enhanced value of specific heat for nanoclay added C-CE composites. This can lead to better insulation characteristics for nanoclay added C-CE composites when compared to conventional unfilled C-CE composite.

4.5.11. Effect of Nanoclay Content on Mass Ablation Rate of Type - II Composites

Image of the oxy-acetylene torch test under progress at at heat flux 125 W/cm^2 on type -II composite is shown in **Figure 4.18**. Images of the ablated samples after oxy-acetylene torch test at heat flux 125 W/cm^2 are shown in **Figure 4.19.**

Figure 4.18. Oxy-acetylene torch test of type -II composite at heat flux 125 W/cm^2

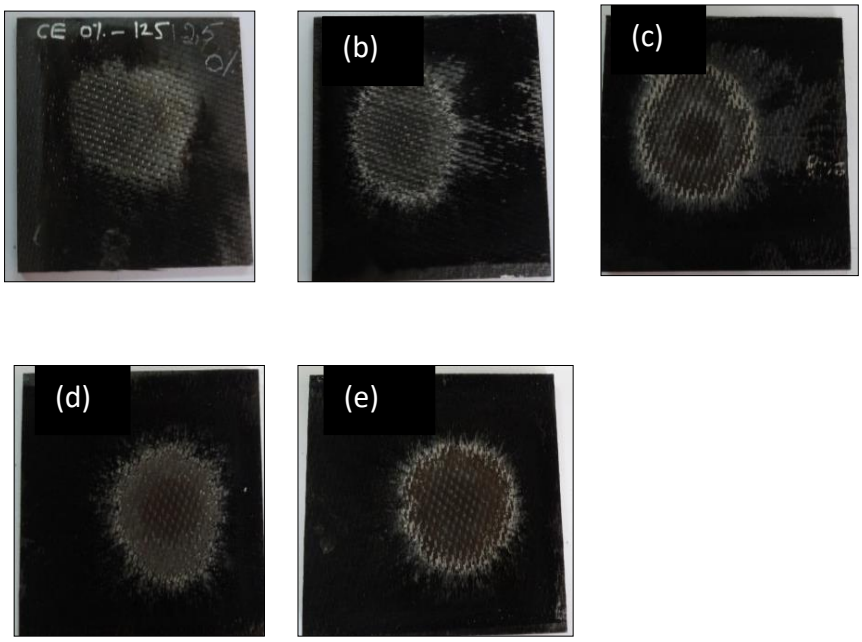

(**Sample size: 100 mm x 100 mm x 4 mm**)

Figure 4.19. Images of the ablated samples after oxy-acetylene torch test at heat flux 125 W/cm^2 (a) blank C-CE (b) 1 wt% nanoclay added C-CE (c) 2 wt% nanoclay added C-CE (c) 4 wt% nanoclay added C-CE (d) 6 wt% nanoclay added C-CE composites

The images of the oxy- acetylene torch test carried out on type-II composites at heat flux 500 W/cm^2 are shown in **Figure 4.20**. The images of the ablated samples after oxy-acetylene torch test at heat flux 500 W/cm^2 are shown in **Figure 4.21.**

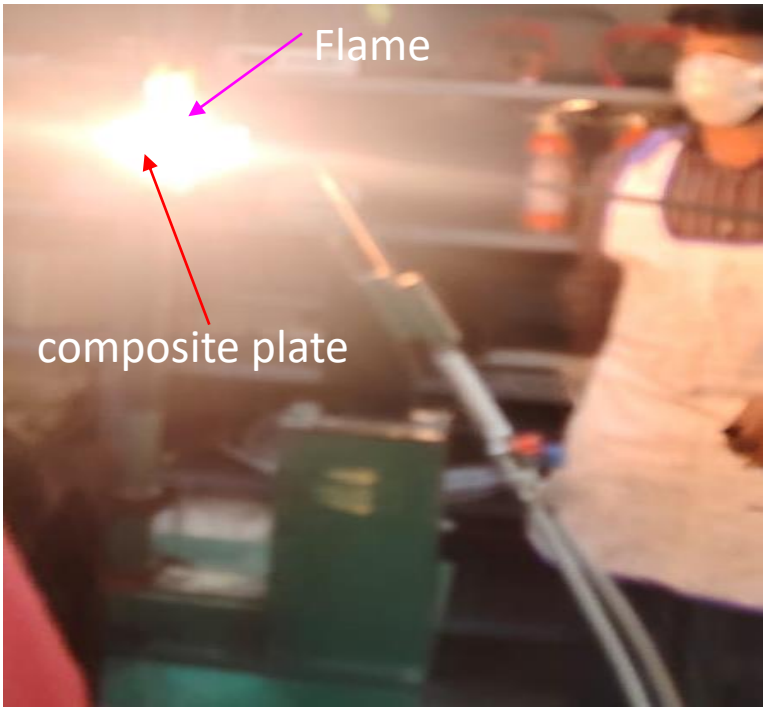

Figure 4.20.Oxy-acetylene torch test of type -II composite at heat flux 500 W/cm^2

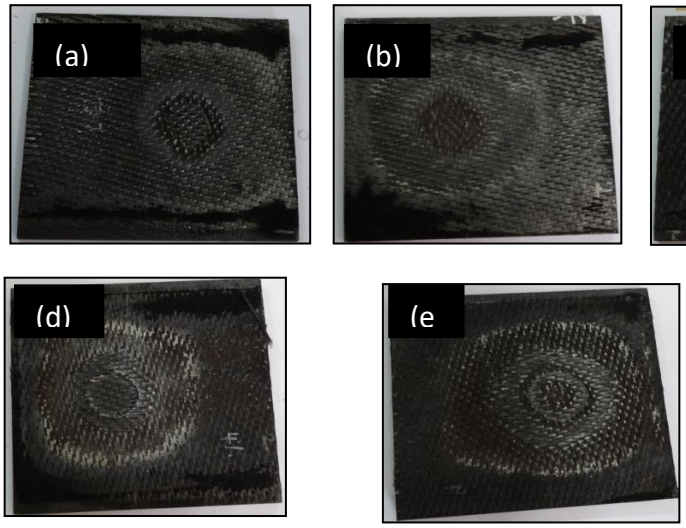

(**Sample size: 100 mm x 100 mm x4 mm**)

Figure 4.21. Images of the ablated samples after oxy-acetylene torch test at heat flux 500 W/cm^2 (a) blank C-CE (b) 1 wt% nanoclay added C-CE (c) 2 wt% nanoclay added C- CE (c) 4 wt% nanoclay added C-CE (d) 6 wt% nanoclay added C-CE composites.

The results of the mass ablation rate of blank carbon fiber - cyanate ester resin composite and nanoclay added carbon fiber - cyanate ester resin composites tested at low heat flux 125 W/cm^2 and high heat flux at 500 W/cm^2 are presented in **Table 4.12.**

Table 4.12 Mass ablation rate of nanoclay added C-CE composites

Composite description	**Nanoclay in Resin (wt%)**	**Mass ablation rate(mg/sec) at Heat flux:125 W/cm^2**	**Mass ablation rate(mg/sec) at Heat flux:500 W/cm^2**
C-CE (blank)	0	84	123
1 NC / C- CE	1	114 (35%)*	142 (15%)*
2 NC / C- CE	2	134 (59%)*	163 (24%)*
4 NC / C-CE	4	151 (79%)*	174 (42%)*
6 NC / C-CE	6	181 (115%)*	227 (84 %)*

Values given in parenthesis indicates the percentage of increase in mass ablation rate with respect to C-CE composite (blank)

The mass ablation rates have increased with an increasing weight percentage of nanoclay content in type -II composites when compared to blank type -II composites at both heat fluxes (125 W/cm^2 and 500 W/cm^2). During the oxyacetylene torch ablation, several degradation processes operate simultaneously. The first one is the chemical degradation of composite, which involves endothermic pyrolysis of cyanate ester resin matrix into char and other gaseous products as shown in **Equation (1**). Another one is, mechanical erosion and removal of the char and fibers. The microstructure of the ablated surface gives inference on the mechanisms operated during the ablation. Ablation mechanisms are discussed in light of the microstructure of the ablated surface in the subsequent sections.

4.5.12. Microstructural Behaviour of Ablated Surface of Type - II Composites

Microstructures of ablated surfaces of nanoclay added carbon fiber reinforced cyanate ester resin composites tested at heat flux 125 W/cm^2 are shown in **Figure 4.22.**

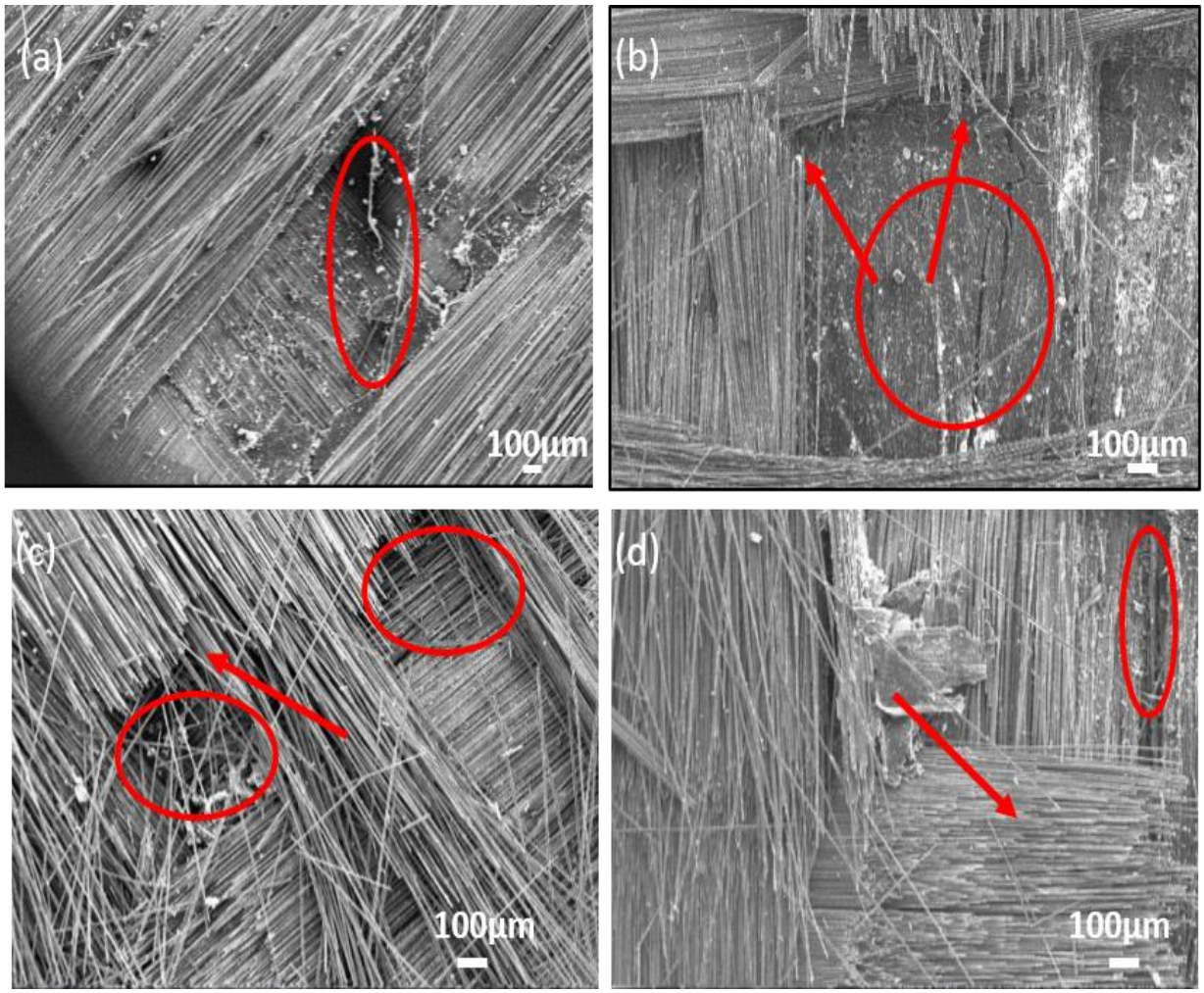

Figure 4.22. Microstructure of ablated samples tested at 125 W/cm^2 (a) blank C-CE, encircled zones showing traces of matrix (b) 1 wt% nanoclay added C-CE, arrows indicating fiber breakage, traces of matrix can be seen in encircled zones (c) 4 wt% nanoclay added C-CE, arrows indicating fiber breakage, encircled zones indicating severe damage to fiber up to the next ply,(d) Arrows indicating fiber breakage, encircled zone indicating severe damage across resin-rich tow interface.

It can be seen that, in the case of a blank C-CE composite **(Fig.4.22 (a)),** there is no appreciable damage to the fibers. Highlighted zones of **Fig.4.22 (a),** indicate that the traces of matrix are still present on the surface of the ablated composite. Even with low concentration (1 wt%) addition of nanoclay to C-CE composites, fiber breakage can be seen as indicated with arrows **(Fig. 4.22 (b)).** As the clay content got increased in the C-CE composite, severe damage of the fibers was noticed with the damage spreading to the next ply across the thickness (encircled zone in **Fig.4.22 (c)** and **4.22 (d))** of the composite. It is interesting to note that, in the case of blank C-CE and 1 wt% C-CE, trace amounts of charred matrix is visible on the ablated surface (encircled

zones in **Fig 4.22 (a)** and **4.22 (b)),** whereas in the case of a higher amount of nanoclay added composites (**Fig 4.22 (c)** and **Fig 4.22 (d)),** matrix vanished completely though the ablative flux levels for the test are same, indicating that, the species formed due to the degradation of organic part of nanoclay are reacting with char formed from the matrix and converting it into the gaseous states on the lines of the reaction 3 shown previously. Since the interfaces of the tows on the fiber become the matrix rich zones in the fabricated composites, degradation along the depth of the interface between the tows will be maximum (reaction 3 will be maximum) as highlighted in the encircled zones of **Figure 4.22 (c)** and **4.22 (d**). This leads to large craters and an increased ablation rate.

Microstructures of ablated surfaces tested at heat flux 500 w/cm^2 are shown in **Figure 4.23.**

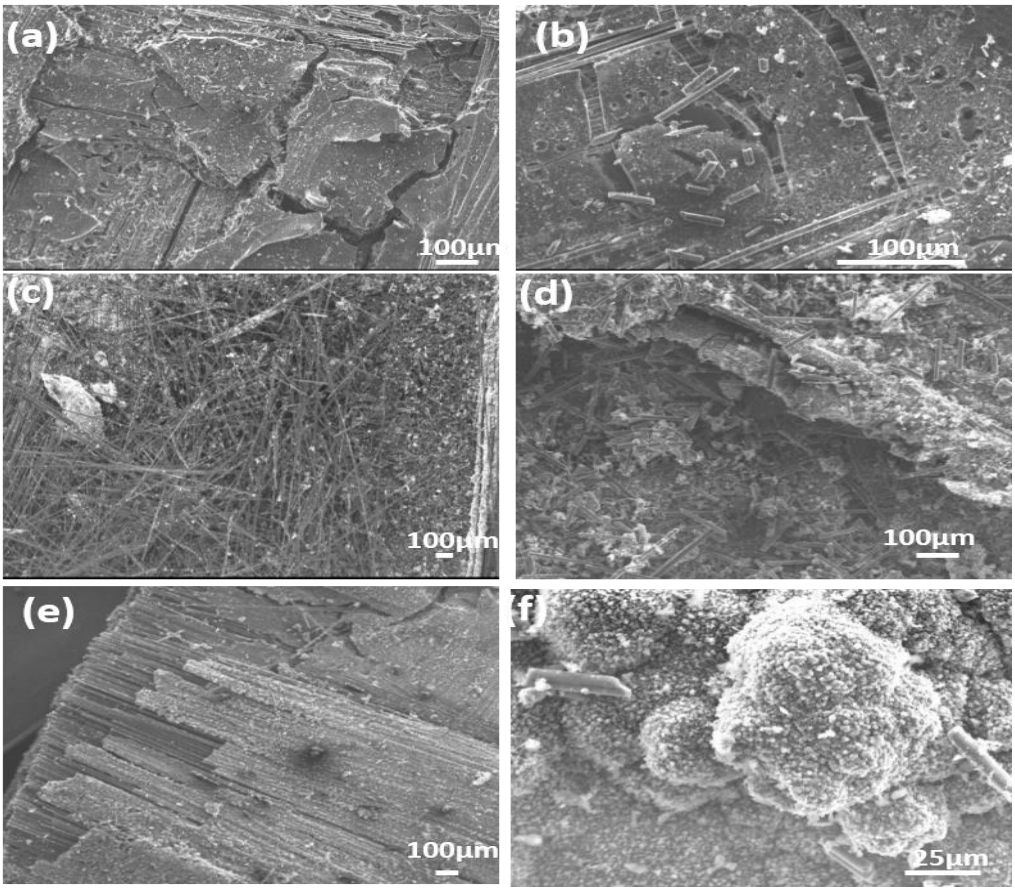

Figure 4.23. Microstructure of ablated samples tested at 500 W/cm^2 a) blank C-CE with a significant amount of matrix present (b) 1 wt% nanoclay added C-CE with bubble-like zones on the matrix (c) 1 wt% nanoclay added C-CE, with fiber breakage, traces of matrix can be seen (d) Molten clay balls on the surface of 4 wt% nanoclay added C-CE (e) Minimum damage to fibers due to continuous melting of nanoclay protected fiber from erosion in 4 wt% nanoclay added C-CE (f) Large size molten nanoclay ball formed in 4 wt% nanoclay added C-CE.

It can be seen from **Figures 4.22** and **4.23**, that the ablative patterns at the higher flux of 500 W/cm^2 are different from the low flux of 125 W/cm^2. It can be seen that there is a deep damage to the matrix and fibers at a high flux (**Fig. 4.23.a**). This is in contrast to almost uniform matrix removal for the nanoclay C-CE composites tested at a low flux of 125 W/cm^2. At 1 wt% nanoclay added C-CE composite, the retained matrix can be seen to have porous openings indicating the release of a gaseous product during ablation (**Fig.4.23.b**). However, as the nanoclay amount has increased, more amount of molten clay/silica would have melted on the ablation surface (as per reaction 2) thereby covering the entire surface of ablating material. However, the reactions that are releasing gases (**as per equation 2** and **3**) will try to lift the molten silica upwards and escape by forming porous surface. This gives a ball like structure to the molten clay. The size of molten clay balls helps keep increasing with increasing clay content (**Fig.4.23 c** and **d, Fig 4.23 e** and **f**). This mechanism (mechanism –I) becomes more prominent at a reasonably good amount of addition of nanoclay which is 4 wt% in this study (**Fig.4.23 (a), (b), (c), (d)).** Large balls of molten clay formed on the surface of ablated fibers indicate liquid clay which was about to evaporate has condensed back in the form of liquid **(Fig.4.23 (d)** and **(e)**). Thus, continuous melting of the nanoclay protects the fibers from erosion. It can be seen that, as the fibers got protected there is minimum damage to the fibers as seen in **Fig 4.23 (e).** However, on the other hand, an alternate mechanism (mechansim –II) operates, which involves the reaction of oxidising species evolved from the organic part of o-MMT, thereby opening the craters for direct exposure of the fibers beneath the flame leading to the removal of fibers. These two mechanisms (melting of clay and protection of fibers, the opening of the protective layer of clay, and exposure of the composite beneath for the flame) compete with each other. Up to 4 wt% addition of nanoclay, clay melting, and protection mechanism plays a significant role. This can be evidenced from the fact that, up to 4 wt% addition of nanoclay, though ablation rate has increased, an overall increase in the percentage ablation with respect to its blank is less when compared to the same samples tested at low heat flux (**Table.**4.12). At low heat flux, mechanism (i) is absent and only mechanism (ii) operates which leads higher rate of ablation. However, at the higher flux of 500 W/cm^2, at 6 wt% loadings of nanoclay, the mechanism (ii) dominates leading to complete removal of char with significant exposure of the fibers and removal of fibers (**Fig.4.24. a** and **b**). Hence, at this loading, there is an abrupt rise in the rate of ablation when compared to the trend of ablation rate observed up to 4 wt% loading.

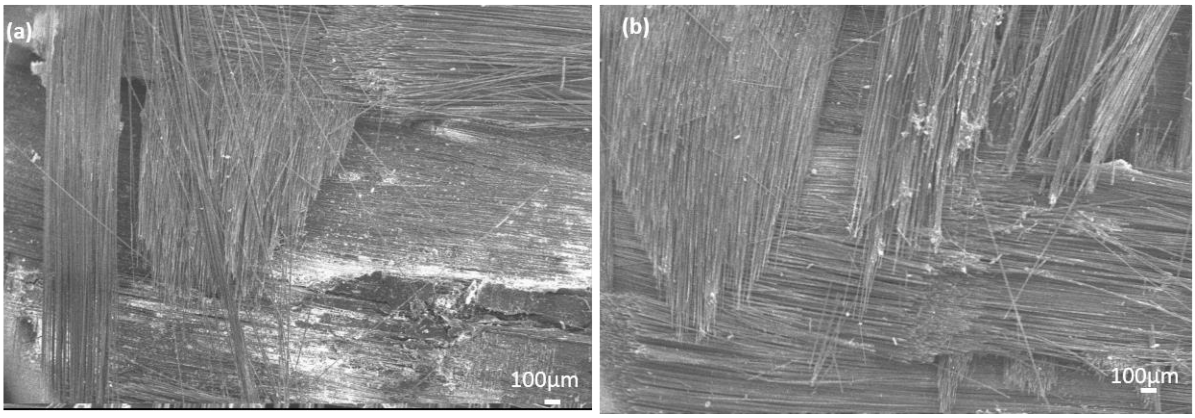

Figure 4.24. Both (a) and (b) shows the microstructure at different locations for 6 wt% nanoclay added C-CE tested at 500 W/cm^2

4.6. Conclusions

This study brings out the mechanical, thermal, and ablative performance of carbon fiber - cyanate ester resin (type -II) composites when added 0,1,2,4 and 6 wt% nanoclay. To understand the underlying changes in the thermal and ablative properties, pure cyanate ester resin was added with o-MMT nanoclay (type - I composites) and its thermal degradation was evaluated up to 900 °C. The results obtained in this research work are summarized below.

- Nanoclay in cyanate ester resin got dispersed up to 1 wt%, intercalated at 2 wt%, agglomerated at 4 wt% and 6 wt%. Even with intercalation, at 2 wt% nanoclay addition to type -II composites, ILSS was found to be maximum, while flexural strength was on par with 1 wt% nanoclay added type - II composites. Overall, 17%, 21% improvement in ILSS and flexural strength respectively were obtained.
- Thermal stability, char yield of carbon fiber – cyanate ester resin composites marginally decreases due to nanoclay addition.
- Mass ablation rate of type - II composites, increased at all concentrations of nanoclay addition when compared to the blank carbon fiber – cyanate ester resin composite.
- 2 wt% nanoclay addition can be considered as optimum for better mechanical properties for the carbon fiber – cyanate ester resin composites with minimum compromise in the thermal stability and ablation performance.
- Though absolute mass ablation rate is higher for type - II composite samples tested at 500 W/cm^2, the percentage increase in mass ablation rate is lower as compared to mass ablation rates of the same samples tested at a low flux (125 W/cm^2). This is attributed to the additional protection from the molten clay at higher flux.

References

1. Ian Hamerton, John N. Hay. Recent developments in the chemistry of cyanate esters, Polymer International. 1998; 47, 465 – 473.
2. Kurt J. Schellhase, Ethan Liu, Ty Templin, Noel Arguello, Logan Head, Andrew Adlof, and Joseph H. Koo. Development of new thermal protection systems based on polysiloxane/silica composite. 58thAIAA/ASCE/AHS/ASC Structures, structural dynamics, and materials conference. doi:10.2514/6.2017-1367
3. D. Njoyaa, F.S. Tadjuidjea, E.J.A. Ndzanaa, A. Pountouonchia, N.Tessier-Doyenb,G. Lecomte-Nana. Effect of flux content and heating rate on the microstructure and technological properties of mayouom (western-cameroon) kaolinite clay based ceramics. Journal Asian Ceramic Societies. 2017; 5, 422-426.
4. Y. Lin, C. A. Stone, S. J. Shaw, M. Song. Effect of carbon nanotubes on the curing dynamics and network formation of cyanate ester resin. Journal of Polymer Research. 2013; 20, 106-117.
5. Denis A. Kissounko, Joseph M. Deitzel, Shawn P. Doherty, Apoorva Shah, John W.Gillespie. Understanding the role of clay silicate nanoparticles with organic modifiers in thermal curing of cyanate ester resin. *European Polymer Journal* 2008, 44, 2807–2819.
6. Jayita Bandyopadhyay, Suprakas Sinha Ray. The quantitative analysis of nano-clay dispersion in polymer nanocomposites by small angle X-ray scattering combined with electron microscopy. Polymer. 2010; 51, 1437–1449.
7. P. A.Hassan, Gunman Verma, Chapter 1: Soft Materials - Properties and applications in the text book: functional materials: preparation, processing and applications, Edited by S. Banerjee and A.K. Tyagi, Elsevier, 2012.
8. Sabyasachi Ganguli, Derrick Dean, Kelvin Jordan, Gary Price, Richard Vai. Mechanical properties of intercalated cyanate ester–layered silicate nanocomposites. Polymer. 2003; 44, 1315–1319.
9. Luiza MP Campos, Letı´cia C Boaro, Tamiris MR Santos, Pamela A Marques, Sonia RY Almeida, Roberto R Braga, and Duclerc F Parra. Evaluation of flexural modulus, flexural strength and degree of conversion in BISGMA/TEGDMA resin filled with montmorillonite nanoparticles. Journal of composite materials. 2016; 51, 927-937.

10. L. Le Pluart, J. Duchet, H. Sautereau, P.Halley, and J.-F. Gerard. Rheological properties of organoclay suspensions in epoxy network precursors. Applied Clay Science. 2004, 25, 207– 219.

11. S. T. Knauert, J. F. Douglas, and F. W. Starr. The effect of nanoparticle shape on polymer-nanocomposite rheology and tensile strength. Journal of Polymer Science, Part B: Polymer Physics. 2007; 45, 1882–1897.

12. L Asaro, G Rivero, LB Manfredi, VA Alvarez, and ES Rodriguez. Development of carbon fiber/phenolic resin prepregs modified with nanoclays. Journal of Composite Materials. 2016; 50, 1287-1300.

13. Golla Rama Rao, Ivautri Srikanth, K. Laxma Reddy. Effect of organo-modified montmorillonite nanoclay on mechanical, thermal, and ablation behavior of carbon fiber/phenolic resin composites. Defence Technology. 2021; 17, 812-820.

14. Bibin John, C.P. Reghunadhan Nair, K.N. Ninan. Effect of nanoclay on the mechanical, dynamic mechanical and thermal properties of cyanate ester syntactic foams. Materials Science and Engineering A, 2010**,** 527, 5435–5443

15. Michael L. Ramirez, Richard Walters, Richard E. Lyon, Edward P. Savitski, Thermal decomposition of cyanate ester resins. Polymer Degradation and Stability. 2002; 78, 73–82.

16. Yongsheng Zhao, Kejian Wang, Fuhua Zhu, Ping Xue, Mingyin Jia. Properties of poly (vinyl chloride) / wood flour/montmorillonite: effect of coupling agents and layered silicate. Polymer Degradation and Stability. 2006; 91, 2874-2883.

17. *Q. Wu, Y. Lei; F. Yao; Y. Xu; K. Lian*. Properties of HDPE/clay/wood nanocomposites. J. Plastic Technology. 2007; 27, 108-124.

18. Yong Lei, Qinglin Wu, Craig M. Clemons, Fei Yao, Yanjun Xu. Influence of nanoclay on properties of HDPE/wood composites. Journal of Applied Polymer Science. 2007;106, 3958 – 3966.

19. B.Suresha and Manpinder S Saini. Influence of organo-modified montmorillonite nanolayers on the static mechanical and dynamic mechanical behavior of carbon/epoxy composites. Journal of Composite Materials. 2016; 50, 3589-3601.

20. G.J. Withers, Y. Yu, V.N. Khabashesku, L. Cercone, V.G. Hadjiev, J.M. Souza,D.C Davis. Improved mechanical properties of an epoxy- glass fiber composite reinforced with surface organo-modified nanoclays. Composites Part B. 2015; 72, 175–182.

21.Emrah B, Elcin K and Metin T. Mechanical and thermal behavior of non-crimp glass fiber reinforced layered clay/ epoxy nanocomposites. Compos Science and Technology. 2007; 67, 3394 – 3403.

22.I. Srikanth, Alex Daniel, Suresh Kumar, N. Padmavathi, Vajinder Singh, P. Ghosal, Anil Kumar, and G. Rohini Devi. Nano Silica modified carbon–phenolic composites for enhanced ablation resistance. Scripta Materials. 2010; 63, 200-203.

Chapter - V

Organo Montmorillonite Nanoclay Added Carbon Fiber – Benzoxazine Resin Composites

Preparation and Characterisation of Organo Montmorillonite Nanoclay Added Carbon Fiber – Benzoxazine Resin Composites

5.0. Introduction: Due to the ability to offer low thermal conductivity and high thermal stability, Phenolic resin-based ablative composites are widely used in aerospace applications. Phenolic resin has processing disadvantages such as volatiles evolution due to condensation polymerization reaction [1]. Because of this, many researchers are exploring alternate resin systems for high temperature applications like cyanate ester resins, polyimide and benzoxazine resin (BZ). These resin systems undergo addition cured polymerization giving no process volatiles. In addition to this, benzoxazine resin offers additional advantages such as good shelf life and good flame-retardant properties, excellent mechanical and thermal properties, near-zero volumetric shrinkage of resin and low moisture absorption [2-4]. Thus, there are many technical advantages in using benzoxazine resin (BZ) instead of phenolic resin. However, there is limited literature available on the processing, properties of the fiber reinforced polybenzoxazine resin for ablative applications. Aim of this research is to investigate suitability of carbon fiber reinforced benzoxazine resin composite for thermal protection system applications.

Many researchers investigated the thermal stability of benzoxazine resin composites with nanoclay and the mechanical properties of glass fiber reinforced benzoxazine composites [5-12]. However, no investigations on the ablative performance of benzoxazine resin composites have been published.

Though, a lot of literature is available in the area of nanoclay reinforced polybenzoxazine resin composites, no research work was reported so far on nanoclay added carbon fiber-benzoxazine resin (C-BZ) composites. Hence preparation and characterisation of organo-montmorillonite nanoclay added carbon fiber - benzoxazine resin composites is taken up in the present study.

5.1. Materials: Major raw materials used in this work are benzoxazine resin, PAN-based carbon fabric, and surface modified montmorillonite (o-MMT) nanoclay. Below is a detailed specifications for each of the raw materials.

5. 1.1 Benzoxazine resin: The benzoxazine precursor-based aniline, formaldehyde, bisphenol F with the trade name Anazine, having a softening point of 80-85 °C and a viscosity of 500 to 2500 cP at 100 °C, was procured from M/s Anabond Limited, Chennai, India. Benzoxazine resin (250 g) was taken into a vessel and added methyl ethyl ketone solvent

(123 g).The mixture was stirred for four hours to get a clear solution of benzoxazine resin. Benzoxazine resin has a solid content of about 65 wt% and solvent (methyl ethyl ketone) content of about 35%. Char yield of the cured benzoxazine resin is about 48 wt% in an inert atmosphere at a temperature of 900 °C. The chemical structure of bisphenol F based benzoxazine (BZ) resin is shown in **Figure 5.1.**

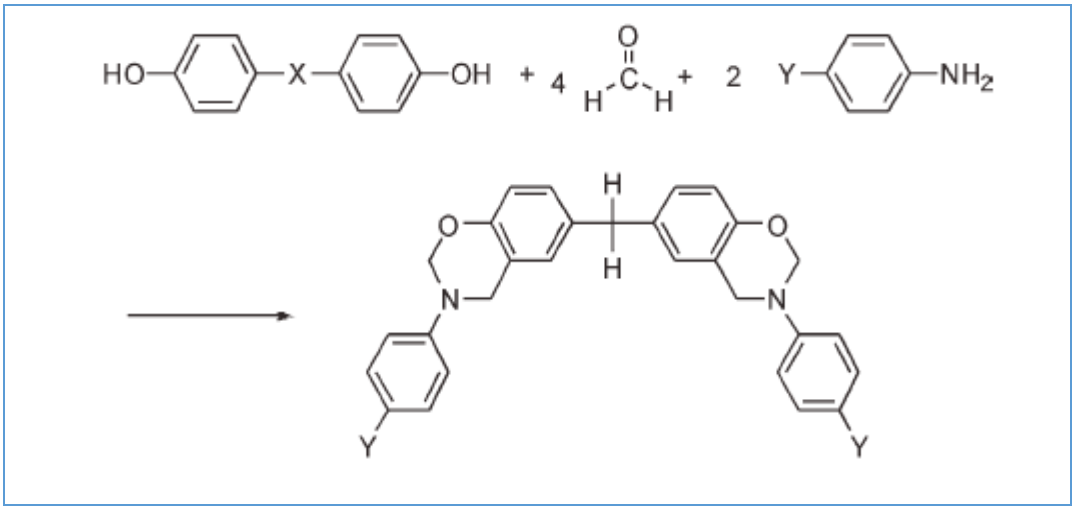

Figure 5.1. Chemical structure of bisphenol F based benzoxazine resin (BZ)

The brief specifications of benzoxazine resin are given below.

Sl. No	Test Parameter	Specification
1	Chemical name	Bisphenol F based benzoxazine resin
2	Viscosity at 30 °C	40 cP
3	Specific gravity at 30 °C	1.07
4	Solid resin content	67 (wt%)
5	Volatile content	33 (wt%)
6	Gel time at 190 °C	10 minutes
7	Commercial name	Anazine

5.1.2 PAN Based Carbon Fabric: A polyacrylonitrile (PAN) based high strength carbon fabric (bidirectional) woven with 3K fiber of T-300 grade was chosen for the manufacturing of three –phase (carbon fiber – benzoxazine resin- nanoclay) composites. The fabric's brief specifications are listed below.

S. No	Test Parameter	Specification
1	Tow type	3k (3000 filaments in tow)
2	Grade of carbon fiber	T- 300 Fiber (M/s Torayca carbon)
3	Thickness of fabric	0.38 ± 0.05 mm
4	Areal density	380 ± 20 g/m^2
5	Fabric weave style	8 Harness satin
6	Fabric count (warp direction)	24 ± 1 Ends /inch
7	Fabric count (weft direction)	24 ± 1 Ends /inch
8	Fabric breaking strength	250-300 kg/inch (in both warp & weft)
9	Carbon content	93 wt%
10	Density	1.8 g/cc

PAN based woven carbon fabric was procured from M/s Urja Products Pvt Ltd, Ahmedabad, India and it was used without any modification in the present study. The image of fabric is shown in **Figure 5.2.**

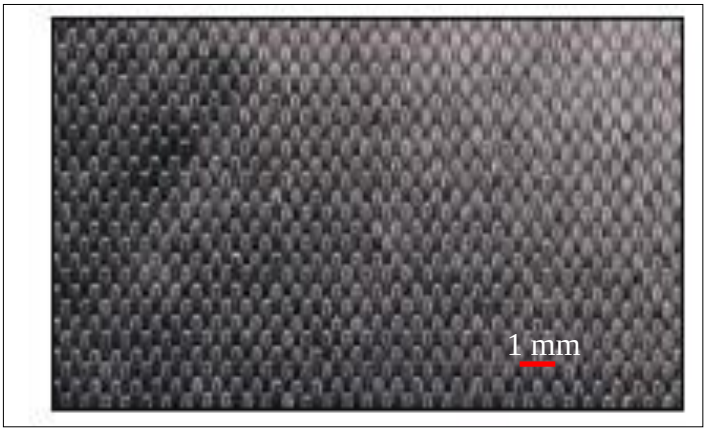

Figure 5.2 PAN based woven carbon fabric

5.1.3. Organo Modified Montmorillonite (o- MMT) Nanoclay

o-MMT nanoclay used in this study is nanomer 1.31 PS. Nanomer 1.31PS nanoclay was surface-modified montmorillonite (o-MMT) with 0.5-5 wt% aminopropyltriethoxysilane, 15-35 wt% octadecyl amine. The nanoclay (Nanomer 1.31 PS) was supplied by Sigma-Aldrich chemical Pvt Limited, Hyderabad, India. Brief specifications of the Nanomer 1.31PS nanoclay are as given below.

S. No	Test Parameter	Specification
1	Appearance	Off white free-flowing powder
2	Surface modifier	Octadecyl ammonium /silane
3	Bulk density	250-300 kg/m^3
4	Specific gravity	1.9
5	Particle size (mean)	14-18 micron

Figure 5.3 shows the structure and compositions of modified montmorillonite (o- MMT) nanoclay.

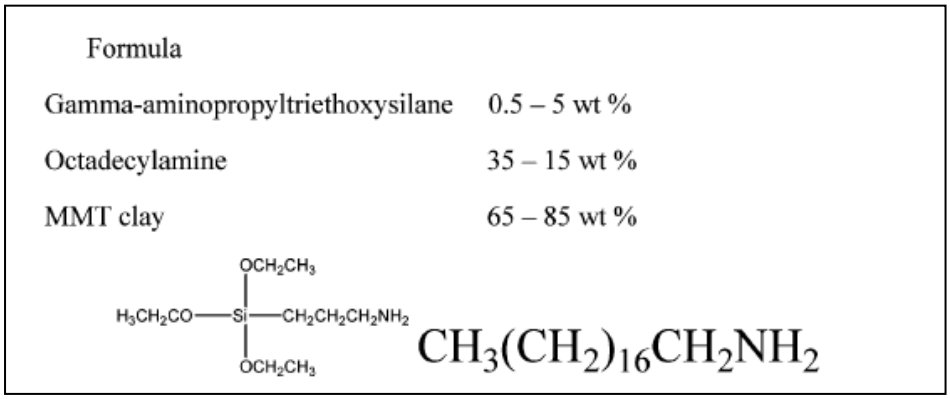

Figure 5.3. Structure and composition of modified montmorillonite nanoclay

5.2. Experimental Work: The flow chart below provides a quick overview of the experimental work carried out.

Flow chart: Schematic flow of experimental work

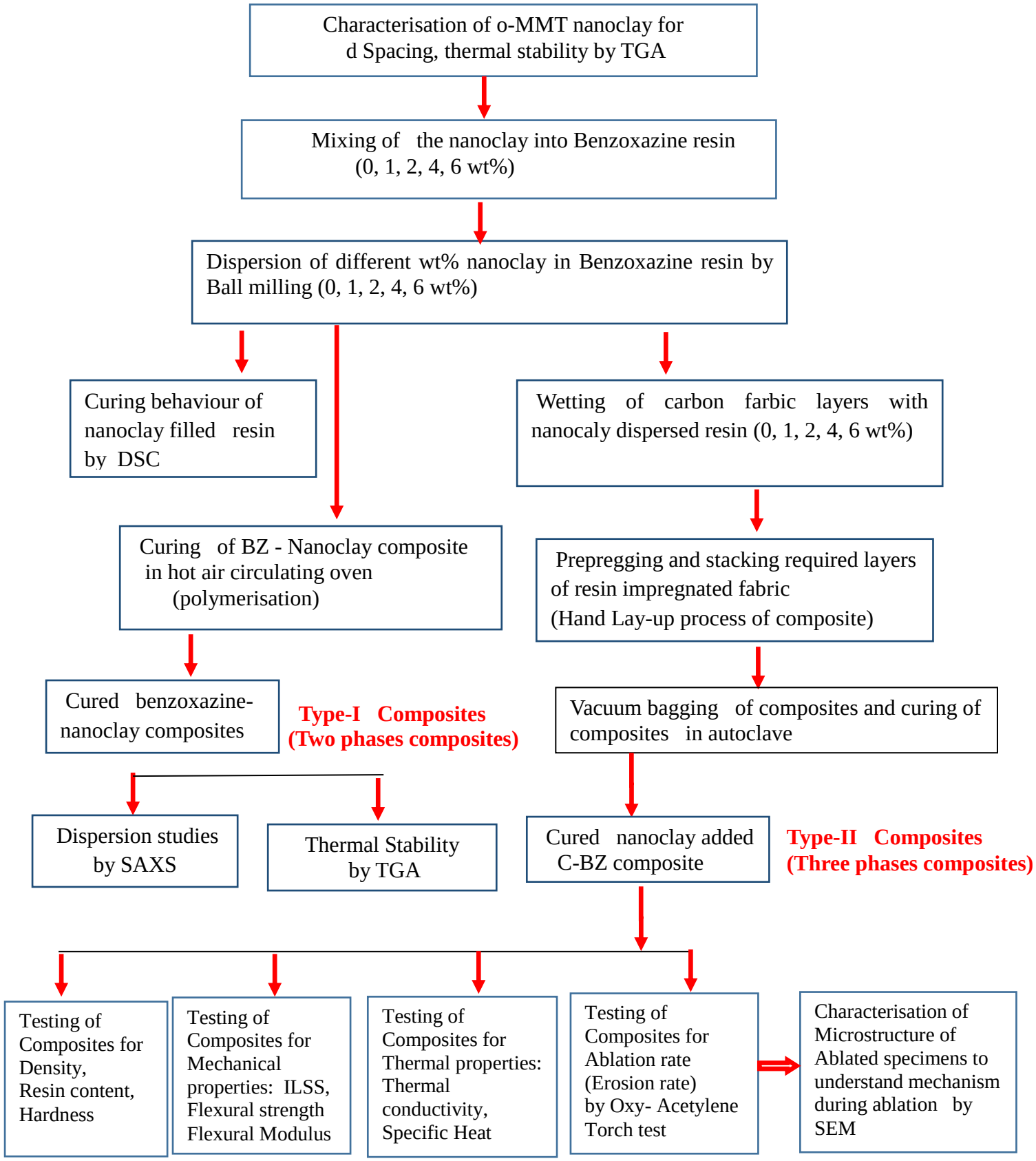

5.2.1 Dispersion of Nanoclay in Benzoxazine Resin

Approximately 198 grams of benzoxazine resin and 2 grams of o-MMT nanoclay were taken into a 500 ml stainless steel (SS) bowl for preparation of 1 wt% nanoclay filled benzoxazine resin. This mixture was initially stirred with a glass rod for approximately 5 mins. Then this mixture along with the bowl was placed into a planetary ball mill (M/s Insmart Systems) and ball milled for 2 h at 250 rpm using SS balls. Ball to charge ratio was maintained at 0.5:1. Thus, four different o-MMT nanoclay benzoxazine resin compositions were prepared by adding 1, 2, 4 and 6 wt% of nanoclay to benzoxazine resin. The composition of two-phase (benzoxazine resin-nanoclay) composites is as given in **Table 5.1.**

Table 5.1. The composition of benzoxazine resin-nanoclay composites (Type-I).

Composite designation	**Nanoclay (NC) (wt%) in resin**	**Composition**
Benzoxazine resin (BZ)	0	
1NC - BZ	1	99 g of resin + 1 g of nanoclay
2 NC - BZ	2	98 g of resin + 2 g of nanoclay
4 NC - BZ	4	96 g of resin + 4 g of nanoclay
6 NC - BZ	6	94 g of resin + 6 g of nanoclay

Viscosity changes to the benzoxazine resin due to the nanoclay addition was measured using a Brookfield viscometer at 30 °C. Using these mixtures, type -I and type -II composites were fabricated as per the details given below.

5.2.2 Preparation of Nanoclay Added Benzoxazine Resin Composites (Type-1): Volatiles of the resin were removed by heating the nanoclay resin mix in a petri dish at 60 ^{0}C for one hour in hot air oven. Subsequently nanoclay dispersed resin mixture was cured in a hot air oven by exposing resin to 60 °C/1 h + 80 °C /1 h + 140 °C /1 h + 170 °C /3 h + 180 °C /2 h + 200 °C/ 4 h. Thus, four different variants of type-I composites were made along with a blank benzoxazine resin matrix sample. Details of the prepared type-I composites are given in Table 5.2. Cured blank benzoxazine resin and nanoclay filled benzoxazine resin composites are shown in **Figure 5.4.**

Figure 5.4 Cured blank BZ resin and 1, 2, 4, 6 wt% nanoclay filled BZ resin composites

5.2.3 Preparation of Nanoclay Added Carbon Fiber Reinforced Benzoxazine Resin Composites (Type-II): Processing steps involved in the preparation of type-II composites are shown in **Figure 5.5**. For fabricating each type-II composite, twelve carbon fabric layers having a size of 300 x 300 X 0.38 mm were cut and impregnated with nanoclay dispersed benzoxazine resin mixture using a nylon brush. These layers were stacked on a metal plate by hand layup process followed by vacuum bagging. This stack was cured in the autoclave as the per cure cycle given in **Figure 5.6.**

Hand impregnation of carbon cloth (fabric) with clay filled benzoxazine resin

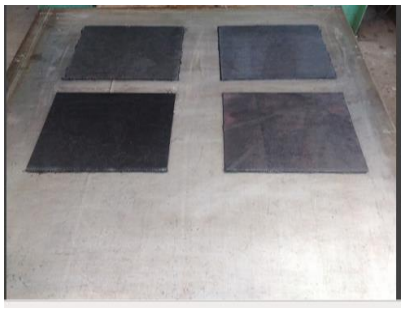

Hand Lay - up of composites (12 Layers ,Size : 300 x300 mm)

Vacuum bagging of composites and vacuum application

Curing of composite by autoclave process

Figure 5.5 Processing steps for preparation of nanoclay added C-BZ composites

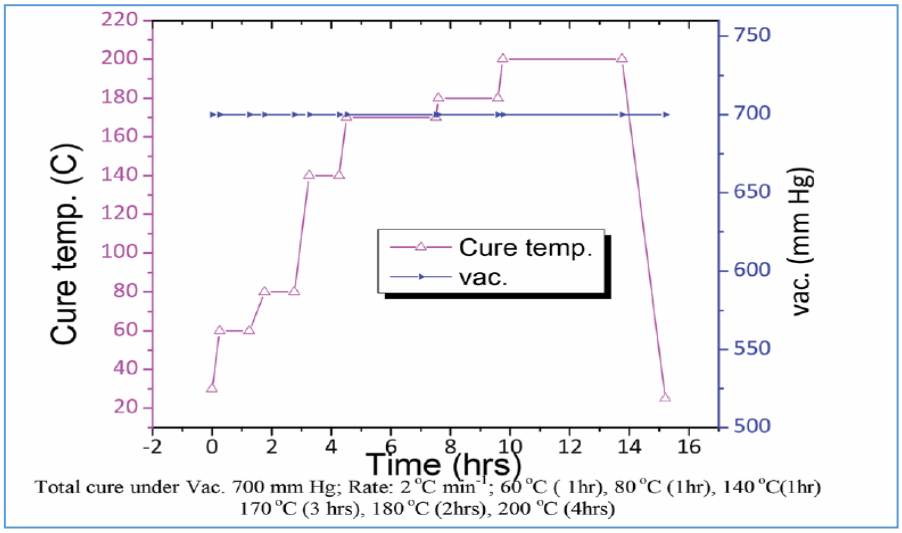

Figure 5.6 Cure cycle followed for curing of nanoclay added C-BZ composites

Five different variants of the type -II composites were prepared along with the blank carbon-benzoxazine resin composite. Details of the prepared nanoclay added carbon fiber-benzoxazine resin composite (type -II) are given in **Table 5.2.**

Table 5.2 Details of the prepared nanoclay added carbon fiber-benzoxazine resin composite (type -II)

Composite designation	**Nanoclay (NC) (wt%) in resin**	**Composition**
C- BZ (blank)	0	Carbon Fabric + Resin
1 NC/ C-BZ	1	Carbon Fabric + Resin + 1 wt% nanoclay
2 NC/ C-BZ	2	Carbon Fabric + Resin + 2 wt% nanoclay
4 NC/ C-BZ	4	Carbon Fabric + Resin + 4 wt% nanoclay
6 NC/ C-BZ	6	Carbon Fabric + Resin + 6 wt% nanoclay

Blank carbon fiber-benzoxazine resin composite and 1, 2, 4 and 6 wt% of nanoclay added carbon fiber-benzoxazine resin composite (type -II) are shown in **Figure 5.7.**

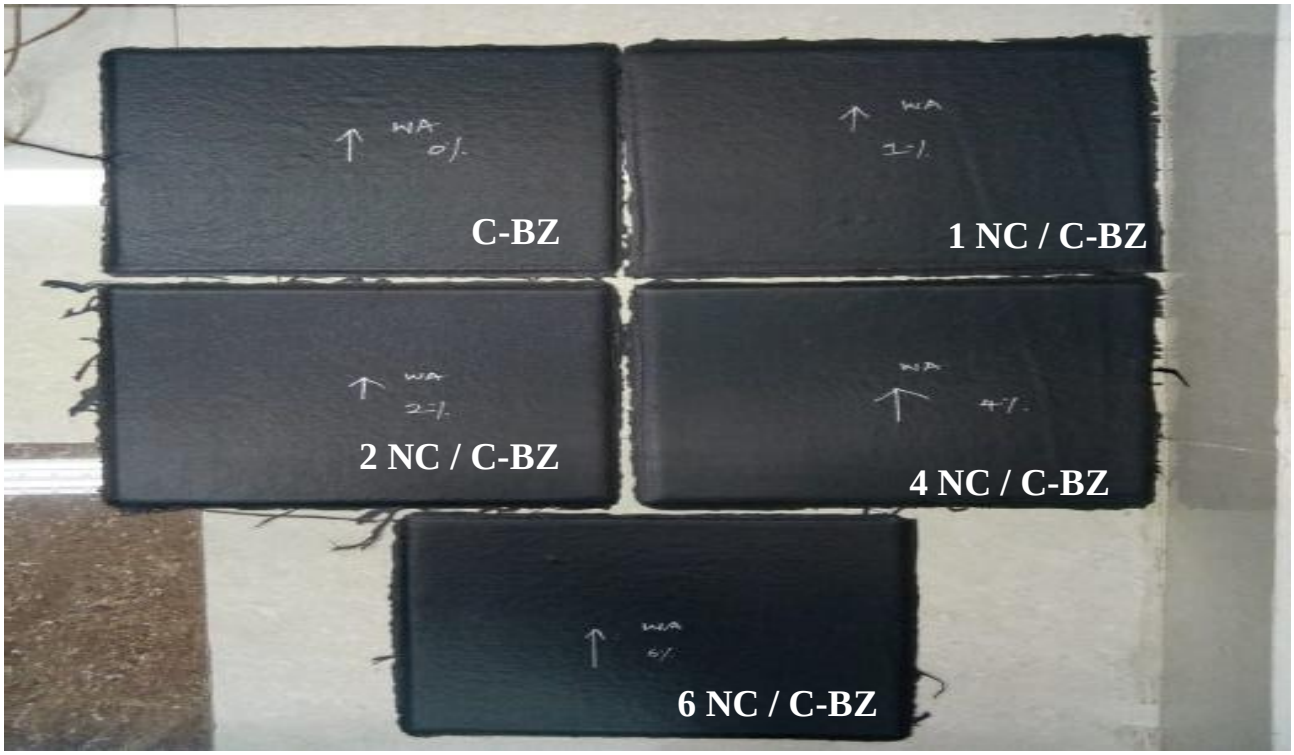

Figure 5.7 Blank carbon fiber - benzoxazine resin composite and 1, 2, 4, 6 wt% nanoclay added carbon fiber - benzoxazine resin composites

(**Size of each composite: 100 mm x 100 mm x 4 mm)**

5. 3 Characterisation and Testing

5.3.1 Curing Studies of Benzoxazine Resin - Nanoclay Composites

Differential scanning calorimetry (DSC: M/s TA instruments, Q200) was used to study the effect of o-MMT nanoclay on the curing reaction of benzoxazine resin composites. DSC was carried out from 30 to 400 °C by taking a sample mass of 10 ± 2 mg. A heating rate of 10 °C /min and a nitrogen flow of 50 mL/min were employed for these studies.

5.3.2 Dispersion Studies of Nanoclay in Benzoxazine Resin - Nanoclay Composites

Small angle X-ray scattering (SAXS: Antonpaar, Model: SAXS Point 2.0) was used to study the dispersion of o-MMT nanoclay in type-I composites. Dispersion of nanoclay in resin is also evaluated using a scanning electron microscope (SEM) (Table Top SEM, Make: SEC, Korea, Model: SN4500 Plus). Before SEM studies, the surface of the samples was coated with a thin gold film with a sputtering unit (Make: M/s Hind HiVacuum India, Model: Scancoat Six) to increase surface conductivity.

5.3.3 Fourier-Transform Infrared Spectroscopy (FTIR): The Ge-ATR attachment on an Agilent 640 series was used to record FTIR spectrums of benzoxazine resin - nanoclay composites. As received nanoclay, nanoclay heated at 200 °C for 2 hours, liquid benzoxazine resin, cured benzoxazine resin, and type -I composites were investigated in transmission mode with a spectral resolution of 4 cm^{-1}, and spectra from 4000 to 700 cm^{-1} were collected.

5.3.4 Density and Fiber Volume fraction: Type - II composites were tested for density and fiber volume fraction as per ASTM D 790 and ASTM D 3171.

5.3.5 Thermal Stability Test: Thermogravimetric analysis (TGA, M/s TA instruments, Q500) runs were carried out for samples collected from type -I and type -II composite from room temperature to 900 °C at a heating rate of 10 °C/min under a continuous flow of nitrogen (flow rate 60 ml/min). Temperature at 5% weight loss ($T_{5\%}$ / °C) and residual carbonaceous char (CR) were recorded. The thermal stability of the as received o-MMT nanoclay was also studied using the same TGA program under similar heating and nitrogen flow conditions.

5.3.6 Interlaminar Shear Strength and Flexural Test: ASTM D 790 was followed for the flexural strength test and ASTM D 2344 was followed for interlaminar shear strength (ILSS) test for type-II composites. Tests were carried out with UTM (M/s ADMET Model 2505). Minimum six samples were tested for each property. The average value and standard deviation were calculated.

5.3.7 Oxy-Acetylene Torch Test: For the oxy-acetylene torch test, the ASTM E285 methodology was utilised to evaluate the mass ablation rate of nanoclay added carbon fiber reinforced benzoxazine resin composites. Samples having a size of 100 mm × 100 mm x 4 mm were collected from the type- II composites to carry out test. Thus, one set of samples of type-II samples were subjected to a constant heat flux of 500 W/cm^2 for 60 seconds, while the other set of type-II composites were subjected to a constant heat flux of 125 W/cm^2 for 60 seconds. The mass ablation rate for these samples was calculated as mass loss per second. Two samples were tested at each flux and the average mass ablation rate was reported.

5.4. Microstructure Characterisation: Microstructure of the type-II composite samples exposed to oxy-acetylene torch was studied using a scanning electron microscope (Table Top SEM, Make: SEC, Korea, Model: SN4500 Plus).

5.5. Results and Discussion

5.5.1. Effect of Nanoclay Content on Viscosity of Benzoxazine Resin:

The results of viscosity measurements of blank benzoxazine resin and 1, 2 4, 6 wt% nanoclay filled benzoxazine resin are given the **Figure 5.8.**

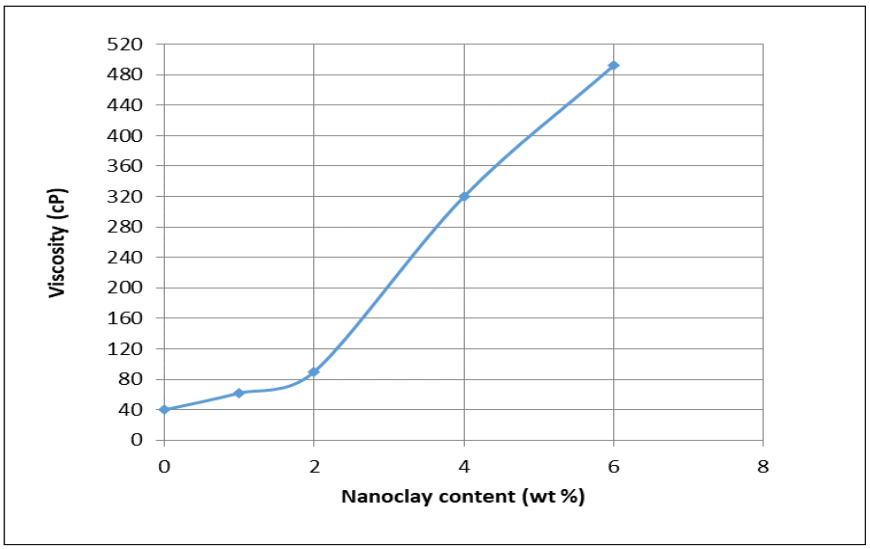

Figure 5.8: Effect of nanoclay content (wt%) on the viscosity of benzoxazine resin

The viscosity of benzoxazine resin at 30 °C is about 40 cP and that of 6 wt% nanoclay filled benzoxazine resin is about 492 cP. The viscosity of resin increased by increasing the weight percentage of nanoclay addition to the resin.

5.5.2. Effect of Nanoclay Content on Curing Behaviour of Benzoxazine Resin: **Figure 5.9** shows the curing behaviour of the neat benzoxazine resin and type-I composites. Initially observed endothermic peaks can be ascribed to the process of evaporation of solvent from the resin. **Table 5. 3** shows the cure initiation temperature (T_i), cure onset temperature (T_e) and Peak cure temperature (T_p), end set of cure exotherm (T_f), and heat generated during curing (ΔH). It was observed from Table 5.3, that with the increase in nanoclay content, Ti, Te, Tp values shifted to lower temperatures with an increase in heat of polymerisation (ΔH) for type-I composites as compared to that of neat BZ resin. This is due to the catalytic effect of organo nanoclay on BZ monomer ring opening [9]. It can be seen that the ΔH is initially coming down up to 2 wt% by the addition of nanoclay, followed by an increase. Initially with the addition of nanoclay, hindrance for the diffusion of polymeric monomers increases during cross-linking. This is reducing the overall cross-link density. However, from 4 wt% nanoclay addition onwards, as the nanoclay is agglomerating and thus not spread throughout the matrix, it can't hinder the

molecular diffusion during curing. However, as the organic part of nanoclay is playing the catalytic role with ring-opening of BZ resin, it is triggering the reactions and acting as nucleating sites for their completion. This could have resulted in the higher ΔH at higher loading of o-MMT nanoclay. The observed trends were found to be matching with the previously reported data of heat of polymerization of nanoclay added polymers [8]. Thus, the present study indicates that, o-MMT acts as a catalyst for curing benzoxazine resin.

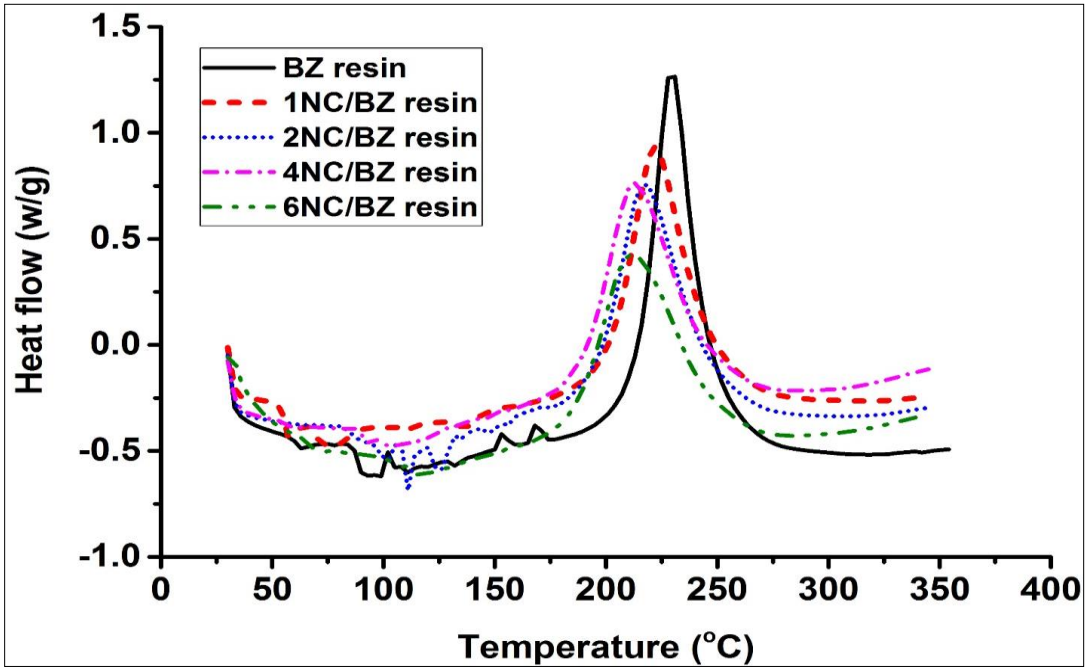

Figure 5.9. DSC scans for the Benzoxazine resin and BZ resin – nanoclay composites

Table5.3 Effect nanoclay content on cure characteristics of BZ resin – nanoclay composites

Sl. No	**Nanocomposites description**	**Nanoclay (wt%)**	**Ti** (°C)	**Te** (°C)	**Tp** (°C)	**T_f** (°C)	**ΔH** (J/g)
1	BZ resin	0	177	213	230	291	275
2	1 NC/ BZ	1	160	200	222	294	253
3	2 NC/BZ	2	158	195	217	299	247
4	4 NC/ BZ	4	113	186	212	295	300
5	6 NC/ BZ	6	110	183	211	286	285

5.5.3. Curing Studies of Benzoxazine Resin-Nanoclay Composites by Fourier-Transform Infrared Spectroscopy

Fourier-Transform Infrared spectrums of nanoclay (NC at RT) as received, nanoclay heated at 200 °C for 2 hours (NC at 200 °C), liquid Benzoxazine resin (L-BZ), cured benzoxazine resin (C-BZ), and type-I composites and resultant spectrum (subtracted cured BZ spectrum from cured BZ- NC composite spectrum) are shown in the **Figure 5.10.**

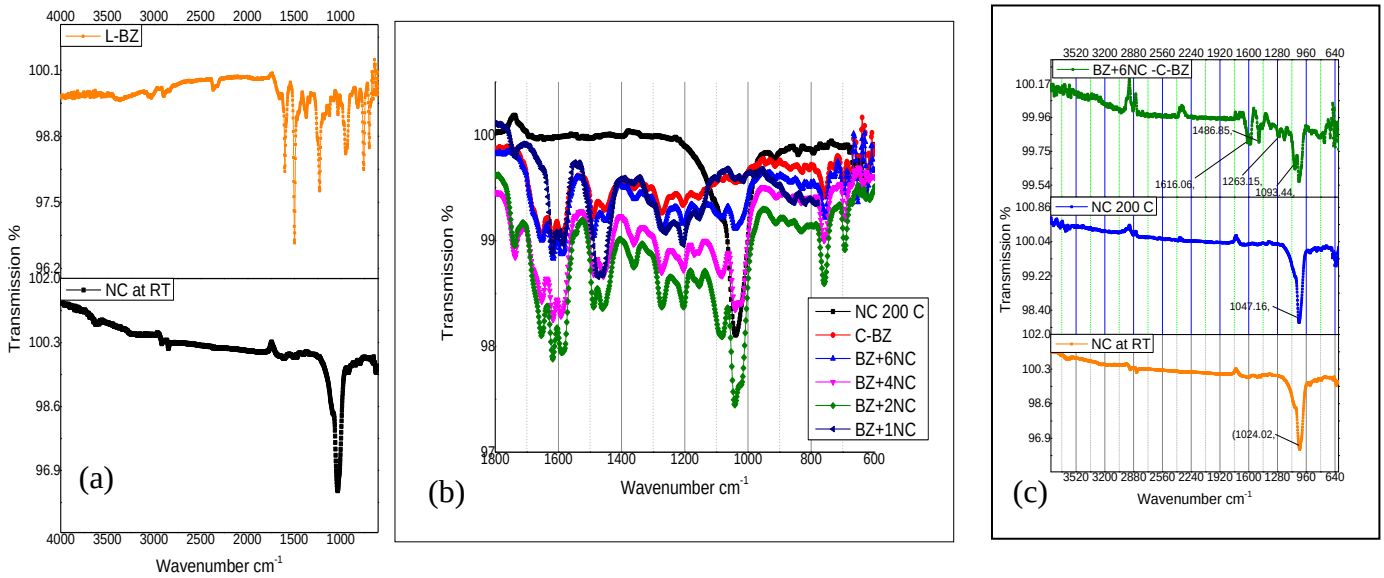

Figure 5.10. FTIR spectrums of (a) Nanoclay (as received) and liquid BZ resin (b) Nanoclay heated at 200°C, cured benzoxazine resin and type -I composites (c) Nanoclay (as received), Nanoclay heated at 200°C and resultant spectrum (subtracted cured BZ spectrum from cured BZ - NC composite spectrum).

Fig. 5.10 (a) represents the FTIR spectrums of nanoclay and liquid benzoxazine resin, which shows the characteristic peaks of siloxane (Si-O) at 1024 cm^{-1} for nanoclay and benzoxazine at 942 cm^{-1}(oxirane), 1027 cm^{-1}, 1232 cm^{-1} and 1490 cm^{-1} (tri substitued benzene ring). **Fig. 5.10 (b)** shows the FTIR spectrums of cured benzoxazine resin, nanoclay sample heated at 200 ^{0}C, and cured type - I composite samples. FTIR spectrums of cured type -I composite samples and cured benzoxazines show the disappearance of all characterstic peaks of BZ and appear a new peak at 1477 cm^{-1} (tetra substituted benzene ring) indicates that complete polymerization of benzoxazines in all composites samples. The effect of nanoclay in benzoxazine resin-nanoclay (BZ-NC) composites was determined by FTIR subtraction method, in which cured BZ FTIR spectrum was subtracted from cured BZ-NC FTIR spectrum. The resultant FTIR

subtracted spectrum was compared with that of nanoclay (NC) before and after heating the samples. **Figure 5.10 (c)** shows the FTIR spectrums of nanoclay (as received), nanoclay heated at 200 ^{0}C, and resultant spectrum of nanoclay (subtracted BZ resin from BZ-NC composite). Nanoclay before and after heating shows the characteristic broad peak at 1027 cm^{-1} which corresponds to siloxane structure, which indicates that there is no change of siloxane and other functional groups on heating. Subtracted FTIR spectrum shows that characteristic peak of nanoclay and also shows additional peaks at 1093, 1202, 1263, 1486, and 1616 cm^{-1}, this could be attributed to new siloxane and secondary amine structures stretching and bending vibrations. FTIR subtracted spectrum indicates that the amine and hydroxyl groups present on the organo modified montmorillonite nanoclay participate in the ring-opening reaction and also form the part of the product.

5.5.4. Dispersion of Nanoclay in Benzoxazine Resin- Nanoclay Composites

Figure.5.11 shows the SAXS patterns of the as-received nanoclay and cured type-I composites for dispersion studies.

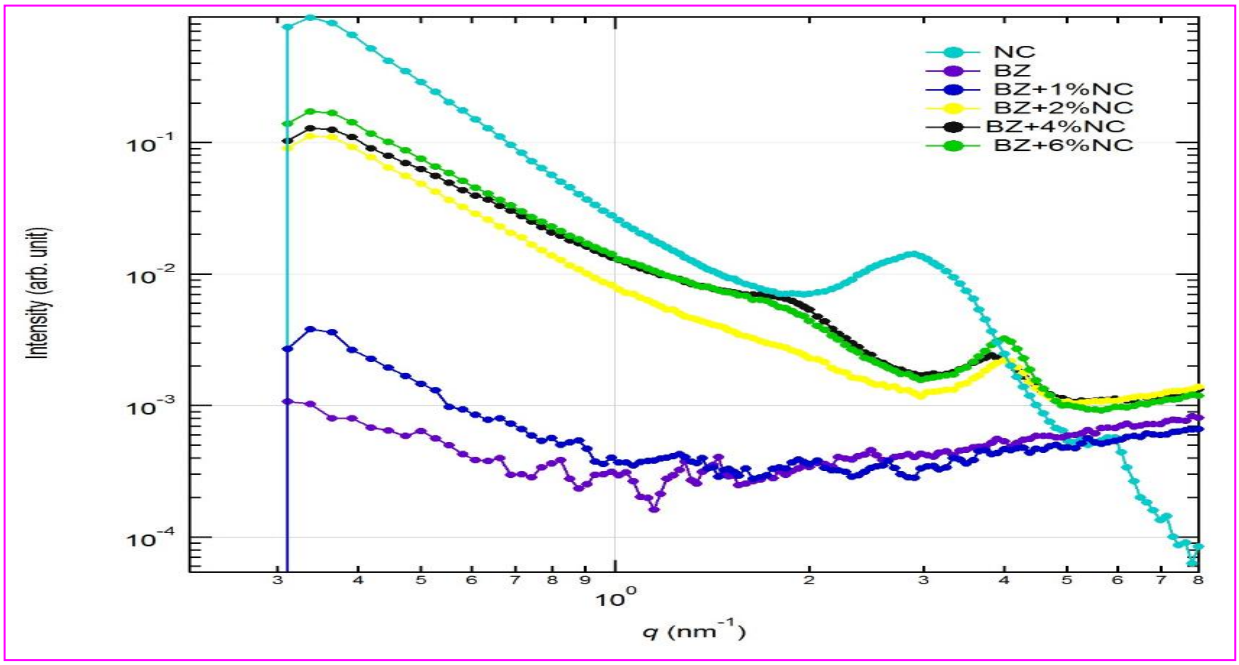

Figure 5.11. SAXS scans of nanoclay and benzoxazine resin-nanoclay composites

Bragg's law is used to calculate the *d* spacing of nanoclay and type-I composites. The results of d spacing values are shown in **Table 5.4.**

Table 5.4 *d* spacing values for nanoclay and benzoxazine resin-nanoclay composites

S. No	Nanocomposites description	Nanoclay (wt%) loading in resin	d 001 (Å)
1	Nanoclay	Nanomer 1.31 PS	32
2	1 NC-BZ	1 wt%	No crystalline peak
3	2 NC-BZ	2 wt%	No crystalline peak
4	4 NC-BZ	4 wt%	40
5	6 NC-BZ	6 wt%	40

It can be seen from **Figure 5.11**, that, the characteristic peak observed for the pure nanoclay (o-MMT nanoclay) was not observed in 1 wt% and 2 wt% of nanoclay addition in type-I composites, indicating that, clay platelets got exfoliated in the benzoxazine resin. SAXS patterns of 1 wt% and 2 wt% nanoclay added benzoxazine resin composite have not shown any crystalline peak of nanoclay at lower scattering vector (q). SAXS of 4 wt% and 6 wt% nanoclay added benzoxazine resin composites have shown crystalline peaks. However, the d spacing of nanoclay has increased from 32 Å to 40 Å in 4 wt% and 6 wt% nanoclay added benzoxazine resin composites. This shows that the nanoclay in 4 wt% and 6 wt% composites are partly intercalated.

The SAXS data shows clay platelet segregation, while the SEM shows clay distribution in the matrix on a macroscopic scale. **Figure 5.12** shows SEM images of nanoclay dispersed in type-I composites. The white spots in **Figure 5.12** are correlated with the silicon molecule, which is one of the main constituents of o-MMT nanoparticles. As a result, the larger amount of white spots with a uniform distribution around the exposed region indicates the presence of o- MMT nanoclay in the matrix.

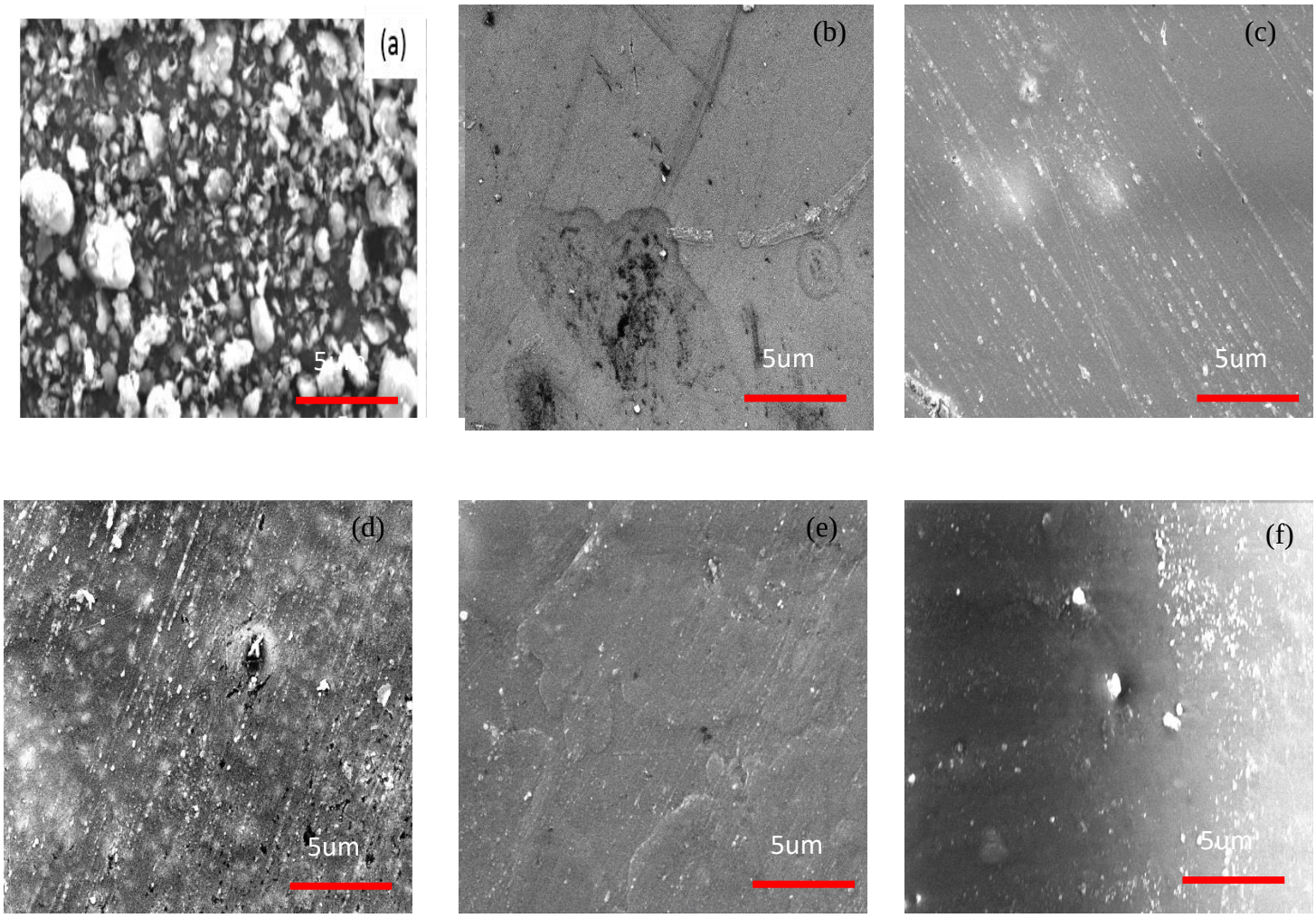

Figure 5.12. SEM images (a) as received o-MMT nanoclay (b) neat benzoxazine resin (c) 1 wt% o-MMT nanoclay added benzoxazine composite (d) 2 wt% o-MMT nanoclay added benzoxazine composite (e) 4 wt% o-MMT nanoclay added benzoxazine composite (f) 6 wt% o-MMT nanoclay added benzoxazine composite.

5.5.5 Density and Fiber Volume Fraction of Nanoclay Added Carbon Fiber - Benzoxazine Resin Composites

It can be seen from **Table 5.5** that, the fiber volume fraction (%V_f) of the composites decreased as the nanoclay content increased in benzoxazine resin. This is because of the increased viscosity of the resin at higher loading of nanoclay which don't squeeze out from the fabric layers during the processing of composites, leading to higher lower fiber volume fraction [13].

Table 5.5 Density and fiber volume fraction of nanoclay added C-BZ composites

Sl No	Composite description	Nanoclay (wt%)	Density (g/cc)	Resin content ($W_{R)}$) (wt%)	Fiber content ($W_{F)}$) (wt%)	Fibre volume fraction, V_f (%)
1	C- BZ	0	1.44	28	72	58
2	1 NC/ C-BZ	1	1.47	30	70	58
3	2 NC/ C-BZ	2	1.45	31	69	56
4	4 NC/ C-BZ	4	1.44	31	69	56
5	6 NC/ C-BZ	6	1.44	34	66	53

5.5.6. Barcol Hardness of Nanoclay Added Carbon Fiber-Benzoxazine Resin Composites

Barcol hardness of fabricated composites is shown in **Table 5.6**. Barcol Hardness values are found to be the same for blank C-BZ composite and nanoclay added C-BZ composites.

Table 5.6 Barcol hardness of nanoclay added C-BZ composites

Sl. No	Composite description	Nanoclay in resin (wt%)	Barcol hardness
1	C-BZ (blank)	0	65-70
2	1 NC/ C- BZ	1	65-70
3	2 NC/ C- BZ	2	66-70
4	4 NC/ C- BZ	4	65-70
5	6 NC/ C-BZ	6	65-70

Barcol hardness value indicates the extent of curing of composite. Data shows that all nanoclay added carbon fiber-benzoxazine resin composite is cured on par with blank carbon fiber-benzoxazine resin composite.

5.5.7. Thermal Stability of the Type -I and Type -II Composites

The TGA and DTGA thermograms for o-MMT nanoclay, neat benzoxazine resin, and benzoxazine resin-nanoclay composites (type -I) are shown in **Figures** 5.13 (a), 5.13 (b) respectively.

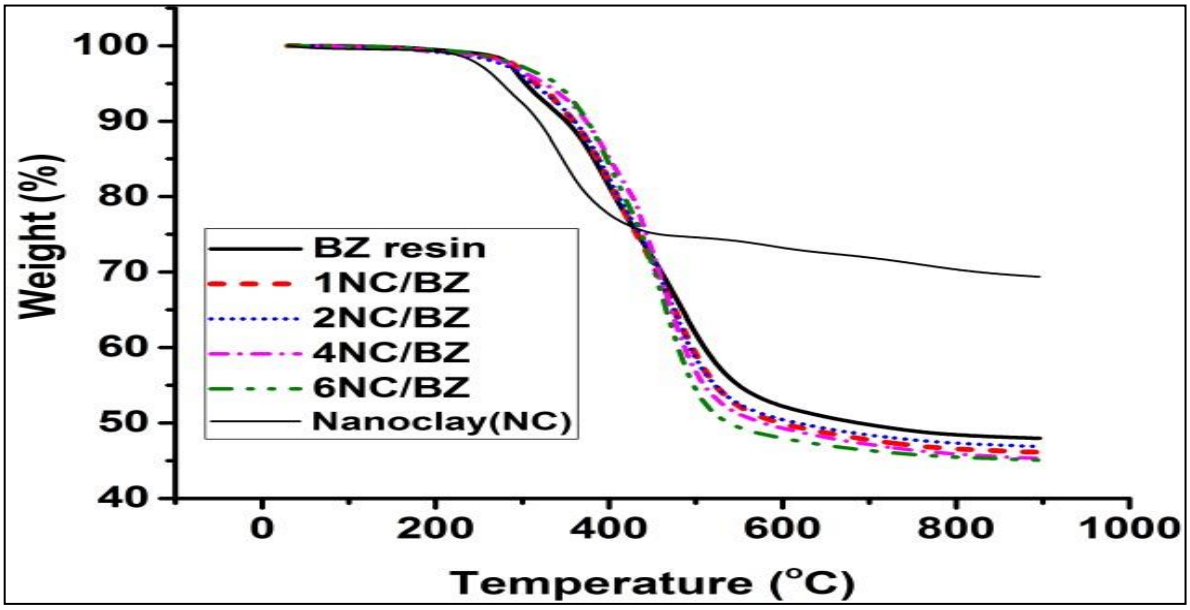

Figure 5.13 (a) TGA scans of nanoclay and benzoxazine resin-nanoclay composites

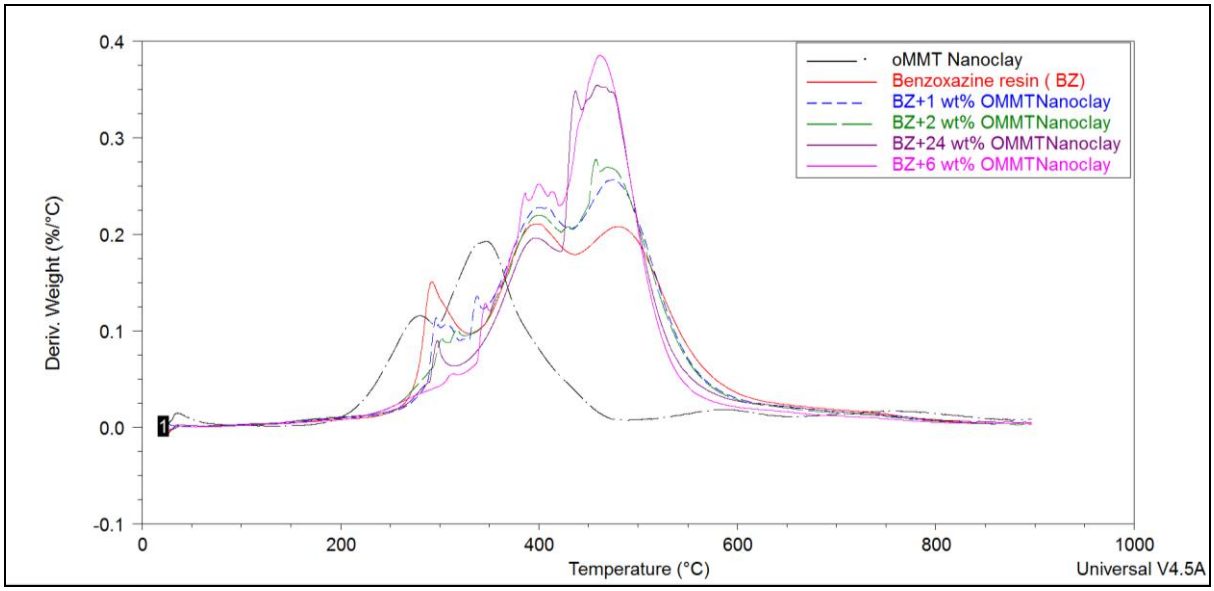

Figure 5.13 (b) DTGA scans of nanoclay and benzoxazine resin - nanoclay composites

The TGA and DTGA thermograms for blank carbon fiber-benzoxazine resin composite and nanoclay added carbon fiber - benzoxazine resin composites (type -II) are shown in **Figures 5.14 (a), 5.14 (b)** respectively.

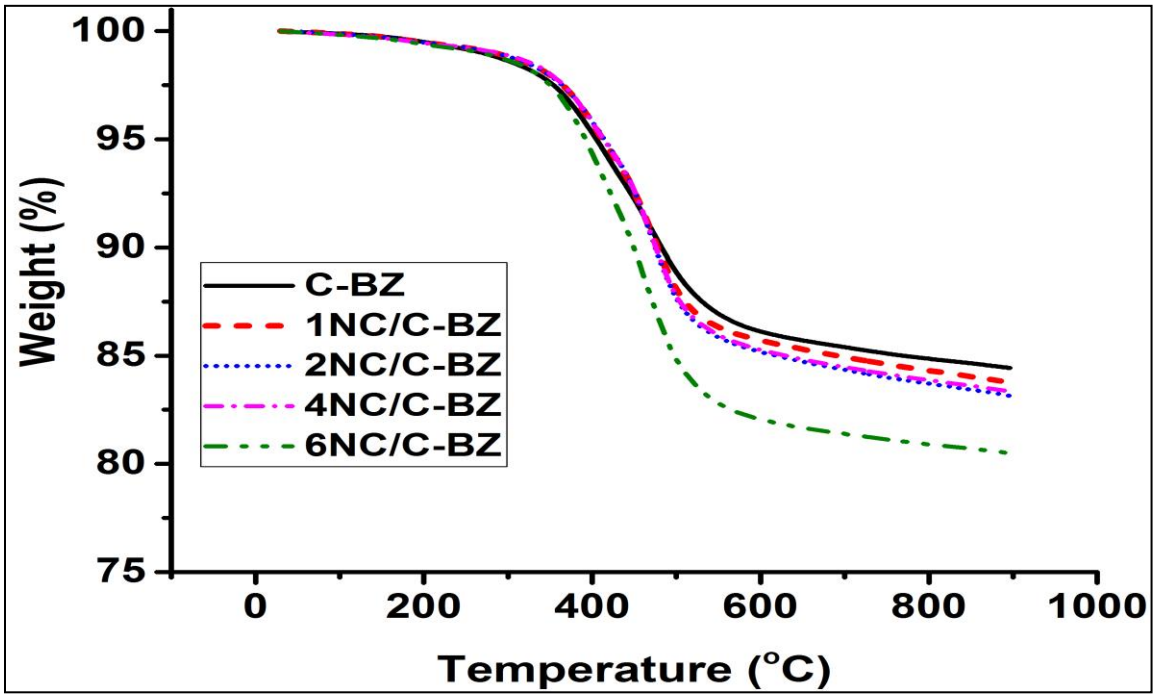

Figure 5.14 (a) TGA scans of nanoclay added C-BZ composites (type -II)

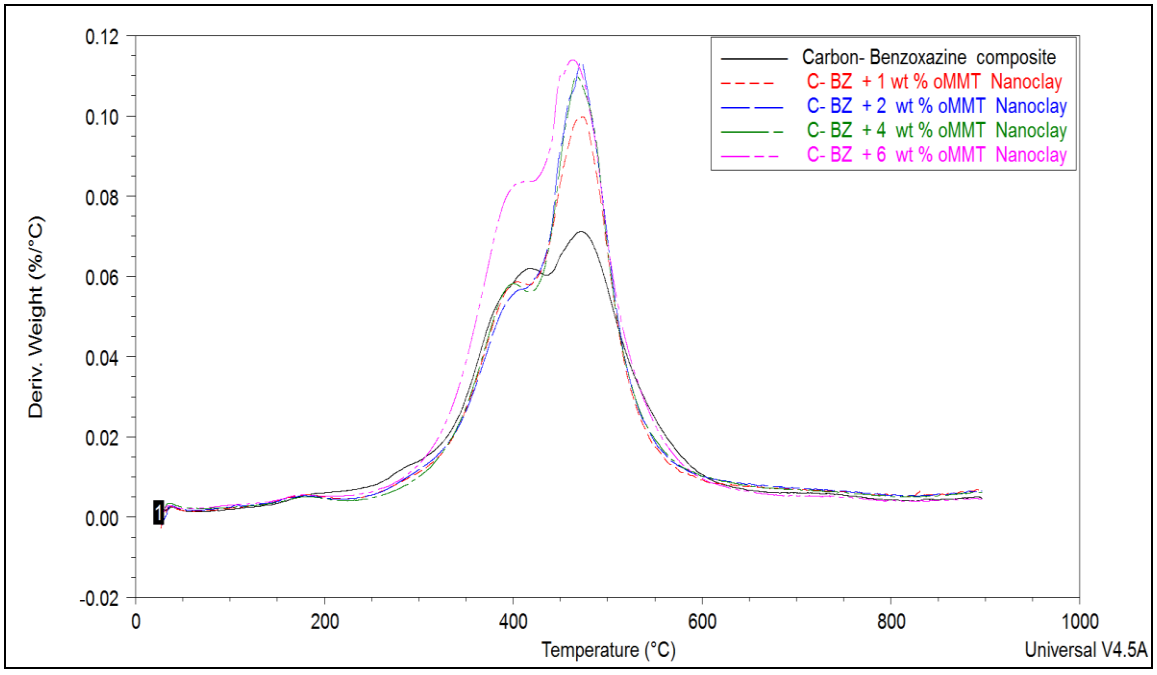

Figure 5.14 (b) DTGA scans of nanoclay added C-BZ composites (type -II)

Char residue at 900 °C and temperatures at 5% weight loss ($T_{5\ \%/°C}$) are shown in **Table 5.7** for type -I and type -II composites.

Table.5.7 Thermal stability of type -I and type -II composites

Nanoclay (wt %) in composite	*$T_{5\ \%/°C}$		% Residue at 900 °C	
	Type-I	Type-II	Type-I	Type-II
0	303	405	48	84
1	315	413	46	84
2	315	415	47	83
4	325	414	45	83
6	340	390	45	80

Temperature at 5% weight loss of the sample

It can be seen that the thermal decomposition and resultant weight loss of the o-MMT nanoclay started at around 250 °C and completed at around 450 °C. From the residual weight of nanoclay at 900 °C, it can be inferred that around 70% of the weight of clay is inorganic and the rest is organic. It is observed that from **Figure 4**, that the degradation of benzoxazine resin is a three-step process starting at 303 °C with a resultant end char of 48 wt% at 900 °C. It can be seen that the temperature at 5% weight loss ($T_{5\ \%/°C}$) has increased marginally with an increasing weight percentage of nanoclay content in type -I composites as compared to blank composite. When compared to blank composites, the temperature at 5% weight loss (T5%/°C) increased nanoclay concentration up to 4% in type -II composites. The increase of thermal stability is due to hindrance offered by nanoclay to oxygen diffusion and matrix interactions [14, 15]. At 6 wt% loading of nanoclay, $T_{5\ \%/°C}$ has come down when compared to the blank due to increased resin content of composites at higher loadings of nanoclay. Moreover, organic part of the nanoclay is known to give oxidizing volatiles which reduces the thermal stability of the matrix. This effect becomes prominent at higher loading of the nanoclay [16].

5.5.8 ILSS of Nanoclay Added Carbon fiber – Benzoxazine Resin Composites

ILSS values of individual specimens for each composition of type-II composites are shown in **Table 5.8.**

Table.5.8 ILSS test results of nanoclay added C-BZ composite

Specimen No	ILSS (MPa)				
	C-BZ	1 NC/ C-BZ	2 NC/ C-BZ	4 NC/ C-BZ	6 NC/ C-BZ
1	20	25	25	24	23
2	20	25	26	24	23
3	20	24	25	24	24
4	20	25	25	24	21
5	20	25	25	24	23
Average	**20**	**25**	**25**	**24**	**23**
Standard deviation	**--**	**0.45**	**0.45**	**-**	**1.09**

The effect of the weight percentage of nanoclay on ILSS is shown in **Figure 5.15**. With 1 wt% loading of nanoclay, ILSS value increased (25% increase at 2 wt% nanoclay loading) as compared to the blank C-BZ composites. This is because of the good dispersion of nanoclay up to 2 wt%. Beyond 2 wt%, ILSS started to come down, yet higher than blank C-BZ composites. Increased ILSS due to nanoclay can be attributed to the higher interfacial area of clay platelets and the ability of organic part of nanoclay platelets to effectively bind with matrix [17-19].

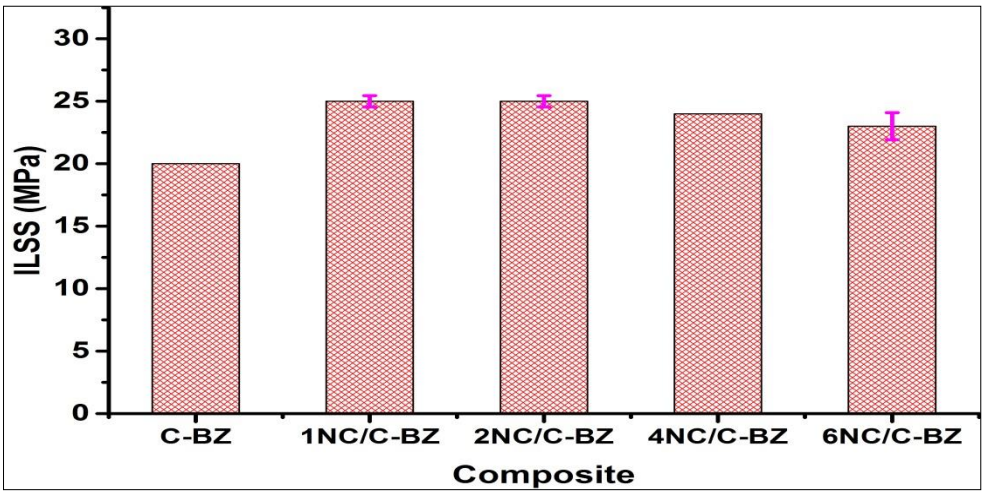

Figure 5.15 ILSS of nanoclay added carbon fiber – benzoxazine resin composites

5.5.9 Flexural Strength and Flexural Modulus of Nanoclay Added C – BZComposites

Individual specimen's flexural strength and flexural modulus values for each composition of type-II composites are shown in **Table 5.9**. The effect of nanoclay loading on the flexural strength of type - II composites is shown in **Figure 5.16**.

Table 5.9. Flexural strength (FS) and Flexural modulus (FM) of nanoclay added C-BZ composites

Specimen No	C- BZ		1 NC/ C-BZ		2 NC/ C-BZ		4 NC/ C-BZ		6 NC/ C-BZ	
	FS (MPa)	FM (GPa)	FS (MPa)	FM (GPa)	FS (MPa)	FM (GPa)	FS (MPa)	FM (GPa)	FS (MPa)	FM (GPa)
1	342	61	436	62	452	62	375	59	364	56
2	364	61	446	63	473	62	380	58	368	55
3	355	64	445	62	461	60	374	58	364	54
4	372	63	445	62	436	60	377	58	366	55
5	355	63	431	62	443	62	371	57	352	56
Average	**358**	**62**	**440**	**62**	**453**	**61**	**375**	**58**	**362**	**55**
Standard deviation	**11.23**	**1.34**	**6.7**	**0.44**	**14.6**	**1.1**	**3.4**	**0.71**	**6.3**	**0.84**

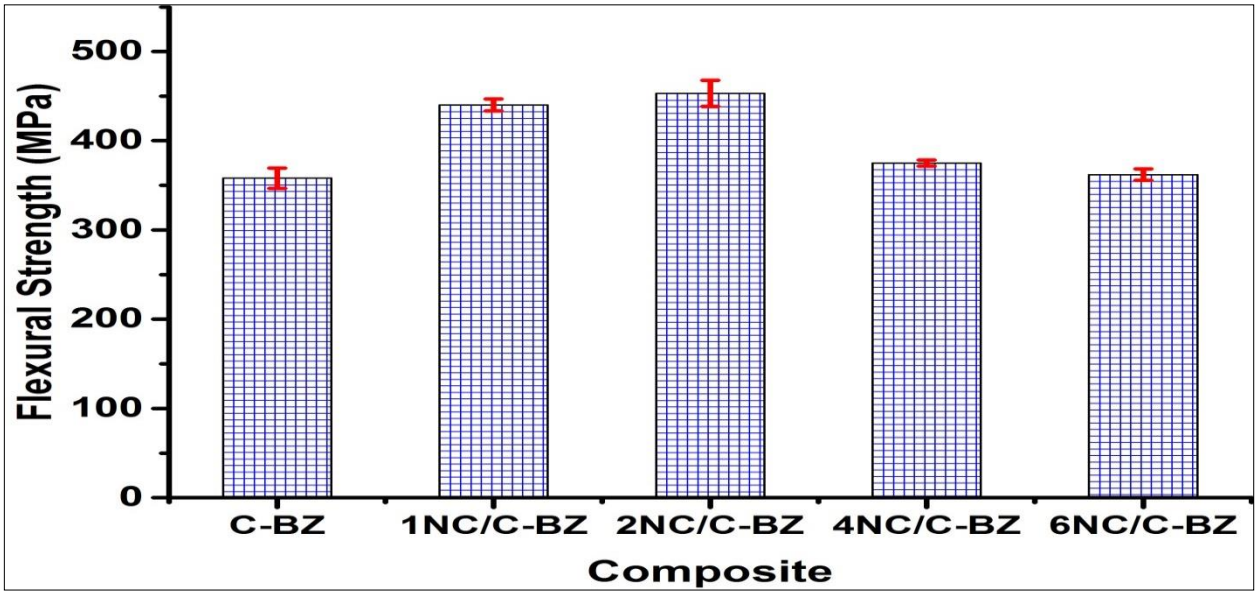

Figure 5.16. Flexural strength of nanoclay added carbon fiber – benzoxazine resin composites

Flexural strength increased significantly with 1 wt% addition of nanoclay with further marginal improvement up to 2 wt% nanoclay addition by about 27%. Beyond 2 wt% addition of nanoclay, flexural strength decreased. This can be attributed to good dispersion up to 2 wt% nanoclay addition. However, nanoclay at 4 wt% and 6 wt% loadings in composites have similar flexural strength as that of the blank composites, though the fiber volume fraction in these composites is less as compared to the blank. This indicates nanoclay platelets are strengthening the composite. Moreover, the results indicate that the nanoclay platelets under non exfoliated conditions (intercalated as per SAXS data) also could impart significant positive influence on the overall flexural properties of the composites due to strong chemical bonds, they form with the matrix, thereby resisting its cracking or debonding. These additional chemical bonds generated in the matrix adds to the overall strength of the composites [20-22].

5.5.10 Thermal Conductivity of Nanoclay Added Carbon Fiber – Benzoxazine Resin Composites

Thermal conductivity of the type-II composites is shown in **Table 5.10.** It can be seen that the thermal conductivity of the composite is decreasing as the nanoclay content in the composite is increasing. This can be attributed to the fact that, nanoclay acts as scattering centers for the heat energy-carrying phonons [23]. This results in energy loss at these inclusions, thereby reducing the overall thermal conductivity of the composite.

Table. 5.10 Thermal conductivity data of nanoclay added C-BZ composites

Sl. No	Composite description	Nanoclay (wt%)	Thermal conductivity (W/ m °C) at 30 °C
1	C-BZ (blank)	0	1.28
2	1 NC/ C-BZ	1	1.20
4	2 NC/C-BZ	2	1.09
3	4 NC/ C-BZ	4	1.01
5	6 NC/C-BZ	6	0.78

5.5.11. Specific Heat of Nanoclay Added Carbon Fiber – Benzoxazine Resin Composites

Specific heat of each composition of type -II composites was measured by differential scanning calorimetry (DSC) at different temperatures from 50 °C to 350 °C. Results of Specific heat of type-II composites samples are given in the following **Table 5.11.**

Table 5.11 Results of Specific heat of nanoclay added C-BZ composites

Composite description	**Specific heat (J/ kg ℃) at temperature (** ℃)					
	50 °C	100 °C	150 °C	200 °C	250 °C	300 °C
C-BZ (blank)	899	1125	1306	1443	1454	1439
1NC/ C-BZ	983	1262	1436	1556	1570	1555
2 NC/ C-BZ	934	1166	1318	1410	1422	1404
4 NC/ C-BZ	910	1162	1364	1468	1471	1429
6 NC/ C-BZ	1094	1373	1584	1651	1660	1646

Comparison of specific heat of blank C - BZ composite with different weight percentages of nanoclay added C - BZ composites are plotted and shown in **Figure 5.17.**

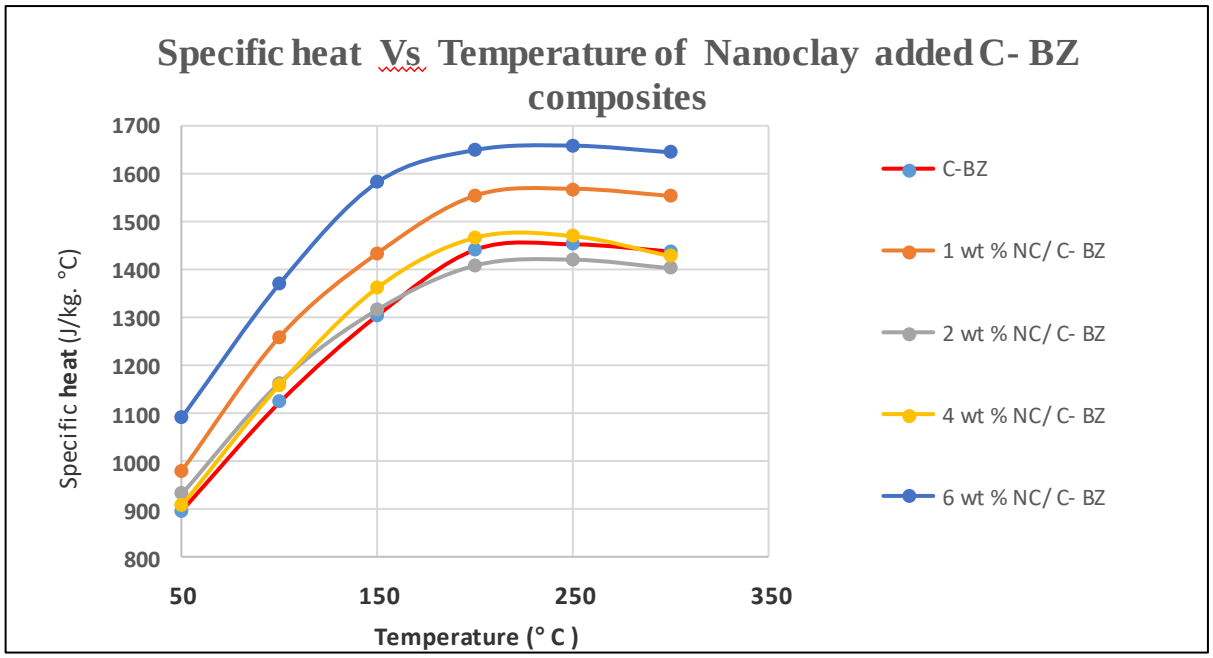

Figure 5.17. Specific heat versus temperature of nanoclay added C-BZ composites

Specific heat of nanoclay added C - BZ composites increased with an increase of nanoclay content as compared to blank C - BZ composite. The thermally stable, inorganic residue of silicate layers is responsible for the enhanced value of specific heat for nanoclay added C-BZ composites. This can lead to better insulation characteristics for nanoclay added C -BZ composites as compared to conventional unfilled C- BZ composite.

5.5.12. Effect of Nanoclay Content on Mass Ablation Rate of Type -II Composites

Figures 5.18 (a), 5.18 (b), and 5.18 (c) show images of type - II composite samples before and after oxy-acetylene torch testing (carried out on type-II composites at heat flux 125 W/cm^2 and 500 W/cm^2, respectively).

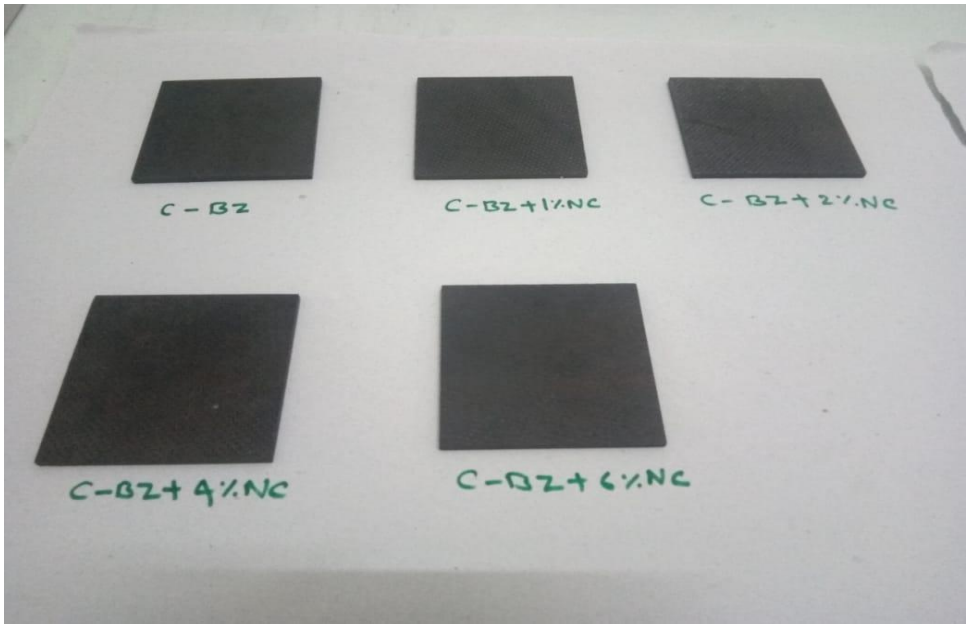

Figure.5.18 (a) Type -II composite samples (size: 100 mm x 100 mm x 4 mm) before oxy-acetylene torch test at 125 W/cm^2

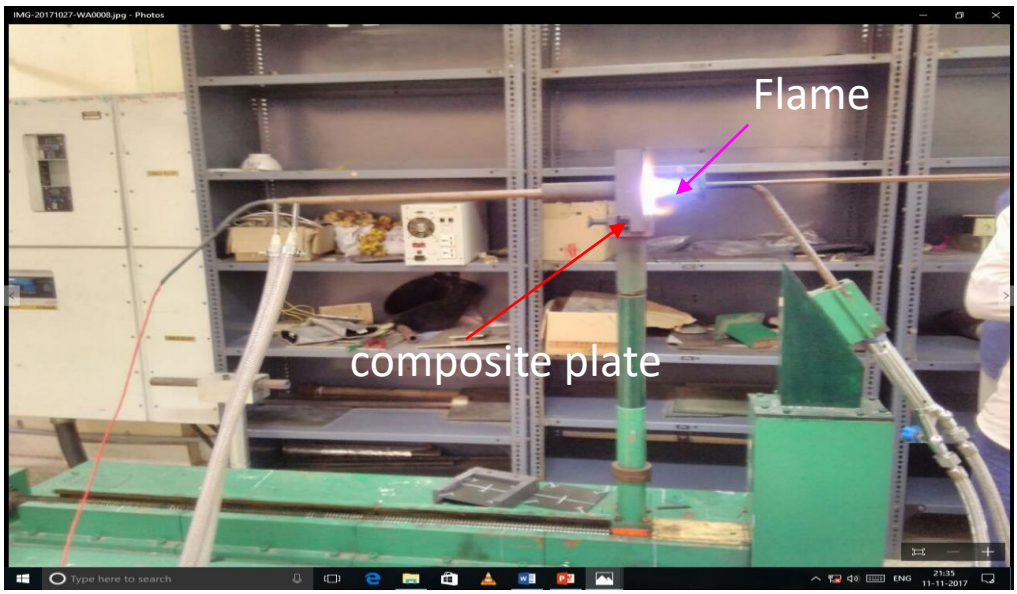

Figure 5.18 (b) Oxy-acetylene torch test of type -II composite at heat flux 125 W/cm^2

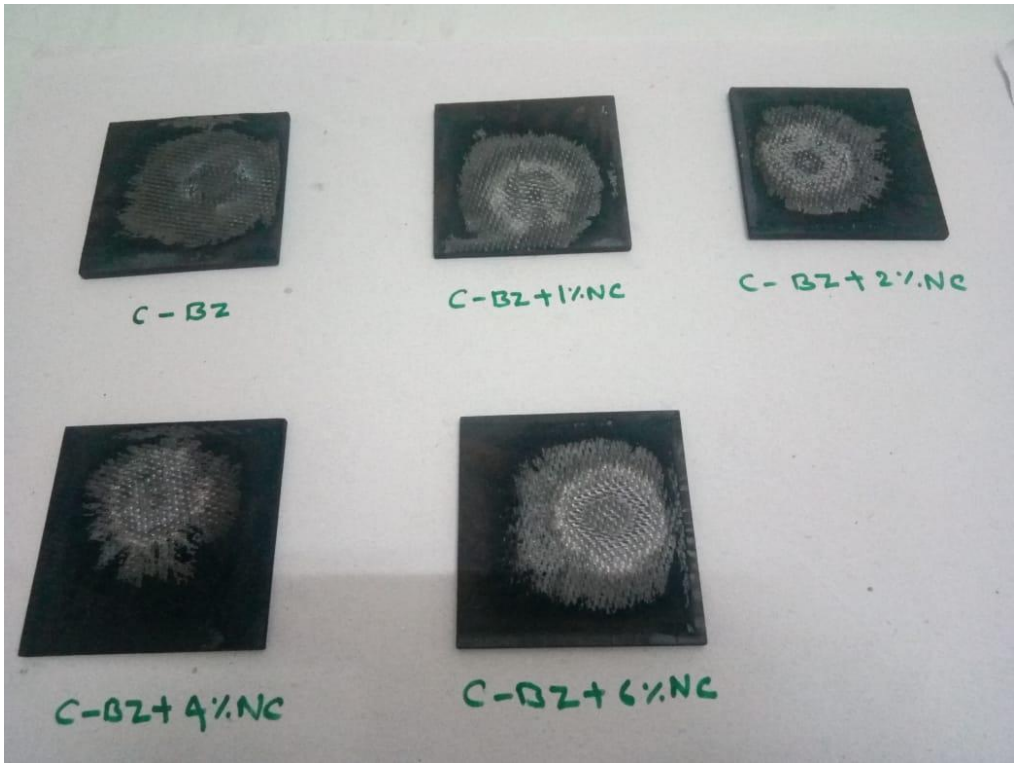

Figure 5.18 (c) Type-II composite samples after oxy-acetylene torch test at 125 W/cm^2

Figures 5.19 (a), 5.19 (b), and 5.19 (c) show images of type-II composite samples before oxy-acetylene torch testing, during oxy-acetylene torch testing on type-II composites at heat flux 500 w/cm^2, and sample after test, respectively.

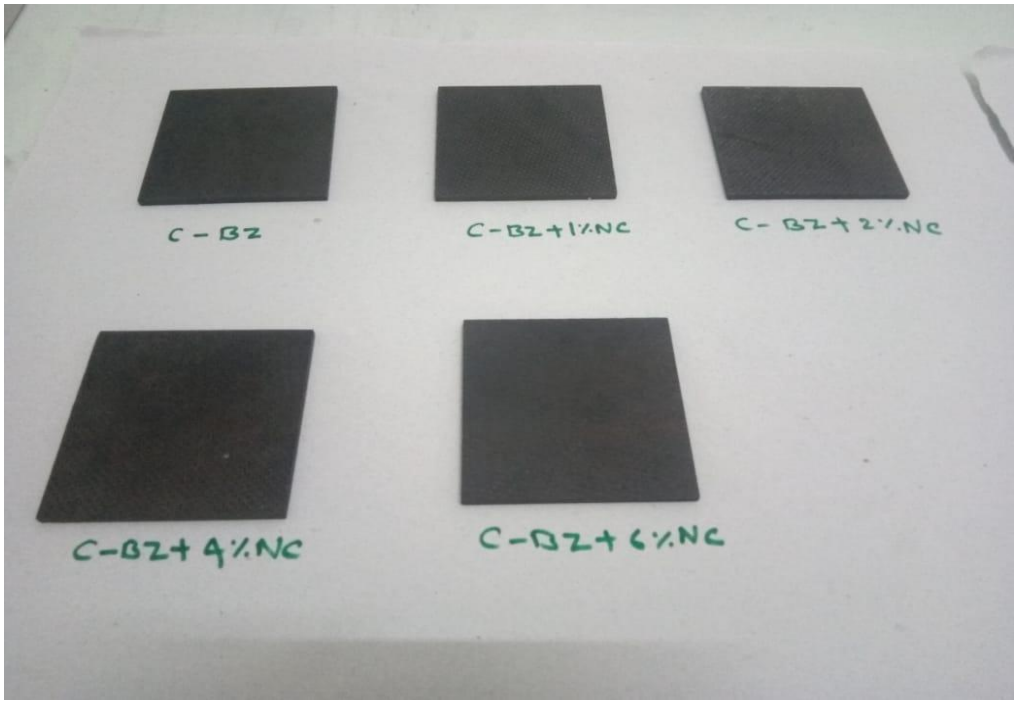

Figure 5.19 (a) Type-II composite samples (size: 100 mm x 100 mm x 4 mm) before oxy- acetylene torch test at 500 W/cm^2

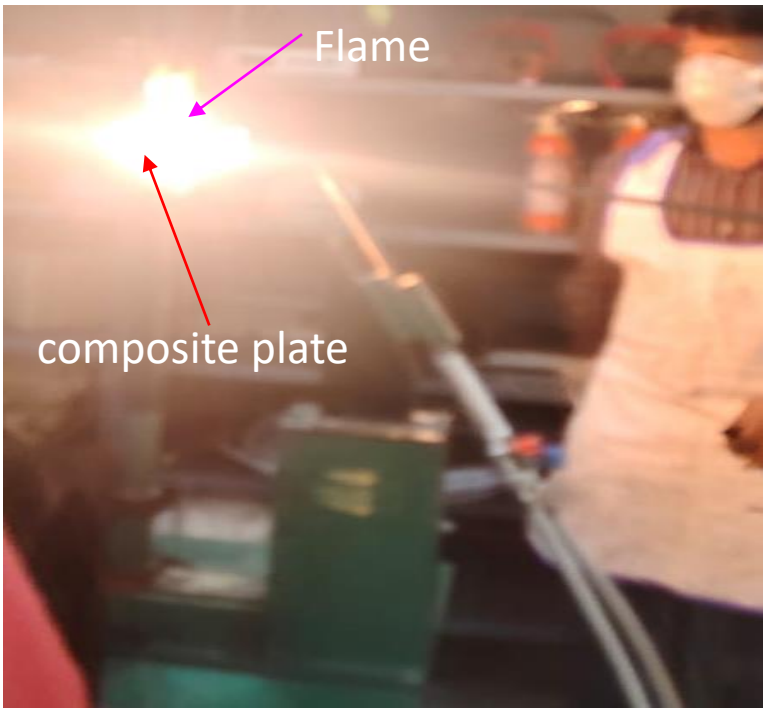

Figure 5.19 (b) Oxy-acetylene torch test of type-II composite at heat flux 500 W/cm^2

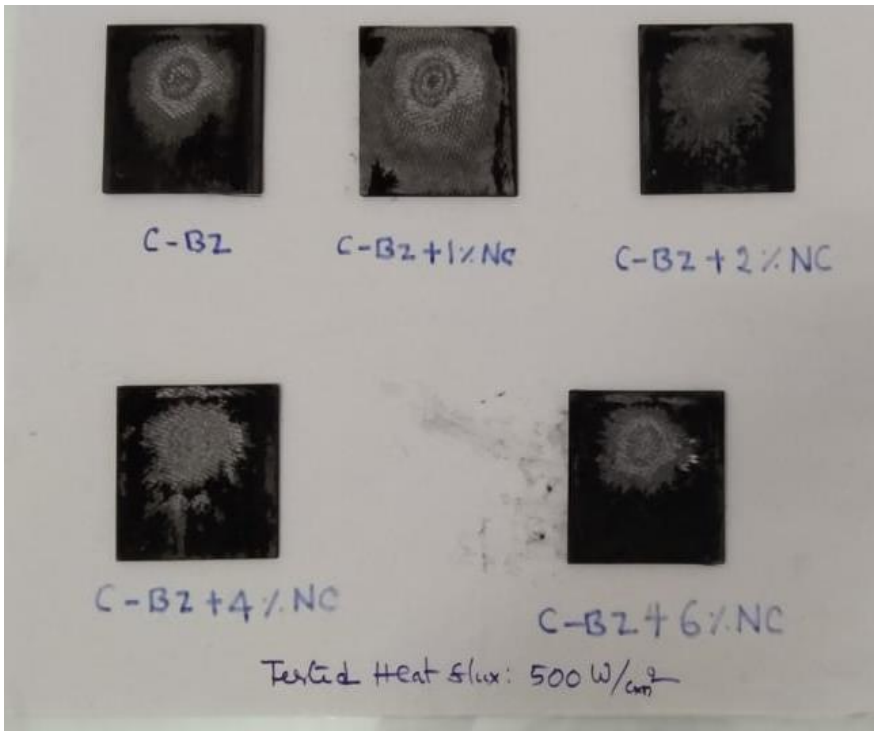

Figure 5.19 (c) Type-II composite samples after oxy-acetylene torch test at 500 W/cm^2

The results of the mass ablation rate of blank carbon-benzoxazine resin composite and nanoclay added carbon fiber-benzoxazine resin composites tested at low heat flux at 125 W/cm^2 and high heat flux at 500 W/cm^2 are presented in **Table 5.12.**

Table 5.12 Mass ablation rate of nanoclay added C-BZ composites

Composite description	**Nanoclay (wt%)**	**Mass ablation rate (mg/sec) at Heat flux 125 W/cm^2**	**Mass ablation rate (mg/sec) at eat flux 500 W/cm^2**
C- BZ (blank)	0	115	147
1 NC/ C-BZ	1	133 (15. 65)*	193 (31. 29)*
2 NC/ C-BZ	2	154 (33. 91)*	197 (34. 00)*
4 NC/ C-BZ	4	163 (41. 73)*	207 (40. 82)*
6 NC/ C-BZ	6	179 (55. 65)*	228 (55. 10)*

****Values shown in parenthesis indicate a percentage of increase in mass ablation rate as compared to blank.***

With increasing weight percentage of nanoclay content, mass ablation rates have increased as compared to blank at low heat flux 125 W/cm^2 and high heat flux 500 W/cm^2.

The degradation of the benzoxazine resin in the composite under inert atmosphere can undergo as per reaction shown in equation-1[25].

Benzoxazine resin $\longrightarrow$ C (Char) + CO + CO_2 + NH_3 - Heat ------- (1)

On the other hand, organic part of nanoclay degrades and gives oxygen as one of the byproducts[8].

Char formed in the reaction (1) can further react with the oxygen evolved from the organic part of the clay as per reaction (2) as shown below.

C (Char) + O_2 $\longrightarrow$ CO_2 + H_2O+ CO – Heat ---------- (2).

Because of the reaction shown in equation (2), char gets removed at a faster rate from the sample under ablation, thus bare fibers get exposed to the flame thereby removing large chunks of composites. Effect of char removal and subsequent increase in the ablation rate will be more pronounced at higher loading of o-MMT nanoclay leading to more ablation. This aspect can be understood from the microstructural changes of the ablated surfaces as discussed in subsequent sections.

5.5.13. Microstructural Behaviour of Ablated Surface of Type -II Composites

Microstructures of ablated surfaces, which were tested at a heat flux 125 W/cm^2 by oxy-acetylene torch test were shown in **Figure 5.20.**

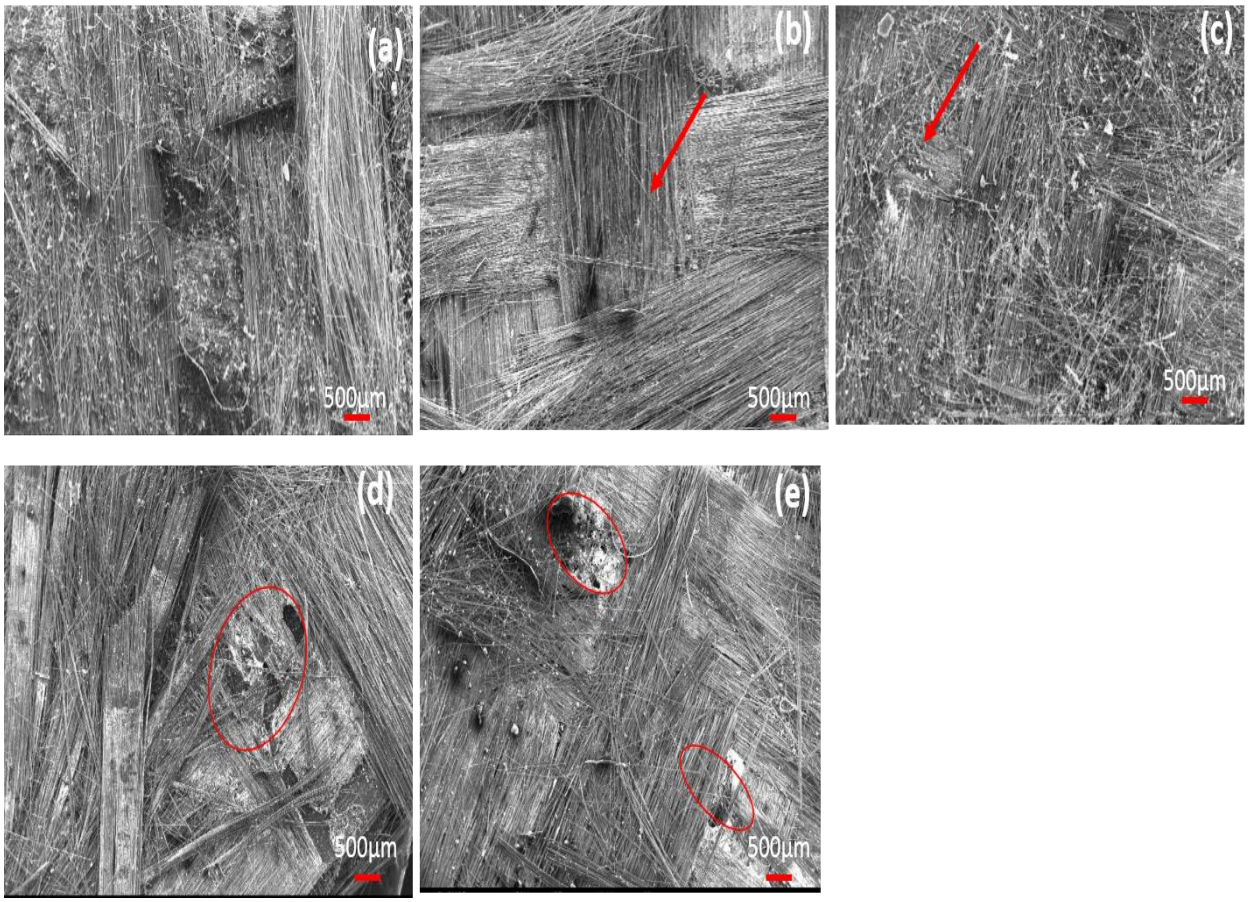

Figure 5.20: Microstructure of ablated samples tested at 125 W/cm^2 (a) blank C-BZ (b) 1 wt% nanoclay added C-BZ, an arrow indicating minor fiber breakage with traces of matrix present (c) 2 wt% nanoclay added C-BZ, arrow increasing depth of damage on carbon fiber tows (d) 4 wt% nanoclay added C-BZ, encircled zone showing deep grooves of damage with large of chunks of composites removed (e) 6 wt% nanoclay added C-BZ, encircled zones showing deep grooves of damage with large of chunks of composites removed.

Figure 5.20 (a) shows the blank C-BZ composite after ablation. It can be seen that there is no significant damage to the fibers for the blank C-BZ composite. Traces of charred matrix holding the fibers together can be noticed for blank C-BZ composite. However, in the case of nanoclay added composites, because of the reaction of char with nanoclay, bare fibers are being exposed. More is the nanoclay content, more is the damage to the matrix resulting in more damage area. At 4 wt% and 6 wt% nanoclay loading, deep grooves in the thickness direction of

the composite can be seen (encircled zones in **Figure 15.20 d & e**). This is because of the advancement of heat front ahead of ablation front which creates a situation, where, composite starts to degrade much ahead it sees the oxyacetylene flame. As the damage in the heat advancement zone increases, the erosive losses of the material when it sees the oxyacetylene flame will be more. This is resulting in more ablation rate for the nanoclay added type-II composites.

Microstructures of ablated surfaces that were tested at a heat flux 500 W/cm^2 by oxy-acetylene torch test were shown in **Figure 5.21.**

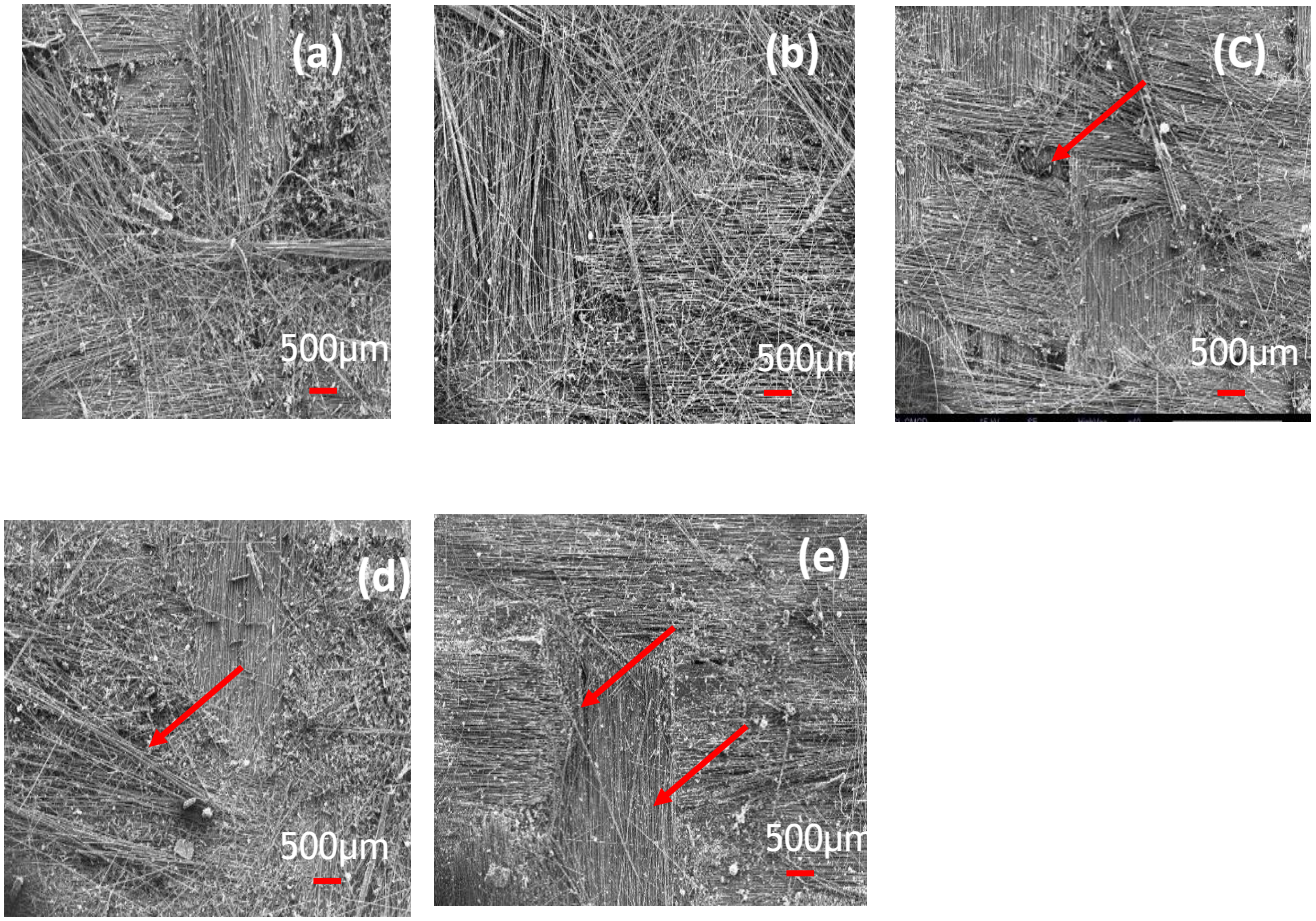

Figure 5.21: Microstructure of ablated samples tested at 500 W/cm^2 (a) blank C-BZ composite (b) 1 wt% nanoclay added C-BZ composite (c) 2 wt% nanoclay added C-BZ composite (d) 4 wt% nanoclay added C-BZ composite (e) 6 wt% nanoclay added C-BZ composite

Overall damage to the fibers at high heat flux 500 W/cm^2 was higher when compared to the low heat flux ablation. It can be seen that, in the case of the blank sample tested at high heat flux, large chunks of tows got damaged in **Figure 5.21 a.** This is because of the high heat flux. As

the nanoclay was added, damage to the tows increased significantly due to more heat input which accelerates the matrix degradation in the heat front which moves ahead of the ablation front. High heat flux coupled with higher nanoclay concentration, resulted in severe damage of tows of C-BZ composites added with 4 wt% and 6 wt% of nanoclay (**Figure 5.21 d** and **e**).

5.6. Conclusions: The effect of adding different weight percentages (0, 1, 2, 4 and 6 wt%) of organo modified montmorillonite (o-MMT) nanoclay on the thermal, mechanical characteristics of carbon fiber reinforced benzoxazine (type -II) was investigated. To understand the changes in the curing behaviour and thermal stability of the matrix part of the composite, nanoclay added benzoxazine composites (type -I) were also fabricated and the results obtained from type -I composites were correlated with thermomechanical behavior of type-II composites. The results obtained in this research work are summarised as below.

- Up to 2 wt% addition of o-MMT nanoclay in benzoxazine resin, exfoliation of clay platelets in resin was observed, beyond which clay platelets are not getting segregated effectively.
- Thermal stability increased for type-I composites up to 6 wt% addition of nanoclay, whereas thermal stability increased for type-II composites up to 4 wt% addition of nanoclay.
- Interlaminar shear strength and flexural strength of type-II composites increased by about 25%, 27% respectively at 2 wt% addition of nanoclay and beyond which these properties decreased.
- Mass ablation rate of type-II composites has increased with increased weight percentage addition of nanoclay as compared to the blank of carbon fiber reinforced benzoxazine composite.
- Based on mechanical properties, thermal stability, and mass ablation rate, 2 wt% o-MMT nanoclay as filler is optimum for improving the performance of carbon fiber reinforced benzoxazine resin composites without much compromise in the ablation performance.

7. References

1. P.D. Mangalgiri. Polymer - matrix composites for high-temperature applications. Defence Science Journal. 2005; 55**,** 175-193.
2. H. Ishida and P. Froimowicz. Advanced and emerging polybenzoxazine science and technology, Elsevier, 2017.
3. M.W. Wang, R.J. Jeng, C.H. Lin. Study on the ring-opening polymerization of benzoxazine through multi substituted polybenzoxazine precursors. Macromolecules. 2015; 48, 530–535.
4. H. Ishida and T. Agag. Handbook of benzoxazine resins. Elsevier, 2011.
5. Sanjeev K. Joshi, Ashavani Kumar$, and M.G.H. Zaidi. Effect of nanographite on electrical, mechanical and wear characteristics of graphite - epoxy composites. Defence Science Journal. 2020; 70, 306-312.
6. Corina Andronescu, Sorina Alexandra Gârea, Georgeta Voicu, Eugeniu Vasile, Horia Iovu. Nanocomposites based on a new polybenzoxazine resin and MMT. U.P.B. Sci. Bull., Series B. 2012; 74, 69-76.
7. .Hui-Wang, Cui, Shiao-Wei Kuo. Nanocomposites of polybenzoxazine and exfoliated montmorillonite using a polyhedral oligomeric silsesquioxane surfactant and click chemistry. Journal Polymer Research. 2013; 20, 114.
8. Tarek Agag, Tsutomu Takeichi. Preparation and cure behavior of organoclay-modified allyl - functional benzoxazine resin and the properties of their nanocomposites. Polymer composites. 2008; 29, 750-757.
9. Tsutomu TakeichI, Takehiro Kawauchi, and Tarek agag. High-Performance polybenzoxazines as a novel type of phenolic resin. Polymer Journal. 2008; 40, 1121-1131.
10. G.J. Withers, Y. Yu, V.N. Khabashesku, L. Cercone, V.G. Hadjiev, J.M. Souza,D.C Davis. Improved mechanical properties of an epoxy- glass fiber composite reinforced with surface organo-modified nanoclays. Composites Part B. 2015; 72, 175–182.
11. S. Rajesh Kumar, S. Krishna Mohan, J. Dhanasekaran. Novel glass fabric reinforced polybenzoxazine-silicate composites along with polyvinyl butyral for high service temperature applications, New Journal Chemistry. 2018; 19, 15499 - 16386.

12. S. Rajesh Kumar, S. Krishna Mohan, J.Dhanasekaran. Epoxy benzoxazine based ternary systems of improved thermo-mechanical behavior for structural composite applications, RSC Advances. 2015; 5, 3709-3719.

13 L Asaro, G Rivero, LB Manfredi, VA Alvarez and ES Rodriguez. Development of carbon fiber / phenolic resin prepregs modified with nanoclays. Journal of Composite Materials, 2016, 50, 1287-1300.

14. Ahmed Akelah, Ahmed Rehab, Mohamed Abdelwahab & Mohamed A.Betiha. Synthesis and thermal properties of nanocomposites based on exfoliated organoclay polystyrene and poly (methylmethacrylate). Nanocomposites. 2017; 3, 20-29.

15. M.S. Senthil Kumar, N. Mohana Sundara Raju, P.S. Sampath, M.Chithirai Pon Selvan. Influence of nanoclay on mechanical and thermal properties of glass fiber reinforce polymer nanocomposites. Polymer Composites. 2016; 39, 1861-1868.

16. Golla Rama Rao, Ivautri Srikanth, K. Laxma Reddy. Effect of organo-modified montmorillonite nanoclay on mechanical, thermal and ablation behavior of carbon fiber/phenolic resin composites. Defence Technology. 2021; 17, 812-820.

17 Yongsheng Zhao, Kejian Wang, Fuhua Zhu, Ping Xue, Mingyin Jia. Properties of Poly (vinyl chloride)/ wood flour/montmorillonite: effect of coupling agents and layered silicate, Polymer Degradation and Stability. 2006; 91, 2874-2883.

18. Q. Wu, Y. Lei; F. Yao; Y. Xu; K. Lian. Properties of HDPE/clay/wood nanocomposites. Journal Plastic Technology. 2007; 27, 108-124.

19. Yong Lei, Qinglin Wu, Craig M. Clemons, Fei Yao, Yanjun Xu, Influence of nanoclay on properties of HDPE/wood composites. Journal of Applied Polymer Science. 2007' 106, 3958-3966.

20.B Suresha and Manpinder S Saini. Influence of organo-modified montmorillonite nanolayers on the static mechanical and dynamic mechanical behavior of carbon/epoxy composites. Journal of Composite Materials. 2016; 50, 3589-3601.

21. Emrah B, Elcin K, and Metin T. Mechanical and thermal behavior of non-crimp glass fiber reinforced layered clay / epoxy nanocomposites. Compos Science and Technology. 2007; 67, 3394-3403.

22. I. Srikanth, Alex Daniel, Suresh Kumar, N. Padmavathi, Vajinder Singh, P. Ghosal, Anil Kumar and G. Rohini Devi. Nano silica modified carbon–phenolic composites for enhanced ablation resistance. Scripta Materials. 2010; 63, 200-203.

23. K.Hemvichian, H.D. Kim, H. Ishida. Identification of volatile products and determination of thermal degradation mechanisms of polybenzoxazine model oligomers by GC-MS. Polymer Degradation and Stability. 2005; 87, 213–224.

Chapter -VI

Kinetic studies on Thermal degradation of Phenolic resin, Cyanate Ester resin and Benzoxazine resin

Kinetics Studies on Thermal Degradation of Phenolic Resin, Cyanate Ester Resin, and Benzoxazine Resin

6.0. Introduction

Thermal shields made of polymeric ablative composite materials are used to protect spacecraft during re-entry from the massive quantity of heat created by friction with the atmosphere. Endothermic reactions cause ablative materials to disintegrate, absorbing heat and protecting the vehicle's interior. Heat transmission, chemical reactions, and fluid flow are the key phenomena that occur during the ablation process. As an ablator, the polymeric ablative must essentially perform two roles. First, it should degrade endothermically, absorbing energy, and second, it should act as a binder. Heat rejection through reradiation, transpiration of gases formed by degradation of the materials, insulation, heat absorption due to the heat capacity of the materials, and the latent heat of thermal degradation due to endothermic processes involved in degradation are some of the mechanisms by which ablative materials provide thermal protection. The principal heat absorbing mechanism among all of these is an endothermic breakdown of the ablating substance. Bond breaking happens during the endothermic breakdown process, resulting in smaller molecules [1]. Degradation mass losses of polymers acquired by thermogravimetric analysis (TGA) can be used to understand this degradation process. Typical weight loss profiles can be examined in TGA to determine the percentage of weight loss at each temperature and the residue at the final temperature. It can also be used to figure out how degradation progresses as a function of temperature. TGA data can be used to derive kinetic parameters for polymer decomposition, such as the degradation reaction rate constant, activation energies (Ea), reaction orders (n), and pre-exponential factors[2].

Assessment of thermal stability of matrix necessitate an understanding of the kinetic parameters that describe mass losses caused by thermal degradation.

Due to their good thermal stability, better heat absorption, and high char yield, phenolic resins, cyanate ester resin, and benzoxazine resin are the most favoured polymeric ablative materials [3, 4]. When three cyanate ester monomers with the –OCN functional group undergo a thermally induced cyclotrimerization (addition) reaction to generate a six-member oxygen linked ring, the phenolic triazines are formed (cyanurate), phenolic resin, on the other hand, forms crosslinks by forming methyl bridges between the phenolic groups during crosslinking. [5]. Benzoxazine ring is known to be stable at moderate temperatures, but at high temperatures, the ring-opening process takes place, resulting in novolac-type oligomers (benzoxazine resin)

containing both the phenolic hydroxyl group and the tertiary amine group [6]. Phenolic resin has high thermal stability due to crosslinked network of aromatics. Cyanate ester resin has high thermal stability due to polycyanurate and benzoxazine resin has high thermal stability due to mannich bridge and inter and intra hydrogen bonding.

Since the last one decade, cyanate ester resin and benzoxazine resin are under development and finding applications. Phenolic resin, on the other hand, has been used in ablative applications for over a century. However, there have been no systematic investigations comparing the thermal stability and degradation kinetic characteristics of these three resin systems.

In the present work, it is aimed at studying thermal stability and activation energy during degradation of phenolic resin, cyanate ester resin, and benzoxazine resin using TGA and to bring out a comparative summary on their ablative performance.

6.1. Degradation Kinetics: Theoretical Background

The Arrhenius law and the theory of chemical reaction rate can be used to define solid-state breakdown kinetics. The rate of decomposition is governed by the temperature and the number of reactants as given in the equation 1, when considering the decomposition process as a one-stage chemical reaction.

$$A_{solid} \longrightarrow B_{solid} + C_{gas}$$

$$d\alpha/dt = k(T)\, f(\alpha) \quad \text{-------- (equation 1)}$$

Where $d\alpha/dt$ is the rate of decomposition (i.e the rate of mass loss), t is time, T is temperature, k (T) is rate constant (i.e k(T) describes the effect of temperature) , $f(\alpha)$ is a differential form of the kinetic model.

α is the degree of decomposition

$$\alpha = (m_0 - m(T)) / (m_0 - m_f)$$

where, m_0 and m_f denote the initial and residual mass, respectively, and m (T) refers to the actual mass of the sample at temperature T.

$f(\alpha)$ is the effect of the reactant quantity on the reaction rate and it can be expressed as

$$f(\alpha) = (1-\alpha)^n \quad \text{-------- (equation 2)}$$

Where n is the reaction order (dimensionless)

While the function k (T) can be obtained from the Arrhenius equation

$k(T) = A \exp(-E_a/RT)$ -------- (equation 3)

Where, A is a preexponential factor, R is the universal gas constant and E is the activation energy. The activation energy (Ea) is the minimum amount of energy required to initiate a chemical reaction. During TGA tests, a constant heating rate (β) is used.

$\beta = dT/dt$ -------- (equation 4)

Combining equations 1, 2, 3, 4 gives equation 5

$d\alpha/dT = (A/\beta) \exp(-E_a/RT)(1-\alpha)^n$ -------- (equation 5)

From equation 5, the degree of decomposition can be determined as a function of temperature, T, if the kinetic parameters A, E_a, and n are known

Ozawa, Flynn, and Wall have solved equation 5 to get equation 6 for the calculation of activation energy, Ea

$Ea = -(R/b) \{d \log\beta / d(1/T)\}$ -------- (equation 6)

Where: b = Constant (0.457/k), assuming, n = 1

β = Heating rate (°C /minute)

T = Temperature of weight loss (°C)

For first-order reactions (*n* =1), the value of the preexponential factor (*A*) may be determined using equation 7

$A = (-\beta R/E) (\ln [1-\alpha] 10^a$----------(equation 7)

Where *a* = the Doyle approximation value

Using a point of equivalent weight loss (decomposition) which is beyond any initial weight loss due to volatiles evolution, a plot of 1og β vs 1/T to be constructed. The slope of the straight-line plot is then used to calculate activation energy (Ea), and the pre-exponential factor (Z) can be calculated by the interactive method of Zsako and Zsako.

Determining the kinetic parameters for thermal decomposition is an important step to evaluate the thermal stability of a material. Different techniques, models, and standards have been developed for a better understanding of these kinetics. The method applied was the one described by the ASTME1641-16 standard, which uses the Ozawa/Flynn/Wall isoconversional method [7]. The method which requires three or more determinations at different linear heating rates, usually between 0.5 and 50 °C/minute.

6.2 Materials: Table 6.1 summarises the resins selected for kinetic studies of thermal degradation.

Table 6.1. Resins selected for kinetic studies of thermal degradation

Sl.No	Resin
1	Phenolic resin (Ph)
2	Cyanate ester resin (CE)
3	Benzoxazine resin (BZ)

Preparation of the cured resin samples, which are described in previous chapters (chapter-III, section 3.2.3, chapter-IV, section 4.2.3 and chapter-V, section 5.2.3). Cured phenolic resin, cyanate ester resin, and benzoxazine resin samples are shown in **Figure 6.1.**

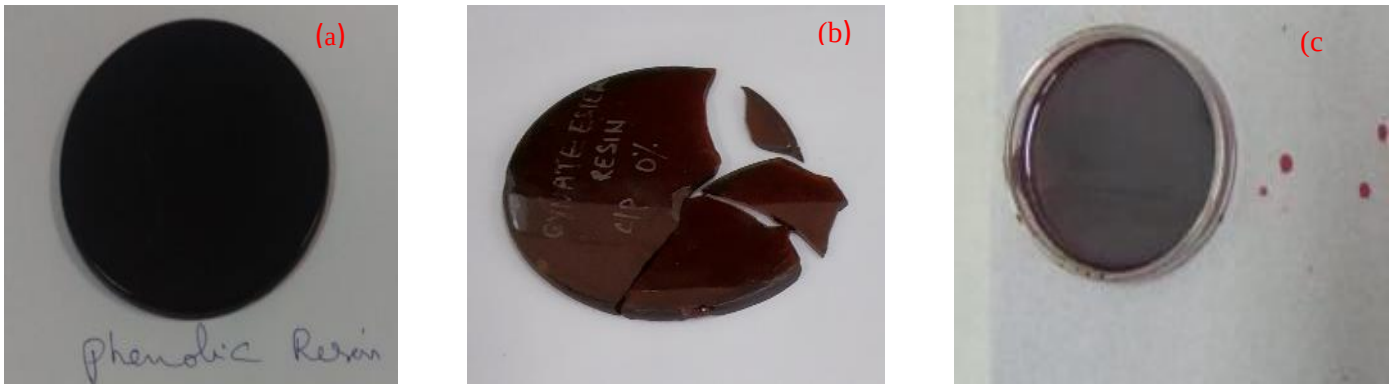

Figure 6.1 (a) Cured phenolic resin, (b) Cured cyanate ester resin (c) Cured benzoxazine resin

6.3 Experimental Work

6.3.1 Thermogravimetric Analysis of Resin Systems

Thermal degradation of the resins (mentioned in **Table 6.1**) was studied by thermogravimetry analysis. A sample mass of 10 ± 2 mg was collected from the resins. TGA runs were carried out for three resins, from room temperature to 900 °C at a heating rate of 10 °C /min under continuous flow of nitrogen (flow rate 60 ml/min) for thermal decomposition temperture and char yield. TGA runs were carried out for three resins with sample mass 10±2 mg, at heating rates of 5 °C / min, 10 °C / min, 20 °C / min, and 30 °C / min from 30 to 900 °C for determination of degradation kinetic parameters.

6.4 Results and Discussion

6.4.1 Char Yield of Cyanate Ester Resin, Benzoxazine Resin, and Phenolic Resin

Char yield of three resins was compared by comparing of percent of the residual mass of resin at 900 °C from TGA studies carried out at a heating rate of 10 °C / min, from room temperature to 900 °C in an inert atmosphere. TGA and DTGA scans for neat cyanate ester resin, benzoxazine resin, and phenolic resin are shown in **Figures 6.2 (a)** and **6.2 (b).**

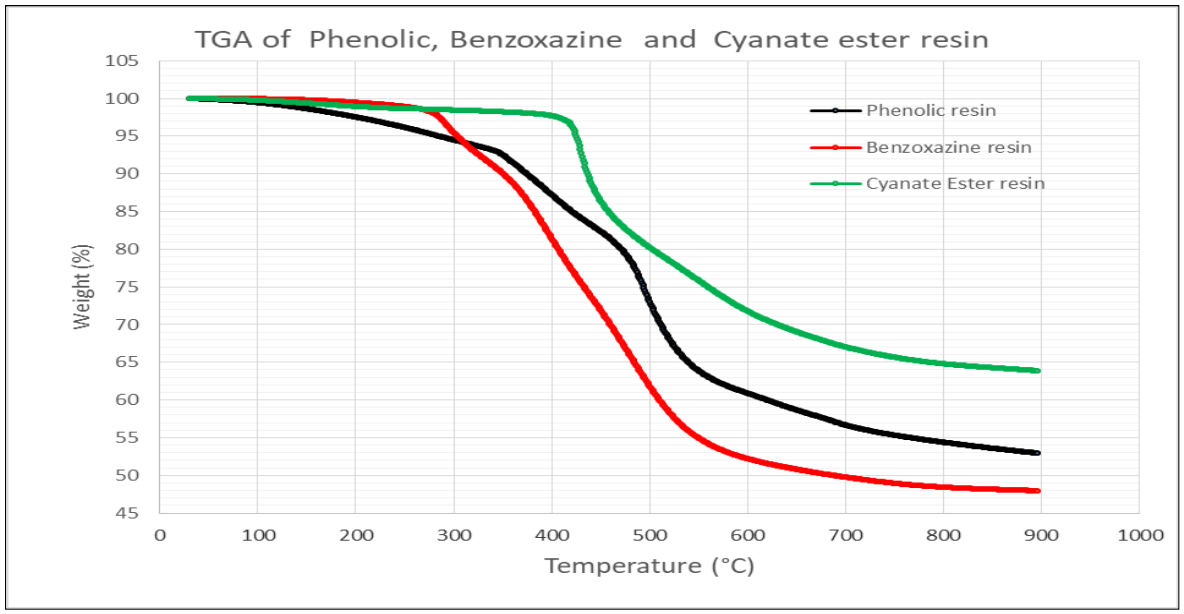

Figure. 6.2 (a) TGA scans for cyanate ester resin, benzoxazine, and phenolic resin

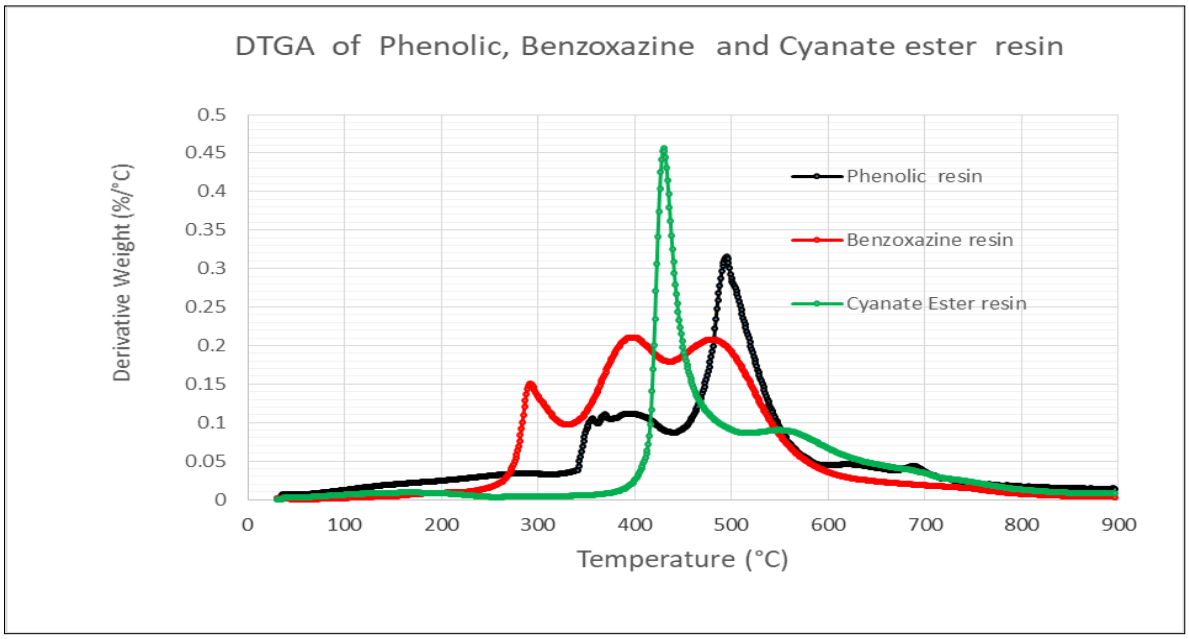

Figure 6.2 (b) DTGA scans for cyanate ester resin, benzoxazine resin, and phenolic resin

Characteristic temperatures namely $T_{5\ \%}$ / °C (temperature at 5% weight loss of material), $T_{10\ \%}$ / °C (temperature at 10% weight loss of material), and char yield obtained from thermogravimetric analysis of phenolic resin, benzoxazine resin and cyanate ester resin at a heating rate of 10 °C / min are given in **Table 6.2**.

Table 6.2: Characteristic temperatures and char yield of cyanate ester resin, phenolic resin and benzoxazine resin

Sl.No	**Material description**	**$T_{5\ \%}$ / °C**	**$T_{10\ \%}$ / °C**	**Char yield at 900 °C / %**
1	Cyanate ester resin (CE)	422	436	64
2	Phenolic resin (Ph)	285	370	53
3	Benzoxazine resin (BZ)	303	350	48

It is observed from **Figure 6.2 (a)** and **6.2 (b)** that, cyanate ester resin undergoes single-step degradation, which occurs at 430 °C suggesting a uniform decomposition for this resin system. Char yield of cyanate ester is about 64 wt% at 900 °C. From **Figure 6.2 (a)** and **(b)**, phenolic resin shows three distinct decomposition reactions that occur at 280 °C, 380 °C, and 495 °C, and the char yield of phenolic is about 53 wt%. **Figure 6.2 (a)** and **(b),** benzoxazine resin shows three distinct decomposition reactions that occur at 295 °C, 400 °C, and 480 °C, and the char yield of benzoxazine is about 48 wt%.

Ascending order for char yield of three resin systems are benzoxazine resin, phenolic resin, and cyanate ester resin.

6.4.2 Estimation of Decomposition Kinetic Parameters of Phenolic Resin, Cyanate Ester Resin and Benzoxazine Resin

The temperature at which 10% mass loss and char yield obtained from thermogravimetric analysis of phenolic resin, cyanate ester resin and benzoxazine resin at heating rates of 5 °C /min, 10 °C /min, 20 °C /min, and 30 °C /min are given in **Table 6.3.**

Table 6.3. Char yield and 10% mass loss data for the three resin systems

Resin	**10% weight loss ($T_{10\,\%}$ / °C)**				**Char yield (%) (Residue at 900 °C / %)**			
	5 °C / min	10°C **/min**	20 °C **/min**	**30** °C **/ min**	**5**°C **/min**	10°C **/min**	20 °C **/min**	**30** °C **/min**
Phenolic	365	370	391	413	58.43	53.00	50.70	50.78
Cyanate ester	428	436	446	453	65.71	64.20	62.33	60.35
Benzoxazine	345	350	383	389	48.40	48.44	47.07	45.51

From **Table 6.3**, it is observed that temperatures at 10% weight loss ($T_{10\,\%\,/°C}$) for three resin systems are increasing with increasing heating rates (5 °C / min, 10 °C / min, 20 °C / min, and 30 °C / min). This is due to the increase in temperature lag of resins with increasing heating rates.However, the char yield of the three resin systems is decreasing with an increasing heating rate.

The TGA and DTGA scan for cyanate ester resin, phenolic resin, and benzoxazine resin at heating rates of 5 °C/min, 10 °C /min, 20 °C /min, and 30 °C /min in **Figure 6.3, 6.4** and **6.5** respectively**.**

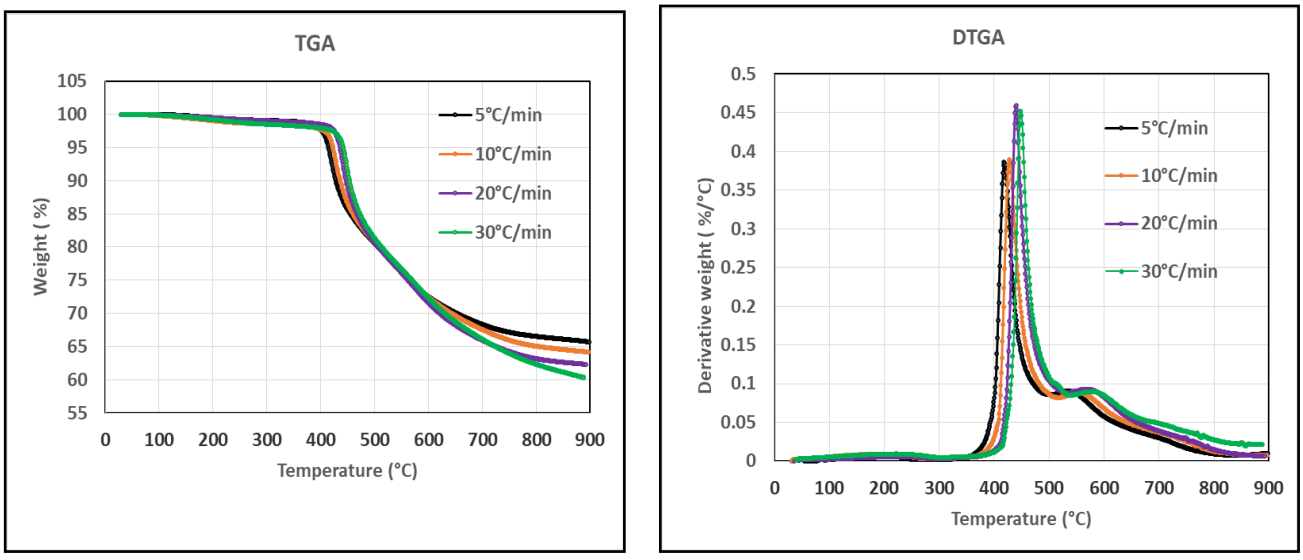

Figure 6.3: TGA and DTGA scans for neat cyanate ester resin at heating rates of 5 °C /min,10 °C /min, 20 °C/min and 30 °C /min

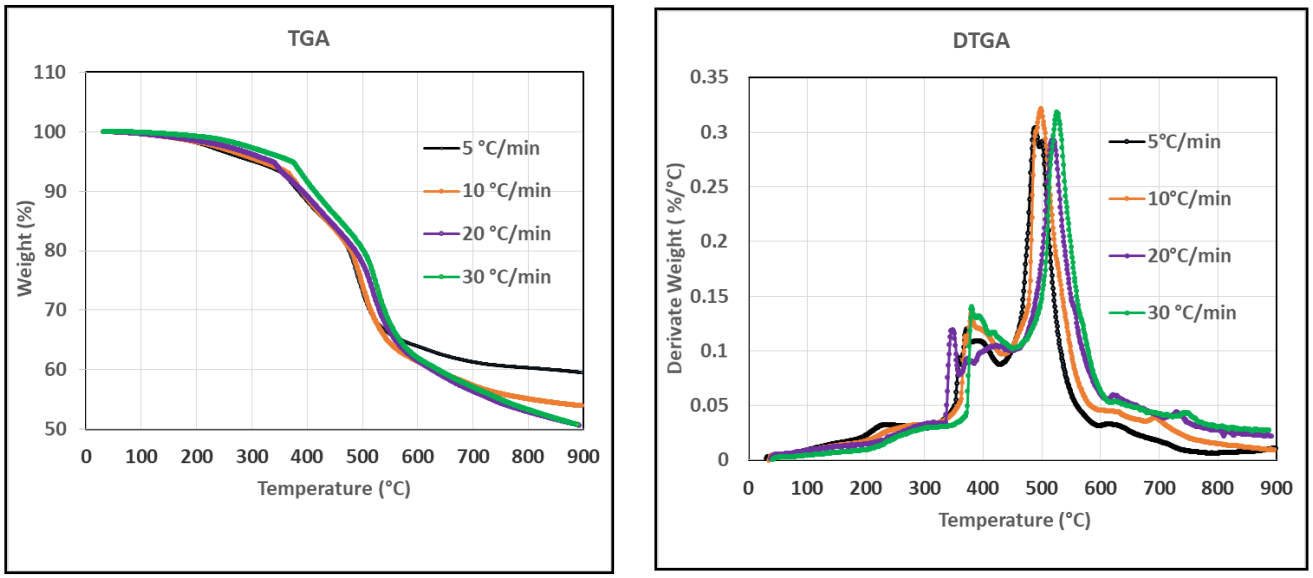

Figure 6. 4: TGA and DTGA scans for neat phenolic resin at heating rates of 5 °C /min, 10 °C /min, 20 °C /min and 30 °C /min

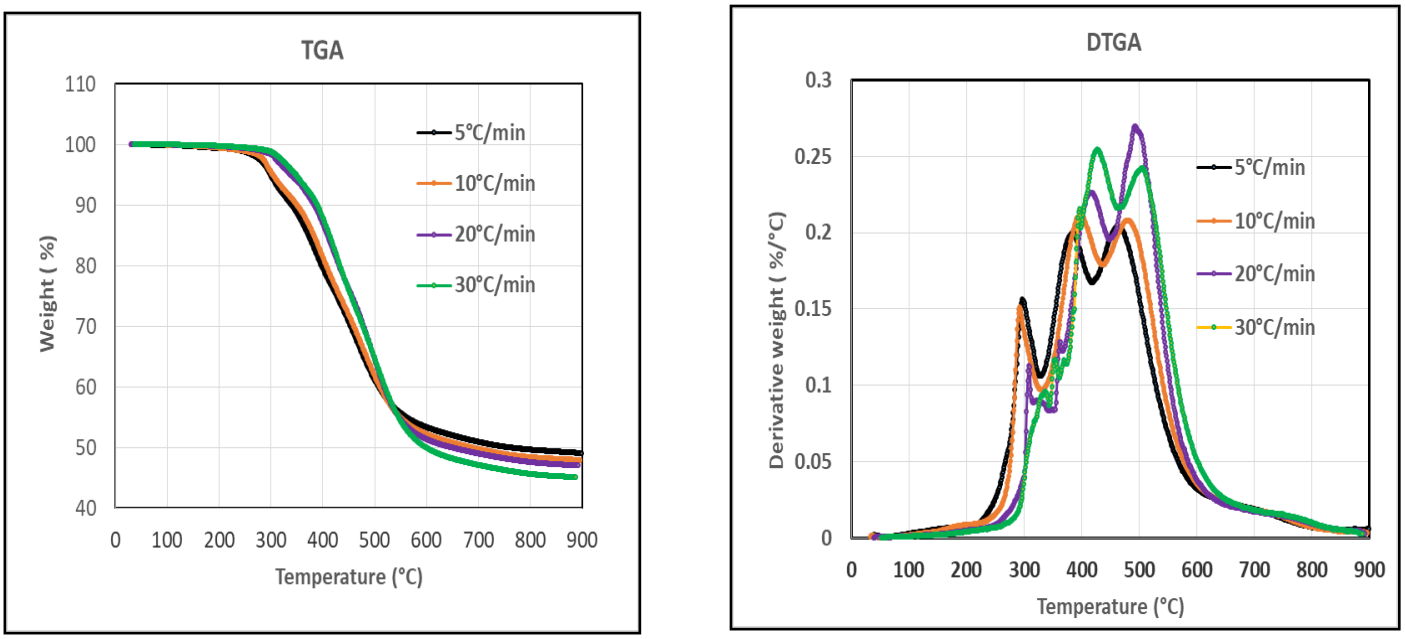

Figure 6.5. TGA and DTGA scans for neat benzoxazine resin at heating rates of 5 °C /min, 10 °C / min, 20 °C / min and 30 °C /min

A conversion 10% (degree of decomposition) was selected as the failure criterion. The absolute temperatures corresponding to the conversion of 10% for cyanate ester resin, phenolic resin,

and benzoxazine resin were determined and these are shown in **Figure 6.6 (a), 6.6 (b)** and **6.6 (c)** respectively

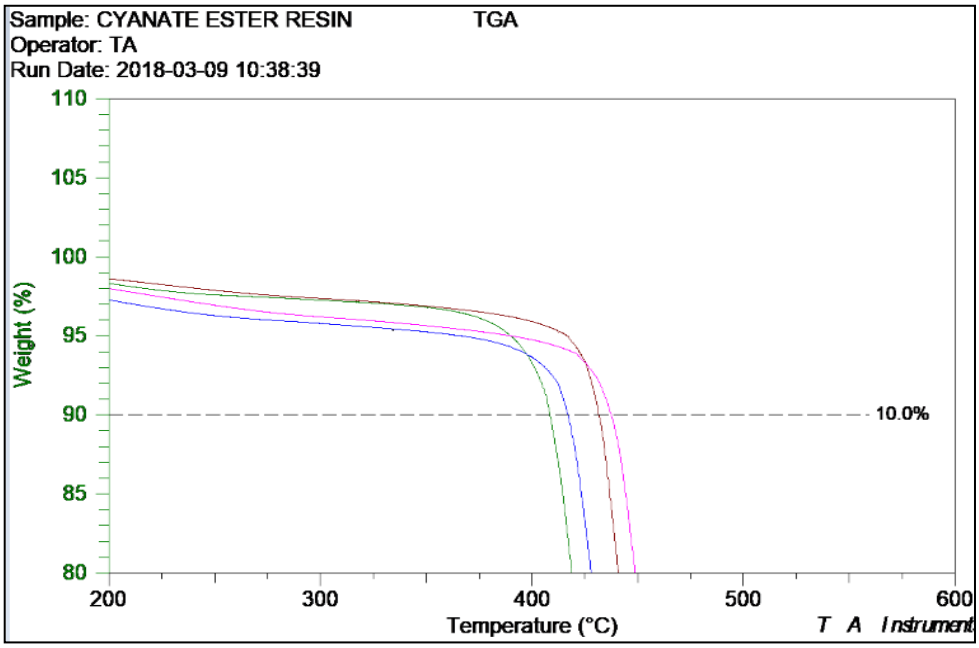

Figure 6.6 (a) 10% Conversion curves of cyanate ester resin at heating rates of 5 °C /min, 10 °C /min, 20 °C /min and 30 °C /min

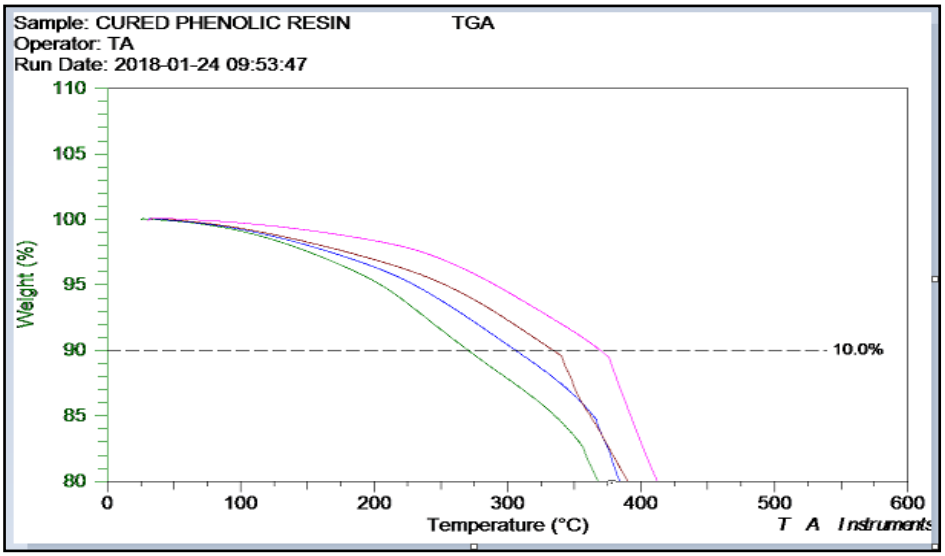

Figure 6.6 (b) 10% Conversion curves of phenolic resin at heating rates of 5 °C /min, 10 °C /min, 20 °C / min and 30 °C /min

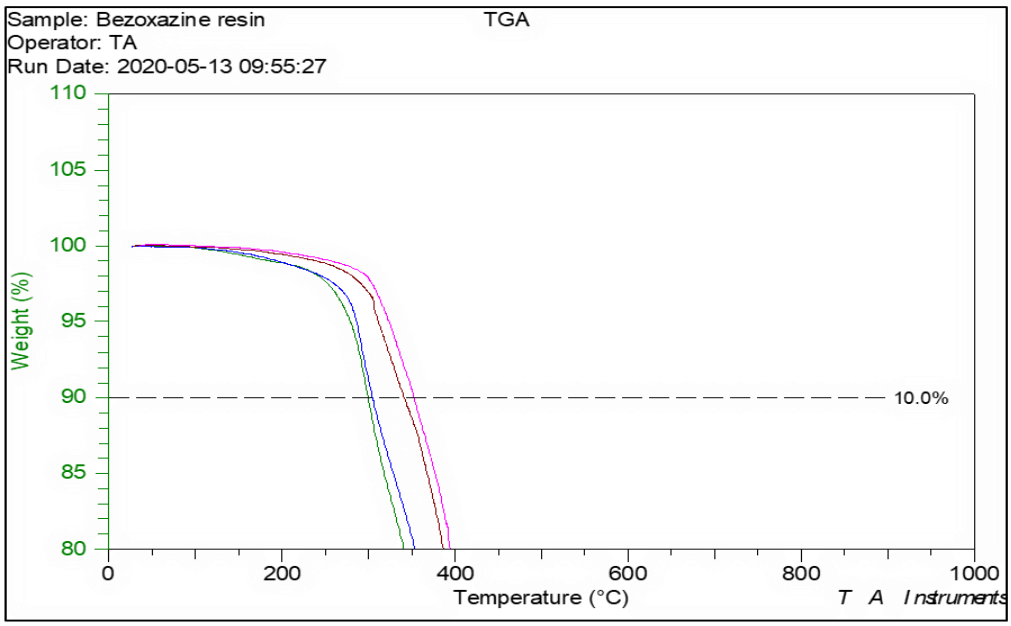

Figure 6.6 (c) 10% Conversion curves of benzoxazine at heating rates of 5 °C / min, 10 °C /min, 20 °C /min and 30 °C /min

From the thermal curves, the absolute temperatures at degree of decomposition (α) 10% were determined for CE, Ph, and BZ resins for the above heating rates. Plotting the logarithms of heating rate versus the reciprocal temperatures, the slope of the curve was estimated by linear regression using kinetics software of Q 500 TGA instrument. Log (Heating rate) as a function of 1/T for cyanate ester resin, phenolic resin, and benzoxazine resin is shown in **Figure 6.7 (a), 6.7 (b),** and **6.7(c)** respectively.

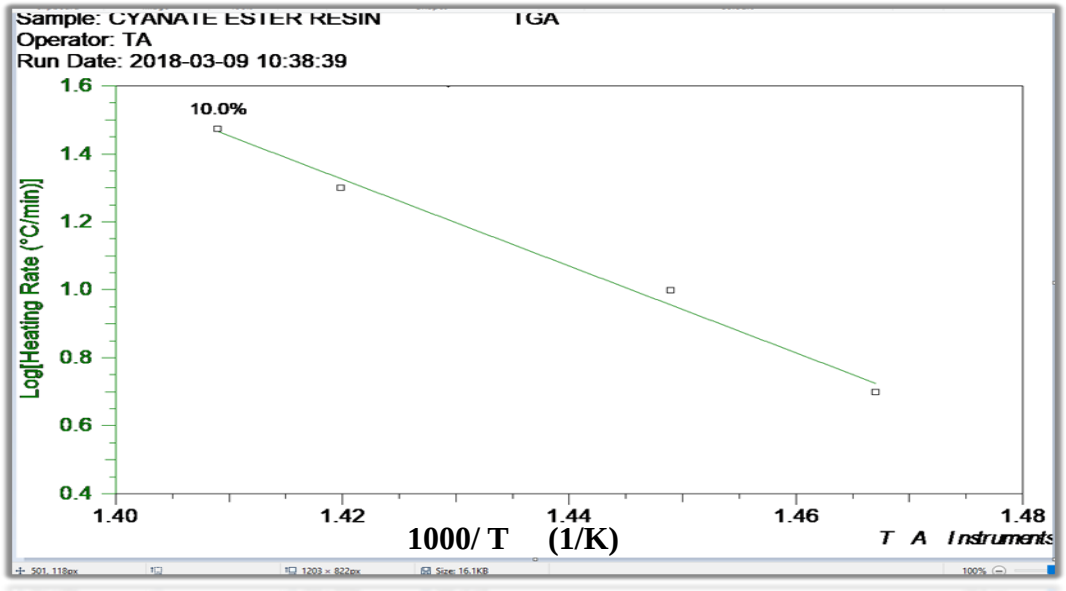

Figure. 6.7 (a) Log (Heating rate) versus 1/T for cyanate ester resin.

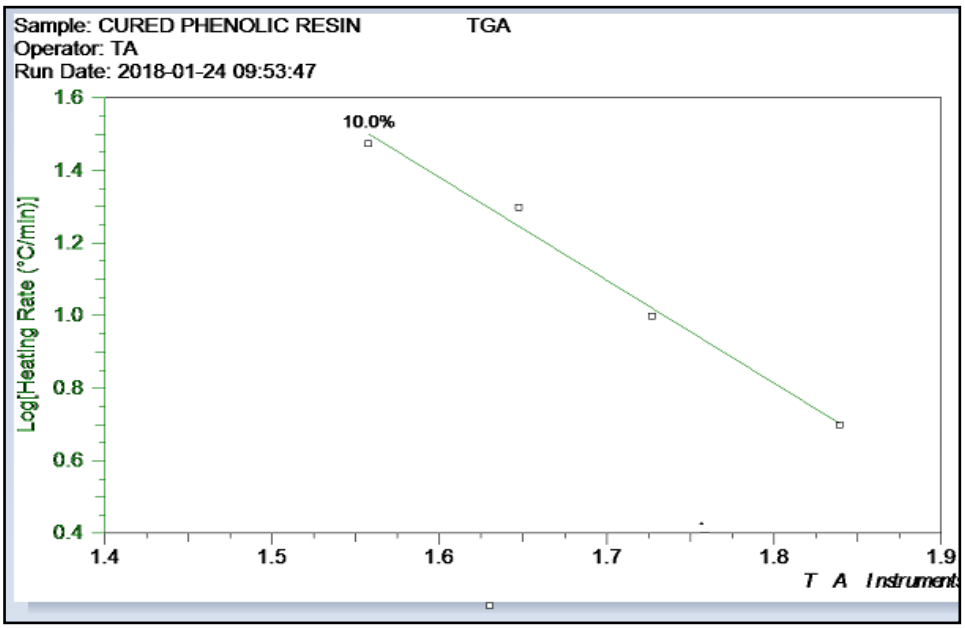

Figure 6. 7(b). Log (Heating rate) versus 1/T for phenolic resin

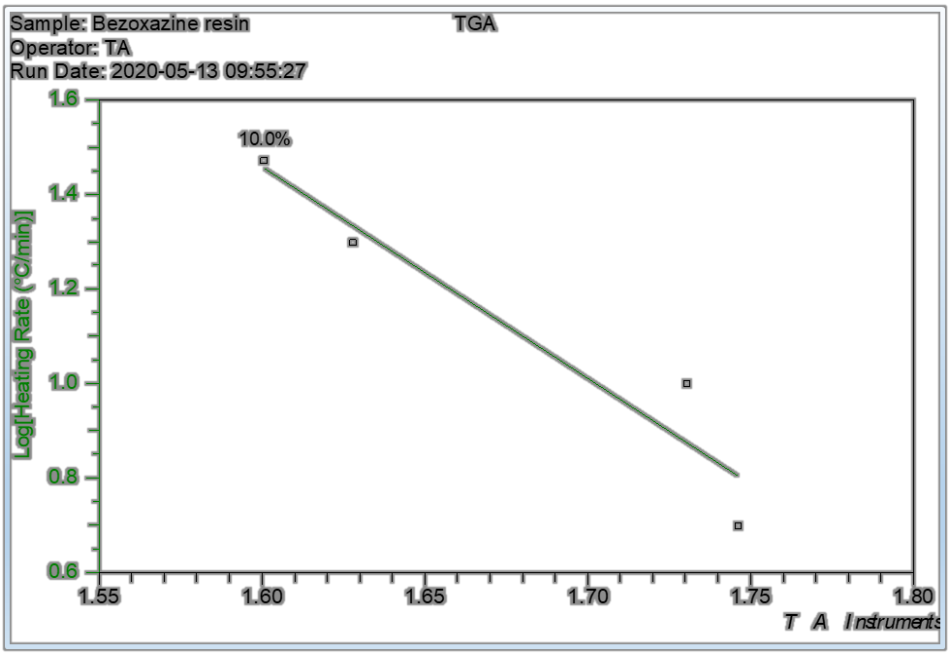

Figure 6.7 (c). Log (Heating rate) versus of 1/T for benzoxazine resin

The values of the slope from **Figure 6.6** were calculated and used for the determination of the activation energy of cyanate ester resin, phenolic resin, and benzoxazine as per the equation 6. The pre-exponential factor 'A' for cyanate ester resin, phenolic resin and benzoxazine resin are also calculated as per equation 7**.** Decomposition kinetic parameters of cyanate ester resin, phenolic resin, and benzoxazine resin at 10% degree of decomposition (conversion) are tabulated in **Table 6.4.**

Table 6.4 Decomposition kinetics parameters for cyanate ester resin, phenolic resin and benzoxazine resin at 10% degree of decomposition.

Sl. No	**Resin**	**Activation Energy (Ea) (k J/ mole)**	**Log(pre-exponential factor A (min^{-1})**
1	Cyanate Ester resin (CE)	240	16.47
2	Phenolic resin (Ph)	41	1.98
3	Benzoxazine resin (BZ)	75	5.24

Ascending order for activation energy for 10% decomposition among three resin systems studied are phenolic resin, benzoxazine resin, and cyanate ester resin.

6.5 Conclusions

Cyanate ester resin has higher char yield than phenolic resin and benzoxazine resin. Activation energy and pre-exponential factor of phenolic resin, cyanate ester resin, and benzoxazine resin have been determined by thermogravimetric analysis (TGA) data using Flynn-Wall-Ozawa (FWO) kinetic model as per ASMT E1641. The activation energy of cyanate ester resin for 10% degree of decompositio was found to be higher than that of benzoxazine resin and phenolic resin. This shows that cyanate ester resin is more thermally stable than phenolic resin and benzoxazine resin.

References

1. L.Torre, J. M. Kenny, and A. M. Maffezzoli. Degradation behaviour of composite material for thermal protection systems Part I – Experimental characterization. Journal of Materials Science. 1998; 33, 3137-3143.

2. M. Day, and D. R. Budgell. Kinetics of thermal degradation of poly(phenylene sulfide), Thermochimica Acta. 1992; 203, 465-474.

3. G. Pulci, J. Tirillò, F.Marra, F. Fossati, C. Bartuli, T.Valente. Carbon-phenolic ablative materials for re-entry space vehicles: Manufacturing and Properties, Composites: Part A. 2010; 41: 1483-1490.

4. Puglia D, Kenny JM, Manfredi LB, Va´zquez A. Influence of chemical composition on the thermal degradation and fire resistance of resol type phenolic resins. Material Engineering, 2001; 12, 55–72.

5. Michael L. Ramirez, Richard Walters, Richard E. Lyon, Edward P. Savitski. Thermal decomposition of cyanate ester resins. Polymer Degradation and Stability. 2002; 78, 73–82.

6. K.Hemvichian, H.D. Kim, H. Ishida. Identification of volatile products and determination of thermal degradation mechanisms of polybenzoxazine model oligomers by GC-MS. Polymer Degradation and Stability. 2005; 87, 213–224.

7. American society for testing and materials. ASTM E1641: Standard test method for decomposition kinetics by thermogravimetry using the Ozawa/Flynn/Wall Method.West Consho-hocken, PA, 2016.

Chapter- VII

COMPARATIVE PERFORMANCE OF MATRIX SYSTEMS REINFORCED WITH CARBON FIBER AND NANOCLAY

Comparative Performance of Matrices Reinforced with Carbon fiber and Nanoclay

7.0 Introduction

In the aerospace and defence sectors, polymeric-based ablative materials are extensively used as thermal protection system (TPS) applications. This type of material requires special properties that allow it to withstand the mechanical loads and high heat flux environment experienced by spacecraft and rocket motors. TPS material selection is based on the mechanical, thermal, and ablation properties of the material.

Three resins namely phenolic resin, cyanate ester resin, and benzoxazine resin were used as a matrix material for fabrication of carbon fiber reinforced polymer composites for thermal protection system (TPS) applications. Organo modified montmorillonite nanoclay was dispersed in these polymers and prepared nanoclay added carbon fiber reinforced polymer composites.

The char yield, thermal stability, and kinetic parameters of each neat resin were compared. Experiments were carried out to compare mechanical, thermal, and ablative properties of carbon fiber reinforced composites and nanoclay added carbon fiber reinforced composites with each of the resin.

To fully understand the effectiveness of matrix on the properties of composites with carbon fiber and nanoclay, it is necessary to compare the properties of composites with respect to the resin system.

The following points will be taken into consideration for the present study.

(i) Comparision of mechanical, thermal, and mass ablation properties of carbon fiber reinforced polymer composites with respect to phenolic resin, cyanate ester resin, and benzoxazine resin.

(ii) Comparision of thermal stability, mechanical, thermal, and mass ablation properties of carbon fiber reinforced polymer composites with the addition of nanoclay in the above resin systems.

7.1 Materials: Phenolic resin, cyanate ester resin and benzoxazine resin, nanoclay added carbon fiber – phenolic resin composites, nanoclay added carbon fiber –cyanate ester resin composites, and nanoclay added carbon fiber –benzoxazine resin composites were used for comparative performance study.

Resin reinforced with carbon fiber and nanoclay reinforcements were prepared as per the process described in previous chapters (Chapter -III, Chapter -IV, and Chapter -V). Details of various composites fabricated are shown in **Table 7.1.** 2 wt% nanoclay added carbon fiber reinforced composites with phenolic resin, cyanate ester resin, and benzoxazine resin were selected for comparative performance. Thermal stability, mechanical properties, thermal properties, and ablation rate of the composite materials were reported in the chapters III, IV, and V. The properties of composite with carbon fiber and nanoclay were compared with respect to phenolic resin, cyanate ester resina and benzoxazine resin.

7.2 Results and Discussion

7.2.1 Comparison of Thermal Stability and Char Yield of Resins and Composites

Temperature at 5% weight loss ($T_{5\ \%}$ /°C) and temperature at 10% weight loss ($T_{10\ \%}$ /°C) and char yield at 900 ºC of resins and their composites measured by TGA at heating rate of 10 ºC / min in nitrogen atmosphere are shown in **Table 7.1.**

Table 7.1 Characteristic temperatures and char yield of resins and composites

Sl. No	Material description	$T_{5\ \%}$ / ºC	$T_{10\ \%}$ / ºC	Char yield at 900 ºC (%)
1	Phenolic resin (Ph)	285	370	53
2	Benzoxazine resin (BZ)	303	350	48
3	Cyanate ester resin (CE)	422	436	64
4	Oragano modified montmorillonite nanoclay (NC)	275	300	70
5	Carbon fiber reinforced phenolic resin composite (C-Ph)	430	580	82
6	2 wt% nanoclay added C-Ph compsoite (2 NC/C-Ph)	445	575	85
7	Carbon fiber reinforced benzoxazine resin composite (C-BZ)	405	480	84
8	2 wt% nanoclay added C-BZ compsoite (2 NC/C-BZ)	415	475	83
9	Carbon fiber reinforced cyanate ester resin composite (C- CE)	459	721	88
10	2 wt% nanoclay added C-CE compsoite (2 NC/C-CE)	440	599	87

From **Table 7.1,** ascending order of thermal stability (for 10 wt% loss) and char yield was observed for benzoxazine resin, phenolic resin, and cyanate ester resin. In the fiber reinforced matrix category (matrix+ fiber) and nanoclay added carbon fiber reinforced matrix category (matrix + fiber + nanoclay), the ascending order of thermal stability was observed for benzoxazine resin, phenolic resin, and cyanate ester resin. The values of 10 wt% loss and char yield of composites have shifted towards higher values than their neat resins. This is due to the fact that composites contain 60-70 wt% of carbon fiber.

The thermal stability (for 10 wt% loss) and char yield of 2 wt% o-MMT nanoclay added carbon fiber reinforced polymer composites are lower than pristine carbon fiber reinforced polymer composites. This is due to thermal degradation of organic modified montmorillonite (o-MMT) nanoclay that occurs between 250 ºC and 450 ºC. This low temperature degradation of nanoclay is due to the degradation of organic modifier part of clay. Moreover, organic part of the nanoclay is known to give oxidizing volatiles which reduces the thermal stability of the matrix. Also, fiber volume fraction for 2 wt% added carbon fiber reinforced polymer composites are lower than blank carbon fiber reinforced polymer composites. Since at lower fiber volume fraction, the thickness of the thermally degrading matrix layer is higher between the fabric layers, effective mass loss (due to matrix degradation) from these composites is more as compared to the higher fiber volume fraction composites.

As a summary of this section, cyanate ester resin-based composites shown higher thermal stability among these three resin systems that were studied.

7.2.2 Comparision of Mechanical Properties of Composites: Interlaminar shear strength (ILSS) and flexural strength of carbon fiber reinforced polymer composites and nanoclay added carbon fiber reinforced polymer composites are shown in **Table 7.2.**

Table 7.2 Results of ILSS and flexural strength of composites

Sl. No	Material description	Fiber volume fraction	ILSS (MPa)	Flexural Strength (MPa)
1	Carbon fiber reinforced phenolic resin composite (C-Ph)	63	21	417
2	2 wt% nanoclay added C-Ph compsoite (2 NC/C-Ph)	61	26	466
3	Carbon fiber reinforced benzoxazine resin composite (C-BZ)	58	20	358
4	2 wt% nanoclay added C-BZ compsoite (2 NC/C-BZ)	56	25	440
5	Carbon fiber reinforced cyanate ester resin composite (C- CE)	68	30	535
6	2 wt% nanoclay added C-CE compsoite (2 NC/C-CE)	63	35	650

The mechanical properties namely ILSS and flexural strength are higher for 2 wt% nanoclay added carbon fiber reinforced composites than the blank composites. The increase of ILSS values can be due to the organo modified montmorillonite, which aids in increasing the bonding between the fibers and resin and thereby better transfer of stress. The increase of flexural strength values can be due to the good mechanical properties of carbon fiber and good bonding between fiber and resin with o-MMT nanoclay.

Flexural strength of carbon fiber reinforced cyanate ester resin composites and 2 wt% nanoclay added carbon fiber reinforced cyanate ester resin composites are higher than carbon fiber reinforced phenolic resin composites, as well as 2 wt% nanoclay added carbon fiber reinforced phenolic resin composites. Even when compared with carbon fiber reinforced benzoxazine resin composites and 2 wt% nanoclay added carbon fiber reinforced benzoxazine resin composites, flexural strength of cyanate ester resin-based composites are better. This could be due to higher ILSS and higher fiber volume fraction in carbon fiber reinforced cyanate ester resin composites than carbon fiber reinforced phenolic resin composites and carbon fiber reinforced benzoxazine resin composites.

In a summary, cyanate ester resin-based composites are showing superior interlaminar shear strength and flexural strength among these three resin systems that were studied.

7.2.3 Comparision of Thermal Properties of Composites: Thermal properties namely specific heat and thermal conductivity of carbon fiber reinforced composites and 2 wt% nanoclay added carbon fiber reinforced composites with the three resin systems were compared. The values of specific heat of composites are shown in **Table 7. 3.**

Table 7.3 Results of Specific Heats of Composites

Composite description	Specific heat (J/Kg ºC) at different temperatures					
	50 ºC	100 ºC	150 ºC	200 ºC	250 ºC	300 ºC
C-Ph (blank)	915	968	1022	1104	1182	1276
2 NC/ C-Ph	928	986	1068	1167	1274	1356
C-BZ(blank)	899	1125	1306	1443	1454	1439
2 NC/ C-BZ	934	1166	1318	1410	1422	1404
C-CE (blank)	957	1109	1245	1369	1477	1585
2 NC/ C-CE	1031	1204	1343	1460	1563	1674

Specific heat values are higher for 2 wt% nanoclay added carbon fiber reinforced polymer composites when compared to their blank carbon fiber reinforced polymer composites. This is due to fact that nanoclay contains silicon oxide. This can lead to better insulation characteristics for nanoclay modified carbon fiber reinforced polymer composites as compared to conventional unfilled carbon fiber reinforced polymer composites. Among the above composites, C-CE composite and 2 NC/C-CE composites have higher specific heat than C-Ph composites, 2 NC/C-Ph composites, C-BZ composites and 2NC/C-BZ composites. Higher values of specific heat of cyanate ester composites are due to higher thermal stability than phenolic resin composites and benzoxazine resin composites.

Thermal conductivity data of the composites is shown in **Table 7.4.**

Table 7.4. Thermal conductivity data of composites

Composite description	**Thermal Conductivity (W/ m ºC) at 30 ºC**
C-Ph (blank)	1.30
2 NC/ C-Ph	1.12
C-BZ(blank)	1.28
2 NC/ C-BZ	1.09
C-CE (blank)	1.26
2 NC/ C-CE	1.08

Nanoclay addition has decreased the thermal conductivity of the carbon fiber reinforced polymer composites significantly as shown in **Table 7.4**. The lattice vibrations and the microstructure (micro-cracks, grain boundaries, porosity, etc.) of composites influence their thermal conductivity. This can lead to better insulation characteristics for nanoclay added carbon fiber reinforced polymer composites when compared to conventional blank carbon fiber reinforced polymer composites. Among the above composites, C-CE composite and 2 NC/C-CE composites have lower thermal conductivity than C-Ph composites, 2 NC/C-Ph composites, C-BZ composites and 2NC/C-BZ composites.

In a summary, cyanate ester resin-based composites with carbon fiber and nanoclay are showing higher specific heat and lower themal conductivity among these three resin systems that were studied.

7.2.4 Comparision of Mass Ablation Rate of Composites: The results of the mass ablation rate of blank carbon fiber reinforced resin composites and 2 wt% nanoclay added carbon fiber reinforced resin composites tested at a low heat flux at 125 W/cm^2 and high heat flux at 500 W/cm^2 are presented in **Table 7.5.**

Table No: 7.5. Mass ablation rate of composites

Sl. No	Composite description	Nanoclay (wt%)	Mass ablation rate (mg/sec) at heat flux : 125 W/cm^2	Mass ablation rate (mg/sec) at heat flux : 500 W/cm^2
1	C-Ph (blank)	0	100	138
2	2 NC/ C-Ph	2	110	176
3	C-BZ (blank)	0	115	147
4	2NC/ C-BZ	2	154	197
5	C- CE(blank)	0	84	123
6	2NC/ C-CE	2	134	163

The mass ablation rates are lower for carbon fiber reinforced cyanate ester resin composites when compared to carbon fiber reinforced phenolic resin composites and carbon fiber reinforced benzoxazine resin composites at both low heat flux (125 W/cm^2) and high heat flux (500 W/cm^2). This is due to cyanate resin has higher thermal stability and char yield than phenolic resin and benzoxazine resin. The mass ablation rates have increased with the addition

of 2 wt% of nanoclay content in carbon fiber reinforced polymer composites when compared to blank carbon fiber reinforced polymer composites at both heat fluxes.

In a summary, cyanate ester resin - based composites with carbon fiber and nanoclay are showing low ablation rates at high heat flux 500 W/cm^2 among these three resin systems that were studied.

7.3 Conclusions: The results are summarised as below from the comparative performance of matrices reinforced with carbon fiber and nanoclay.

- Among the three resin systems studied, thermal stability and char yield are higher for cyanate ester resin than phenolic resin and benzoxazine resin. Thermal stability decreased for 2 wt% nanoclay added carbon fiber reinforced polymer composites when compared to their blank composites with the above resin systems.
- Interlaminar shear strength, flexural strength of 2 wt% nanoclay added carbon fiber reinforced polymer composites increased when compared to their blank composites with the above resin systems.
- Specific heat increased and thermal conductivity decreased for 2 wt% nanoclay added carbon fiber reinforced polymer composites when compared to their blank composites with the resin systems.
- The mass ablation rates of carbon fiber reinforced cyanate ester resin composites are lower as compared to carbon fiber reinforced phenolic resin composites and carbon fiber reinforced benzoxazine resin composites. Mass ablation rate of 2 wt% nanoclay added carbon fiber reinforced polymer composites increased when compared to their blank composites with the resin systems.
- Based on comparisons of thermal stability, mechanical properties, thermal properties, and mass ablation rate, it is inferred that carbon fiber reinforced cyanate ester resin composite (C-CE) and 2 wt% nanoclay added C-CE are the superior ablative composites when compared to conventional carbon fiber reinforced phenolic resin composite. Hence they can be considered as alternative ablative thermal protection systems for aerospace applications. They have the potential to reduce the total weight of aerospace systems, if used.

Chapter - VIII

Summary and Conclusions

Summary and Conclusions

8.0. Conclusions: The primary findings are drawn from each chapter III, IV, V, VI, and VII. The implications of the findings, are also discussed in this chapter.

Organo modified montmorillonite (o-MMT) nanoclay added polymer composites were prepared by dispersing 0, 1, 2, 4 and 6 wt% of nanoclay in three different thermoset matrices namely phenolic resin, cyanate ester resin, and benzoxazine resin by ball milling dispersion process (type-I composites). Dispersion studies of nanoclay in these resins were studied by SAXS and SEM. Viscosity changes, curing behavior, and thermal stability changes to these resins due to the addition of nanoclay were studied. Organo modified montmorillonite nanoclay added carbon fiber reinforced polymer composites were prepared by adding 0, 1, 2, 4 and 6 wt% nanoclay dispersed resins to carbon fiber (type –II composites). Nanoclay added carbon fiber reinforced polymer composites were evaluated for thermal stability, mechanical properties, thermal properties, and mass ablation rate. Results from the studies of polymer – nanoclay composites (type –I) are used to understand the mechanical, thermal, and ablation behaviour of nanoclay added carbon fiber reinforced polymer composites (type–II). Comparative performance of matrices reinforced with carbon fiber and nanoclay was also studied.

Major conclusions of the present study are as follows

- From the results of the chapter -III, it can be concluded that 2 wt% o-MMT nanoclay as filler is optimum in carbon fiber reinforced phenolic resin composites for increased mechanical properties, thermal stability without much compromising on ablative properties.
- From the results of the chapter -IV, it can be concluded that 2 wt% of o-MMT nanoclay as filler is optimum for better mechanical properties for the carbon fiber reinforced cyanate ester resin composites with minimum compromise in the thermal stability and ablation performance.
- From the results of the chapter -V, it can be concluded that 2 wt% of o-MMT nanoclay as filler is optimum for improving the mechanical performance of carbon fiber reinforced benzoxazine resin composites without much compromise in the ablation performance.

- From the results of the chapter -VI, it can be concluded that cyanate ester has higher thermal stability, char yield, and activation energy than the phenolic resin and benzoxazine resin

- Based on the results of the chapter -VII, it can be concluded that carbon fiber reinforced cyanate ester resin composite with 2 wt% of o-MMT nanoclay is a superior alternative ablative composite to the traditional carbon fiber reinforced phenolic resin composite for thermal protection system applications in the areas of aerospace and defence sectors.

9.0 Future Scope of Work

Nanoclay added carbon fiber reinforced polymer composites (type –II) were characterised for ILSS and flexural strength in the present study. In future work, type –II composites can be characterised for other mechanical properties namely tensile, compressive, and shear to study the effect of nanoclay addition. Type –II composites should also be characterised for limited oxygen index to study the effect of nanoclay. This data will be useful for use of type –II composite for aircraft interior applications.

Type–II composites should be characterised for dynamic mechanical properties using a dynamic mechanical analyser to study the effect of nanoclay. One of the potential of o-MMT nanoclay to replace the unfilled carbon fiber – polymer composites in many applications that require very high-load bearing capabilities with high temperature resistance.

List of Publications

1. **Golla Rama Rao**, Ivautri Srikanth, K. Laxma Reddy. Effect of organo-modified montmorillonite nanoclay on mechanical, thermal and ablation behaviour of carbon fiber / phenolic resin composites**. Defence Technology. 2021; 17(3), 812-820.**

   doi.org/10.1016/j.dt.2020.05.012

2. **Golla Rama Rao**, Ivautri Srikanth, K. Laxma Reddy. Mechanical, thermal and ablative behaviour of organo nanoclay added carbon fiber/cyanate ester resin composites and effect of heat flux on its ablative performance. **Polymers and Polymer Composites. 2021.**

   doi.org/10.1177/0967391121998833

3. **Golla Rama Rao**, Ivautri Srikanth, K. Laxma Reddy. Effect of organo modified montmorillinite nanoclay on mechanical properties, thermal stability and ablative rate of carbon fiber / polybenzoxazine resin composites. **Defence Science Journal. 2021; 71(5), 682-690.**
   doi org: 10.14429/dsj.71.16630

Papers Presented in Conferences

1. Presented a paper on "Preparation and characterisation of nanoclay modified carbon fiber reinforced polymer compoistes**"** at National Conference on **"Recent Developments in Chemical Sciences and allied Technologies (RDCST-17)**", organized by the Department of Chemistry, NIT Warangal, Warangal, India, during 29-30, June 2017**.**

2. Presented a paper on "Comparative kinetic analysis on thermal degradation of phenolic resin and phenolic triazine cyanate ester resin**"** at National Conference on "***Telangana State Science Congress*** (**TSSC-2018)**", organized by NIT Warangal, Warangal, India, during 22-24, December 2018.

3. Presented a paper on "Influence of chemical structure of polymer on thermal stability, mechanical properties and ablation rate of carbon fiber reinforced polymer composites" at Inter National Conference on "***Conventional and Digital Methods in Chemical Education*** (**CDCE-2021)**", organized by the Department of Chemistry, NIT Warangal, Warangal, India, during 29-31, July 2021.

Defence Technology 17 (2021) 812–820

Contents lists available at ScienceDirect

Defence Technology

journal homepage: www.keaipublishing.com/en/journals/defence-technology

Effect of organo-modified montmorillonite nanoclay on mechanical, thermal and ablation behavior of carbon fiber/phenolic resin composites

Golla Rama Rao [a,*], Ivautri Srikanth [a,**], K. Laxma Reddy [b]

[a] Advanced Systems Laboratory, DRDO, Hyderabad, India
[b] National Institute of Technology, Warangal, India

ARTICLE INFO

Article history:
Received 7 December 2019
Received in revised form
7 March 2020
Accepted 8 May 2020
Available online 18 May 2020

Keywords:
Carbon/phenolic
Nanoclay
Mechanical properties
Thermal stability
Ablation rate

ABSTRACT

The mechanical, thermal and ablation properties of carbon phenolic (C-Ph) composites (Type-I) reinforced with different weight percentages of organo-modified montmorillonite (o-MMT) nanoclay have been studied experimentally. Ball milling was used to disperse different weight (wt) percentages (0, 1,2,4,6 wt.%) of nanoclay into phenolic resin. Viscosity changes to resin due to nanoclay was studied. On the other hand, nanoclay added phenolic matrix composites (Type-II) were prepared to study the dispersion of nanoclay in phenolic matrix by small angle X-ray scattering and thermal stability changes to the matrix by thermogravimetric analyser (TGA). This data was used to understand the mechanical, thermal and ablation properties of Type-I composites. Inter laminar shear strength (ILSS), flexural strength and flexural modulus of Type I composites increased by about 29%, 12% and 7% respectively at 2 wt.% addition of nanoclay beyond which these properties decreased. This was attributed to reduced fiber volume fraction (%V_f) of Type-I composites due to nanoclay addition at such high loadings. Mass ablation rate of Type-I composites was evaluated using oxy acetylene torch test at low heat flux (125 W/cm^2) and high heat flux levels (500 W/cm^2). Mass ablation rates have increased at both flux levels marginally up to 2 wt.% addition of nanoclay beyond which it has increased significantly. This is in contrast to increased thermal stability observed for Type-I and Type-II composites up to 2 wt.% addition of nanoclay. Increased ablation rates due to nanoclay addition was attributed to higher insulation efficiency of nanolcay, which accumulates more heat energy in limited area behind the ablation front and self-propagating ablation mechanisms triggered by thermal decomposition of organic part of nanoclay.

1. Introduction

Thermal protection systems (TPS) are essential sub systems of rockets and ballistic re-entry vehicles. Increased shear strength and flexural strength with reduced thermal conductivity are the main requirements for the TPS used under ballistic conditions. This is because, the liners of the rocket nozzles and thermal insulating shields of the re-entry vehicle structures encounters aerodynamic shear forces due to high velocity gases from the plume of the propulsion systems. Hence, TPS should withstand such harsh aerodynamic shear loads while simultaneously acting as heat insulator to protect the subsystems that are behind them. Carbon fiber reinforced phenolic (C-Ph) composites are widely used in fabrication of TPS. Though C-Ph composites have established themselves as the best TPS materials, there is always an urge to further improve their properties to realize relatively thinner TPS which can reduce the overall weight of aerospace systems [1].

Researchers have explored addition of various nano materials like, nano silica, carbon nanotube, carbon black, nanoclay, polyhedral oligomer silsesquioxane (POSS) to C–Ph composites for enhancing their thermo mechanical performance [2–8]. Among all these, nanoclay is the most versatile nano filler due to its low cost and ease of dispersion in the resin systems. Many researchers have

* Corresponding author.
** Corresponding author.
E-mail addresses: ramanogolla@asl.drdo.in (G.R. Rao), isrikanth@asl.drdo.in (I. Srikanth).
Peer review under responsibility of China Ordnance Society

https://doi.org/10.1016/j.dt.2020.05.012

Original Research Article

Polymers and Polymer Composites

Polymers and Polymer Composites
1–12

DOI: 10.1177/09673911211998833
journals.sagepub.com/home/ppc
SAGE

Mechanical, thermal and ablative behavior of organo nanoclay added carbon fiber/cyanate ester resin composites and effect of heat flux on its ablative performance

Golla Rama Rao[1], Ivautri Srikanth[1] and K Laxma Reddy[2]

Abstract

Nanoclay added cyanate ester resin (Type I) composites were fabricated by adding different weight percentages (0,1,2,4 & 6 wt%) of organo-modified Montmorillonite (o-MMT) and tested for dispersion by Small angle X-ray scattering(SAXS), thermal stability using Thermogravimetric analyser (TGA) and curing behavior using Differential scanning calorimeter (DSC). This data was correlated with the thermomechanical properties of nanoclay added carbon fiber reinforced cyanate ester resin composites (C-CE composites /Type II). Interlaminar shear strength (ILSS), flexural strength of type II composites increased by about 17%, 21% respectively at 2 wt% addition of nanoclay although at this loading nanoclay was found to show intercalation. Thermal stability of type II composites got reduced whereas the ablation rate has increased for type II composites with increased loading of nanoclay. However, percentage increase in ablation rate was found to be lower when type II composites were tested at 5000 kWm^{-2} as compared to the ablation testing carried out at 1250 kWm^{-2}. Scanning electron microscopy studies indicates significant melting of nanoclay at high flux resulting in additional protection mechanisms for the composites at high flux. Present study indicates the possibility of using o-MMT nanoclay for improved mechanical properties of C-CE composites used in thermal protection systems (TPS).

Keywords

Carbon fiber, cyanate ester resin, nanoclay, mechanical properties, thermal stability, ablation, microstructure

Received 21 January 2021; accepted 27 January 2021

Introduction

Phenolic resin based ablative composites are more popular in aerospace applications due to its low cost, ease of availability raw materials.[1] However, phenolic resin suffers from low shelf life and out life due to easy crosslinking of methylol groups present in the aromatic structure leading to variation in properties of the resultant components as function of storage life. One of the alternate choice as ablative matrix is cyanate ester (CE) resin, which is an addition cured thermoset polymer synthesized by the reaction of phenolic resin with cyanogen bromide.[2]

It was reported that, the CE resin has higher decomposition temperature and char yield than phenolic resins.[3,4] Moreover CE undergoes addition curing without releasing any gaseous by products which enables easy processing.[5] However, there is limited literature available on the processing, properties of the fiber reinforced cyanate ester resins for ablative applications.

On the other hand, researchers have explored addition of various nano materials like nanosilica, carbon nanotube, nanoclay, polyhedral oligomer silsesquioxane, nanozirconium tungstate to neat cyanate ester resin for enhancing their

[1] Advanced Systems Laboratory, DRDO, Hyderabad, Telangana, India
[2] Department of Chemistry, National Institute of Technology, Warangal, Telangana, India

Corresponding author:
Golla Rama Rao, Advanced Systems Laboratory, DRDO, Hyderabad, Telangana 500058, India. K Laxma Reddy, Department of Chemistry, National Institute of Technology, Warangal, Telangana 506004, India.
Email: ramaraogolla@asl.drdo.in; ramaraogolla@rediffmail.com; laxma@nitw.ac.in

Defence Science Journal, Vol. 71, No. 5, September 2021, pp. 682-690, DOI : 10.14429/dsj.71.16630

Effect of Organo-Montmorillonite Nanoclay on Mechanical Properties, Thermal Stability and Ablative Rate of Carbon fiber /Polybenzoxazine Resin Composites

Golla Rama Rao[#,@], Ivautri Srikanth[#,*], and K. Laxma Reddy[@]

[#]*DRDO-Advanced Systems Laboratory, Hyderabad - 500 058, India*
[@]*Department of Chemistry, National Institute of Technology, Warangal - 506 004, India*
[*]*E-mail: isrikanth@asl.drdo.in*

ABSTRACT

Organo-Montmorillonite (o-MMT) nanoclay added polybenzoxazine resin (type I composites) were prepared with varying amounts of clay (0, 1, 2, 4 and 6 wt %). Clay dispersion, changes in curing behaviour and thermal stability were assessed in type I composites. Findings from these studies of type I composites were used to understand thermal stability, mechanical, and mass ablation rate behaviour of nanoclay added carbon fiber reinforced polybenzoxazine composites (type II). Interlaminar shear strength and flexural strength of type II composites increase by 25% and 27%, respectively at 2 wt% addition of clay. An oxy-acetylene torch test with a constant heat flux of 125 w/cm^2 was used to investigate mass ablation rate of type II composites. The ablation rate has increased as the weight percentage of clay has increased. This is contradicting to type I composites with up to 6 wt% clay and type II composites with up to 4 wt% clay, which have improved thermal stability. The microstructure of the ablated composites was examined using scanning electron microscopy. Increased ablation rates are due to the reaction of charred matrix with nanoclay, which exposes bare fibers to the ablation front, resulting in higher mechanical erosion losses.

Keywords: Carbon fiber; Polybenzoxazine resin; Organo-montmorillonite nanoclay; Thermomechanical properties; Ablation rate; Microstructure

1. INTRODUCTION

Composites made of phenolic matrix are used for high temperature thermal protection application due to their ability to provide good thermomechanical properties, thermal stability with low ablation rate. Phenolic resin has processing disadvantages such as volatiles evolution due to condensation polymerisation reaction. In addition to this, phenolic resin has low shelf life which adds to the processing cost[1-2]. In view of this, many researchers are exploring alternate resin systems for high temperature applications like cyanate ester resins, polyimide and benzoxazine resin (BZ). These resin systems undergo additional cured polymerisation giving no process volatiles. In addition, benzoxazine resin offers additional advantages such as good shelf life, and good flame retardant properties, coupled with good thermo mechanical properties with low volumetric shrinkage and moisture absorption[3-5]. Thus, there are many technical advantages in using BZ instead of phenolic resin. As a result, the current research focused on the carbon fibre reinforced polybenzoxazine resin composite as a candidate material for use in thermal protection systems (TPS).

Many studies on nanofillers such as nanosilica, nanographite, carbon nanotube, organo-nanoclay, polyhedral oligomer silsesquioxane (POSS), and nanozirconium have been published in the literature to improve the thermomechanical efficiency of high temperature polymer composites[6-11]. Organic treated montmorillonite nanoclay is the most commonly used filler since it is readily available and miscible with resin systems. Previous studies have shown that introducing nanoclay particles to polymer composites enhances their thermomechanical properties significantly[12-16]. TPS applications need excellent thermomechanical properties. It is reported that nanoclay can impart these properties to polymer matrices[17-18]. For instance, Agag[19], *et al.* reported organo-nanoclay modified polybenzoxazine nanocomposites with allyl dimethyl stearyl ammonium-montmorillonite and propyl dimethyl stearyl ammonium-montmorillonite with clay loadings (3,7,10 wt%). Organo-nanoclay catalysed polymerisation of benzoxazine resin was reported. It is also reported that thermal stability of resin has increased with increased nanoclay content[19]. Many researchers studied the thermal stability of nanoclay added polybenzoxazine composites and mechanical properties of glass fibre reinforced benzoxazine composites[20-24]. Furthermore, no studies on the ablative performance of benzoxazine resin composites have been published.

Although there is a lot of literature on nanoclay reinforced polybenzoxazine resin matrices, no research on nanoclay modified carbon fibre – polybenzoxazine matrix (C-BZ) composites has been done to the author's knowledge, despite the fact that carbon fibre composites are the most promising for end applications. The present work aims at addressing this gap.

Received : 30 December 2020, Revised : 12 April 2021
Accepted : 01 July 2021, Online published : 02 September 2021

Bio Data

Name: Rama Rao Golla

Contact: +91 4024309239

Email: ramaraogolla@rediffmail.com

Address: Advanced Systems Laboratory,
DRDO, Ministry of Defence,
Government of India,
Kanchanbagh, Hyderabad-500058,
Telangana, India.

Area of Research: Development of high performance polymers for fibre reinforced composite materials and nanocomposite materials for defence applications. Characterisation of composite materials for the generation of design input data for design and analysis of composite products.

Educational Qualification:

Degree	Institute	Specialization	Year of Passing
B.Sc	Nagarjuna University, Guntur, Andhra Pradesh	Mathematics, Physics, Chemistry	1995
M. Sc	Pondicherry University, Pondicherry	Chemical Science	1997
M. Tech	Indian Institute of Technology, Delhi	Polymer Science and Technology	1998
Ph. D.	National Institute of Technology, Warangal	Nanoclay Reinforced Composites	Pursuing from 2016

Work Experience:

1. 1999 - 2000 : Project Associate, Indian Institute of Technology, Delhi
2. 2001 - Present : Scientist, Advanced Systems Laboratory, DRDO, Hyderabad

Publications: 18 (Peer Reviewed Journals: 8 and Conference Proceedings: 10)

Membership: Life Member – Indian Society for Advancement of Materials and Process Engineering (ISAMPE).

Awards: Laboratory Scientist of the Year-2017 and Agni Award for Excellence in Self Reliance-2018